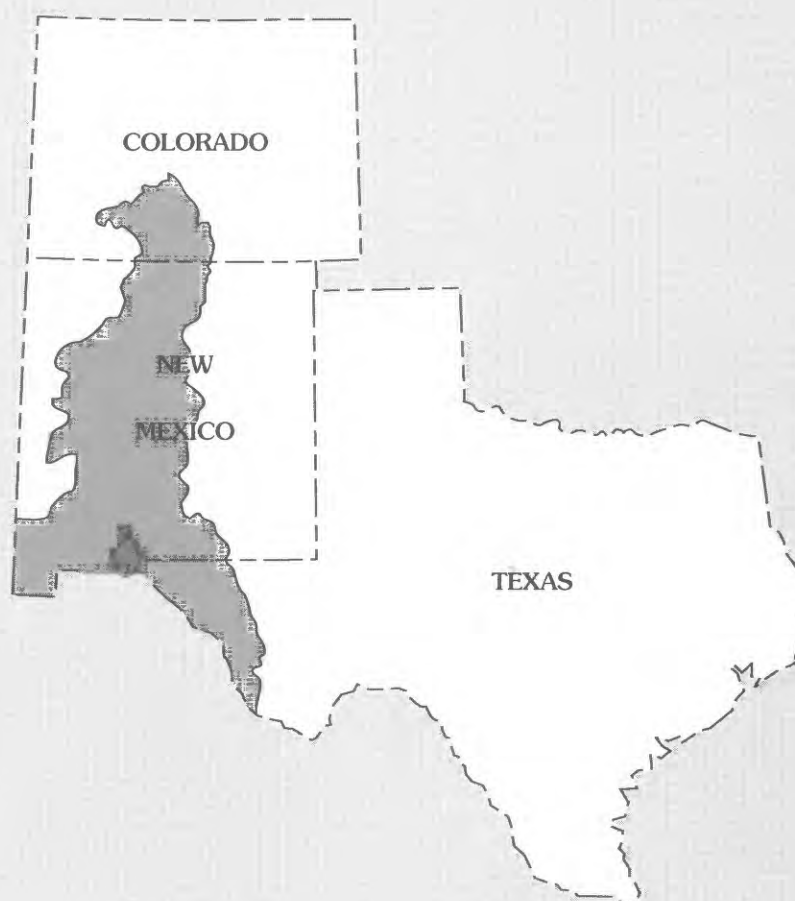


GEOHYDROLOGY AND SIMULATION OF GROUND-WATER FLOW IN THE MESILLA BASIN, DOÑA ANA COUNTY, NEW MEXICO, AND EL PASO COUNTY, TEXAS

REGIONAL AQUIFER-SYSTEM ANALYSIS



Geohydrology and Simulation of Ground-Water Flow in the Mesilla Basin, Doña Ana County, New Mexico, and El Paso County, Texas

By PETER F. FRENZEL *and* CHARLES A. KAEHLER

With a section on WATER QUALITY AND GEOCHEMISTRY

By SCOTT K. ANDERHOLM

REGIONAL AQUIFER-SYSTEM ANALYSIS—
SOUTHWEST ALLUVIAL BASINS, NEW MEXICO AND ADJACENT STATES

U.S. GEOLOGICAL SURVEY PROFESSIONAL PAPER 1407-C



U.S. DEPARTMENT OF THE INTERIOR

MANUEL LUJAN, JR., *Secretary*

U.S. GEOLOGICAL SURVEY

Dallas L. Peck, *Director*

Any use of trade, product, or firm names in this publication is for
descriptive purposes only and does not imply endorsement by the
U.S. Government

Library of Congress Cataloging-in-Publication Data

Frenzel, Peter F.

Geohydrology and simulation of ground-water flow in the Mesilla Basin, Doña Ana County, New Mexico, and El Paso County, Texas / by Peter F. Frenzel and Charles A. Kaehler; with a section on water quality and geochemistry by Scott K. Anderholm.

p. cm.—(Regional aquifer-system analysis—southwest alluvial basins, New Mexico and adjacent States) (U.S. Geological Survey Professional Paper ; 1407-C).

Includes bibliographical references.

Supt. of Docs. no.: I.19.16:P1407C

1. Groundwater flow—New Mexico—Doña Ana County—Simulation methods. 2. Groundwater flow—Texas—El Paso County—Simulation methods. 3. Water, Underground—New Mexico—Doña Ana County—Simulation methods. 4. Water, Underground—Texas—El Paso County—Simulation methods. I. Kaehler, C.A. II. Anderholm, Scott K. III. Title. IV. Series. V. Series: U.S. Geological Survey Professional Paper; 1407-C.

GB1197.7.F74 1994

551.49'09789'66—dc20

91-47031

CIP

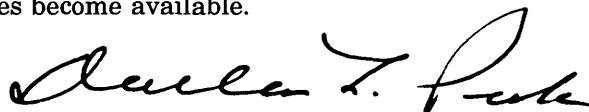
For sale by Book and Open-File Report Sales, U.S. Geological Survey,
Federal Center, Box 25286, Denver, CO 80225

FOREWORD

THE REGIONAL AQUIFER-SYSTEM ANALYSIS PROGRAM

The Regional Aquifer-System Analysis (RASA) program was started in 1978 after a congressional mandate to develop quantitative appraisals of the major ground-water systems of the United States. The RASA program represents a systematic effort to study a number of the Nation's most important aquifer systems that, in aggregate, underlie much of the country and that represent important components of the Nation's total water supply. In general, the boundaries of these studies are identified by the hydrologic extent of each system and accordingly transcend the political subdivisions to which investigations have often arbitrarily been limited in the past. The broad objective for each study is to assemble geologic, hydrologic, and geochemical information; to analyze and develop an understanding of the system; and to develop predictive capabilities that will contribute to the effective management of the system. The use of computer simulation is an important element of the RASA studies, both to develop an understanding of the natural, undisturbed hydrologic system and any changes brought about by human activities as well as to provide a means of predicting the regional effects of future pumping or other stresses.

The final interpretive results of the RASA program are presented in a series of U.S. Geological Survey Professional Papers that describe the geology, hydrology, and geochemistry of each regional aquifer system. Each study within the RASA program is assigned a single Professional Paper number, and where the volume of interpretive material warrants, separate topical chapters that consider the principal elements of the investigation may be published. The series of RASA interpretive reports begins with Professional Paper 1400 and thereafter will continue in numerical sequence as the interpretive products of subsequent studies become available.

A handwritten signature in black ink, appearing to read "Dallas L. Peck". The signature is fluid and cursive, with a large, stylized initial 'D'.

Dallas L. Peck
Director

CONTENTS

	Page		Page
Abstract	C1	Simulation of ground-water flow—Continued	
Introduction	2	Description of the model—Continued	
Purpose and scope	2	Boundary conditions—Continued	
Previous investigations	2	No-flow boundary	C33
Well-numbering systems	4	Recharge	33
Acknowledgments	4	Underflow	33
Description of the Mesilla Basin	4	Mesilla Valley boundary	33
Physical features	4	Ground-water withdrawals	39
Climate	6	Model adjustments	39
Population, industry, and agriculture	6	System properties used for comparison	39
Surface-water system	7	Hydraulic heads	41
Geohydrology	9	Surface-water depletions	48
Geologic units and their water-bearing properties	9	Drain discharges	52
Igneous-intrusive and metamorphic rocks	11	System properties adjusted	52
Paleozoic and Mesozoic sedimentary rocks	11	Recharge	53
Lower Tertiary sedimentary and volcanic rocks	12	Hydraulic conductivity	54
Santa Fe Group	12	Specific yield	54
Post-Santa Fe Group deposits	14	Mesilla Valley boundary	54
Ground-water flow system	16	Model evaluation	54
Ground-water/surface-water relation	18	Sensitivity tests	55
Net irrigation flux	18	Sources of water withdrawn for nonirrigation uses ..	59
Evapotranspiration from nonirrigated lands	20	Predictive capability	61
Stream seepage	20	Some possible ways to improve the model	61
Ground-water withdrawals	21	Additional model adjustment	61
Ground-water recharge	22	Shorter time increments	62
Summary of concepts	23	Restructuring of the grid	63
Simulation of ground-water flow	23	Simulation of inelastic beds	63
Description of the model	24	Conclusions concerning the model	63
Model grid	24	Water quality and geochemistry of the Mesilla Basin	
Aquifer characteristics	25	by Scott K. Anderholm	64
Hydraulic conductivity and transmissivity	25	Area west of the Mesilla Valley	65
Specific yield and storage coefficients	32	Mesilla Valley	67
Initial condition and time periods	32	Area east of the Mesilla Valley	69
Boundary conditions	32	Conclusions concerning basin geochemistry	73
		Summary	74
		Selected references	75

ILLUSTRATIONS

[Plates are in pocket]

PLATES 1–5. Maps showing:

1. Approximate water-level contours and gaging stations on drains, Mesilla Basin, New Mexico and Texas
2. Major faults and approximate saturated thickness of basin fill, Mesilla Basin, New Mexico and Texas
3. Estimated hydraulic conductivity of the Santa Fe Group, Mesilla Basin, New Mexico
4. Estimated hydraulic conductivity of the shallow part of the aquifer (flood-plain alluvium and upper part of the Santa Fe Group), Mesilla Valley, New Mexico and Texas
5. Concentration of dissolved constituents for selected sites in the Mesilla Basin and adjacent areas, New Mexico and Texas

FIGURE 1. Map showing study area boundary and basin divisions for the eastern part of the Southwest Alluvial Basins Regional Aquifer-System Analysis	C3
2. Diagram showing system of numbering wells in New Mexico	4
3. Diagram showing system of numbering wells in Texas	5
4. Map showing location of the Mesilla Basin study area	6
5-9. Graphs showing:	
5. Annual and April-to-October precipitation at New Mexico State University near Las Cruces, and at La Tuna, near Anthony, 1926-80	7
6. Number of irrigated acres in the Mesilla Valley, 1880-1980	7
7. Annual discharge of the Rio Grande at Leasburg and El Paso Narrows, 1912-75	8
8. Net diversions and depletions in the Mesilla Valley, 1930-75	8
9. Annual drain discharge and total length of drains upstream from gaging stations in the Mesilla Valley, 1923-79	9
10. Map showing general geology of the Mesilla Basin and adjacent areas	10
11. Generalized geohydrologic section of the northern Mesilla Basin	11
12. Stratigraphic column of the Santa Fe Group in the Mesilla Basin and adjacent areas	13
13. Diagram showing distribution of hydraulic conductivity with depth for the Santa Fe Group	15
14. Graph showing frequency distribution of hydraulic-conductivity estimates for the shallow part of the aquifer in the Mesilla Valley	16
15. Diagram showing interactions between ground water and surface water	19
16. Graph showing estimate of net irrigation flux in the Mesilla Valley, 1915-75	20
17. Graph showing estimates of net ground-water withdrawal rate for nonagricultural uses in the Mesilla Valley	22
18-25. Maps showing:	
18. Mountain-front and slope-front recharge	23
19. Model grid and basin boundary	26
20. Hydraulic conductivity assigned to model layer 1, the top layer	27
21. Transmissivity assigned to model layer 2	28
22. Transmissivity assigned to model layer 3	29
23. Transmissivity assigned to model layer 4	30
24. Transmissivity assigned to model layer 5, the bottom layer	31
25. Recharge, underflow, and evapotranspiration boundaries for layer 1, steady-state version	34
26. Graphs showing major basinwide flow rates, 1910-75	35
27-29. Maps showing:	
27. Location of model blocks where flow to and from the prestabilized Rio Grande was simulated (steady-state version)	36
28. Location of gaging stations and model blocks where flow to and from the stabilized Rio Grande and drains was simulated (transient version)	37
29. Model-derived evapotranspiration from nonirrigated lands for 1975 and area of net irrigation flux	40
30. Diagram showing estimated time of pumpage for wells in the Las Cruces well field	41
31-35. Maps showing comparison of measured hydraulic heads and:	
31. Model-derived steady-state potentiometric surface, layer 1	43
32. Model-derived potentiometric surface for 1947-48, layer 1	44
33. Model-derived potentiometric surface for 1975-76, layer 1	45
34. Model-derived potentiometric surface for 1975-76, layer 2	46
35. Model-derived potentiometric surface for 1975-76, layer 3	47
36. Graphs showing comparison of hydrographs of measured and model-derived hydraulic heads, 1910-80	48
37. Map showing potentiometric surface (for 1975-76, layer 2) that might exist without nonirrigation withdrawals	50
38. Map showing potentiometric surface (for 1975-76, layer 3) that might exist without nonirrigation withdrawals	51
39-42. Graphs showing:	
39. Annual surface-water depletions calculated from measured discharges compared to depletions calculated from model-derived discharges	52
40. Comparison of hydrographs of measured and model-derived drain discharges, 1910-80	53
41. Comparison of hydrographs of measured and model-derived hydraulic heads when values of transmissivity were one-half those in the standard model	56
42. Sources of nonirrigation withdrawals	60
43-44. Graphs showing:	
43. Effect of changes in diffusivity on the sources of water for nonirrigation withdrawals	61
44. Effect of changes in diffusivity on the sources of water for hypothetical nonirrigation withdrawals	62
45. Piper diagram showing selected ground-water analyses from the area west of the Mesilla Valley	66
46. Piper diagram showing selected ground-water analyses from the area east of the Mesilla Valley	70
47. Map showing the location of the thermal anomaly along the east side of the Mesilla Basin	72
48. Graph showing chloride versus potassium concentrations for selected ground-water analyses in the area east of the Mesilla Valley	73

TABLES

	Page
TABLE 1. Estimated values of hydraulic conductivity of the Santa Fe Group.....	C80
2. Estimated values of hydraulic conductivity of the shallow part of the aquifer in the Mesilla Valley (flood-plain alluvium and upper part of the Santa Fe Group)	81
3. River and drain specifications	83
4. Schedule of nonagricultural withdrawals specified in the model.....	89
5. Differences between measured and model-derived hydraulic heads.....	92
6. Description of sensitivity tests	97
7. Comparison of flows and heads of sensitivity tests with those of the standard	98
8. Average differences, in feet, between model-derived and measured heads for the standard and each sensitivity test	99
9. Differences between model-derived and measured drain discharges, surface-water depletions, and 1975 heads.....	100
10. Selected ground-water analyses from the area west of the Mesilla Valley	101
11. Concentrations of dissolved ions in excess applied irrigation water for different irrigation efficiencies and chemical reactions.....	102
12. Selected ground-water analyses from the area east of the Mesilla Valley	103
13. Well depth, water level, and percentages of calcium plus magnesium and sulfate plus chloride for selected sites in the northeastern part of the Mesilla Basin	105
14. Calculated chemical-geothermometer temperatures for selected ground-water analyses in the Mesilla Basin	105

CONVERSION FACTORS AND VERTICAL DATUM

In this report, figures for measurements are given in inch-pound units only. The following table contains factors for converting to metric units.

<i>Multiply inch-pound units</i>	<i>By</i>	<i>To obtain metric units</i>
inch	25.4	millimeter
inch	0.02540	meter
foot	0.3048	meter
foot per day	0.3048	meter per day
foot per year	0.3048	meter per year
per foot	3.281	per meter
square foot	0.0929	square meter
foot squared per day	0.0929	meter squared per day
foot squared per second	0.0929	meter squared per second
cubic foot	0.02832	cubic meter
cubic foot per second	0.02832	cubic meter per second
cubic foot	28.32	cubic decimeter cubic
foot per second	28.32	liter per second
cubic foot per second	28.32	cubic decimeter per second
foot per mile	0.1894	meter per kilometer
mile	1.609	kilometer
acre	4,047	square meter
acre	0.4047	square hectometer
acre	0.004047	square kilometer
square mile	2.590	square kilometer
gallon	3.785	liter
gallon	3.785	cubic decimeter
gallon	0.003785	cubic meter
gallon per minute	0.06309	liter per second
gallon per minute	0.06309	cubic decimeter per second
gallon per minute	0.00006309	cubic meter per second
gallon per minute per foot	0.2070	liter per second per meter
acre-foot	1,233	cubic meter
acre-foot	0.001233	cubic hectometer
acre-foot	0.000001233	cubic kilometer
acre-foot per year	0.001233	cubic hectometer per year
acre-foot per acre	0.003048	cubic hectometer per hectare

Temperature in degrees Fahrenheit (°F) may be converted to degrees Celsius (°C) as follows:

$$^{\circ}\text{C} = 5/9(^{\circ}\text{F} - 32)$$

Sea level: In this report “sea level” refers to the National Geodetic Vertical Datum of 1929 (NGVD of 1929)—a geodetic datum derived from a general adjustment of the first-order level nets of both the United States and Canada, formerly called “Sea Level Datum of 1929.”

REGIONAL AQUIFER-SYSTEM ANALYSIS—SOUTHWEST ALLUVIAL BASINS, NEW MEXICO AND
ADJACENT STATES

**GEOHYDROLOGY AND SIMULATION OF GROUND-WATER FLOW IN THE
MESILLA BASIN, DOÑA ANA COUNTY, NEW MEXICO, AND
EL PASO COUNTY, TEXAS**

By PETER F. FRENZEL and CHARLES A. KAEHLER

ABSTRACT

The ground-water hydrology and geochemistry of the Mesilla Basin in south-central New Mexico and western Texas were studied as part of the Southwest Alluvial Basins Regional Aquifer-System Analysis program of the U.S. Geological Survey. The Mesilla Basin, hydrologically representative of many alluvial basins, was studied by simulating the ground-water flow system using a digital model. The basin fill, composed of Santa Fe Group and younger deposits, forms a three-dimensional ground-water flow system whose lateral extent and depth are defined by bedrock that has a much smaller hydraulic conductivity than the basin fill. Near Las Cruces, ground-water flow generally is away from the Mesilla Valley and is toward the valley in the southern part of the basin. Most flow into and out of the ground-water system occurs at or near land surface in the Mesilla Valley and is the result of interaction of the Rio Grande, drains, canals, evapotranspiration, and ground-water withdrawals. These flows fluctuate in the short and intermediate term (as much as about 5 years) with the availability of surface water, but in the long term, they do not change much. The general direction of ground-water flow is southeastward along the Mesilla Valley. Some recharge results from torrential surface runoff, mainly near mountain fronts. Recharge over most of the West Mesa area is unlikely but occasionally may occur in places.

A finite-difference ground-water flow model of the basin consisting of 36 rows, 64 columns, and 5 layers was used to simulate hydrologic conditions from 1915 to 1975. The model simulated ground-water flow to and from the Rio Grande and a series of drains that empty into the Rio Grande. The model also simulated evapotranspiration from nonirrigated lands in the Mesilla Valley (about 2 acre-feet per acre) as a function of the difference between the altitude of the land surface and the model-derived altitude of the water table. Mountain- and slope-front recharge (about 15 cubic feet per second) was estimated by an empirical formula and modeled as specified fluxes. No recharge was simulated for the West Mesa. Pumpage of ground water for municipal, industrial, and domestic uses (about 58 cubic feet per second in 1975) was either reported or estimated from population data and was simulated as specified fluxes. Net ground-

water pumpage for irrigation (pumpage minus recharge) was estimated from a summation of estimated evapotranspiration from irrigated lands, effective rainfall, and water diverted from the Rio Grande.

Hydraulic conductivity of the uppermost layer generally was about 22 feet per day in the case where the layer represented the Santa Fe Group and about 70 feet per day in the case where the layer represented the flood-plain alluvium plus the upper part of the underlying Santa Fe Group. Hydraulic conductivity of other layers ranged from about 22 feet per day for the upper part of the Santa Fe Group to 3 feet per day for the lower part. The ratio of horizontal to vertical hydraulic conductivity was estimated by simulations to be 200:1.

Model-derived hydraulic heads, drain discharges, and river depletions compared well with measured values except that model-derived hydraulic heads in the Las Cruces well-field area were about 20 feet higher than measured hydraulic heads. These comparisons were not very sensitive to changes in the aquifer characteristics of plus 100 percent or minus 50 percent. The model was found to be insensitive to changes in specific yield and storage coefficient.

According to simulations for the 1970's, about 80 percent of ground water pumped for municipal, industrial, and domestic uses may have come from the Rio Grande. About 10 percent may have come from salvaged evapotranspiration and about 10 percent from aquifer storage. Drawdowns of 1 to 10 feet in 1975, caused by historical nonirrigation withdrawals, may be measurable at distances of about 5 miles west of well fields at Las Cruces and Cañutillo in or below the deep producing zones. The accuracy of predicted effects of future withdrawals on depletion of streamflow would depend largely on the accuracy of hydraulic-conductivity, specific-yield, and specific-storage values, especially if the withdrawals were distant from the Mesilla Valley.

The chemical composition of ground water in the Mesilla Valley varies areally and vertically. The large variation is due to mixing of excess applied irrigation water with ground water. The location of the transition zone between these two water types probably moves in response to ground-water pumpage.

Some ground water enters the basin fill from bedrock at depth. Along the northwestern margin of the basin, sulfate and sodium are the dominant ions in ground water flowing into the basin, and the specific conductance of this water ranges from 1,400 to 2,310

microsiemens per centimeter at 25 degrees Celsius. Ground-water inflow along the southwestern margin of the basin consists of two types: bicarbonate and sodium are the dominant ions in one type, and chloride and sodium are the dominant ions in the other type.

Inflowing geothermal water, which has large concentrations of chloride, silica, and potassium, mixes with cool, less mineralized water along the eastern side of the Mesilla Basin. Calculated chemical-geothermometer temperatures indicate that geothermal-reservoir temperatures may be as great as 230 degrees Celsius.

INTRODUCTION

This report is a product of the Southwest Alluvial Basins (SWAB) study, which is part of the Regional Aquifer-System Analysis (RASA) program of the U.S. Geological Survey. The SWAB study area is divided, for administrative reasons, into two parts. The western part includes the southern tip of Nevada, the eastern part of California (from Hoover Dam to the Mexican border), and the southern part of Arizona. The eastern part, which includes the Mesilla Basin, includes parts of southern Colorado, New Mexico, and West Texas (fig. 1).

The main purposes of this part of the SWAB study were to enhance the understanding of the regional hydrology of the alluvial basins in parts of Colorado, New Mexico, and Texas that serve as major ground-water reservoirs and to study the hydrologic effects of stresses on the system. Twenty-two alluvial basins were chosen for study within the area. Each basin study consisted of a literature review of the hydrology and geology, data compilation, data collection, data evaluation, and digital simulations of the aquifer system where sufficient data were available. A planning report by Wilkins and others (1980) provides a more detailed description of the SWAB study.

The SWAB regional analysis is described in Professional Paper 1407, which consists of three chapters. Chapter A is a summary of the project. Chapter B summarizes ground-water flow models developed for the area and provides guidelines for developing generalized models applicable to basins within the study area. Chapter C (this report) describes the geohydrology and ground-water quality of the Mesilla Basin.

PURPOSE AND SCOPE

The purpose of this report is to provide a summary of hydrologic data, a brief description of hydrogeologic and geochemical characteristics, and an explanation of the digital model of the Mesilla Basin ground-water flow system. Preexisting data were used.

The Mesilla Basin was studied in detail by using a model to help assess the consistency of hypotheses, concepts, estimates, and observations. Creating a tool

for management of water resources was not the purpose of this study, and use of this model for such a purpose may not be justified.

PREVIOUS INVESTIGATIONS

Ground-water investigations in the Mesilla Valley began in the early part of the 20th century. Slichter (1905) and Lee (1907) investigated the hydrology of the shallow ground-water system in the Mesilla Valley. A reconnaissance survey for municipal water supplies was made by Theis (1936) for the Las Cruces area.

A number of reports have been written that present information on ground-water conditions and geology of the area. Bryan (1938) included a hydrogeologic description of the types of intermontane basins along the Rio Grande depression. He recognized that most of the basin sediments are part of the Santa Fe Group, as did Dunham (1935), and that an ancestral Rio Grande emptied into a closed Mesilla Basin prior to development of the present through-flowing river system. Conover (1954) conducted an extensive study of ground-water conditions in the Mesilla Valley and adjacent areas. Conover prepared a water-table and depth-to-water map and presented drillers' logs, aquifer-test results, and other data. From this information, he was able to describe ground-water movement and outline a water budget for the valley.

Leggat and others (1962) discussed in detail the ground-water conditions in the southern part of the Mesilla Valley. They described the shallow, medium, and deep zones of the aquifer in this part of the valley and provided information on aquifer tests, recharge and discharge, and the quantity of freshwater in storage. This information was also summarized by Gates and others (1978).

A comprehensive hydrogeologic study of central and western Doña Ana County was presented by King and others (1971). Their report contains data on the configuration and stratigraphy of the Mesilla and southern Jornada del Muerto Basins (fig. 1) and on the occurrence of ground water. A water-level map and detailed lithologic logs are included.

A recent study involving ground water, geology, and surface water was conducted by Wilson and others (1981). Their report includes descriptions of the geology, hydraulic characteristics of the aquifer, occurrence and movement of ground water, and the chemical quality, use, and availability of water in the Mesilla and southern Jornada del Muerto Basins. Water-level, depth-to-water, and water-quality maps were presented, and hydrologic sections were constructed from vertical electrical-resistivity sounding data. The present digital-model study relied heavily on their report as a source of data.

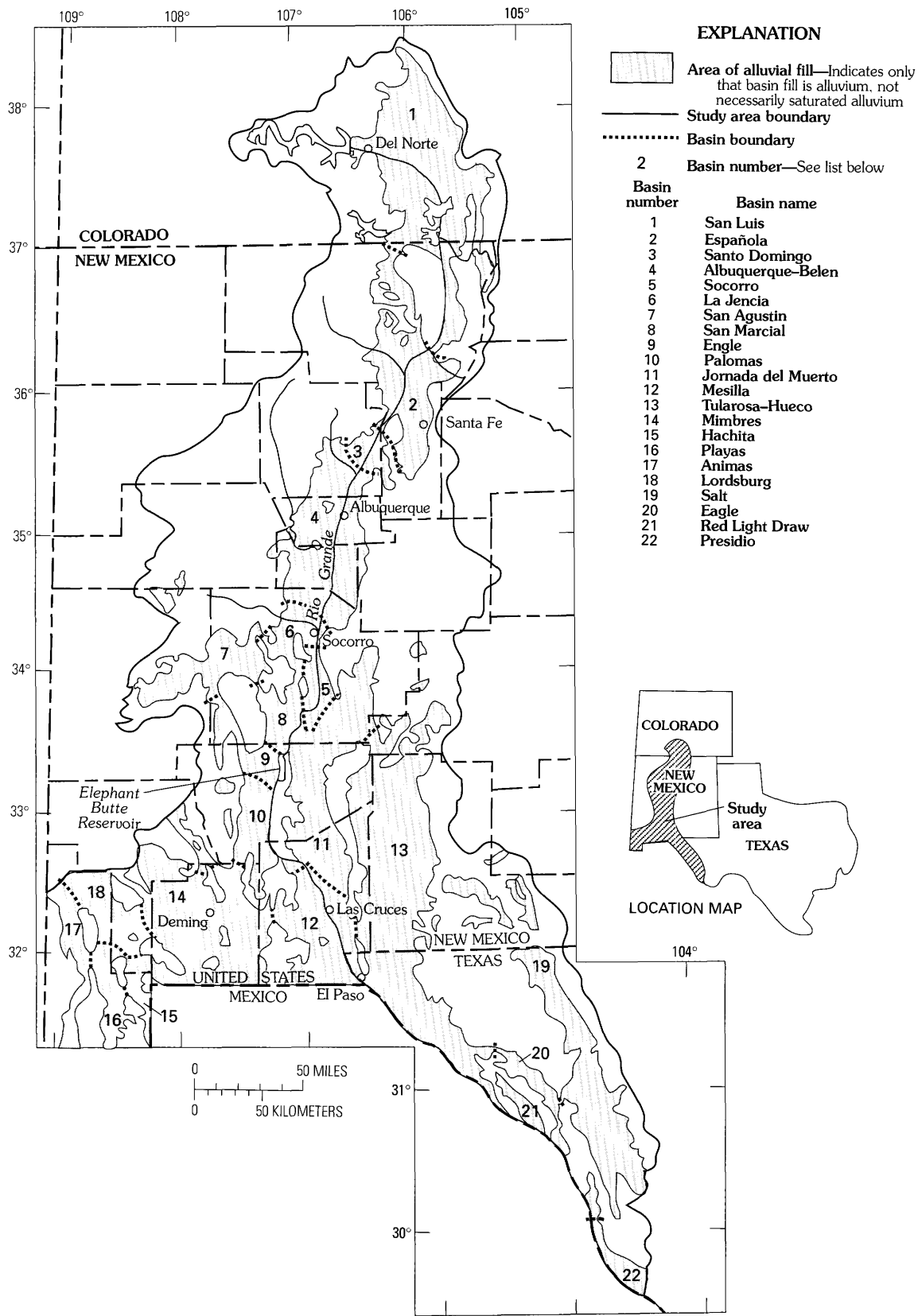


FIGURE 1.—Study area boundary and basin divisions for the eastern part of the Southwest Alluvial Basins Regional Aquifer-System Analysis. Modified from Wilkins and others (1980, p. 3).

Spiegel (1958) presented data on wells and information on the movement and discharge of ground water in the Mesilla Valley. The Tertiary and Quaternary geology and the geomorphic evolution of the Mesilla Basin have also been investigated. Reports on these topics include those by Kottowski (1953), Strain (1966, 1969), Ruhe (1967), Hawley and Kottowski (1969), Hawley and others (1969), Seager and others (1971), Belcher (1975), Hawley (1975, 1978, 1984), and Lovejoy and Hawley (1978).

WELL-NUMBERING SYSTEMS

Wells in New Mexico are identified by a location-number system based on the township-range system of subdividing public lands. The location number consists of four segments separated by periods, corresponding to the township, range, section, and tract within a section (fig. 2). The townships and ranges are numbered according to their location relative to the New Mexico base line and the New Mexico principal meridian. The smallest division, represented by the third digit of the final sequent, is a 10-acre tract. If a well has not been located precisely enough to be placed within a particular section or tract, a zero is used for that part of the location number.

Wells in Texas are officially given a well number consisting of five parts (fig. 3). The first part is a two-letter prefix used to identify the county. El Paso

County is represented by JL, whereas NM signifies wells in New Mexico that have been given a number using the Texas system. The second part of the number has two digits indicating the 1-degree quadrangle. Each 1-degree quadrangle is divided into 64 7½-minute quadrangles: this is the third part of the well number. The first digit of the fourth part indicates the 2½-minute quadrangle, and the last two digits comprise a sequence number that identifies the well from others in the same 2½-minute quadrangle. As an example (fig. 3), well JL-49-04-501 is in El Paso County (JL), in 1-degree quadrangle 49, in 7½-minute quadrangle 04, in 2½-minute quadrangle 5, and was the first well inventoried in this 2½-minute quadrangle. The wells used in the study also were given a latitude-longitude location number to aid data processing.

ACKNOWLEDGMENTS

Many people contributed to this study. During the data collection phase, the personnel of the U.S. Bureau of Reclamation office at El Paso, Texas, supplied streamflow data and drain profiles. Personnel of the U.S. Geological Survey at El Paso, Las Cruces, and Albuquerque assisted with pumpage data, conceptualization of the hydrologic system, implementation of the model programs, and preprocessing and postprocessing programs. J.W. Hawley and students at the New Mexico Institute of Mining and Technology contributed geologic information. Owen Lockwood and Sheryl Wilson at New Mexico State University supplied pumpage and student-population data. Jerry Mayfield, Leonard Valdez, and others with the City of Las Cruces provided city pumpage and return-flow information. Stuart Meerscheidt and others of Jornada Water Company and personnel of the Doña Ana Mutual Domestic Water Consumers Association supplied pumpage data for those organizations.

DESCRIPTION OF THE MESILLA BASIN

The Mesilla Basin is the southernmost of a series of basins along the Rio Grande in New Mexico. The basin primarily is in Doña Ana County, New Mexico, and extends into El Paso County, Texas, and the State of Chihuahua, Mexico (fig. 4).

PHYSICAL FEATURES

The Mesilla Basin is encircled by mountains. The East and West Potrillo Mountains, Aden Hills, and Sleeping Lady Hills are on the west. The Robledo

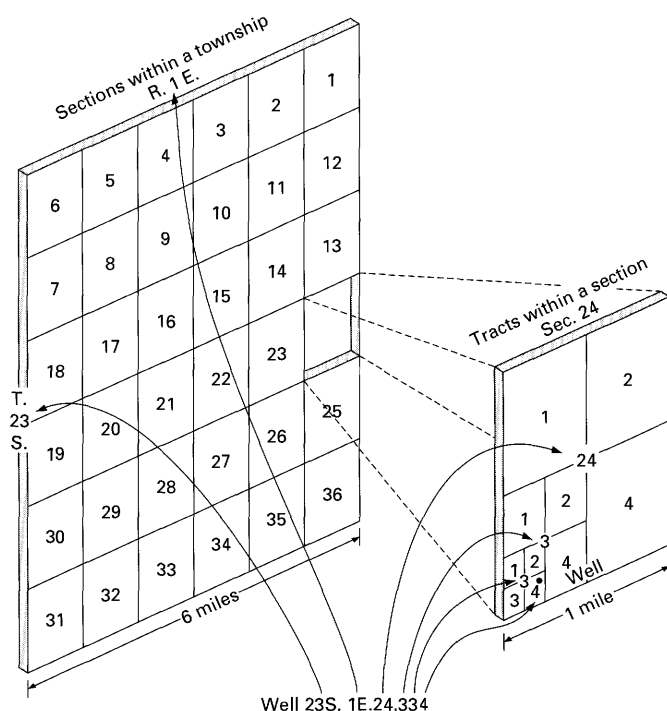
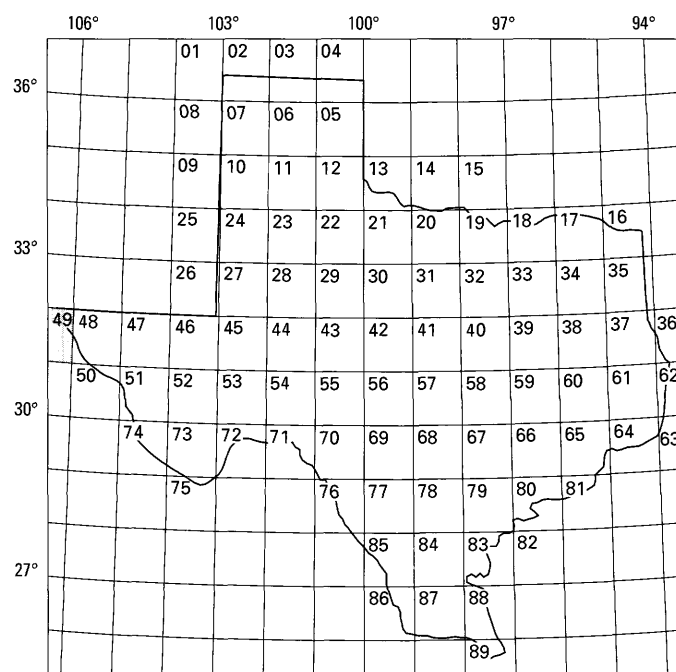
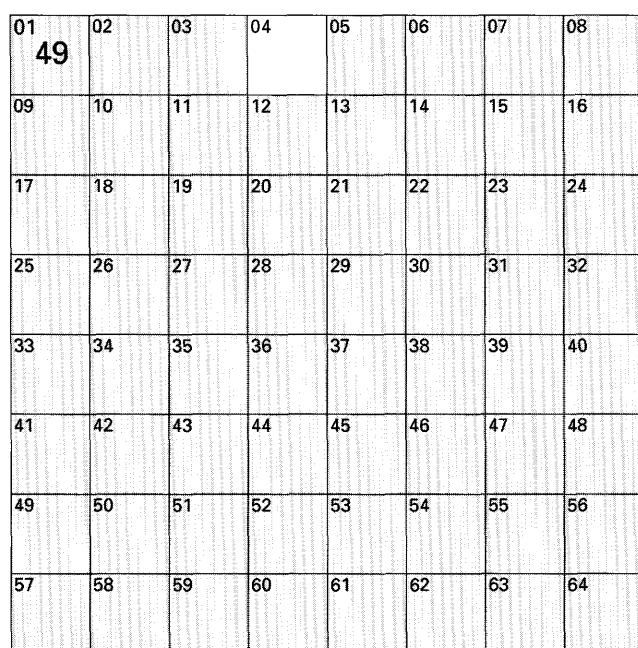


FIGURE 2.—System of numbering wells in New Mexico.

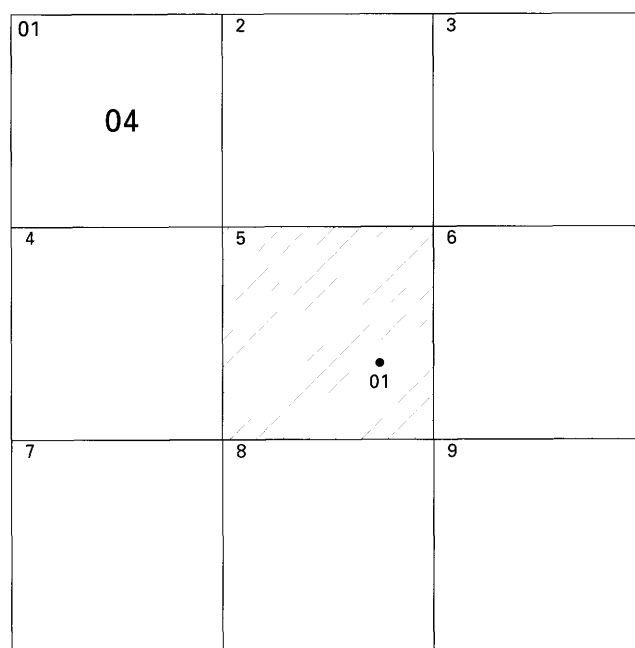


1-degree quadrangles



7 1/2-minute quadrangles

- LOCATION OF WELL JL-49-04-501
- 49 1-degree quadrangle
 - 04 7 1/2-minute quadrangle
 - 5 2 1/2-minute quadrangle
 - 01 Well number within 2 1/2-minute quadrangle
 - JL Symbol for El Paso County



2 1/2-minute quadrangles

FIGURE 3.—System of numbering wells in Texas.

Mountains and Doña Ana Mountains are on the north. Goat Mountain, Tortugas Mountain, the Organ Mountains, Bishop Cap Mountain, and the Franklin Mountains are on the east; on the southeast, the Sierra de Cristo Rey is on the International Boundary and the Sierra de Juarez is just south of the International Boundary. The highest point in Doña Ana County is in

the Organ Mountains (9,012 feet above sea level), whereas mountains on the west side of the basin have relatively low relief (high point 5,979 feet).

The Rio Grande enters the basin through Selden Canyon between the Robledo and Doña Ana Mountains and exits through El Paso Narrows between the Franklin Mountains and the Sierra de Cristo Rey. The broad



FIGURE 4.—Location of the Mesilla Basin study area.

area west of the Rio Grande from the International Boundary to the Rough and Ready Hills is called West Mesa (or La Mesa). West Mesa is relatively level, has some closed drainage basins, and generally slopes slightly toward the southeast. The area contains scattered extinct volcanoes and an extensive area of lava flows. Incision of the Rio Grande into the mesa surface by as much as 400 feet has formed the Mesilla Valley, which is more than 50 miles long and as much as 5 miles wide. The total area of the Mesilla Valley is about 110,000 acres. The altitude of the Mesilla Valley ranges from 3,980 feet, at Leasburg Dam, to 3,729 feet, at El Paso Narrows. East of the Mesilla Valley, the land slopes upward toward the Organ and Franklin Mountains.

The ground-water basin can be defined in two ways. One area is defined by ground-water divides (King and others, 1971, pl. 1) and generally follows topographic divides. The other, smaller, area is defined geologically and hydrologically by structural boundaries. The word

“basin” as used in this report means the smaller area unless otherwise indicated. The smaller basin is bounded by uplifted blocks of bedrock or by relatively impermeable volcanic rocks and is filled with alluvial sediment from the surrounding mountains and with fluvial sediment carried in by an ancestral Rio Grande. The area between the basin and the mountains generally is covered by similar, but relatively thinner, sediments. Although the western piedmont slope of the Organ Mountains topographically might be included in the Mesilla Basin, that area is within the southern Jornada del Muerto structural basin and is excluded from this study. Gravity anomalies and bedrock outcrops indicate that the basin extends about 7 miles into Mexico. However, no hydrologic data were available for that area.

CLIMATE

The climate primarily is arid but becomes semiarid in high, mountainous regions. The average annual precipitation, mostly in the form of rain, in the Las Cruces area for 1851 to 1976 is 8.39 inches. About one-half of the annual rainfall results from thunderstorms during July through September. The mean annual temperature at University Park is 60 degrees Fahrenheit. Temperatures often range over a span of 30 degrees Fahrenheit during 24-hour periods in the summer. The average frost-free period at Las Cruces is 197 days. Pan evaporation averages about 94 inches a year and is greatest during late spring and summer. Annual and April-to-October (growing season) precipitation at New Mexico State University and La Tuna is shown in figure 5.

POPULATION, INDUSTRY, AND AGRICULTURE

The main population center within the basin is Las Cruces, which had a population of 8,325 in 1940, 29,367 in 1960, and 45,086 in 1980 (U.S. Department of Commerce, 1952a, p. 31–38; 1982a, p. 33). Other population centers in New Mexico include Doña Ana, Mesilla, Mesilla Park, San Miguel, La Mesa, Berino, Chamberino, Anthony, La Union, Meadow Vista, Anapra, and residential developments in the Santa Teresa Grant area (pl. 1). New Mexico State University is adjacent to Las Cruces. In the Texas part of the valley are Anthony, Vinton, and Cañutillo. All these communities are dependent upon ground water for domestic and industrial water supply. El Paso, Texas, which had a 1980 population of almost 0.5 million, is south-east of the basin and depends partly on ground water pumped from a well field at Cañutillo.

Industry in the area includes produce canneries, an egg-production plant, a steel mill, and a knitting mill. Mining also is of economic importance.

Agriculture is a major activity, and irrigation is the chief use of water in the Mesilla Basin. The Rio Grande is the primary source of irrigation water—irrigation water is administered by the Elephant Butte Irrigation District (EBID) in the New Mexico part of the Mesilla Valley and by the El Paso County Water Improvement District No. 1 in the Texas part of the valley. Surface water is supplemented by ground water for use in irrigation. As of February 1948, there were about 70 irrigation wells in the Rincon and Mesilla Valleys (Conover, 1954, p. 107). During the drought of 1951–57, several hundred wells were drilled in the Mesilla Valley. Many wells were also drilled during a shortage of surface water from 1963 to 1966. As of 1975, there were about 920 usable irrigation wells in the Mesilla Valley (C.A. Wilson, oral commun., 1979). The irrigation wells, mostly about 100 feet deep, were completed primarily in the flood-plain alluvial aquifer. However, after 1975, a large number of irrigation wells were drilled deeper in order to obtain water of better quality than that available from shallow wells (Wilson and White, 1984). In Doña Ana County in 1979, 86,660 acres were irrigated with both surface and ground water and 9,070 acres with ground water only (Lansford and others, 1980, p. 5). Major crops (in order of total acreage planted) are: cotton, pecans, alfalfa, cereal grains, and vegetables (primarily chile, lettuce, and onions). The number of irrigated acres in Mesilla Valley has increased from about 25,000 acres at about the turn of the century to about 77,000 acres during 1940–75 (fig. 6)—the latter figure is about two-thirds of the area of the valley. Much of the West Mesa area, where there are scattered stock and domestic wells, is used for grazing.

Historical irrigation practices have effectively used the ground-water system as a reservoir in a combined stream-aquifer system. During years of plentiful surface water, most irrigation water is diverted from the Rio Grande. About one-third of applied irrigation water may replenish the ground-water system (Blaney and Hanson, 1965, p. 28). Some ground water seeps into drains that discharge to the Rio Grande. During years of inadequate surface-water supply, the shortfall is made up from ground water, causing lower than usual ground-water levels and diminished drain discharge. Ground-water levels generally return to normal after an irrigation season when surface water is plentiful.

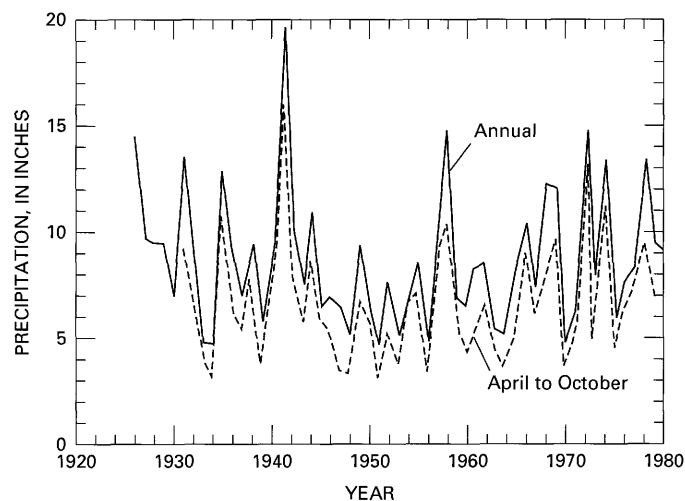


FIGURE 5.—Annual and April-to-October precipitation at New Mexico State University, near Las Cruces, and at La Tuna, near Anthony, 1926–80. Values for 1926–43 are for New Mexico State University station only. Values for 1944–80 are an average of the two stations. Data from U.S. Department of Agriculture and U.S. Department of Commerce.

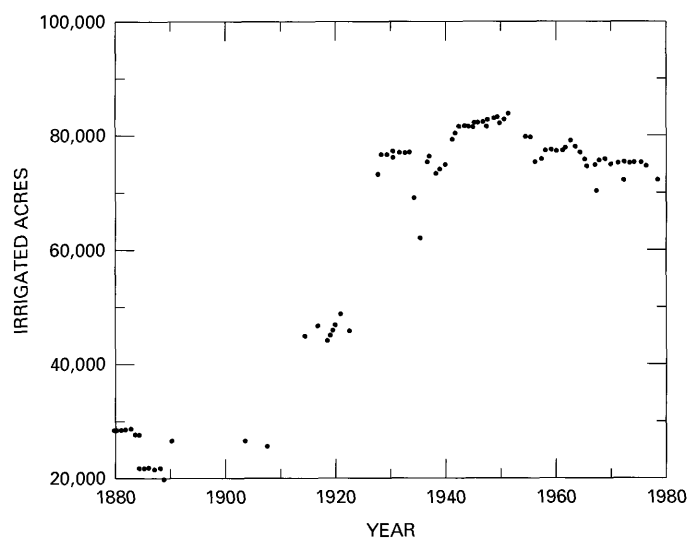


FIGURE 6.—Number of irrigated acres in the Mesilla Valley, 1880–1980. Sources of data: 1880–1905, Yeo (1928); 1906–17 and 1930–46, Conover (1954); 1917–24, Josephine Derryberry (U.S. Bureau of Reclamation, oral commun., 1982); 1925–29, Debler (1932); 1947–75, Wilson and others (1981); 1976–78, Roger Patterson (U.S. Bureau of Reclamation, written commun., 1983).

SURFACE-WATER SYSTEM

The surface-water system is comprised of the Rio Grande and its tributaries, a distribution system of canals and laterals, and drains that return water to the Rio Grande. The main features of the surface-water system are shown on plate 1.

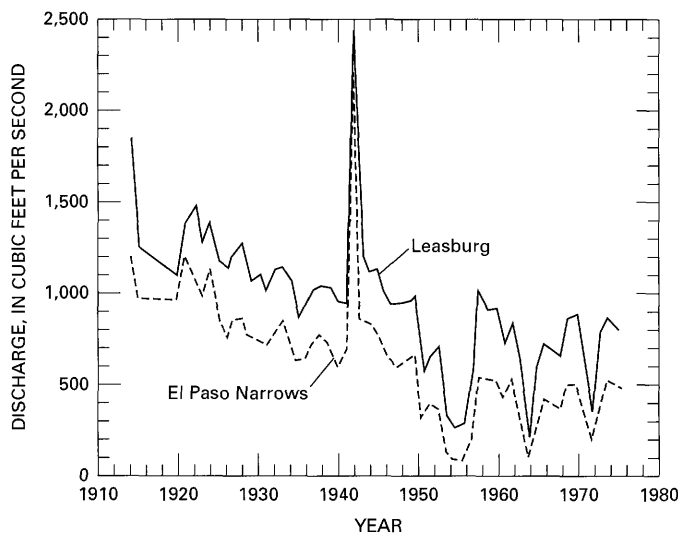


FIGURE 7.—Annual discharge of the Rio Grande at Leasburg and El Paso Narrows, 1912–75. Data for 1912–29 for Leasburg from U.S. Bureau of Reclamation records. Data for 1912–29 for El Paso Narrows from U.S. Department of State (no date). Data for 1930–46 from Conover (1954). Data for 1947–75 from Wilson and others (1981).

The Rio Grande is the primary surface-water feature in the Mesilla Basin. Rio Grande water is stored in Elephant Butte Reservoir, about 75 miles upstream from Leasburg Dam, and in Caballo Reservoir, about 45 miles upstream from Leasburg Dam, as well as in several dams farther upstream. The discharge of the Rio Grande in the Mesilla Valley is regulated by releases of water from Caballo Reservoir that are replaced by releases from Elephant Butte Reservoir. Prior to the first releases from Elephant Butte Reservoir in 1915, discharge in the Rio Grande was not regulated and often ceased for months at a time (Conover, 1954, p. 16, 53). Annual discharges of the Rio Grande passing Leasburg and El Paso Narrows are shown in figure 7.

Arroyos (ephemeral streams with straight-walled, flat-bottomed channels) that are tributary to the Rio Grande include Alameda, Tortugas, Fillmore, Peña Blanca, Mossman, and Vado Arroyos (pl. 1). The arroyos flow only in response to intense rainfall. Those on the east side of the basin drain the Organ and Franklin Mountains. The arroyos directly east of Las Cruces cross the southern end of the Jornada del Muerto structural basin before entering the Mesilla Basin. Several of the large arroyos are blocked by retention dams east of Interstate 25, and the others that reach the valley probably do not contribute much surface discharge to the Rio Grande. Small arroyos drain the eastern slopes of the Robledo Mountains and the western slope of Mesilla Valley.

The Mesilla Valley contains a network of canals and laterals that deliver river water to fields (pl. 1). Small canals were dug in 1841, and the system was expanded after 1848. Improvements in the system were made after about 1890; in 1897, there were five main canals, all north of Chamberino (Barker, 1898, p. 10–12). Leasburg Diversion Dam was built in 1908 (Conover, 1954, p. 53), and Mesilla Diversion Dam was built in 1916, by which time the canal system extended the entire length of the valley. Diversions from the Rio Grande are at Leasburg and Mesilla. Water at Leasburg Diversion Dam either continues down the river or is diverted into the Leasburg Canal for distribution to laterals in the northern part of the Mesilla Valley. At Mesilla Diversion Dam, about 6 miles south of Las Cruces, Rio Grande water is diverted into the West Side or East Side Canals or continues down the river channel. Data on the distribution of diversions for 1930–77 have been compiled from Bureau of Reclamation records by Conover (1954, p. 138) and Wilson and others (1981, p. 506–508). Some of the diverted water is returned as surface flow to the river during normal operation of the distribution system. Net diversions (the amount diverted minus the amount returned to the river) are shown in figure 8.

Depletions (the flow passing Leasburg minus the flow passing El Paso Narrows) and depletions as a percentage of net diversions also are shown in figure 8. The percentage was nearly constant during 1930–50. After 1950, the percentage increased and became more variable. However, the average annual depletion has not changed greatly over the years. The depletion was

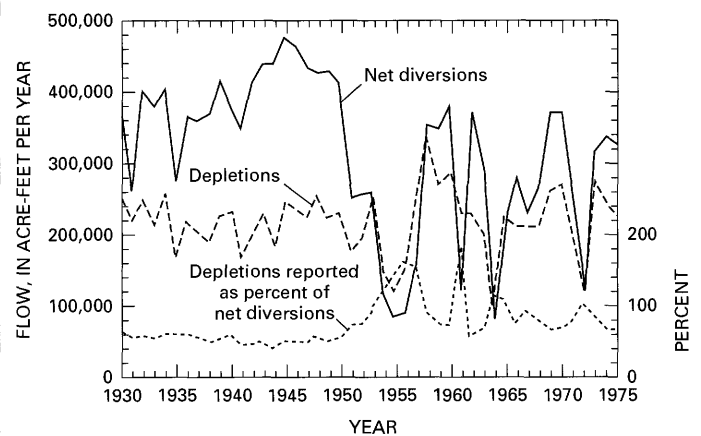


FIGURE 8.—Net diversions and depletions in the Mesilla Valley, 1930–75. Net diversions were estimated from data given by Conover (1954) and Wilson and others (1981). Depletions were estimated as discharge at Leasburg less discharge at El Paso Narrows.

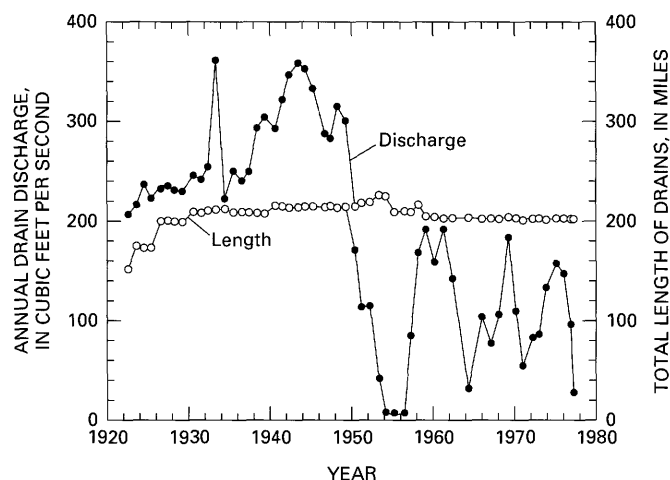


FIGURE 9.—Annual drain discharge and total length of drains upstream from gaging stations in the Mesilla Valley, 1923–79. Drain discharges do not include discharges that were measured twice (such as from Mesilla and Leasburg Drains, which discharge to Del Rio Drain, and from West and Nemexas Drains, which have discharged into Montoya Drain since the mid-1930's). Data are from records at the U.S. Bureau of Reclamation.

222,000 acre-feet per year during 1930–50, 221,000 acre-feet during 1951–60, 218,000 acre-feet during 1961–75, and 221,000 acre-feet overall during 1930–75.

Drains have been constructed to keep the water table below the level of the irrigated fields. The need for drains arose by 1917 after the number of irrigated acres nearly doubled (fig. 6) during the previous 10 years (Conover, 1954, p. 53–56). By summer 1919, approximately 75 miles of drains existed (Conover, 1954, pl. 6). The drainage system was completed in the mid-1920's. The locations of drains and sites for measuring drain discharges are shown on plate 1. The total length of drains is shown in figure 9.

Drain discharge is directly related to the altitude of the water table, which in turn, mainly is related to the amount and seasonal distribution of surface water, irrigation, and ground-water withdrawals. The water-level contours on plate 1 approximate the water table but do not show details in the immediate vicinities of drains, canals, or the Rio Grande. The sum of the average annual drain discharges for all stations is shown in figure 9. The average discharge for 1923–50 was 1.4 cubic feet per second per mile of drain. Since 1950, due to a lower water table, drain discharges have been uneven and intermittent.

The annual evaporation was estimated to be 5.5 feet per year from open water, which is approximately 0.7 times the annual pan evaporation of 7.8 feet per year (Harbeck and others, 1958, p. 52). Evaporation from canal surfaces was estimated to be 4,000 acre-feet per

year (5.5 feet times four canals, each 25 feet wide, running the length of the 60-mile-long valley). The evaporation from drains was assumed to be approximately the same as from canals. Evaporation from the inner, deeper part of the river channel was estimated to be 12,000 acre-feet per year (5.5 feet times the river surface area—assumed to be 300 feet wide by 60 miles long). The widths of the drains and river were estimated to include evapotranspiration from wet soil and adjacent vegetation.

GEOHYDROLOGY

The ground-water system is controlled by geologic boundaries, internal geology of the basin, and the interrelation of ground and surface waters. A brief review of the geology is presented here in the order of the oldest to the youngest rocks. More detailed descriptions of the geology have been given by Ruhe (1967), Hawley and Kottlowski (1969), Hawley and others (1969), King and others (1971), Lovejoy and Hawley (1978), Wilson and others (1981), and other authors referenced in this section.

GEOLOGIC UNITS AND THEIR WATER-BEARING PROPERTIES

A generalized geologic map of the Mesilla Basin is shown in figure 10. The major geologic units mapped are: (1) Pre-Santa Fe Group rocks, including Precambrian through lower Tertiary rocks; (2) Santa Fe Group, consisting of upper Tertiary and Quaternary sedimentary deposits; (3) Quaternary basalt flows and cones that generally postdate the Santa Fe Group; (4) Quaternary alluvial, eolian, and lacustrine deposits that form a thin, discontinuous cover on the Santa Fe Group; and (5) Quaternary alluvium, primarily Rio Grande flood-plain deposits in the Mesilla Valley. The near-surface deposits, except for the flood-plain alluvium, are above the water table. The Santa Fe Group and the flood-plain alluvium constitute the major aquifer and together are referred to as "basin-fill deposits" in this report. The older, generally consolidated rocks form the bottom and side boundaries of the basin and are referred to as "bedrock" (fig. 11).

The geohydrologic properties of the consolidated rocks that crop out in the area have been discussed by Dinwiddie (1967), Titus (1967), King and Hawley (1975), and Wilson and others (1981). The stratigraphy, lithology, and geologic history of the Santa Fe Group and younger units were described by Hawley and others (1969), Seager and others (1971), Hawley

SOUTHWEST ALLUVIAL BASINS RASA PROJECT

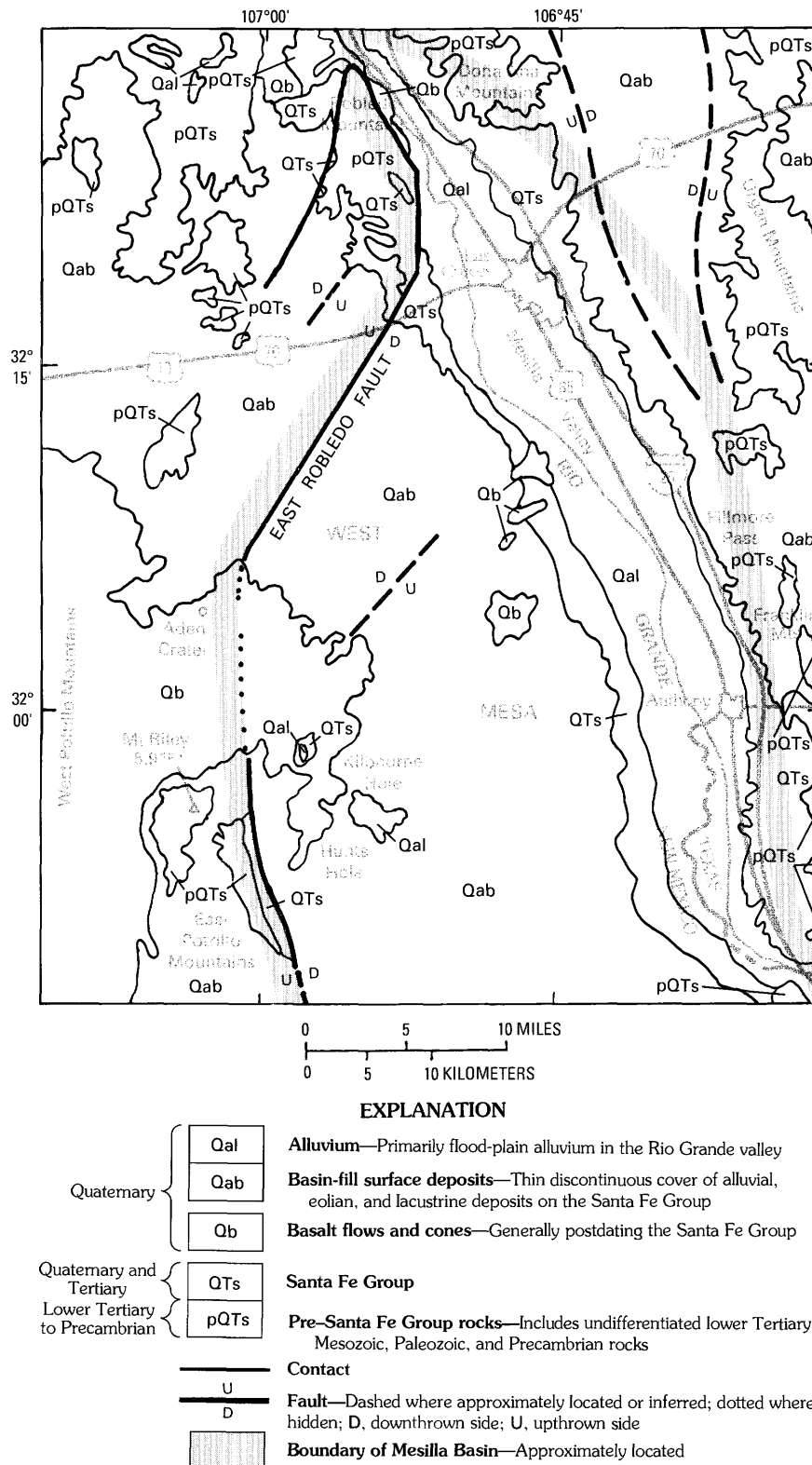
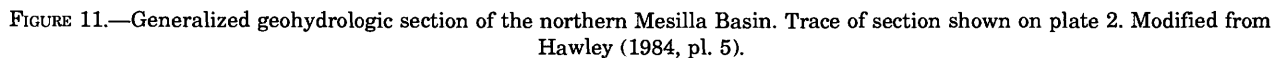


FIGURE 10.—General geology of the Mesilla Basin and adjacent areas (modified from Wilson and others, 1981).



and Picacho Peak also contain igneous rock. These igneous and metamorphic rocks may yield small quantities of water in places where they are weathered or fractured.

PALEOZOIC AND MESOZOIC SEDIMENTARY ROCKS

Consolidated, locally folded sedimentary rocks of Paleozoic and Cretaceous age occur in uplifts and beneath the basin-fill sediments in some parts of the study area. The Paleozoic rocks consist mainly of limestone and dolomite (with some shale and quartzite to quartzite conglomerate in the Cambrian and Devonian strata) and intertongued gypsum and sandstone

to siltstone in Upper Pennsylvanian to Permian rocks (King and Hawley, 1975). Most of the San Andres and Robledo Mountains is composed of rocks of Upper Cambrian(?) through Permian age (Kottlowski, 1975).

The primary permeability is small in all of the rock units discussed above. However, secondary permeability may result from weathered zones, dissolution of limestone and gypsum, or from joints, fractures, or faults, such as along the piedmont slope of the Franklin Mountains. The permeability of these rocks is thought to be several orders of magnitude smaller than that of the basin fill and is considered to be insignificant with regard to the basin-fill ground-water system. However, secondary permeability may be large in places, accounting for minor amounts of underflow of substantially different chemical composition.

LOWER TERTIARY SEDIMENTARY AND VOLCANIC ROCKS

The lowermost Tertiary unit is the Love Ranch Formation of Kottlowski and others (1956). It mainly crops out in the Rincon Hills and on San Diego Mountain to the north of the Mesilla Basin; it consists of conglomerate derived from Paleozoic limestone with some sandstone and mudstone. The Love Ranch Formation is overlain by the Palm Park Formation of Kelley and Silver (1952), which is composed of andesite-boulder tuff breccia; volcanically derived, moderately consolidated sandstone, mudstone, and conglomerate; plus spring deposits (travertine) (Seager and others, 1971, p. 6). The Palm Park Formation mainly crops out north of the study area in the western Selden Hills, Rincon Hills, and the southern Caballo Mountains. The Bell Top Formation of Kottlowski (1953) and the Thurman Formation of Kelley and Silver (1952), which are separated from the underlying Palm Park Formation by an unconformity, contain ash-flow tuffs, tuffaceous sediments, and some basaltic andesite flows. Volcanic rocks and interbedded clastic sedimentary rocks of mainly Eocene to Miocene age (including some of the above formations) form most of the Doña Ana Mountains, the southern Organ Mountains, and Picacho Peak. Some or all of these units probably underlie the Santa Fe Group in most parts of the Mesilla Basin.

There has not been much exploration for ground water in the areas of igneous rock and interbedded sedimentary rock. The amount of consolidation is variable according to rock type, but all rock types generally have small permeability (King and Hawley, 1975, p. 195-196). Conover (1954, p. 29) and Wilson and others (1981, p. 22-26) reported that a few stock wells obtain small quantities of water from these units. King and Hawley (1975, p. 197) mentioned a well

(21S.3E.4.211) near the southern San Andres Mountains that penetrates about 550 feet of rhyolite and interbedded sedimentary rock below the water table and produces less than 50 gallons per minute.

SANTA FE GROUP

The Santa Fe Group of Tertiary and Quaternary age is a rock-stratigraphic unit that is classified mainly on the basis of lithology and depositional environment rather than on fossils or time boundaries. The Santa Fe Group consists of unconsolidated to moderately consolidated sedimentary deposits, minor ash-fall volcanics, and some volcanic rocks. In the study area, the lower limit of the Santa Fe Group generally is placed above the middle Tertiary (Oligocene) igneous rocks and associated sedimentary rocks. The upper limit is placed at the surfaces of the youngest basin-fill deposits that predate initial entrenchment of the present Rio Grande valley in middle Pleistocene time. These surfaces include the Jornada del Muerto, West Mesa, and Doña Ana geomorphic surfaces (Weir, 1965; King and others, 1971).

The Santa Fe Group was deposited as the Mesilla Basin subsided relative to the bordering upland areas (fig. 11) during development of the Rio Grande rift. The early stages of basin filling were marked by closed, intermontane basin (bolson) environments. The sediments include a variety of alluvial-fan, coalescent-fan, and piedmont deposits around the basin margins that grade into or intertongue with fine-grained lacustrine and alluvial basin-floor deposits (King and others, 1971; Hawley, 1984). (The term "basin floor" is used to describe the relatively flat land surface over the middle of the basin and should not be confused with the lower boundary of the ground-water basin.) The greater percentages of fine-grained sediment in the lower part of the Santa Fe Group and toward the southern end of the Mesilla Basin imply smaller permeability in the deep parts of the basin and in the southern part of the West Mesa (Hawley, 1984). The ancestral Rio Grande through the Mesilla Basin probably developed in Pliocene time (Hawley, 1975, p. 146). Medium- to coarse-grained fluvial facies, with small amounts of fine-grained sediment, were deposited in the central part of the basin by axial streams, whereas alluvial-fan facies continued to be deposited at the margins. The surface of the West Mesa represents the highest level of basin fill deposited by distributaries of the ancestral Rio Grande prior to the start of downcutting of the present Rio Grande valley (Mesilla Valley) that began in the later part of middle Pleistocene time (Hawley, 1975, p. 146). An ancestral Rio Grande probably flowed through Fillmore Pass into the Tularosa and Hueco

Basins during the late Pliocene to early Pleistocene (Belcher, 1975, p. 46-49).

The lower part of the Santa Fe Group is not exposed in the Mesilla Basin, but as much as 3,500 feet of it is exposed in the Palomas Basin immediately to the north. Three units, from oldest to youngest, have been recognized within the lower part of the Santa Fe Group in the vicinity of the Mesilla Basin (fig. 12): an unnamed transitional unit composed mainly of conglomerate and sandstone; the Hayner Ranch Formation of Seager and others (1971), composed of conglomerate, sandstone, and volcanic-derived sediment; and the Rincon Valley Formation of Seager and others (1971), composed mainly of red clay plus some gypsum beds and thin sand layers.

The lower part of the Santa Fe Group is overlain by the Fort Hancock Formation, which, in turn, is overlain by or interfingers with the Camp Rice Formation of Strain (1966, 1969). These formations comprise the upper part of the Santa Fe Group.

The Fort Hancock Formation (Strain, 1966), exposed in the valley slopes at the southern end of the Mesilla Valley, is composed of alternating sands and lacustrine clays. The formation probably was deposited in a deltaic-lacustrine environment near the mouth of the ancestral Rio Grande in the middle to southern parts of the basin (King and Hawley, 1975, p. 201).

The Camp Rice Formation (Strain, 1966) contains fluvial-facies sediment composed of sand with lenses of gravel, silt, clay, and sandy clay; it also contains alluvial-fan facies sediment composed of sand, gravel, silt, and clay. The fluvial facies is the most extensive and contains most of the freshwater in the basin (Wilson and others, 1981, p. 38). Both facies and their intertonguing relation to each other are visible in the side slopes of the Mesilla Valley.

The distribution of facies of the Camp Rice Formation is not known in detail, but some information is available. King and others (1971, p. 20) reported that Las Cruces city wells produce from intertongued sand and gravel of the alluvial-fan and fluvial facies that contain only minor amounts of silt and clay. New Mexico State University wells are completed in both the fluvial and alluvial-fan facies. The Camp Rice Formation, on the eastern side of Mesilla Valley from about Mesquite to south of Anthony, consists of sandy clay and clay instead of proportionately more sand than clay, as is typically found beneath the center and western side of the Mesilla Valley (Wilson and others, 1981, p. 39).

J.W. Hawley (New Mexico Bureau of Mines and Mineral Resources, oral commun., 1983) reported that the ASARCO well (25S.01E.16.114) may penetrate more than 1,600 feet of the Camp Rice Formation.

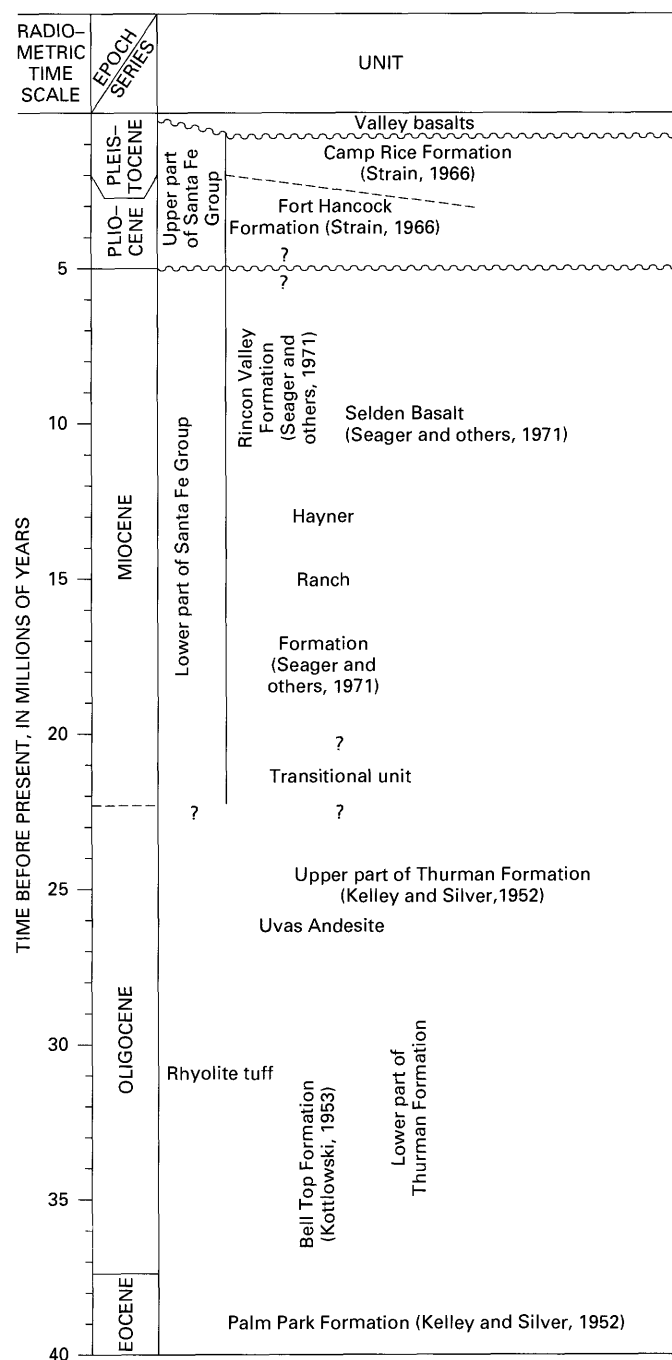


FIGURE 12.—Stratigraphic column of the Santa Fe Group in the Mesilla Basin and adjacent areas. Modified from Hawley (1978, p. 239).

Wilson and others (1981, p. 38) reported more than 1,300 feet of Camp Rice at test hole 23S.1E.13.411 in Las Cruces and 1,932 feet in test hole 25S.2E.3.244 near Mesquite. Wells generally do not produce water from the full thickness of the aquifer.

A City of El Paso well field that extends several miles northward from the town of Cañutillo (pl. 1) produces

water from three production zones described by Leggat and others (1962). The shallow production zone is primarily comprised of flood-plain alluvium to a depth of at least 90 feet (although the production zone extends into the Santa Fe Group to depths of 150–200 feet). The medium-depth production zone (all within the Santa Fe Group) contains alternating beds of sand to sand and gravel (similar to fluvial-facies sediment) and clay to sandy clay (similar to clay-facies material from the Palomas and Rincon Valleys) (King and others, 1971, p. 21). The medium zone is 160–450 feet thick. The deep production zone (all within the Santa Fe Group) consists of a uniform, fine-grained, brown sand with almost no clay and is 500 to possibly more than 1,000 feet thick (Leggat and others, 1962, p. 10–13). In general, the intervals below land surface occupied by each production zone are 0–200 feet for the shallow zone, 200–600 feet for the medium zone, and 600–1,350 feet for the deep zone. The characteristically fine grained sand of the deep production zone at the Cañutillo well field has not been recognized west of the flood plain or north of Berino (J.W. Hawley, New Mexico Bureau of Mines and Mineral Resources, oral commun., 1981).

The Santa Fe Group occurs beneath and to the west of the valley. It apparently decreases from about 3,800 feet in thickness in the downfaulted block between the East Robledo and Fitzgerald faults (pl. 2) to about 1,100 feet near the International Boundary about 40 miles to the south. The thickness of basin fill (pl. 2) was determined from data from deep wells, gravity profiles (Birch, 1980), a seismic profile (Hans Ackermann, written commun., 1980), and vertical electrical-resistivity sounding profiles (Wilson and others, 1981, pl. 2).

A study of well logs by King and others (1971) showed a progressive decrease in grain size from north to south and few, coarse, gravelly zones for the upper 1,330 feet of basin fill—however, the sediments appear to have very good potential for development of ground water according to King and Hawley (1975, p. 201). A decrease in hydraulic conductivity from north to south is not indicated by aquifer-test data from the three West Mesa wells listed by Wilson and others (1981, table 3). The general decrease in grain size probably represents an increase in the percentage of clayey layers or lenses to the south.

Significant amounts of interbedded volcanics in the upper part of the Santa Fe Group are not indicated by drillers' logs. An exception is the apparent subsurface intertonguing of Quaternary basalts with sediments of the upper part of the Santa Fe Group on West Mesa near sec. 31, T. 23 S., R. 1 W. and near sec. 16, T. 26 S.,

R. 1 W. These basalts appear to be above the water table.

Values of hydraulic conductivity for the Santa Fe Group were estimated from values of transmissivity reported by Wilson and others (1981, table 3) for specified intervals within each well. For this study, each hydraulic conductivity was estimated by dividing the transmissivity by the length of the interval tested. This method of estimating hydraulic conductivity yields apparent values that generally are greater than actual values because two-dimensional radial flow is assumed—if a short interval of a very thick aquifer is tested, three-dimensional flow probably occurs. Another reason for large estimates of conductivity may be the selection of the sandiest zones for testing (R.R. White, oral commun., 1984). Several such tests were conducted at various depths at many of the sites (pl. 3).

Variability of hydraulic conductivity with depth is apparent on plate 3 as well as in figure 13. The tests of intervals less than 600 feet below the water table yielded values of hydraulic conductivity that generally were about four times as great as those from tests of deeper intervals. Physical difficulties of testing tend to increase with depth. Such difficulties might be caused, for example, by a limitation of air-compressor capacity in an airlifting test and might be the source of an apparent decrease in hydraulic conductivity with depth. Nevertheless, the values in table 1 (tables are in the back of the report) were judged to be acceptable estimates. The median value was 22 feet per day for intervals shallower than 600 feet and 5 feet per day for deeper intervals. For the same intervals, the upper quartile was 43 and 14 feet per day, and the lower quartile was 9 and 2 feet per day.

POST-SANTA FE GROUP DEPOSITS

After deposition of the Santa Fe Group, there were three major episodes of incision of the Rio Grande, each followed by partial backfilling of alluvium. Thin alluvial and eolian deposits (generally less than 25 feet thick) cover much of the West Mesa surface, and alluvial deposits are present on the piedmont slopes adjacent to upland areas (Hawley, 1975, p. 147). Of these deposits, only the youngest alluvial-fill sequence, consisting of the flood-plain alluvium (figs. 10 and 11) of the Rio Grande as well as interfingering alluvial-fan deposits of tributary arroyos, constitutes an aquifer. The other deposits all "appear * * * to be above the water table" (King and Hawley, 1975, p. 202). The Rio Grande flood-plain alluvium, generally about 80 feet thick, has a thick basal channel sand and gravel unit overlain by finer grained, sand-to-clay flood-plain deposits (King and Hawley, 1975, p. 202). The alluvium

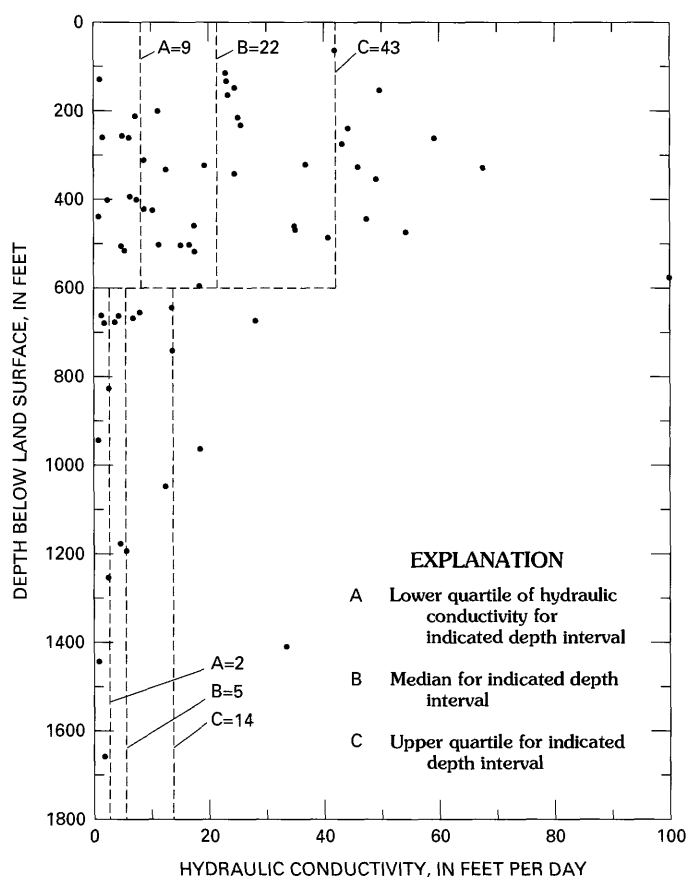


FIGURE 13.—Distribution of hydraulic conductivity with depth for the Santa Fe Group.

generally is very permeable. Values of hydraulic conductivity estimated from specific capacities of irrigation wells were 200 or more feet per day in places.

Most irrigation wells in the valley are from 70 to 200 feet deep (Wilson and others, 1981, table 2), and many obtain water from both the flood-plain alluvium and the underlying Santa Fe Group (King and Hawley, 1975, p. 202). The open interval of most irrigation wells is not known, but Wilson and others (1981, p. 82) described the construction of irrigation wells generally as having slotted casing "from several tens of feet below the water table to the bottom of the hole."

The hydraulic conductivity (pl. 4) of the shallow part of the aquifer in the Mesilla Valley (in flood-plain alluvium and upper part of the Santa Fe Group) was estimated by analysis of the specific capacities of 72 shallow wells described by Wilson and others (1981, table 2). The wells ranged in depth from 65 to 350 feet with a median depth of 133 feet. The bottoms of most of the wells probably were in the Santa Fe Group. The specific capacities of these wells ranged from 10 to about 200 gallons per minute per foot of drawdown and had a median value of 50 gallons per minute per foot.

The hydraulic conductivity, in feet per day, of the saturated interval of the aquifer penetrated by each well was estimated to be 170 times the specific capacity divided by the interval of the well (in feet) open to the aquifer. The conversion factor is from Walton (1962, fig. 6) and is based on the assumptions of an 8-hour test duration (Wilson and others, 1981, p. 43) and the occurrence of unconfined conditions. The conversion factor could have been as small as 133 for a median specific-capacity well if a test duration of 1 hour had been assumed or as large as 186 if a 24-hour test duration had been assumed (Walton, 1962, figs. 4 and 5).

The interval of the well open to the aquifer was assumed to be either (a) the entire distance between the water table and the bottom of the well, or (b) 80 percent of that distance. Assumption (a) probably overestimates the length of well open to the aquifer, especially in the case of the deep wells, and, thus, may cause estimates of hydraulic conductivity to be too small. Assumption (b) might be more consistent with the construction of the wells in that they are not entirely open to the aquifer. However, that assumption does not account for three-dimensional radial flow (due to some vertical flow within the aquifer toward the well openings) and may cause estimates of hydraulic conductivity to be too great. Estimates of hydraulic conductivity shown in figure 14 and table 2 were estimated using assumption (a).

The harmonic mean (50 feet per day) of the estimates of hydraulic conductivity (fig. 14) may be an appropriate value for the overall basinwide hydraulic conductivity, but the arithmetic mean (93 feet per day) may also be a reasonable value. If the harmonic mean, derived using assumption (a), were reduced by the factor 133/170 (accounting for the possibility that the tests were shorter than assumed), the resulting value of 40 feet per day would be a reasonable minimum. If the greater arithmetic mean, derived using assumption (b), were increased by the factor 187/170 (accounting for the possibility that the tests were longer than assumed), the resulting value of 130 feet per day would be a reasonable maximum.

The western part of the West Mesa surface is capped by the extensive Potrillo basalt field of Quaternary age (Hoffer, 1976). The eastern part of the basalt flows, in the areas of Kilbourne Hole and Hunt's Hole, overlies Santa Fe Group sediments, but the volcanic rocks of the West Potrillo Mountains may be underlain by Tertiary and older bedrock units (King and others, 1971, p. 23). On the eastern side of the West Mesa, adjacent to the central Mesilla Valley, the Santo Tomas-Black Mountain basalts (Hoffer, 1971) are present. In total, basalt flows cover an area of at least

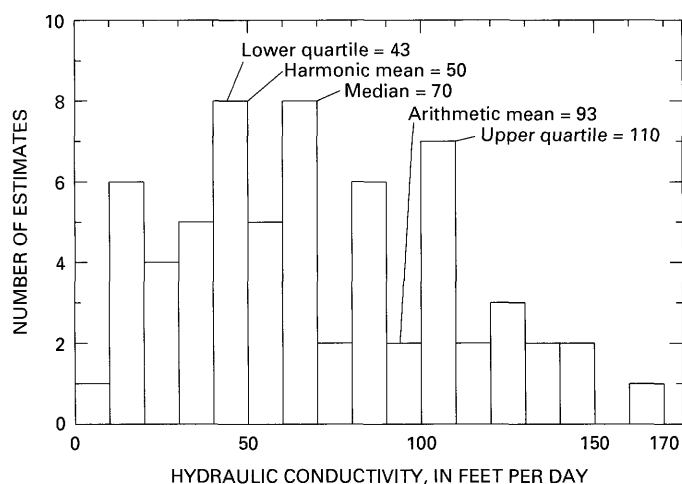


FIGURE 14.—Frequency distribution of hydraulic-conductivity estimates for the shallow part of the aquifer in the Mesilla Valley. Perforated intervals in wells ranged from 0 to 200 feet below the water table. Of 72 values, 8 values were between 170 and 440 and are not shown. The means, quartiles, and median are for all 72 values. These estimates were made assuming unconfined conditions. Estimated values would have been greater if confined conditions were assumed.

350 square miles. The effect of these surfaces on ground-water recharge was not studied.

Approximately 15 wells in the basalt-flow region are shown on a water-table map by King and others (1971, pl. 1). Some of the wells obtain water from the underlying Santa Fe Group, whereas others that are close to the center of the West Potrillo Mountains may obtain water from Tertiary volcanics. There is little subsurface information available for this region.

GROUND-WATER FLOW SYSTEM

The base and lateral boundaries of the ground-water flow system are considered to coincide with the bedrock-Santa Fe Group contact because of the permeability contrast between the two. However, the thickness of the Santa Fe Group throughout the vicinity of the study area is highly variable. Therefore, the perimeter, or farthest lateral extent of the ground-water basin, was defined to be the smaller area shown in figure 4. The perimeter, for the most part, follows structural boundaries. Some ground-water underflow almost certainly crosses these boundaries. Such water probably affects the quality of ground water around the perimeter of the basin and at great depth, but the quantity probably is very small compared to the quantity involved in the interaction with surface waters near the axis of the basin.

Bedrock of the Robledo Mountains, Selden Canyon, and the Doña Ana Mountains bounds most of the

northern end of the basin. There is probably only a small amount of underflow in Selden Canyon due to the small cross-sectional area of the flood-plain alluvium. Because a ground-water divide exists between the Rough and Ready Hills and the Robledo Mountains, most ground water beneath Faulkner Canyon (pl. 1) flows northward and does not enter the Mesilla Basin as underflow (King and others, 1971, pl. 1).

The East Robledo fault forms a significant hydrologic boundary. North of the East Robledo fault, which extends from the east side of Picacho Peak southwestward across the West Mesa (pl. 2), the thickness of the Santa Fe Group (mainly fine-grained sediments) generally is less than 500 feet (King and others, 1971, p. 41-42; Thompson and Bieberman, 1975, p. 171). Wells in this area, most of which penetrate rock older than the Santa Fe Group, generally have small yields (several gallons per minute). An exception is a reported yield of several hundred gallons per minute from sand and gravel in the Santa Fe Group in well 23S.2W.13.111, which is in a small graben.

The northeast border of the ground-water flow system is formed by a bedrock high (primarily andesite, rhyolite, and limestone) that extends from the Doña Ana Mountains through Goat Mountain, Tortugas Mountain, and Bishop Cap Mountain. The irregular surface of the bedrock high between these hills is buried by alluvium of varying thickness, although the saturated thickness generally is small. The valley fill above the Lower Permian Hueco Limestone in the Snowden and Clary State No. 1 (oil-test) well (about 1 mile south of Tortugas Mountain) is about 530 feet thick (Thompson and Bieberman, 1975, p. 173). A 1,000-foot-deep well (22S.2E.21.131) that is 1½ miles south of Goat Mountain penetrates about 500 feet of alluvium, the bottom 30 feet of which are saturated. The well produces only 1 gallon per minute (Wilson and others, 1981, p. 40). The basin fill east of the bedrock high is as much as 2,500 feet thick. There, the basin fill is part of the Jornada del Muerto structural basin, which may end about 6 miles south of Highway 70, where probable volcanic rock was found at a depth of 275 feet (King and Hawley, 1975, p. 198). Buried bedrock ridges extend toward the valley in some locations. For example, rhyolite was penetrated at a depth of 284 feet in a well (22S.2E.30.123) 1 mile east of the flood plain (Wilson and others, 1981, p. 40). The bedrock barrier causes water levels on the east to be higher than those on the west. A ground-water divide may exist in the southern Jornada del Muerto structural basin between the Doña Ana and Organ Mountains (Wilson and others, 1981, pl. 9). The bedrock probably is not a continuous barrier (King and

others, 1971, p. 59), and a small amount of ground water moves from the southern Jornada del Muerto Basin westward into the Mesilla Basin (Wilson and others, 1981, p. 2).

A broad ground-water divide may exist in Fillmore Pass between the Organ Mountains and Franklin Mountains. The direction of ground-water movement in the pass is uncertain.

The eastern boundary of the ground-water flow system for the southern Mesilla Valley is approximately at the western base of the Franklin Mountains. Runoff from the mountains enters the alluvium and becomes a source of recharge to the ground-water system.

The southern end of the Mesilla Valley is bounded by bedrock at El Paso Narrows. The Rio Grande passes through the Narrows. Underflow in the flood-plain alluvium is only about 0.1 cubic foot per second (Slichter, 1905, p. 9–13).

The part of the structural basin beneath West Mesa may continue southward into Mexico for at least 12 miles (Woodward and others, 1978). A basin-fill thickness map drawn from interpretation of gravity data by Wen (1983) shows the structural basin extending about 7 miles south of the International Boundary west of the Sierra Juarez. However, the Santa Fe Group possibly extends as much as 75 miles southward (King and others, 1971, p. 22). Because ground-water flow apparently is mainly parallel to the International Boundary (King and others, 1971, pl. 1; Wilson and others, 1981, pl. 9), a precise determination of the location of the structural boundary may not be critical for a hydrologic analysis of the Mesilla Basin.

The western boundary of the basin is formed by the East Potrillo Mountains, West Potrillo Mountains, Aden Hills, and Sleeping Lady Hills. There is an inferred ground-water divide through the center of these areas of consolidated rock (King and others, 1971, pl. 1). A few wells are in or adjacent to the mountain areas, so the boundary may not be completely impermeable. In addition, some ground water flows toward the basin through the gap between the West Potrillo Mountains and the Aden Hills (King and others, 1971, p. 59) and probably flows toward the basin between the Aden Hills and the Sleeping Lady Hills (Conover, 1954, p. 31). The alluvium in these two areas apparently is shallow, and the amount of water moving through the areas probably is not great. The thickness of the Santa Fe Group is much greater on the southeastern side of the East Robledo fault.

The lower boundary of the ground-water flow system is considered to be the contact between the Santa Fe Group basin-fill sediment and the generally more

consolidated underlying bedrock (pl. 2). In some places, the pre-Santa Fe rocks are slightly to moderately consolidated, but they generally are poorly sorted and have small hydraulic conductivity (R.G. Myers, oral commun., 1985). The maximum thickness of the Santa Fe Group in the Mesilla Basin apparently is about 3,800 feet (King and others, 1971, p. 22); this is present in the Boles No. 1 Federal well (24S.01E.07.440), about 4 miles west of Mesilla Dam. The thickness is less on the south side of the Fitzgerald fault. The Santa Fe Group wedges out against bedrock in the Anapra area and against the East Potrillo Mountains and the Aden and Sleeping Lady Hills (King and others, 1971, p. 22).

The definition of the ground-water basin (fig. 4) does not preclude a small amount of water entering the basin from bedrock at depth. Water levels tend to be higher in the highlands surrounding the Mesilla Basin than those within the basin (King and others, 1971, pl. 1). The amount of such flows would be approximately proportional to the gradient in the hydraulic-head potential between the highlands and the basin area along the flow path, the hydraulic conductivity of the material along the flow path, and the cross-sectional area of the flow path (Darcy's Law). For example, most of the flow would follow path X in figure 11 through the more conductive Santa Fe Group. Less flow would take path Y through the bedrock, depending largely on the ratio of hydraulic conductance between the Santa Fe Group and bedrock. Similarly, even less flow would follow path Z (a still deeper and longer path). Paths X, Y, and Z are examples of an infinite number of stream lines that would be subparallel to each other. The amount of underflow from the highland areas around the periphery of the basin is most likely limited to no more than the amount of recharge in the highland areas. However, it is possible for water to follow a very deep path from areas where a regional divide is more distant than a water-table divide in the shallow rocks.

The approximate direction of the horizontal component of ground-water movement can be inferred from the water-level contour map (pl. 1). The map, modified from Wilson and others (1981, pl. 9), was constructed using January 1976 water-level data; some older data were used in upland areas.

The general direction of movement of ground water in the Mesilla Basin is southeastward. Ground water probably moves southward away from the Mesilla Valley near Las Cruces and back toward the valley in the southern part of the basin—this is consistent with hydraulic conductivity being greater in the Santa Fe Group than in underlying rocks. Ground water probably also moves vertically downward from the valley in the north. Upward movement of water in the southern end of the valley was indicated by increasing hydraulic

head with depth (Leggat and others, 1962, p. 16). Upward flow probably persists except as altered by ground-water withdrawals.

The water-table gradient beneath the West Mesa averages about 4.5 feet per mile: approximately the same as in the Mesilla Valley. Near the edges of the Mesilla Basin, water flows into the basin from the surrounding highlands, and the water-table gradient is steeper in those places due to thinner aquifers and possibly lower permeability. Near the East Robledo fault, where the transmissivity of the basin fill changes greatly, it might be expected that the water-table contours would have a kink in them as shown by the dashed and queried 3,840-, 3,860-, and 3,880-foot contours on plate 1.

Ground water moves horizontally toward well fields at Las Cruces and Cañutillo from surrounding areas. The indistinct cone of depression in the Cañutillo area (pl. 1) indicates that a large part of water pumped from the Cañutillo well field may move vertically toward the production zones from nearby streams and irrigation-return flow from irrigated lands. Some water probably moves upward toward the lowermost production zone. In the Las Cruces area, ground water probably moves vertically toward the production zone. Wells generally do not produce from the full thickness of the aquifer.

GROUND-WATER/SURFACE-WATER RELATION

The ground and surface waters in the Mesilla Valley are closely interrelated. In addition to mountain- and slope-front recharge, recharge takes place when excess irrigation water percolates through the flood-plain alluvium, as shown by the rise in water levels during the summer irrigation season (Spiegel, 1958). After long periods of heavy pumping, ground-water levels rapidly recover when surface water is applied on agricultural lands (Taylor, 1967).

Ground water is discharged to drains and eventually flows back to the Rio Grande when ground-water levels rise above the drain bottoms. However, during periods of drought, the limited surface-water supply is supplemented by ground-water withdrawals from wells, and drain discharge is decreased (King and others, 1971, p. 57). Ground water also is discharged by evapotranspiration from crops and natural vegetation in the valley.

A schematic diagram shown in figure 15 indicates the following ground-water/surface-water interactions:

1. A major group made up of (a) net diversions, (b) effective rainfall on both irrigated and non-irrigated lands (effective rainfall is here defined as that part of rainfall that either recharges

aquifers or reduces ground-water discharge), (c) evaporation from canal surfaces, and (d) evapotranspiration from irrigated lands is summed to provide an overall flux for the valley area (fig. 16). This summation is termed "net irrigation flux" in this report, and it includes by implication the leakage from irrigation canals to ground water and that part of irrigation ground-water pumpage that is not recirculated back to the ground water.

2. A second major group is comprised of seepage to and from the river and drains.
3. A third major group is evapotranspiration from nonirrigated lands.
4. A fourth group, of intermediate significance, consists of water pumped from wells for domestic, municipal, and industrial purposes, and septic-system return flows.
5. Mountain- and slope-front recharge constitutes a relatively minor amount of flow.

Most flows have been reported or estimated. Most of the flows to and from ground water occur at or near the land surface in the Mesilla Valley (with the exceptions of discharges from deep wells and mountain-front recharge). These flows fluctuate seasonally in the short term, but, in the intermediate term (1-5 years), they fluctuate with the availability of surface water, and, in the long term, they do not fluctuate much at all.

NET IRRIGATION FLUX

Net diversions for a given year are estimated to be gross diversions less water returned directly to the river or drains. The error in gross diversions probably is similar to the error in other streamflow measurements and is dependent on conditions of the stream. Such records may have an accuracy within 5 percent of the true value for "excellent" records, 10 percent for "good" records, 15 percent for "fair" records, and greater than 15 percent for "poor" records (U.S. Geological Survey, 1981). If an error of 10 percent were assumed, the measured gross diversion could vary by about 10,000 to 40,000 acre-feet per year. However, because most of the errors may be random, they may cancel each other and the average error over a period of time may be reduced as the time period is increased. The accuracy of measurements of gross diversions may be "good" or "excellent," but accuracy of measurements of irrigation water returned directly to the river may be "poor" (Ray Sanchez, U.S. Bureau of Reclamation, oral commun., 1984).

Basinwide evaporation from canal surfaces was estimated to be 5.5 cubic feet per second, which is equivalent to about 5.5 feet of water annually over an assumed canal surface area of 730 acres (a 100-foot-

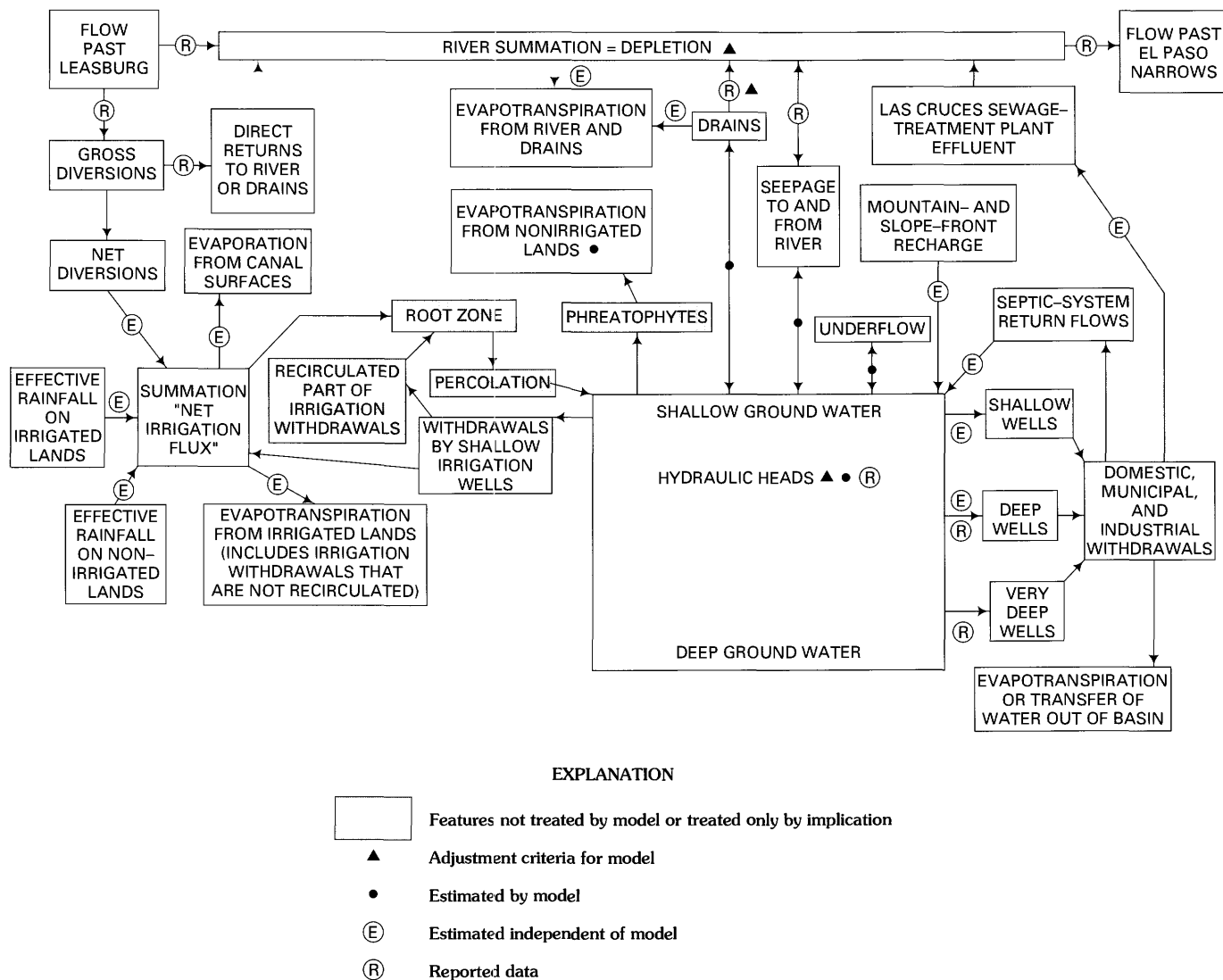


FIGURE 15.—Interactions between ground water and surface water.

wide strip that equals the length of the valley). The percentage of error in this estimate may be very large, but the amount of water that could possibly evaporate is small compared to the potential error in the measurements of diversions.

Effective rainfall is considered in two ways: effective rainfall on agricultural lands and effective rainfall on other surfaces. The effective rainfall (in units of acre-feet) on agricultural land for a given year was estimated, on the basis of methods of Blaney and Hanson (1965, table 5), to be 0.9 times the rainfall (feet) for April through October times the reported irrigated acreage (fig. 5 and fig. 16, line B). The effective rainfall on other surfaces was estimated to be 0.2 times the rainfall times the nonirrigated part of the valley calculated on an annual basis. Evapotranspiration and

effective rainfall on the river channel were treated separately from the ground-water system. Estimated effective rainfall is not a significant amount compared to net diversions (fig. 16, lines A, B, and C) except during years with very small diversions.

Evapotranspiration from agricultural land for a typical year was estimated by the methods of Blaney and Hanson (1965) to be about 2.2 acre-feet per acre for the mixture of crops, mostly cotton and vegetables, grown in Doña Ana County for 1970–75 (Lansford and others, 1976, p. 13). The same mixture of crops was assumed to apply to the Mesilla Valley for earlier times as well as 1970–75. The amount of water consumed each year (fig. 16, line D) was estimated to be 2.2 acre-feet per acre times the irrigated acreage. Errors in estimates of the annual evapotranspiration could arise

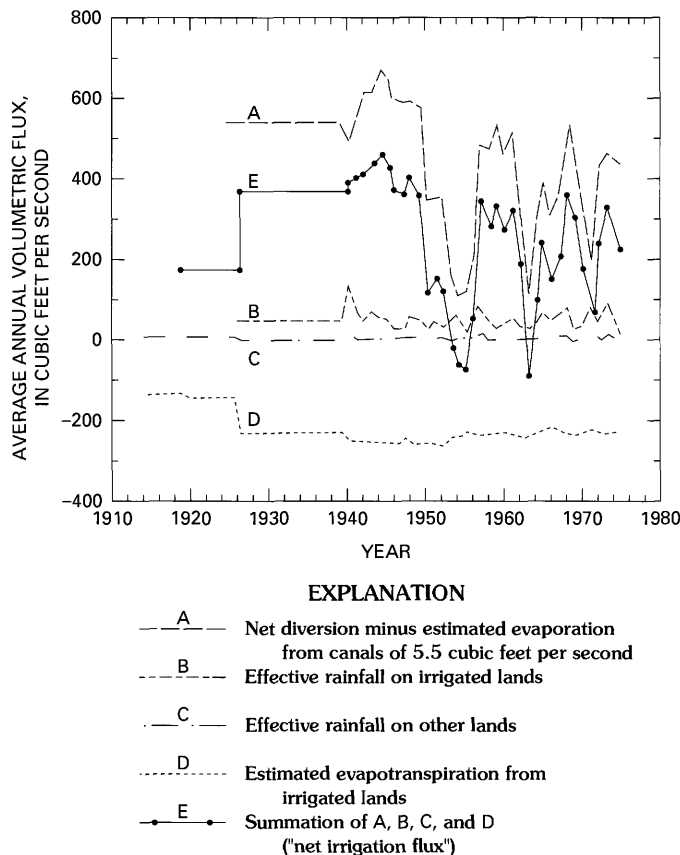


FIGURE 16.—Estimate of net irrigation flux in the Mesilla Valley, 1915–75.

from: (1) use of an inappropriate mixture of crops, (2) errors inherent in the Blaney-Hanson method, and (3) undocumented variations in management practices. For example, during droughts, application of irrigation water may be minimized because of pumping costs. Also, at the beginning of the drought of 1951–53, the ground-water pumping capacity probably was inadequate to supply all the needed irrigation water, but many wells were drilled during that time (Leggat and others, 1962, p. 15–16). Although it was assumed that enough pumping capacity existed at the end of that drought, the transition from inadequate to adequate capacity is not known. It may not be possible to determine the size of these errors.

EVAPOTRANSPIRATION FROM NONIRRIGATED LANDS

Evapotranspiration from nonirrigated lands was not estimated. These lands have highly variable hydrologic properties. They include such features as paved roads that may reduce evapotranspiration and collect rainfall, allowing it to infiltrate to the water table in places. Also included are vegetated areas that lie relatively high above the water table, minimizing the

availability of ground water to plants, and areas where trees grow near surface water or shallow ground water where evapotranspiration may be near a maximum. Evapotranspiration of ground water from surfaces covered by natural vegetation generally is dependent on the depth to the water table: during dry years (when the water table is unusually deep), natural evapotranspiration may be reduced. On the other hand, if the water table were to decline slowly, some vegetation might be able to adapt by growing deeper roots. The estimation of ground-water evapotranspiration from nonirrigated land is complex and difficult to make.

STREAM SEEPAGE

Seepage to and from streams, including drains and canals, accounts for a major amount of water. The river has both gaining and losing reaches that probably change seasonally. The drains gain when ground-water levels are high but may lose in their lower reaches where they join the river or in localities where large amounts of ground water are withdrawn. Irrigation canals generally lose water to the ground during the irrigation season.

The type and amount of interconnection between streams and the aquifer depend on the relative heads in the stream and in the aquifer and on streambed conditions. Where the water table is below the level of the stream, surface-water recharge to the aquifer can take place; however, the rate of recharge is dependent on the head difference and the permeability of the streambed. The beds of streams that recharge ground water tend to be somewhat more plugged than the beds of streams that receive ground water because suspended sediment tends to follow the water from the stream into pores of the aquifer (a condition that does not prevail where flow is from the aquifer to the stream).

It is possible for beds of shallow surface-water bodies to be effectively sealed, even in places where the bed material is permeable. This condition can occur where fine-grained bed material overlies relatively coarse grained material that is not saturated. In this case, the capillary tension in the fine-grained material, being greater than the capillary tension in the coarse-grained material, may restrict downward flow. This is the concept of an inverted water table (Freeze and Cherry, 1979, p. 45). This condition may occur beneath irrigation canals where the velocity of the water slows and allows suspended material to settle, or it may occur where drains flow near a well field. In this case, the effective vertical hydraulic conductivity could change greatly not only from place to place but from time to time depending on ground-water levels and streamflow velocities.

Two seepage (gain and loss) investigations were made on discharge in the Rio Grande: (1) a complete run made February 12–13, 1974, under minimal-flow conditions (mainly drain-return flow, ground-water inflow, and precipitation); and (2) a partial run made January 12–21, 1975, that ended at Mesilla Dam (Wilson and others, 1981, p. 66). The water table during these periods was generally high due to 2 or more preceding years of full surface-water irrigation allotment. The investigations showed that the river had slight gains in the upper part of Mesilla Valley but was a losing stream from about 6.2 miles north of Las Cruces (SE $\frac{1}{4}$ sec. 20, T. 22 S., R. 1 E.) downstream to El Paso Narrows. The greatest losses occurred from the west side of sec. 3, T. 23 S., R. 1 E., southward to Mesilla Dam. The losses measured in this reach ranged from 1.7 to 4.8 cubic feet per second per river mile and averaged 2.5 cubic feet per second per river mile (Wilson and others, 1981, p. 67). The reach of the Rio Grande between Mesilla Dam and the mouth of Del Rio Drain near Vado usually is dry during much of the nonirrigation season because few drains enter the river in this reach. River losses were 1.2 cubic feet per second per river mile for the reach downstream from Del Rio Drain and about 1.8 cubic feet per second per river mile for the reach opposite the Cañutillo well field. The losses primarily were due to seepage into the aquifer and would be greater during the irrigation season when most surface-water discharge occurs.

Annual drain discharges are shown in figure 9. (Individual drain discharges are shown, for convenience of comparison with model-derived drain discharges, in the section on model adjustment.) The accuracy of drain-discharge measurements probably is "poor" because stream gradients are low—this causes problems with backwater and moss or other vegetation. An additional uncertainty is that drains may receive water from redirected surface water such as excess water from irrigation canals. All drain discharges were assumed to have come from ground water.

GROUND-WATER WITHDRAWALS

Ground-water withdrawals for municipal, domestic, and industrial uses (fig. 17) generally were reported or estimated from population data. The amount and location of ground-water withdrawals by industrial users, small subdivisions, and the city of El Paso were obtained from the files of the U.S. Geological Survey at El Paso (Don White, written commun., 1980). Withdrawals by the city of Las Cruces were estimated or reported. Withdrawals by small towns and villages in

Doña Ana County were mostly estimated from population data. Total estimated nonirrigation withdrawals increased from about 6 cubic feet per second in 1950 to about 60 cubic feet per second in the early 1970's. About one-half was withdrawn by the city of El Paso and about one-fourth by the city of Las Cruces. The remainder was withdrawn by small towns, villages, and industries.

Withdrawals at Las Cruces were estimated to be 50 gallons per day per capita from 1910 to 1940. This rate is consistent with reported rates (Classen and Rowland, 1948) for 1941–47. For 1948–58, annual withdrawals were estimated by linear interpolation between the 1947 and 1959 values. The 1959–75 values were obtained from records of the city.

Withdrawals by small towns and villages mostly were estimated. However, previously estimated or reported withdrawals were used (Dinwiddie and others, 1966; Randall and Dewbre, 1972; U.S. Bureau of Reclamation, 1973, sec. VII–A, sheet 3; Sorensen, 1982; records of the Jornada Water Company; and records of the Doña Ana Municipal and Domestic Water Consumers Association). Withdrawals were estimated to be 50 gallons per day per capita (U.S. Department of Commerce, 1952a, 1952b, 1982a, 1982b; Sorensen, 1982) for the years for which population data exist. Where previous estimates conflicted with each other or with per-capita-derived estimates, one of the estimates was selected on the basis of a subjective assessment of its reliability. The remaining annual withdrawals were estimated for each town or village by linear interpolation. Withdrawals at New Mexico State University were estimated by multiplying the student enrollment by 46,000 gallons per student per year. Enrollment was obtained from New Mexico State University librarians (oral commun., 1984). The average per-student withdrawal was obtained from a combination of withdrawal and enrollment data that were available for several years during the 1960's and 1970's (Field, no date; Owen Lockwood, New Mexico State University, written commun., 1982). It was assumed that the per-student rate was the same in previous years as it was during the 1960's and 1970's.

The amount of error in reported and estimated withdrawals for municipal, industrial, and domestic uses is not known. This error may be important because of resulting drawdowns in the Cañutillo and Las Cruces areas. In other places, the amount of water withdrawn probably is not significant compared to errors in estimates of net irrigation flux.

Return flows of municipal, industrial, and domestic water take several forms. Water withdrawn by El Paso is not returned in the Mesilla Basin. Slightly more than one-half of the wintertime withdrawals by

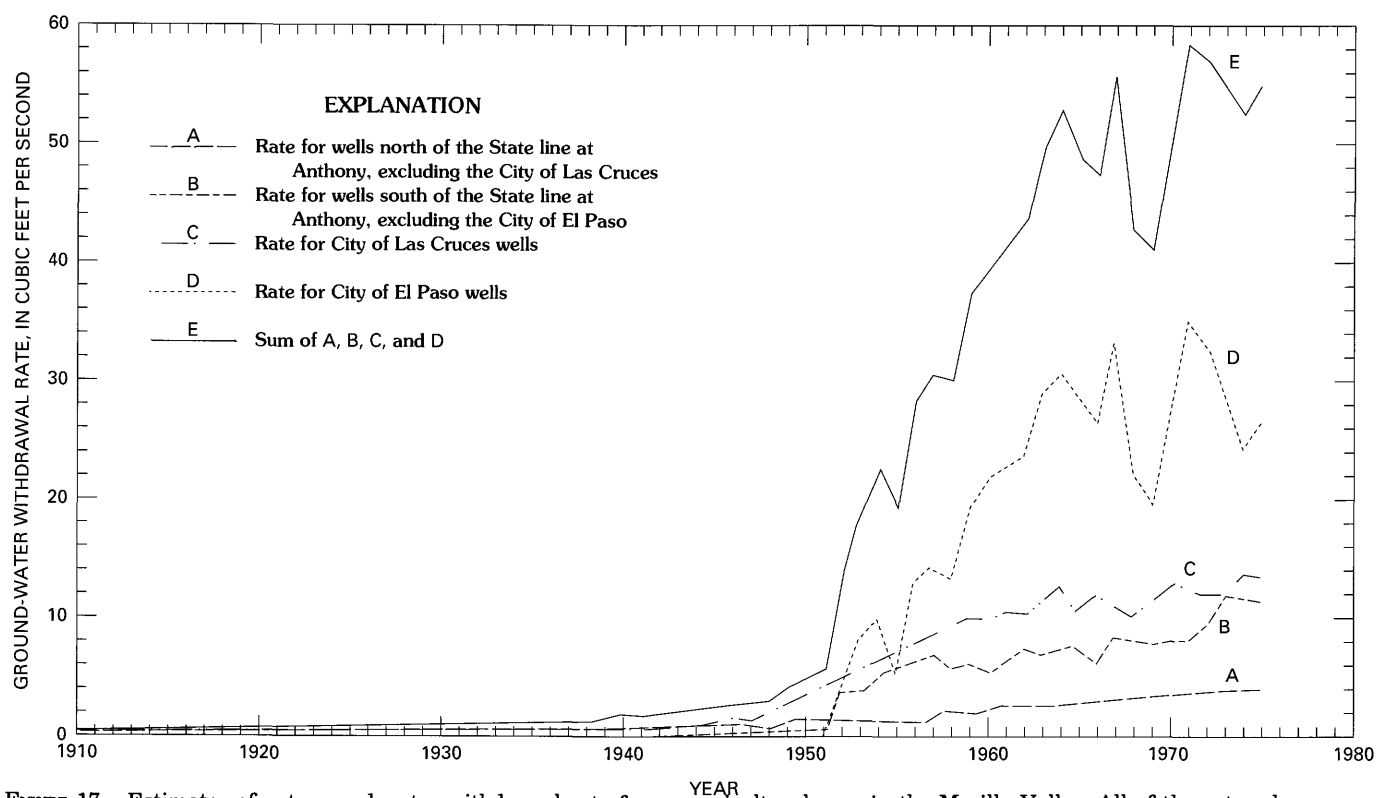


FIGURE 17.—Estimates of net ground-water withdrawal rate for nonagricultural uses in the Mesilla Valley. All of the rates shown were estimates of net ground-water withdrawal made exclusively for this study and may be neither complete enough nor appropriate for any other purpose.

Las Cruces are returned as surface discharge to the Rio Grande (Las Cruces city personnel, oral commun., 1983). On the basis of data in Sorensen (1977, tables 1 and 2), possibly one-half of the water withdrawn by communities where no surface disposal systems are in use is returned by means of septic systems. Errors in estimates of these return flows probably are not critical because the amount is small.

GROUND-WATER RECHARGE

Recharge to the aquifer probably occurs along ephemeral streams in response to intense local storms. Beds of ephemeral streams are composed of sand and gravel, and their relatively flat gradients allow for infiltration of water that comes from upstream, relatively steep reaches that are incised in bedrock around the perimeter of the ground-water basin. This recharge is termed "mountain-front recharge." Hydrologically similar conditions occur on the sides of the Mesilla Valley where sand channels indicate that rainwater from steep slopes flows into less steep sand channels that do not extend to the river. Recharge under these conditions is termed "slope-front recharge." Slope-front

recharge differs from mountain-front recharge in that the steep parts of the drainages are underlain by basin fill instead of bedrock, and the slopes cannot be described as mountains.

Mountain- and slope-front recharge was estimated (fig. 18) by J.D. Dewey (written commun., 1983) using an empirical formula developed from a log-multiple regression analysis of measured streamflows. The method has been documented by Hearne and Dewey (1988). Watersheds underlain by crystalline rock in Colorado and New Mexico were selected for the analysis. The watersheds were divided into groups on the basis of average winter precipitation, and each group was analyzed separately. Only watersheds in New Mexico were used to derive the equation for less than 7.4 inches of winter precipitation. This equation is:

$$Q = (1.074 \times 10^{-5}) A^{1.216} P^{2.749} S^{0.536} \quad (1)$$

where

Q is the mean annual runoff, in cubic feet per second,
 A is the area of the drainage basin, in square miles,
 P is the mean annual winter precipitation, in inches,
 and
 S is the slope of the basin, in feet per mile.

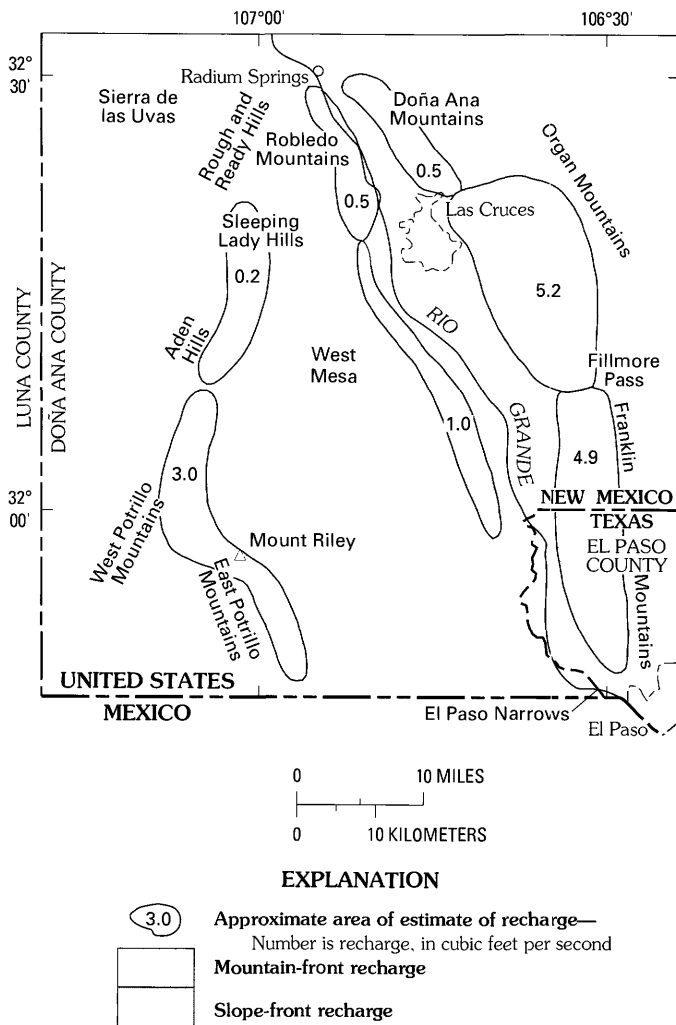


FIGURE 18.—Mountain-front and slope-front recharge.

The drainage basins were combined as shown in figure 18. The entire amount of runoff was assumed to infiltrate the sand channels at the lower ends of the drainage basins and to recharge the aquifer. The total mountain- and slope-front recharge was estimated to be 15.3 cubic feet per second, and most recharge occurred on the eastern side of the basin. The potential error in these estimates is great—perhaps plus 100 percent or minus 50 percent.

Any recharge on gently sloping areas, such as the West Mesa, probably occurs only occasionally and in small amounts. It is hypothesized that, in such areas where average annual rainfall (8 inches) is much less than potential evapotranspiration (50–80 inches), the natural grass and desert shrubs capture all rainfall before it percolates beyond the root zone. Caliche just below the land surface on most of the West Mesa may inhibit the downward movement of water (King and others, 1971, p. 57). Nevertheless, occasional intense

storms could exceed the infiltration capacity of the soil and allow surface water to pond in closed depressions. On such occasions, some ponded water might percolate beyond the reach of vegetation and arrive at the water table. Locally, unvegetated, fractured basalt flows could allow a large part of rainfall to recharge the ground water because of the lack of water-retaining soil. However, recharge on the West Mesa was assumed to be negligible.

SUMMARY OF CONCEPTS

Some generalized concepts can be formulated from the above discussion. (1) The ground-water system is three dimensional: (a) The flood-plain alluvium has a larger hydraulic conductivity than the underlying and laterally contiguous Santa Fe Group; (b) although several water-producing zones have been identified in the southern end of the valley (each with a different hydraulic head), no laterally extensive confining beds have been observed; and (c) wells generally do not produce from the full thickness of the aquifer. (2) The lateral extent and depth of the ground-water flow system are defined by bedrock with values of hydraulic conductivity that are much less than those of the Santa Fe Group. (3) Most water that flows into and out of the ground-water system is at or near the land surface in the Mesilla Valley. These flows are the result of complex interactions of the river, drains, canals, evapotranspiration, and withdrawals from wells. These flows fluctuate seasonally (in the short term), but in the intermediate term (1–5 years), they fluctuate with the availability of surface water, and in the long term (more than 5 years), they do not fluctuate much at all. (4) Basinwide withdrawals of water from deep wells (deeper than about 200 feet) before 1975 were small compared to evapotranspiration, but they were locally significant, especially in the Cañutillo and Las Cruces areas. After 1975, withdrawals from deep wells increased because more deep irrigation wells were installed. (5) A small amount of water recharges the ground-water system near mountain fronts. This water comes from surface runoff from the steep mountain drainages. By a similar mechanism, a small amount may recharge the system along the toe of the steeply sloping bluff along the west side of the Mesilla Valley. (6) Recharge of any significant amount over most of the West Mesa area is unlikely but occasionally may occur in places.

SIMULATION OF GROUND-WATER FLOW

After the basic concepts of the ground-water system were formulated, a computer program was selected for

simulation of ground-water flow. A preliminary steady-state version of the model was made, and then a transient version was made. The transient version incorporated the steady-state version in order to provide an initial condition upon which storage and time-variant pumpage, streamflows, and areal fluxes were superimposed. Because the purpose of modeling was to study the ground-water system, as the understanding of the system improved, the steady-state and transient versions were refined and adjusted simultaneously. The adjustment stage generally is termed "calibration," but in this report the term is not used because it connotes a degree of accuracy that is not appropriate. After some adjustments were made, the model was accepted as adequate for a tentative standard against which to test the effects of changes to certain properties in a sensitivity analysis. These changes were made individually to assess the importance of various hydrologic properties and to assess the predictive capability of the model. Although making a predictive model was not the immediate purpose of the study, it is recognized that the model might be used for preliminary predictive studies; hence, the limits of its predictive capability were explored.

A computer program for modeling the hydrologic system needs to be capable of simulating: (1) a three-dimensional flow system; (2) specified-head and flow boundaries in order to simulate wells, recharge, and underflow; (3) head-dependent flow boundaries in order to simulate evapotranspiration and flow to or from streams; and (4) streams that may be intermittent or perched—this is done by keeping a node-by-node account of the flow in streams, limiting flow to or from the stream nodes. Filling these requirements, the program of Posson and others (1980) as modified by Hearne (1982) was used for the preliminary simulations. During the latter part of the study, the U.S. Geological Survey modular program (McDonald and Harbaugh, 1984) was used. Both programs solve the same basic three-dimensional equation of ground-water flow using the strongly implicit procedure (SIP) of Stone (1968). Both programs treat specified-head, specified-flow, and head-dependent flow boundaries in essentially the same way except that the modular program solves for head-dependent flow boundaries implicitly, whereas the Posson program solves for them explicitly. The implicit solution allows the modular program to complete the simulation more quickly and cheaply. A minor alteration of the modular program was necessary to enable it to keep an account of discharge in streams and to allow for a limit to be specified for the ground-water recharge from streams.

The alterations to the modular program are described by Miller (1988, p. 1). The main features that this alteration allows are the same as those allowed by the program of Posson and others (1980). They are as follows: (1) Excess surface discharge is carried from one node to the next in a specified sequence. This is just an accounting procedure, not a surface-water model. (2) The stream system is divided into reaches to make it convenient to specify streamflow into the upper end of a reach and the destination of outflow either into the upper end of another reach or out of the model. (3) More than one stream can occur at a single node or they can cross (as in the case of a siphon). (4) The amount of flow to the aquifer at any node can be limited by the user. Within this limit, the maximum flow into the aquifer is the amount available in the stream, allowing for the simulation of intermittent streams and drains that have no streamflow routed into their upper reaches. (5) This routine is not a surface-water model. For example, neither a stage-discharge relation nor storage in the stream or streambanks is simulated. Because these streams have a wide range of discharge for slight stage changes, the assumption is that stream stage and storage are not relevant to ground-water simulation—this assumption may not be appropriate for periods of less than 1 year in the Mesilla Valley.

DESCRIPTION OF THE MODEL

The model required specification of a three-dimensional grid, aquifer characteristics, and boundary conditions. Some values were changed during model adjustment. Aquifer characteristics reported in this section are the adjusted values.

MODEL GRID

A model grid was required because the computer program utilizes a finite-difference method in which differential equations of ground-water flow are solved numerically. The equations require that hydraulic properties and boundaries (and stresses in the transient case) be defined for the modeled space. To accomplish this, the modeled space is divided into a three-dimensional grid made up of rows, columns, and layers of blocks. The center point of each block is called a node and is referred to by its layer, row, and column numbers. The average value of each hydraulic property or flux, such as transmissivity, hydraulic head, or pumping rate for an entire block, is assigned to the node at its center. Similarly, model-derived values apply to the node and are "average" values for the entire block. The accuracy of the simulation is affected by the block size relative to the rate of change of

hydraulic properties from one block to the next. The relation is a matter of resolution. For example, although a potentiometric surface is usually a smooth curve, the model-derived surface is made up of steps that are the size of the grid blocks. It is therefore desirable to make grid blocks as small as feasible, especially in places where the surface is most curved, in order to smoothly simulate the surface. This principle holds in all three dimensions.

The rectangular grid that defines the block sizes is shown in figure 19. Horizontally, the grid has 36 rows and 64 columns with dimensions that range from 0.5 to 2.0 miles. The grid spacing is finest in the flood plain and in the Las Cruces and Cañutillo well-field areas.

The model grid contains five layers: layer 1 is at the top. The thicknesses of the top three layers were determined by the approximate average thicknesses of the middle and deep production zones (layers 2 and 3) in the southern Mesilla Valley and of the flood-plain production zone (layer 1 throughout the valley area). The bottom of layer 1 (and top of layer 2) is defined as the 1975 water-table altitude minus 200 feet. Layers 4 and 5 are included to represent deep parts of the basin; each layer was given a thickness equal to 1.5 times the thickness of the layer above. The thicknesses of layers 1 through 5 were 300, 400, 600, 900, and 1,350 feet, respectively. The top layer included about 200 feet of saturated thickness because its bottom was defined as being 200 feet below the 1975 water table. Therefore, the top of the layer had no direct relation to land surface.

AQUIFER CHARACTERISTICS

Aquifer characteristics include hydraulic conductivity, transmissivity, specific yield, and storage coefficient. In the top layer, hydraulic conductivity and specific yield were specified because unconfined conditions were simulated.

HYDRAULIC CONDUCTIVITY AND TRANSMISSIVITY

The hydraulic conductivity (70 feet per day) specified for the top layer in the Mesilla Valley (fig. 20) was the median of estimated values (fig. 14). This value represented a combination of the flood-plain alluvium plus some underlying Santa Fe Group. Outside the Mesilla Valley, the values of hydraulic conductivity for layer 1 (usually 22 feet per day) that represent the upper part of the Santa Fe Group are comparable to estimated values (fig. 13 and table 1). The values of transmissivity of the top layer were calculated by the model as hydraulic conductivity times saturated thickness. The saturated thickness was the difference

between the model-derived hydraulic head and the specified altitude of the bottom of the layer. Therefore, the model-derived transmissivity for layer 1 was approximately 200 feet times the hydraulic conductivity.

The values of transmissivity of the lower four layers (figs. 21–24) were equal to layer thickness times hydraulic conductivity. The hydraulic conductivity for layer 2 was 18 feet per day, corresponding to the values shown in table 1 for the upper part of the Santa Fe Group. The values of hydraulic conductivity for layers 3, 4, and 5 were 8, 5, and 3 feet per day, respectively, corresponding to the values shown in table 1 for the deeper part of the Santa Fe Group. One exception was in layer 3 in the lower Mesilla Valley where the hydraulic conductivity was 13 feet per day, corresponding to the transmissivity reported by Leggat and others (1962, p. 32). In places where the depth of saturated basin fill did not allow for a layer to be its full thickness, transmissivity was reduced proportionately (figs. 23 and 24).

Vertical flow in the aquifer was simulated by specifying a leakance between model layers ("Vcont" of McDonald and Harbaugh, 1984, p. 142). Leakance, in hydrologic terms, is the vertical hydraulic conductivity of a hydrologic unit divided by the thickness of the unit. Analogously, leakance between two model layers was the thickness-weighted harmonic mean of the values of vertical hydraulic conductivity of each layer. The vertical hydraulic conductivity at a given location was assumed to be the horizontal hydraulic conductivity divided by 200.

Thus, leakance was calculated as:

$$L_{(i,j,k)} = \frac{2}{R \left(\frac{(b_{(k)})^2}{T_{(i,j,k)}} + \frac{(b_{(k+1)})^2}{T_{(i,j,k+1)}} \right)} \quad (2)$$

where

R is the ratio of horizontal to vertical hydraulic conductivity (specified as 200),

$b_{(k)}$ is the thickness of layer k , and

$T_{(i,j,k)}$ is the transmissivity of the block located at row i , column j , layer k .

An inconsistency was introduced by this procedure for parts of layers 4 and 5 where transmissivity was reduced in order to account for aquifer thicknesses that were less than the nominal thicknesses of the layers. In these areas, the values of leakance that were approximated using the reduced transmissivity were less than intended. This inconsistency was not considered to be serious because sensitivity tests indicated that the model was relatively insensitive to the existence of layers 4 and 5.

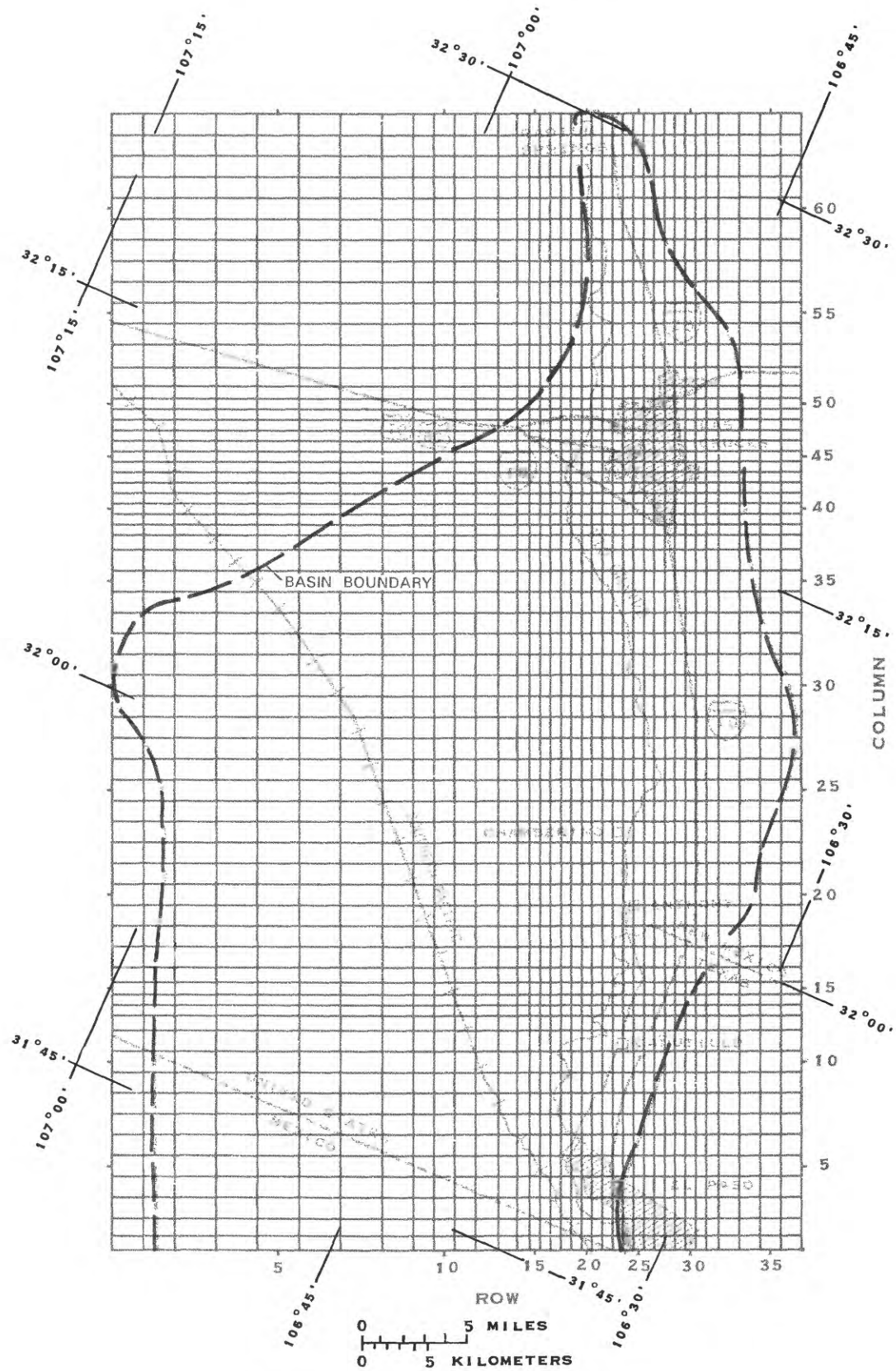


FIGURE 19.—Model grid and basin boundary.

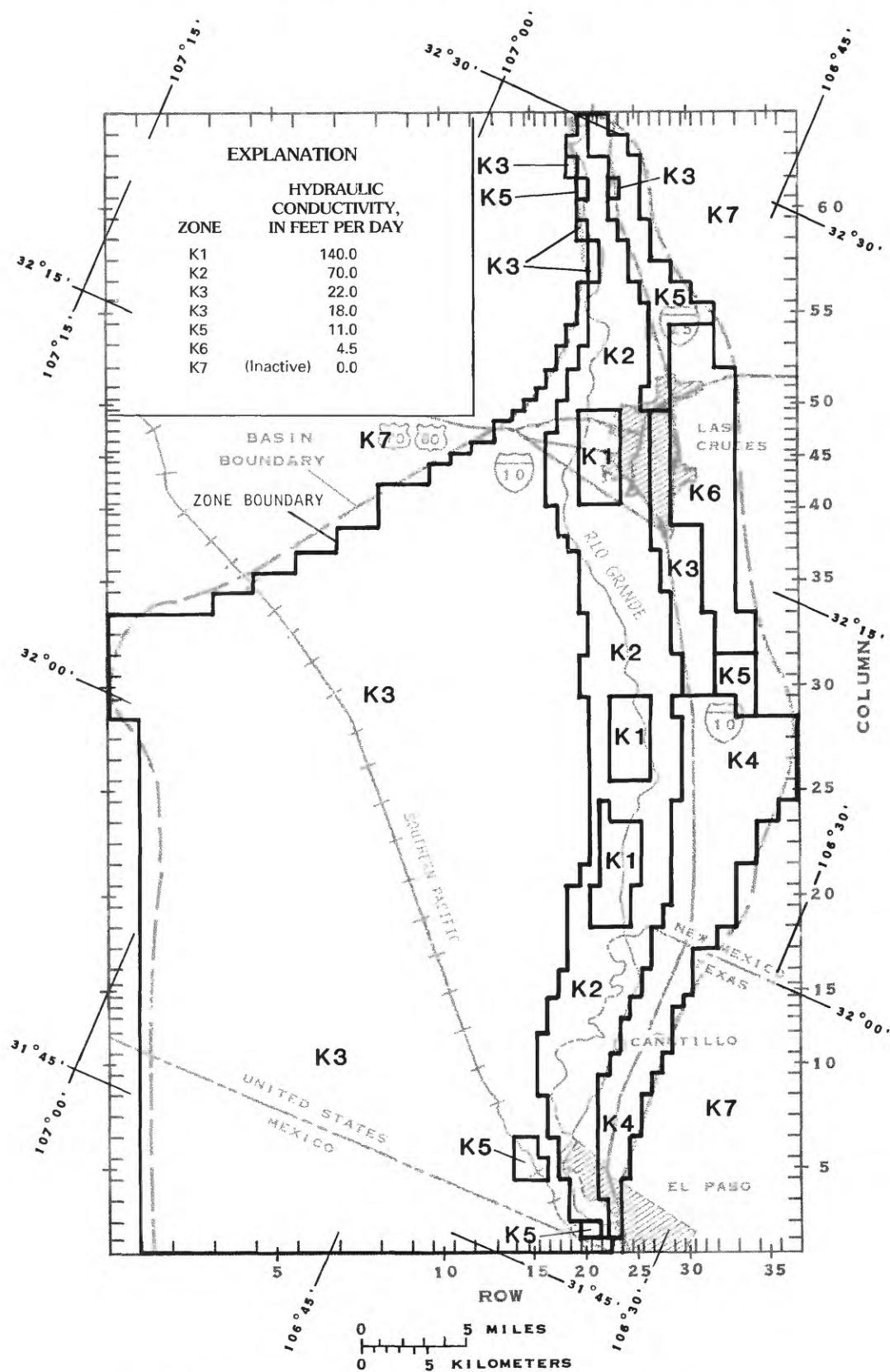


FIGURE 20.—Hydraulic conductivity assigned to model layer 1, the top layer.

SOUTHWEST ALLUVIAL BASINS RASA PROJECT

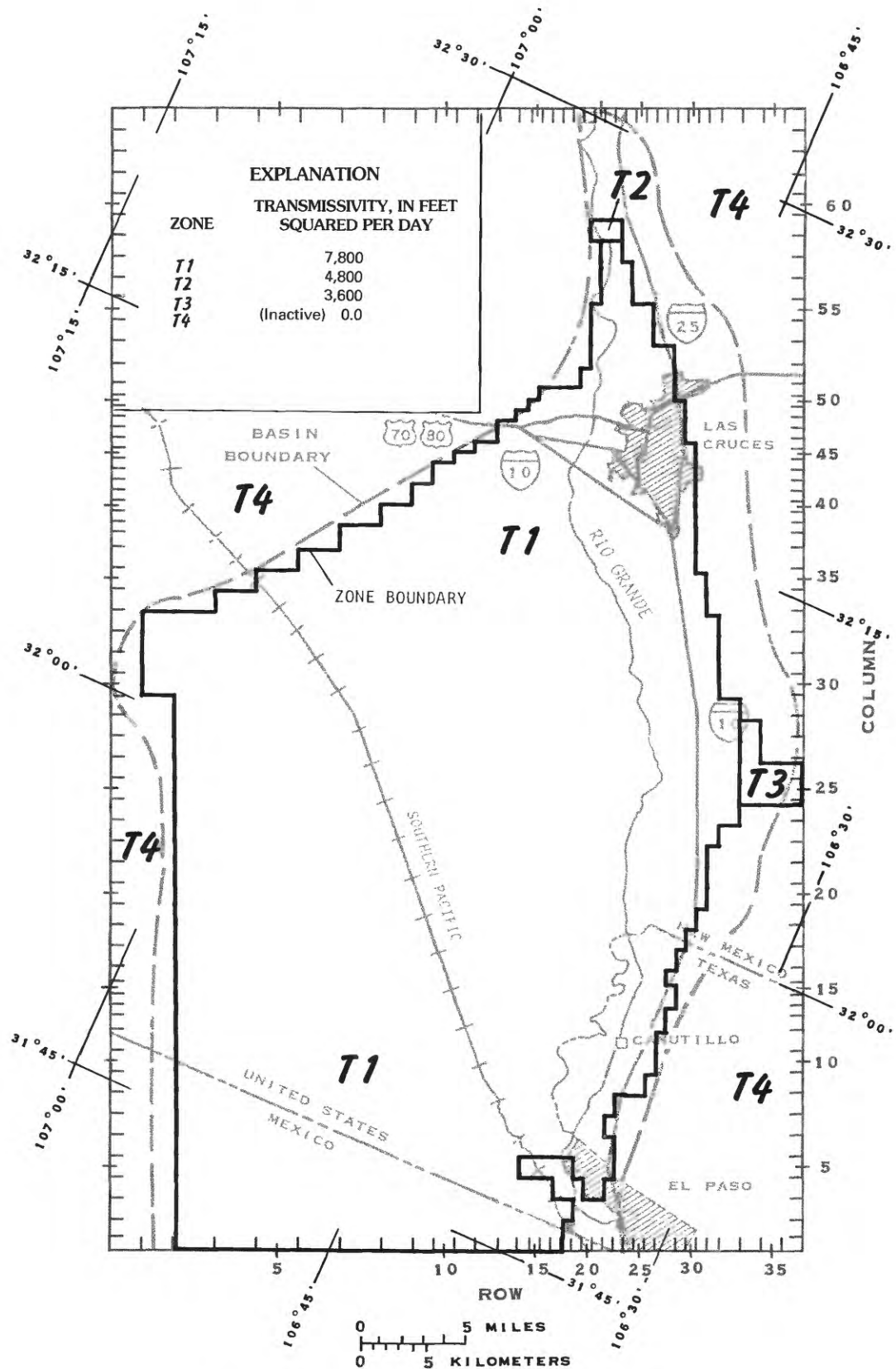


FIGURE 21.—Transmissivity assigned to model layer 2.

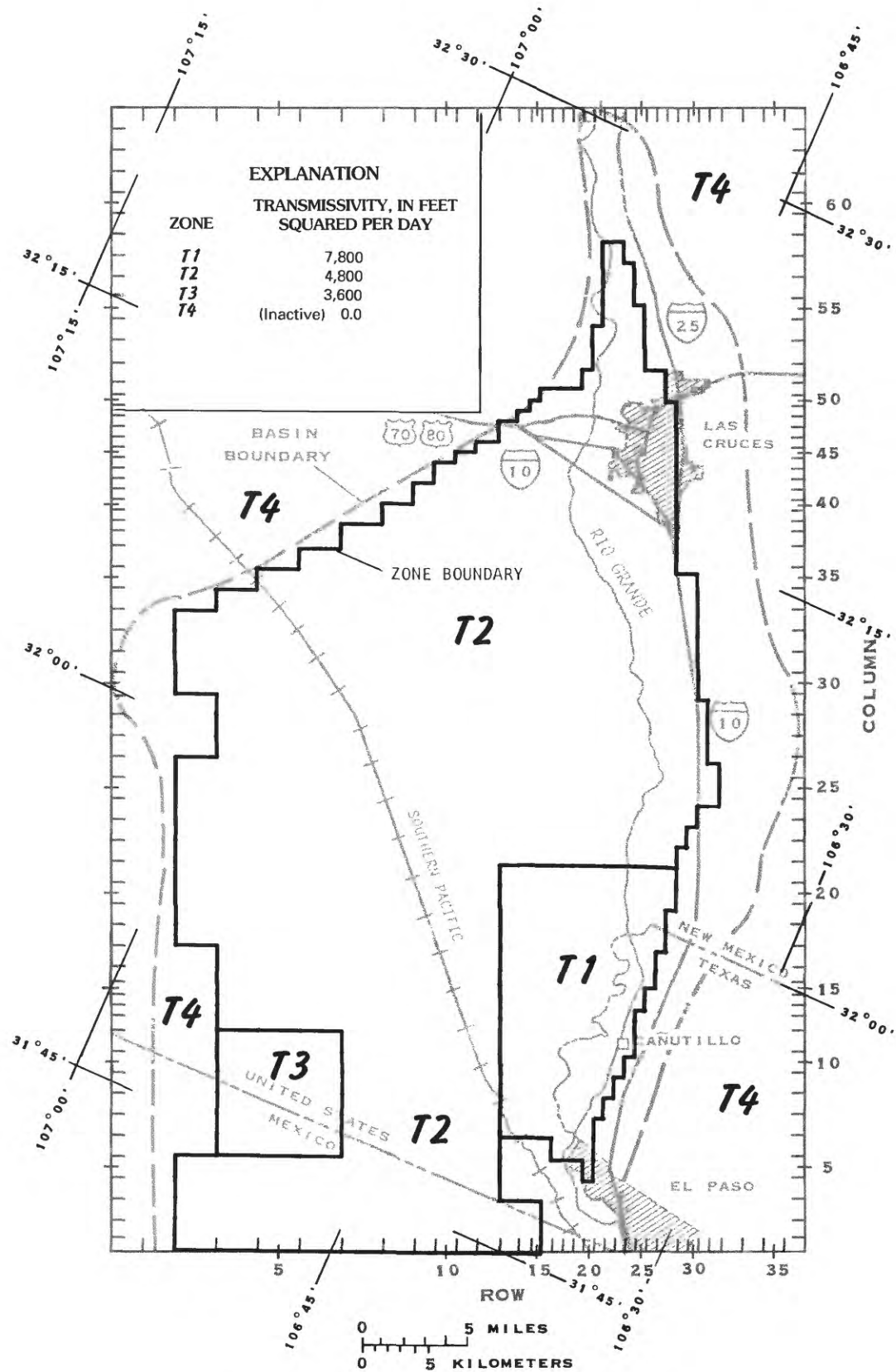


FIGURE 22.—Transmissivity assigned to model layer 3.

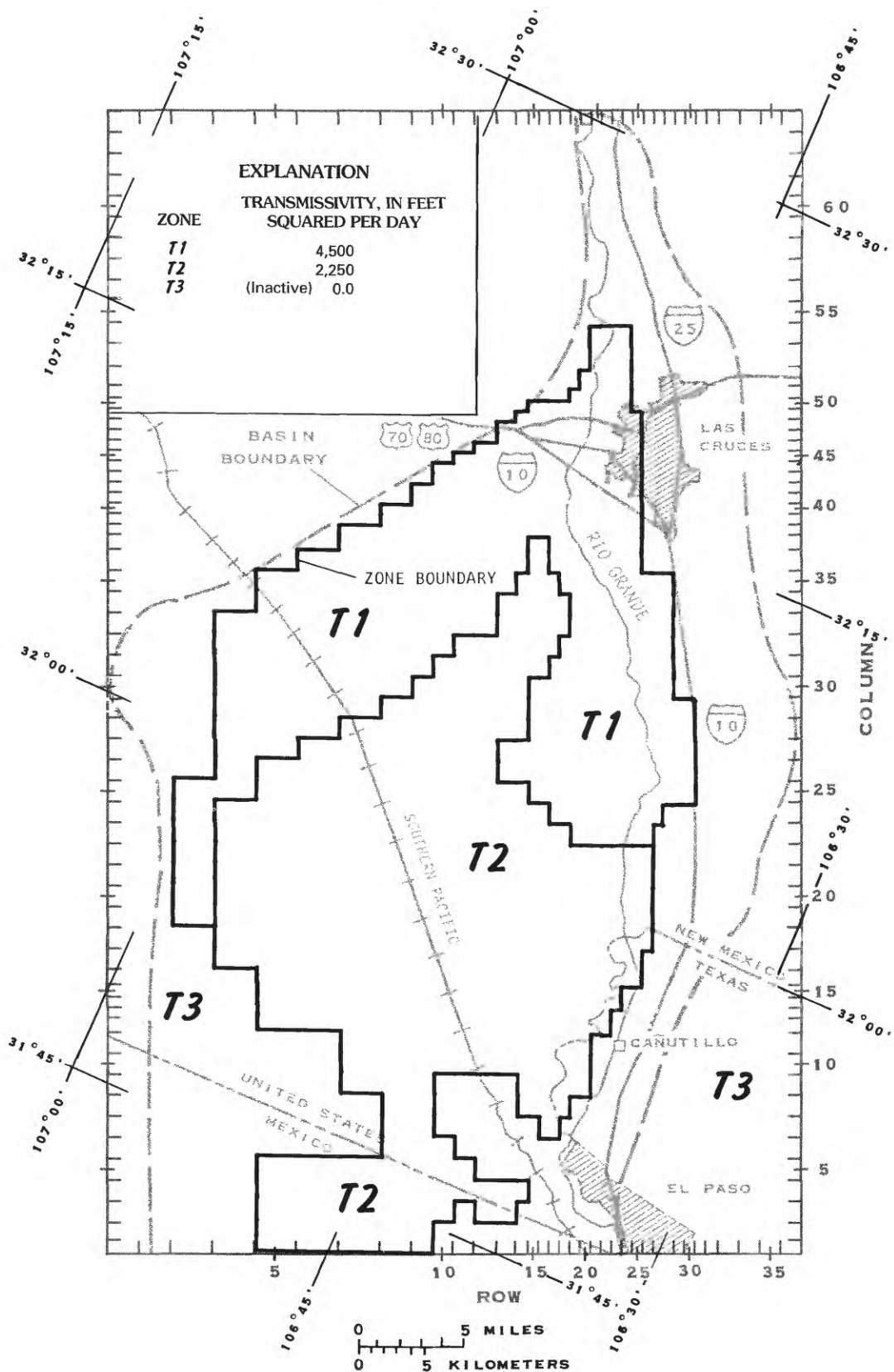


FIGURE 23.—Transmissivity assigned to model layer 4.

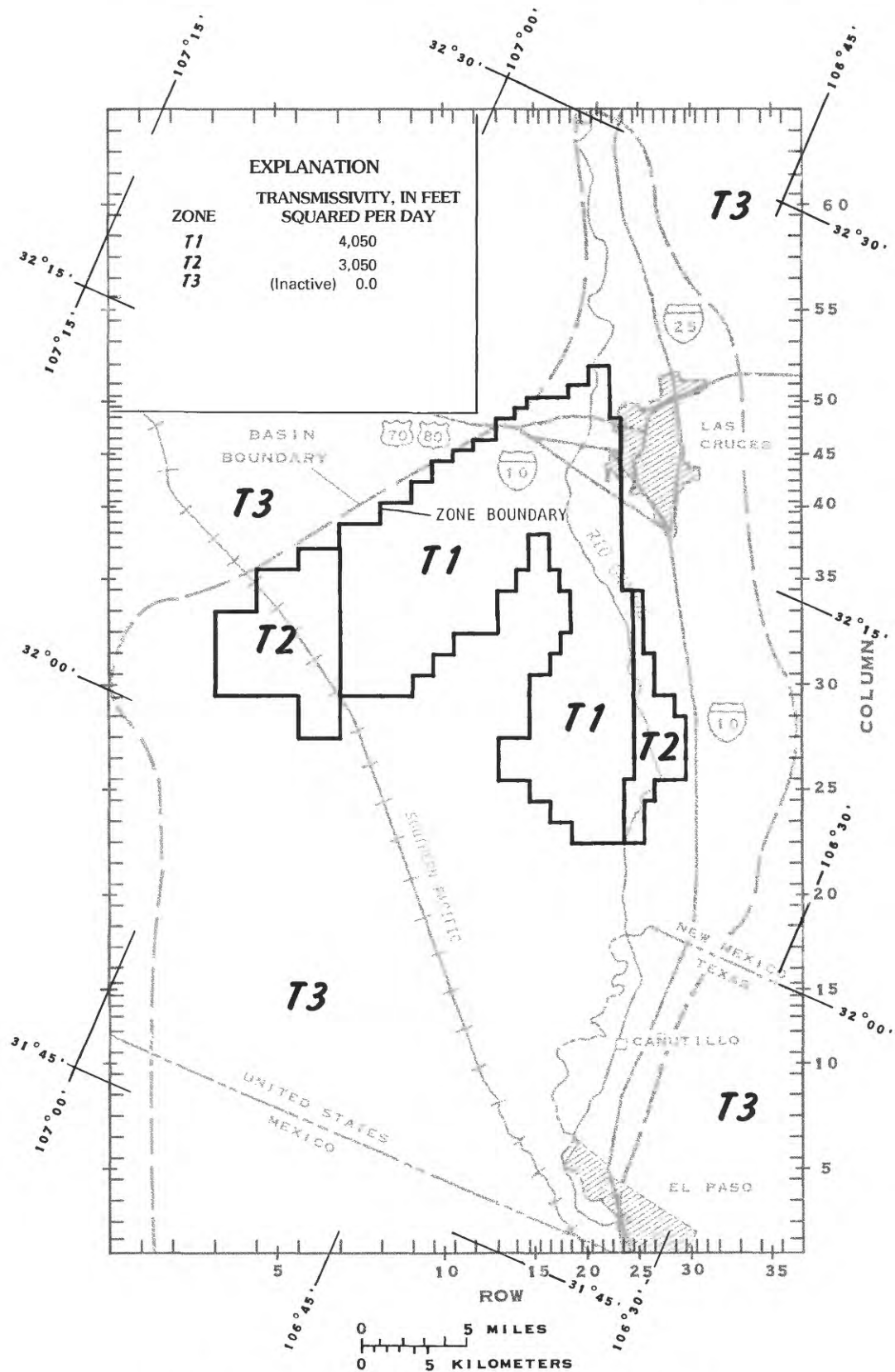


FIGURE 24.—Transmissivity assigned to model layer 5, the bottom layer.

SPECIFIC YIELD AND STORAGE COEFFICIENTS

The specific yield for layer 1, which simulated unconfined conditions, was 0.2 as indicated by previous studies (Richardson and others, 1972, p. 86; Lizarraga, 1978, p. 29; Wilson and others, 1981, fig. 10). The storage coefficients for layers 2–5, which simulated a fully saturated (leaky-confined) condition, were derived by multiplying the thickness of each layer by a specific storage of 1×10^{-6} per foot. This value of specific storage is common in sedimentary rocks (Lohman, 1972, p. 8) and accounts for the expansion of water and some elastic matrix compression in rocks that have ordinary porosity and mechanical properties. The storage coefficients were 0.0004 for layer 2, 0.0006 for layer 3, 0.0009 for layer 4, and 0.00135 for layer 5.

INITIAL CONDITION AND TIME PERIODS

The hydrologic history of the Mesilla Basin was divided into five time periods. Before water became available from Elephant Butte Reservoir in 1915, ground water in the basin was assumed to occur under steady-state conditions. Furthermore, it was assumed that the water-table map of Lee (1907, pl. X) described the unconfined ground-water conditions in the flood-plain alluvium before 1915. During the second period, between 1915 and 1926, the amount of irrigated land was greatly increased (fig. 6), and a drainage system (started in 1917) was installed. The hydrologic history of this period is extensive but incomplete with regard to the progress of these developments from one part of the valley to the next. Also, records of the resulting ground-water levels and streamflow rates are incomplete. The third period, 1927–40, was a time of relatively stable hydrologic conditions. Adequate surface water was available for irrigation, and little ground-water development occurred. Ground-water levels were controlled by drains and were relatively stable except for seasonal changes of a few feet (generally 10 or less). The fourth period, 1941–75, was a time of droughts separated by periods of plentiful surface water. The droughts led to ground-water development for irrigation starting in the early 1950's. Also, pumpage of ground water from municipal well fields grew steadily. These changing conditions are documented by measurements of streamflows, pumpages, and ground-water levels. The fifth period, after 1975, was distinguished by pumpage of irrigation water from deeper zones in the aquifer than previously had occurred (Wilson and White, 1984); however, the locations and amounts of these pumpages were not precisely known, so this period was not simulated.

The model was intended to simulate 1941–75. However, the time before 1941 was simulated in order to

provide initial conditions for 1941. The early times were simulated starting with a steady-state approximation of the pre-1915 period. Subsequent times to 1940 were simulated progressively more precisely. Thus, the total time period for the transient version of the model was 1915–75, which was divided into 16 pumping periods of four time steps each. Pumping periods and time steps (Trescott and others, 1976) allow for changes in model input such as specified fluxes and in model output such as model-derived hydraulic-head values.

The first three pumping periods were selected on the basis of increasing irrigated acreage in the Mesilla Valley. These pumping periods were 1915–19, when it was assumed that 44,000 acres of land were irrigated (fig. 6); 1920–26, when about 46,000 acres of land were irrigated; and 1927–40, when about 75,000 acres were irrigated. The progressive increase in irrigated acreage before 1920 and the progressive construction of drains were simulated in one long pumping period. The buildup of hydraulic head resulting from increased irrigation followed by a decline in hydraulic head from construction of drains was not simulated because both took place in the same period (figs. 6 and 9). Both irrigated acreage and drain lengths approached their maximums by 1926, the end of the second pumping period, when conditions became more stable. This provided an approximation of hydraulic heads to begin the simulation of the relatively stable conditions of 1927–40.

The remaining pumping periods were selected to define major hydrologic changes. The most significant changes were: (1) changes in the amount of diversion of irrigation water (fig. 16) that resulted from droughts and times of plentiful surface water; (2) changes in irrigated acreage (fig. 6); and (3) changes in rates of ground-water withdrawal from municipal well fields (fig. 17). The pumping periods defined, including the first three, were 1915–19, 1920–26, 1927–40, 1941–47, 1948–50, 1951–53, 1954–57, 1958–60, 1961, 1962–63, 1964, 1965–66, 1967–68, 1969–71, 1972, and 1973–75.

BOUNDARY CONDITIONS

A no-flow boundary defined the lateral extent and depth of the basin. Within this boundary, recharge was applied near the mountains and slope fronts, and a recharge-discharge boundary was placed along the Mesilla Valley. The Mesilla Valley boundary consisted of a net flux that mainly represented the river and drains, evapotranspiration from nonirrigated lands, and a combination of irrigation pumpage, evapotranspiration from crops, and irrigation with surface water.

NO-FLOW BOUNDARY

The exterior model boundary was simulated to coincide with the basin boundary. The model blocks outside the boundary (figs. 20–24) were assigned a transmissivity of zero and thus were inactive and formed a no-flow boundary. Similarly, the lower boundary of the basin (the contact between the basin fill and the underlying bedrock) was simulated as a no-flow boundary. It was represented by the bottom surface of a layer in areas where that layer was not underlain by active blocks of a lower model layer. In all of these layers, the blocks outside the boundary were inactive, forming no-flow boundaries for adjacent or overlying blocks. Thus, thickness of basin fill (pl. 2) determined the areal extent of each layer.

RECHARGE

Within the no-flow boundaries, most of the perimeter of the basin was simulated as a specified-flux boundary to represent mountain-front recharge into the top layer. Slope-front recharge was simulated between the West Mesa and the Mesilla Valley. The locations and flow rates of the specified-flux nodes are shown in figure 25. Mountain- and slope-front recharge in the steady-state version was approximately equal to that estimated in the geohydrology section of this report. The estimated recharge for the Aden Hills and Sleeping Lady Hills was applied along the East Robledo fault as underflow.

Recharge in the transient version was applied at the same nodes as in the steady-state version (fig. 25), but the rate of recharge was adjusted to reflect the average precipitation during each pumping period for each node by the formula:

$$R = \frac{RS((PC_1 + PT_1) + (PC_2 + PT_2) + \dots + (PC_n + PT_n))}{2n \text{ PA}} \quad (3)$$

where

R is the recharge rate at the node for the pumping period, in cubic feet per second,

RS is the steady-state recharge rate at the same node, in cubic feet per second,

PC is the annual precipitation at Las Cruces, in inches,

PT is the annual precipitation at La Tuna, in inches,

1,2,... n are the years of the pumping period, and

PA is the long-term average annual precipitation at Las Cruces and La Tuna, in inches.

It was assumed that the recharge rate in the steady-state model reflected the long-term average precipitation and that the recharge rate during any given

pumping period would vary linearly with precipitation. The time-variable rate of recharge for the transient version is shown in figure 26A.

UNDERFLOW

Underflow through the flood-plain alluvium in Selden Canyon and El Paso Narrows was simulated with specified-head nodes where the heads approximated the altitude of the Rio Grande. The model-derived inflow rate at Selden Canyon was 0.15 cubic foot per second, and the model-derived outflow rate at El Paso Narrows was 0.09 cubic foot per second. Neither flow is significant compared to net irrigation flux and river leakage. Underflow through the bedrock was considered to be negligible. However, because the estimated mountain-front recharge was applied at the edge of the active part of the model, underflows in the vicinity of the East Robledo fault and in the vicinity of the bedrock high between the Mesilla and Jornada Basins were included by implication. Underflow was not simulated in layers 2–5 because it was assumed to be insignificant with respect to the magnitude of other flows into the system.

MESILLA VALLEY BOUNDARY

A complex boundary at or near the land surface in the Mesilla Valley was approximated by three overlapping boundary conditions. They were: (1) a head-dependent flux to approximate flow to and from the river and drains; (2) another head-dependent flux to approximate evapotranspiration from nonirrigated lands; and (3) a specified net irrigation flux to approximate the summation of effective rainfall and net diversions (positive) and evapotranspiration from irrigated lands (negative) (fig. 16, line E). By implication, pumpage for irrigation from layer 1 is included in this summation because evapotranspiration is accounted for directly.

Flow to and from the river and drains.—The location of flow to and from the river and drains is shown in figures 27 and 28. Only the Rio Grande was simulated in the steady-state version (fig. 27), following the alignment shown by Lee (1907), which apparently was natural and unaltered. Both the Rio Grande (stabilized alignment) and the complete drainage network were simulated in the transient version; the simulation covers the period beginning in 1915 (fig. 28).

The amount of flow ($QRIV$), in cubic feet per second, to and from the river and drains was calculated by the model at each river or drain node using the following equation:

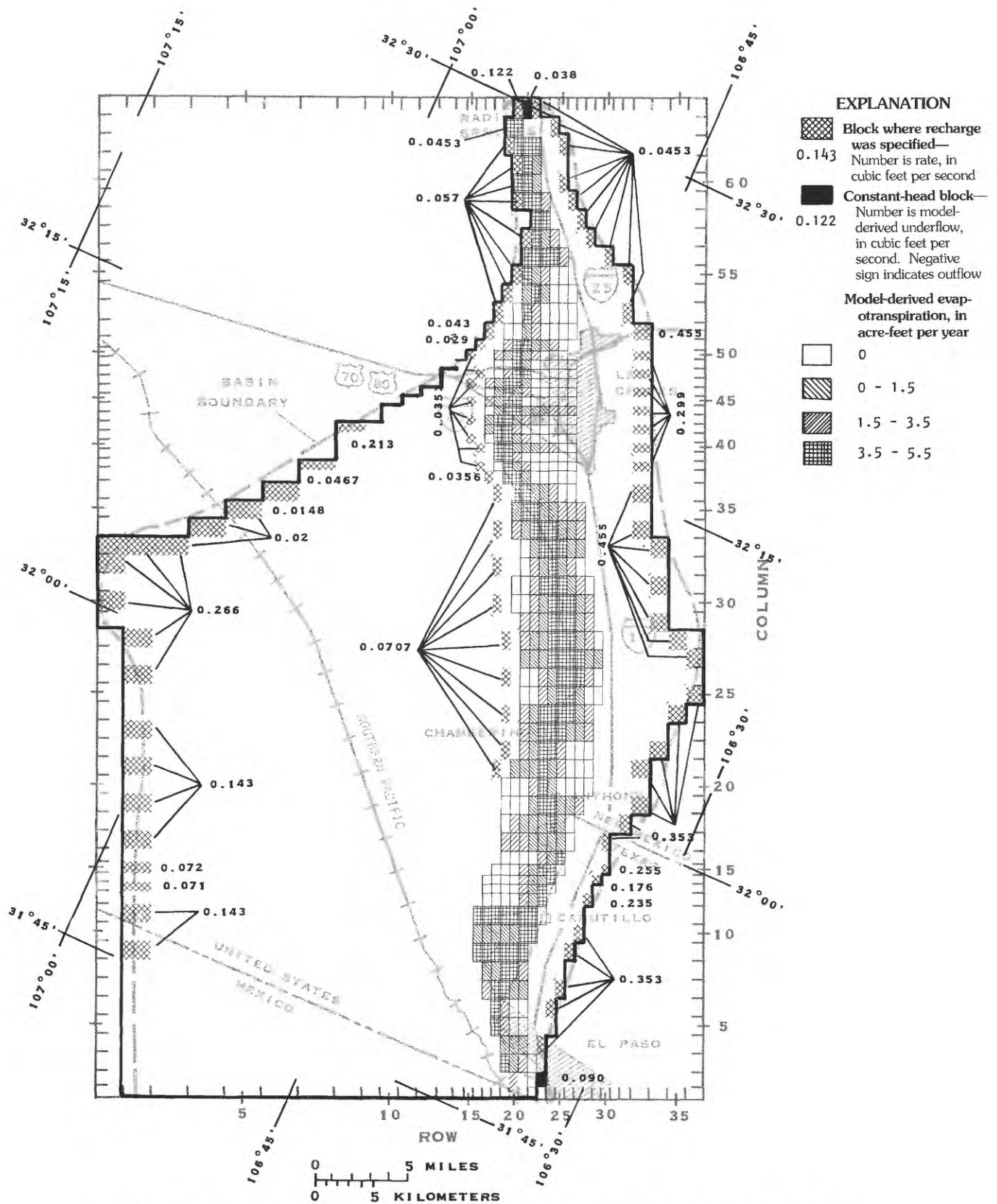


FIGURE 25.—Recharge, underflow, and evapotranspiration boundaries for layer 1, steady-state version.

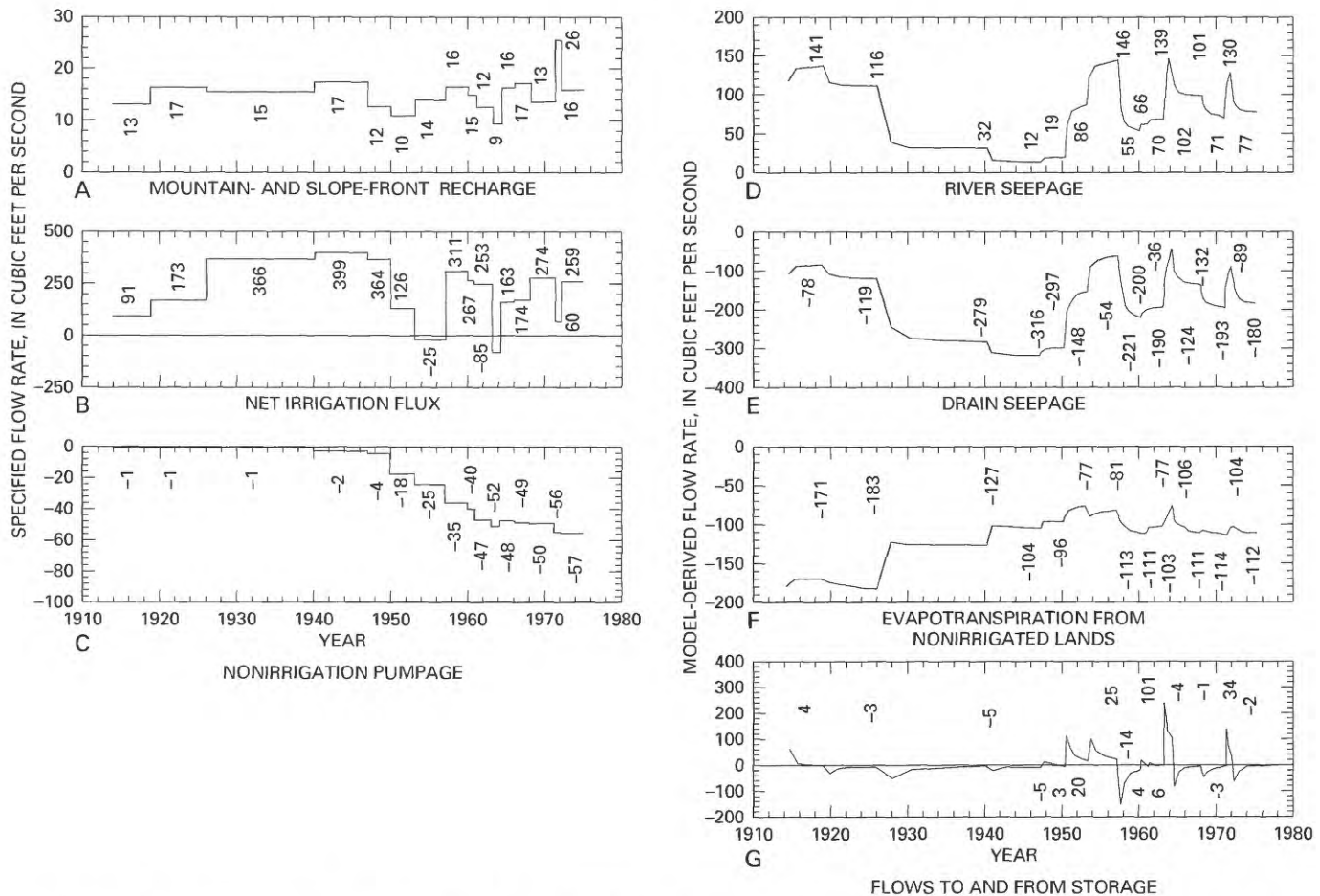


FIGURE 26.—Major basinwide flow rates, 1910–75. Values in graphs A–C are specified; values in graphs D–G are model derived.

$$QRIV = CRIV (HRIV - H) \quad (4)$$

where

$CRIV$ is a specified connection coefficient, in feet squared per second,

$HRIV$ is the specified head for the river, in feet, and H is the model-derived head in the aquifer, in feet.

Independent estimates of $CRIV$ could be derived from Darcy's Law if the model-block size were small with respect to the bottom and side areas of the stream. However, in this model, the block widths are about 200 times the drain widths, and block depths (saturated thickness of the top layer) are about 100 times the depths of the saturated sidewalls of the drains. These conditions may introduce a large discrepancy between the geometry of the simulated flow paths and the geometry that might actually exist in the vicinity of a drain. Instead of using Darcy's Law directly, an approach was taken that introduces a "correction" into the value of $CRIV$. The equation was solved for $CRIV$.

The head difference ($HRIV - H$) was set equal to 3 feet, which was the estimated average difference in altitude between the water table and water in the drains. This estimate was made by visual inspection of plates 4, 6, and 9 of Conover (1954). These plates show a cross-sectional view of the water table between the river and New Mexico State University for June 1927, the water table for drained and undrained areas for September 1919, and the water table between the river and Anthony Drain for July 1930. Generally, the water table was 2–5 feet above water levels in drains, but summer dates for all of these observations indicate that the water table in each case was near a seasonal high (Conover, 1954, p. 58). The flow rate, $QRIV$, for a given block was estimated as the average inflow rate per mile of drain times the length of drain in the block, in miles. The average inflow rate per mile was 1.4 cubic feet per second, calculated from records for the entire valley for 1923–50 (fig. 9). The effect of estimating $CRIV$ in this way is to force the model to calculate an average drain discharge given average hydraulic

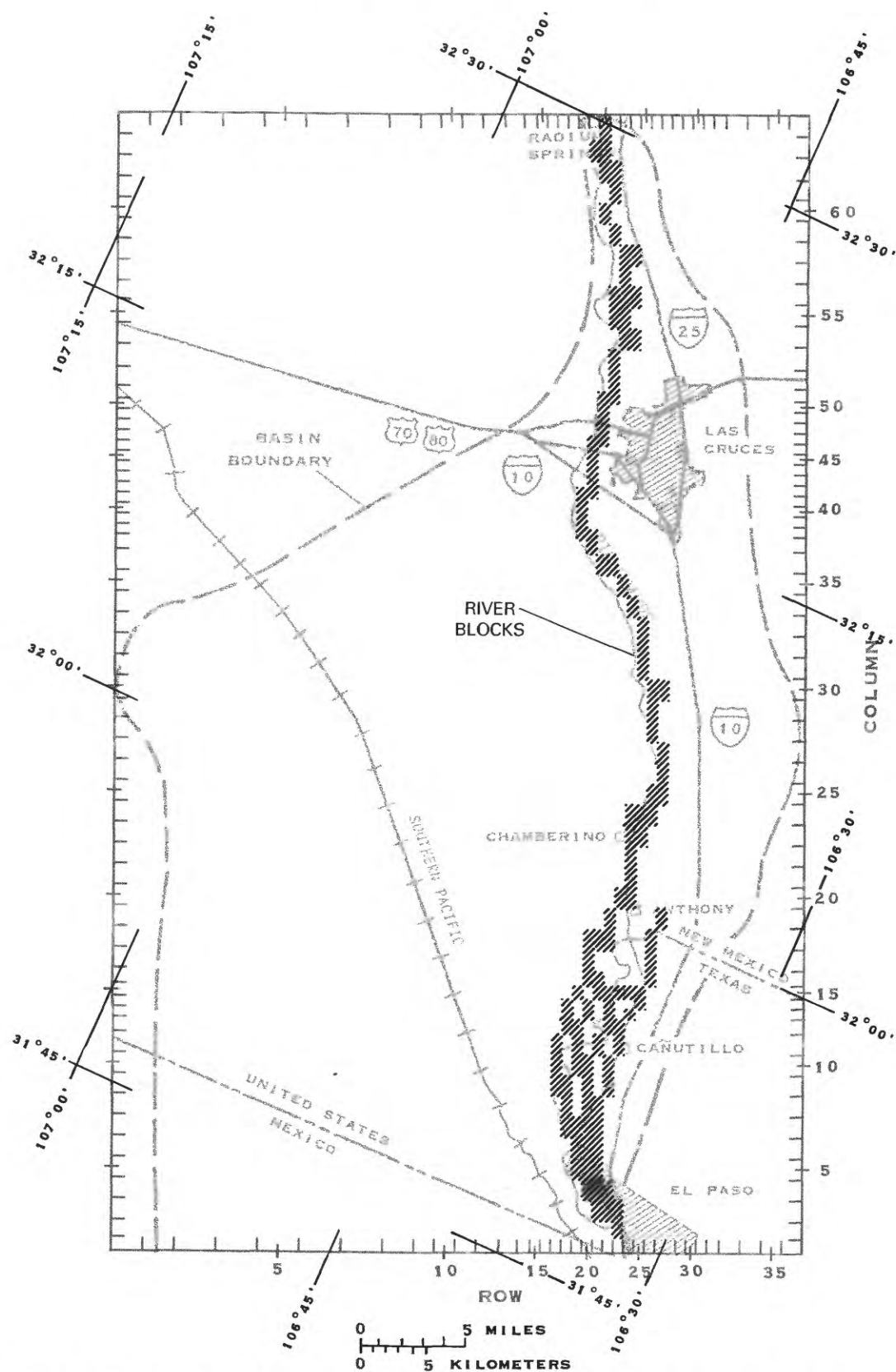


FIGURE 27.—Location of model blocks where flow to and from the prestabilized Rio Grande was simulated (steady-state version).

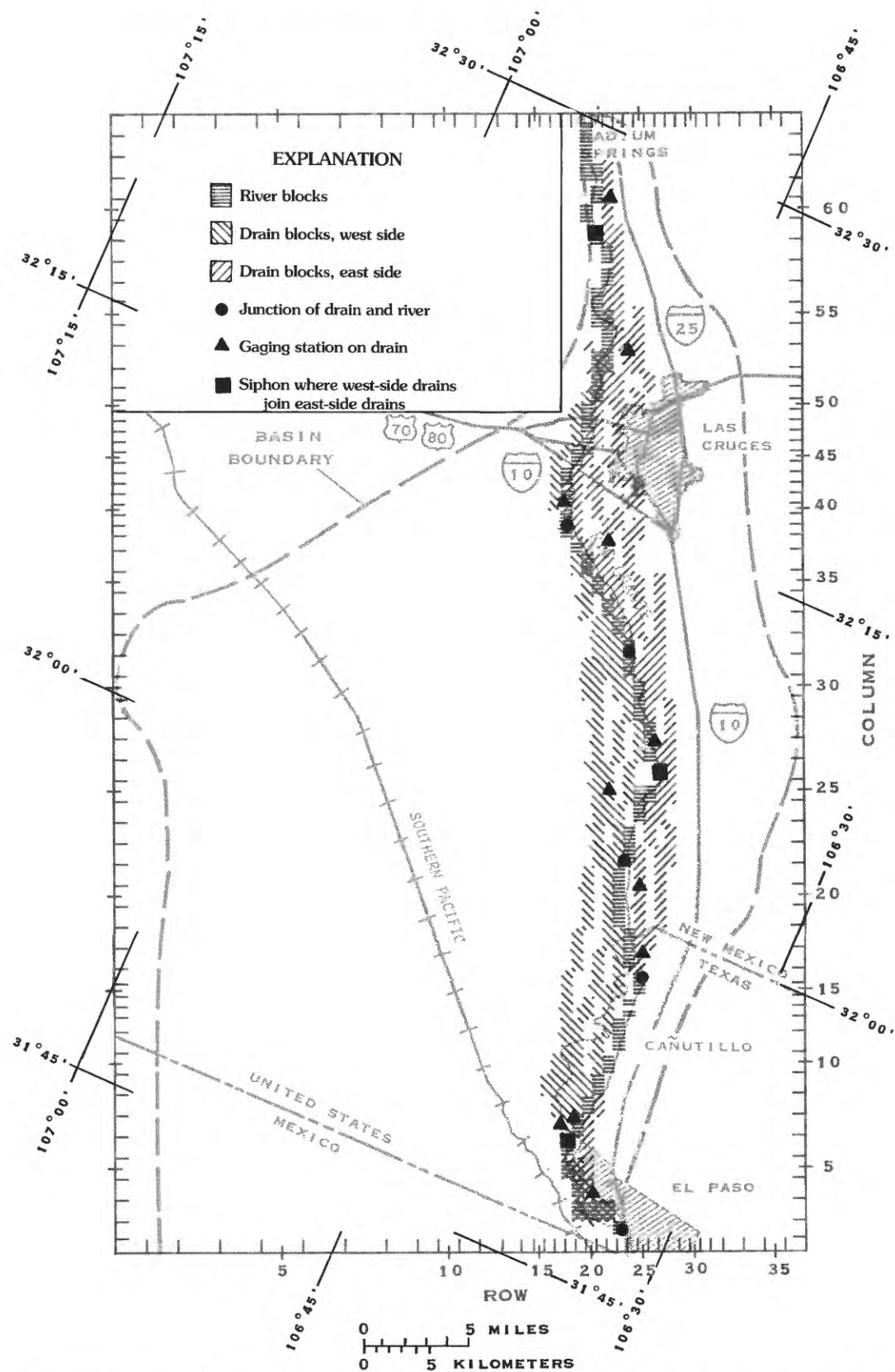


FIGURE 28.—Location of gaging stations and model blocks where flow to and from the stabilized Rio Grande and drains was simulated (transient version).

conditions. That is, *CRIV* is, in effect, an empirical quantity that may not be directly related to the hydraulic conductivity of a streambed or drain.

The values of *CRIV* for the Rio Grande (table 3) were estimated under transient conditions in a trial-and-error manner. They were about twice the values for drains for a given length of channel. However, if the width of the simulated river were 10 times the width of the simulated drains, then the equivalent leakance of the simulated river would be one-fifth of the leakance of a drain. It is reasonable to expect river leakance to be less than drain leakance because sediment-laden river water generally flows into the ground, plugging the river bottom, whereas clear ground water flowing into the drains tends to flush drain bottoms. The *CRIV* values used in the steady-state version were greater and were proportionate to the greater width of the river (Lee, 1907) so that the same leakance was represented.

The values of head assigned to the river (*HRIV*) were 2 feet greater than the riverbed altitude at each river node. A 42-foot datum correction was added to all altitudes on Lee's map (Filiberto Cortez, U.S. Bureau of Reclamation, oral commun., 1983) to obtain the altitude of the river for the steady-state version. For the transient version (stabilized river), topographic maps were used to estimate riverbed altitudes. These altitudes are considered to be accurate to within 2 or 3 feet because, on average, the river probably follows a smooth profile from one diversion dam to the next.

The hydraulic heads assigned to the drain nodes were selected from "condition profiles" of the U.S. Bureau of Reclamation. These profiles, dated 1956–60, show altitudes of the construction grade, cleaning grade, and water level above the same datum as was apparently used on Lee's (1907) map. Although these profiles probably represent the best information available, some judgment was required in selecting the altitudes. Generally, the water level was selected unless the drain was dry. The possible error in selecting altitudes usually was less than about 2 feet. The altitudes were converted to hydraulic heads (feet above sea level) by adding 42 feet. Profiles were not available for the Park or Mesquite Drains—heads were selected, in these cases, from adjacent drains.

The flow of water (*QRIV*) from the river or drain to the aquifer at a given node was limited in the model program to less than or equal to the amount of streamflow that was routed to the node from upstream nodes. That is, if the simulated stream was dry, no flow from the stream to the aquifer was simulated. The model program also provides for the flow to be limited directly to a specified maximum, but the maximum was set high (equivalent to about 6 cubic feet per second per

mile) so that it was never exceeded by the model-derived rate, *QRIV*.

Surface-water inflow was assigned to the farthest upstream river node for Selden Canyon. Realistic rates of surface-water inflow were used in order to allow for the possibility of the simulated river going dry. Also, realistic inflows allowed for simulation of outflows at El Paso Narrows that were used to calculate model-derived depletions. For the steady-state simulations, the surface-water inflow to the uppermost reach on the Rio Grande was arbitrarily set at an average value of 700 cubic feet per second (the approximate average measured streamflow for 1898–1904) (Lee, 1907, p. 32). For the transient simulations, surface-water inflow consisted of the average measured discharge at Leasburg for a given pumping period less net diversion and an estimated evapotranspiration from the river channel and drains of 22 cubic feet per second.

The fact that part of the net diversion took place at Mesilla instead of at Leasburg was not something for which we accounted. This was not considered to be critical because the only possible effect would occur if the simulated river were to go dry between Leasburg and Mesilla Dams. It did not.

Evapotranspiration from nonirrigated lands.—Evapotranspiration from nonirrigated lands in the Mesilla Valley was simulated as a flux that depended on the difference between the model-derived water-table and land-surface altitude at each node. Where the water table was at or above land surface, a maximum rate of 5.5 acre-feet per year per acre of nonirrigated land was simulated. A rate of zero was simulated where the water table was 15 feet or more below the land surface. Between the two limits, the rate of evapotranspiration was proportional to the difference between the model-derived head and the land surface. Land surface for the steady-state version was taken from Lee (1907, pl. X). The model-derived evapotranspiration for the steady-state version is shown in figure 25.

The evapotranspiration flux was also applied over the entire valley area for pumping periods 2 through 16 of the transient version. However, evapotranspiration was intended to apply only to nonirrigated land, so to avoid overestimating it, the maximum evapotranspiration rate of 5.5 acre-feet per acre was adjusted by a factor equal to the nonirrigated acreage divided by the total valley acreage. A similar adjustment was made for pumping period 1 for the area north of Anthony because it was assumed that the area south of Anthony was not irrigated during this period. Because the flux depended on model-derived heads, it was neither uniform over the valley area nor constant in time. The model-derived, valleywide flow rate is shown in figure 26F. The simulated flux for 1975 ranged from

0 to 1.7 acre-feet per year per acre over the entire valley area (fig. 29). However, this discharge only occurs on nonirrigated lands. In 1975, out of a total valley area of 110,000 acres, about 75,000 acres were irrigated (fig. 6). If it is assumed that stream areas totaled 3,000 acres, there were about 32,000 acres of nonirrigated lands. The model-derived evapotranspiration rate (fig. 26F) was about 110 cubic feet per second or 2.5 acre-feet per year per acre.

Evaporation from streams.—Evaporation from streams was estimated independently from the ground-water model in order to compare depletions calculated from model-derived streamflows with those calculated from measured streamflows. The estimated evaporation from canal surfaces of 4,000 acre-feet per year was subtracted from annual net irrigation diversions. The total estimated annual evaporation from the river and drains of 16,000 acre-feet per year (22 cubic feet per second) was added to depletions calculated from model-derived streamflows.

Net irrigation flux.—The net sum of irrigation-return flow to the ground water, canal leakage, effective rainfall, and agricultural pumpage of ground water was represented by a specified flux over the entire valley for pumping periods 2–16. For pumping period 1, the flux was applied only to the area of the valley north of Anthony (fig. 29). In this case, it was assumed that all irrigated acreage was north of Anthony. This assumption was based on the braided stream network of Lee (1907) and on the hypothesis that naturally wet conditions existed in the lower Mesilla Valley due to ground-water upflow. Also, Barker (1898) showed the irrigation canals extending only slightly south of Chamberino. The flux (fig. 16, line E) was averaged within each pumping period (fig. 26B). In figure 26B, the flow rate is shown for the entire valley area. The larger values (250–400 cubic feet per second) represent times of plentiful surface-water supplies for irrigation, and the smaller values (25–85 cubic feet per second) represent times of drought. Negative values occur when simulated irrigation pumpage exceeded infiltration of irrigation water.

GROUND-WATER WITHDRAWALS

Nonagricultural withdrawals were applied at the center (node) of the block in which they occurred (table 4). The withdrawals were averaged for each pumping period. The total nonirrigation withdrawals are shown in figure 26C, which is comparable to line E in figure 17. The values in table 4 are cumulative for each node; hence, the amount that is withdrawn from an individual well is not indicated. Withdrawals at small

towns and villages were assumed to have occurred near the center of each community if the location of the well was not known.

The distribution of withdrawals at Las Cruces may be important to the shape of the cone of depression within the well field. The time of service was estimated (fig. 30) from data in Conover (1954), Dinwiddie and others (1966), and Wilson and others (1981). The total withdrawals were distributed evenly between wells that were thought to be in service during any given time.

The simulated return of nonirrigation withdrawals depended on the type of sewage disposal system. Leach fields were assumed to have been in use unless there was reason to believe another system was used. Return flows by leach-field systems to the shallow ground water were simulated by positive values of withdrawals for layer 1. These return flows tended to offset withdrawals from layer 1. In places where reported withdrawals were mainly from deep wells (layer 2), withdrawals were simulated as negative values for layer 2, and returns were simulated as positive values for layer 1. Return flows by the Las Cruces disposal system were routed to the head of river reach 5 near Mesilla in the amount of 50 percent of the Las Cruces pumpage rate. No return was simulated for water withdrawn from the Cañutillo well field by the city of El Paso because this return was assumed to have occurred downstream from El Paso outside the modeled area. Also, return was not simulated for water withdrawn by major industries and subdivisions in the lower Mesilla Valley because the water was assumed to have evaporated from sealed ponds or returned either to drains or the river where it would constitute a negligible part of surface-water discharge.

MODEL ADJUSTMENTS

The goal of model adjustment was to make model-derived values, such as hydraulic heads, match measured values reasonably well while keeping other simulated properties, such as hydraulic conductivity, plausible. That is, values of any given property should fall within the range of error in the estimate of that property.

SYSTEM PROPERTIES USED FOR COMPARISON

Measured values of head, depletion, and drain discharge were compared with model-derived values. The fit between measured and model-derived values was judged to be reasonably good overall, given the accuracy of measured data.

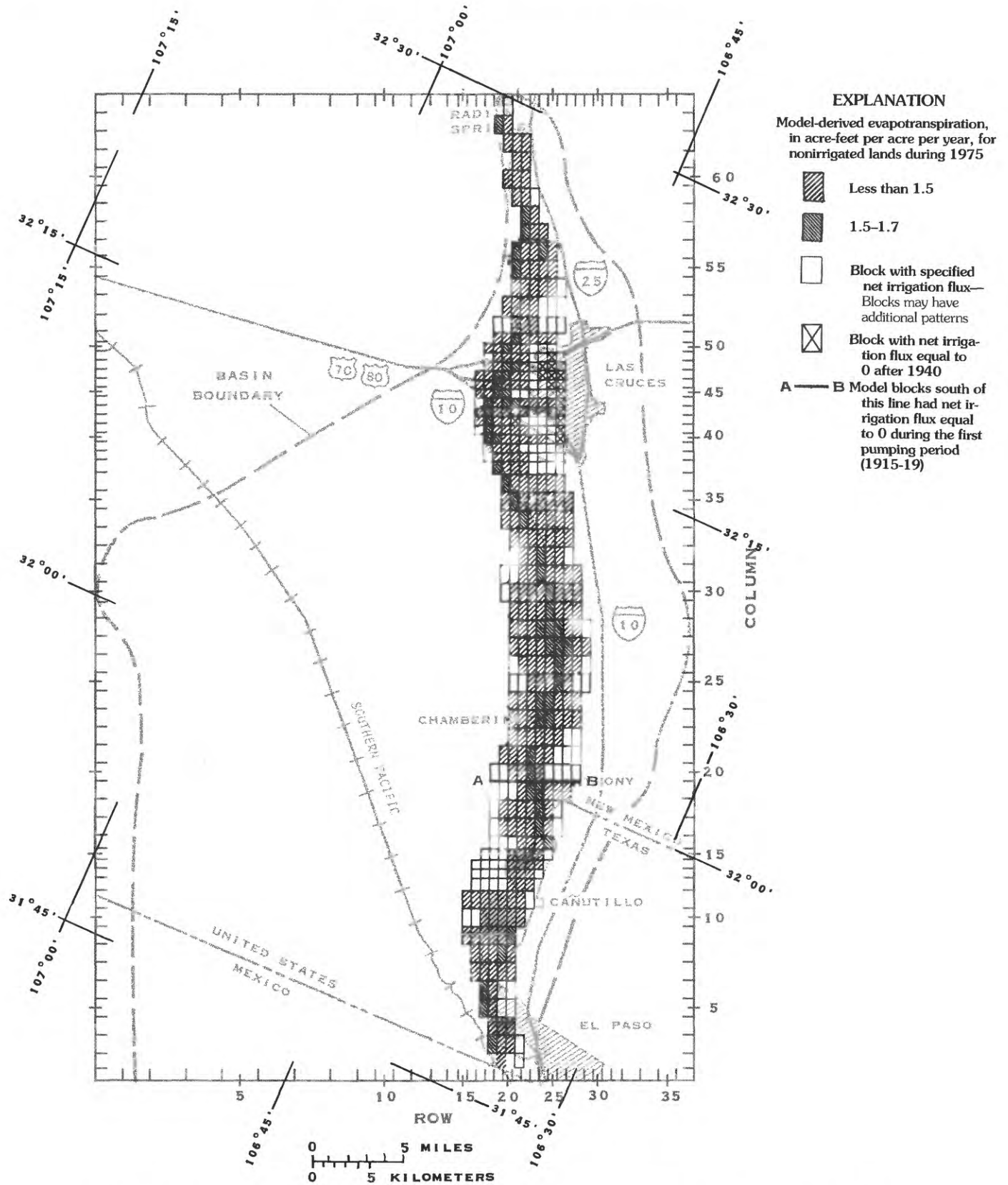


FIGURE 29.—Model-derived evapotranspiration from nonirrigated lands for 1975 and area of net irrigation flux.

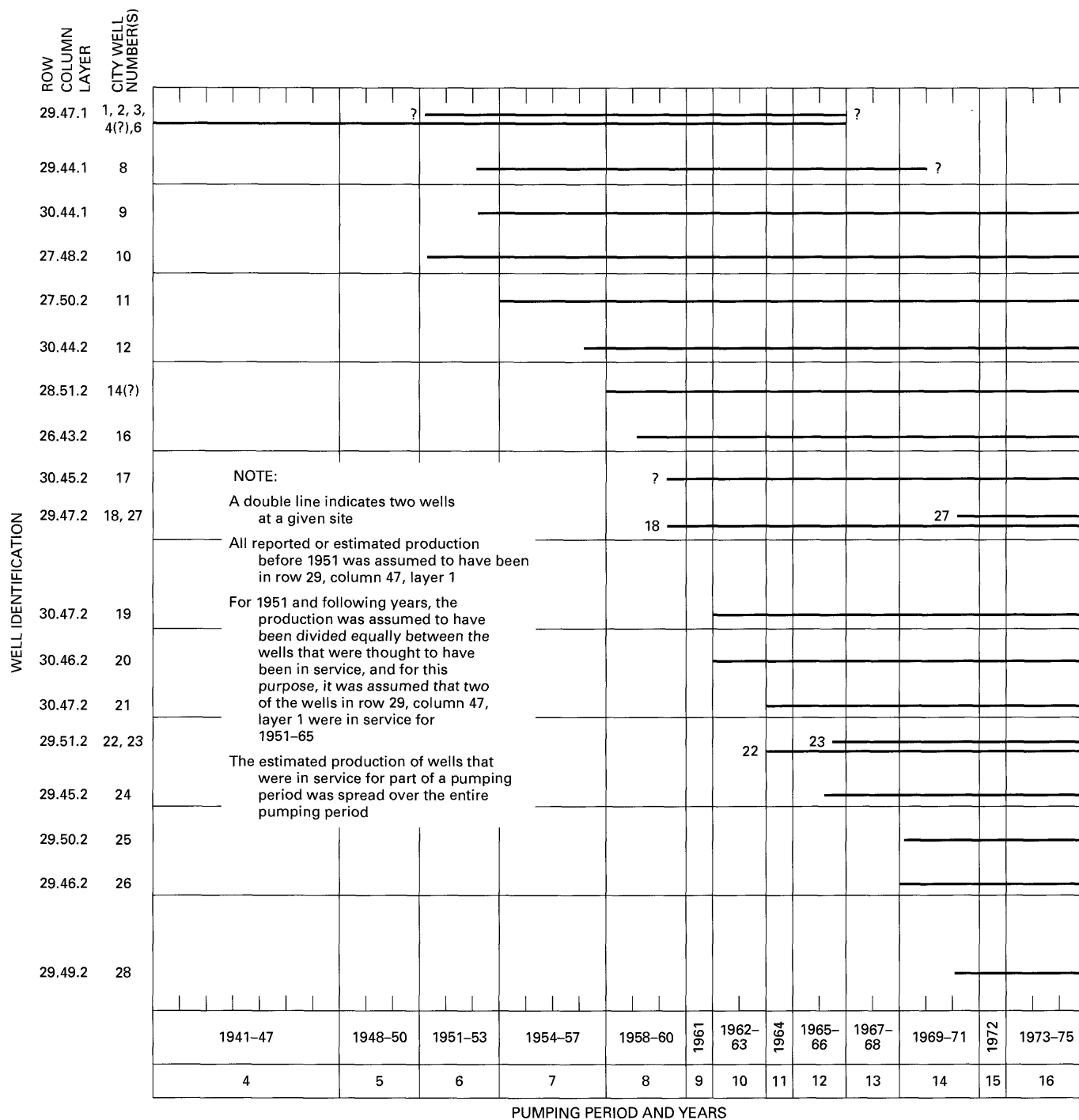


FIGURE 30.—Estimated time of pumpage for wells in the Las Cruces well field.

HYDRAULIC HEADS

The model was adjusted so that model-derived heads for the steady-state version matched conditions that existed during 1905-6. This period was chosen for three reasons. First, it was prior to construction of Elephant Butte Dam and Elephant Butte Irrigation

District drains. Second, the period was prior to pumpage of large amounts of ground water. Third, valley water levels for this time are shown on a map by Lee (1907, pl. X) and may be compared with model-derived levels. Measured heads in wells from later dates were selected for comparison with model-derived heads

outside the valley and for deep layers in the valley. The criteria for selection of wells were: (1) The perforated interval was primarily within the interval represented by a particular model layer; (2) the water level was measured, not reported, and represented near-static conditions; and (3) the water level represented predevelopment conditions as closely as possible—early dates for layers 2 and 3 beneath the valley, any date (preferably 1975 or 1976 from data in Wilson and others, 1981) for areas distant from the valley.

The model was adjusted so that model-derived heads for the transient version would match measured and reported heads in and near the valley for the winters of 1947–48 (Conover, 1954) and 1975–76 (Wilson and others, 1981). The time requirement was relaxed for areas outside the valley: any heads measured during the 1940's were assumed to be representative of 1947, and similarly, any heads measured during the 1970's were assumed to be representative of 1975.

Measured and model-derived heads are shown for comparison in table 5, in figures 31–35, and in the lines marked "STANDARD" in table 8. The comparison was judged to be reasonably good on the basis of the following discussion.

The degree of fit that may be expected between measured heads and corresponding model-derived heads depends partly on the accuracy of the measured heads. Measured heads generally have an error of 5 to 15 feet because they are derived from a land-surface datum that is estimated from topographic maps. Beyond this, a measured head may be accurate; however, if it represents local conditions that cannot be simulated because of the resolution in a regional model, the degree of fit may not be good. That is, the actual well location generally is not at the center of a block, and the measured head at that well will differ from the model-derived "average" head for the entire model block.

The location of measured heads and heads estimated from plate X of Lee (1907) and the model-derived heads and the differences between the two for each location are shown in table 5. Differences are as great as 74 feet, but most are less than 10 feet. Average differences are shown in table 8 on the lines marked "STANDARD." The average difference between model-derived heads and measured heads should be small because errors in measured heads, being random in nature, tend to cancel each other. The average differences shown are calculated in several ways. The arithmetic mean is the sum of all the differences, both positive and negative, divided by the number of sites. A non-zero arithmetic mean may indicate that the model-derived potentiometric surface may be generally too high or too low. The median also reveals the overall goodness of fit

without showing extreme differences, whereas the root-mean-square difference accentuates extreme differences. The root-mean-square difference is the square root of the mean of the squares of the differences. The mean-absolute difference is the arithmetic mean of the absolute values of the differences. It shows the overall goodness of fit without allowing positive and negative values to cancel each other, but it does not reveal a high or low bias in the model-derived surface.

Comparisons of measured and model-derived hydraulic heads are shown by hydrographs in figure 36 in which the solid lines indicate measured heads and the lines with boxes show model-derived heads. The goal of model adjustment was to simulate changes in head by matching the shapes of the hydrographs. Hydrographs of model-derived heads could be as much as 15 feet more than or less than corresponding hydrographs of measured heads in wells except those wells in well-field areas. (For brevity, further reference to hydrographs of model-derived or measured heads will be as model-derived or measured hydrographs.) In the hydrographs at well fields, the potentiometric surface is likely to have small drawdown cones for individual pumping wells within the larger well-field drawdown cone. The small cones would not be defined by the model-derived potentiometric surface because of the size of the model-grid blocks. Therefore, model-derived drawdowns may not be as great as measured drawdowns. The same principle applies to the time dimension. That is, seasonal variations are not simulated because pumping periods were for a year or longer. Following this rationale, model-derived hydrographs were expected to approximate only the highest points of the measured hydrograph—this is generally the case in figure 36.

The approximate horizontal extent of drawdown cones at Las Cruces and Cañutillo is shown in figures 37 and 38 along with potentiometric surfaces that might have existed in 1975 without nonirrigation withdrawals (i.e., no municipal, industrial, or domestic withdrawals). The potentiometric surfaces in figures 37 and 38 were derived by the model with nonirrigation withdrawals set to zero. The lines of equal drawdown were derived by comparing the potentiometric surface in figure 34 with that in figure 37 and the potentiometric surface in figure 35 with that in figure 38. This procedure leads to the assumption that no significant change in transmissivity resulted from simulated-head changes in layer 1. The lines of equal drawdown near Las Cruces are questionable because drawdowns in the well field (fig. 36) were not well simulated. Nevertheless, the lines of equal drawdown

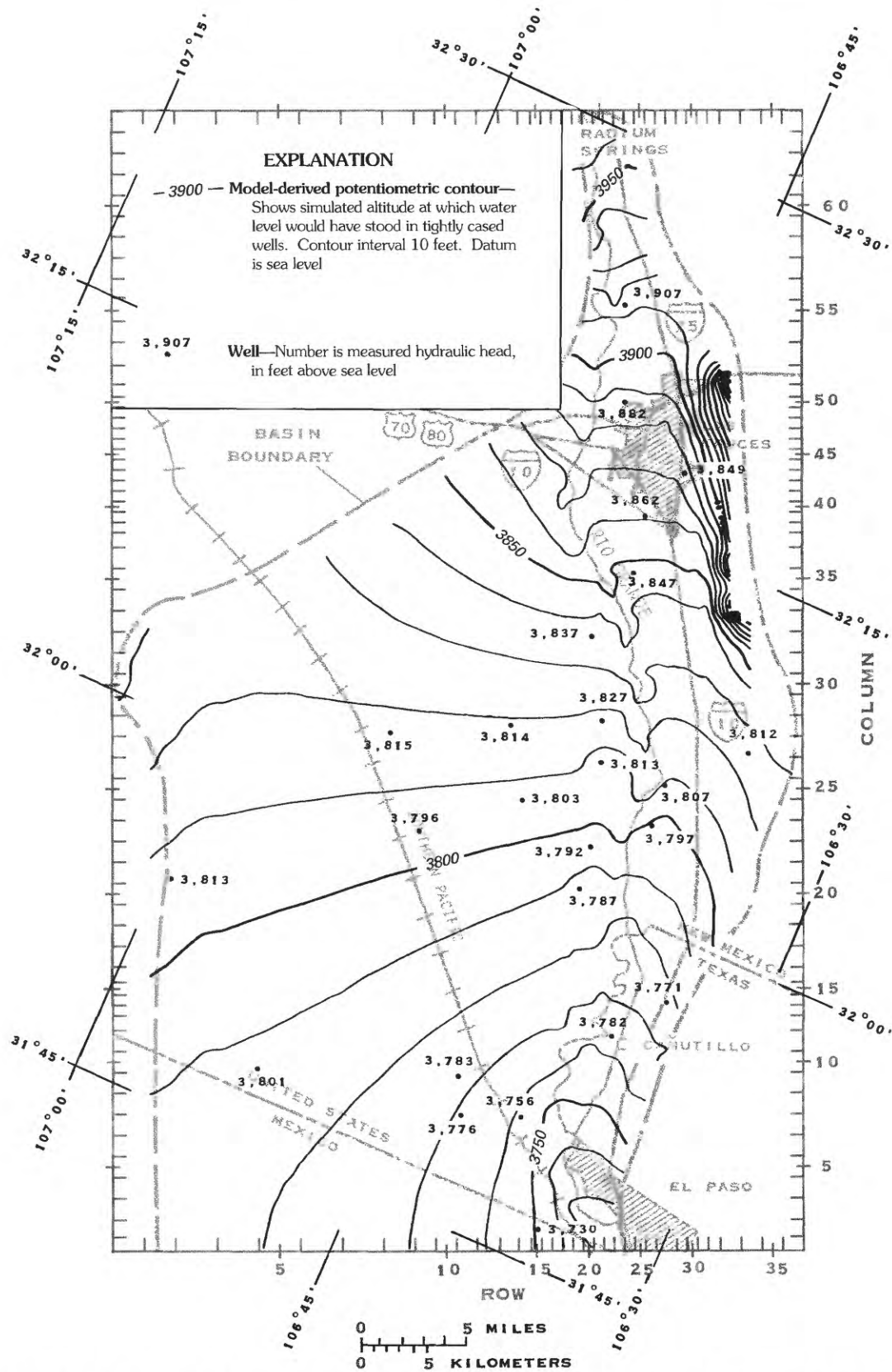


FIGURE 31.—Comparison of measured hydraulic heads and model-derived steady-state potentiometric surface, layer 1.

SOUTHWEST ALLUVIAL BASINS RASA PROJECT

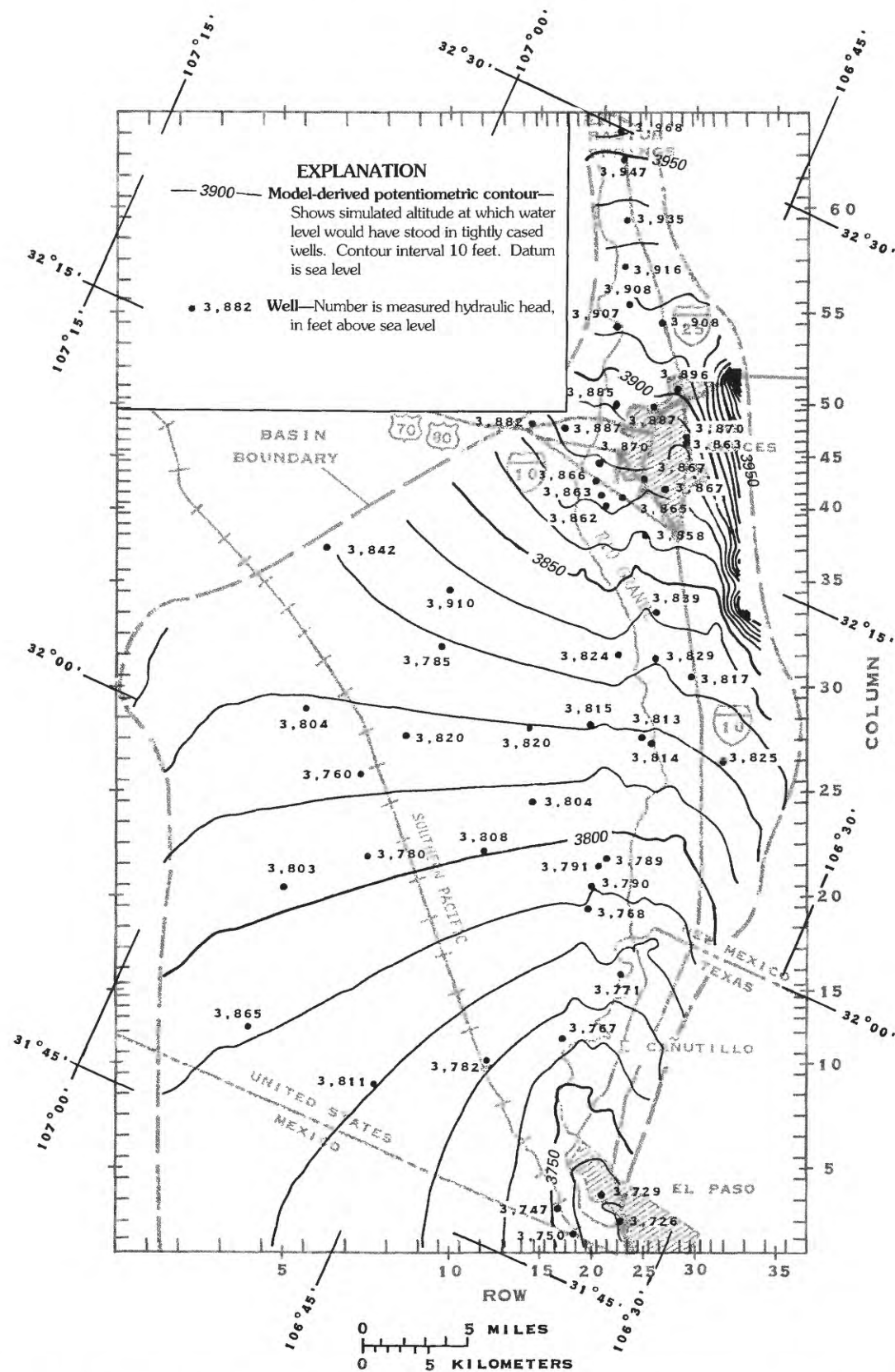


FIGURE 32.—Comparison of measured hydraulic heads and model-derived potentiometric surface for 1947–48, layer 1.

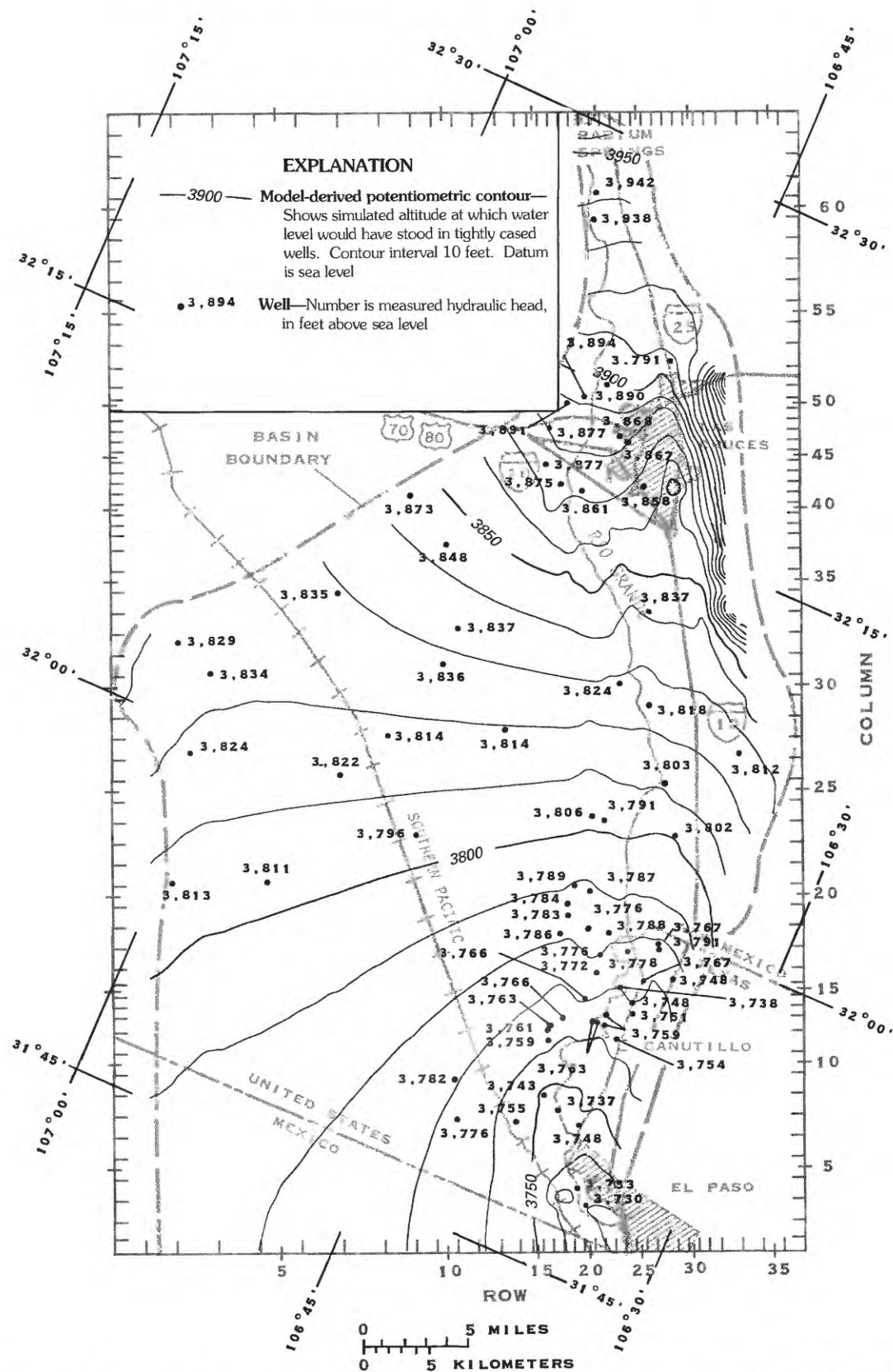
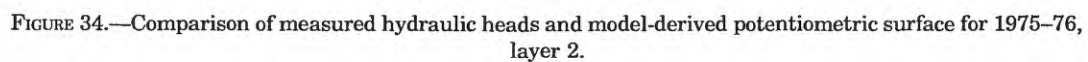


FIGURE 33.—Comparison of measured hydraulic heads and model-derived potentiometric surface for 1975-76, layer 1.



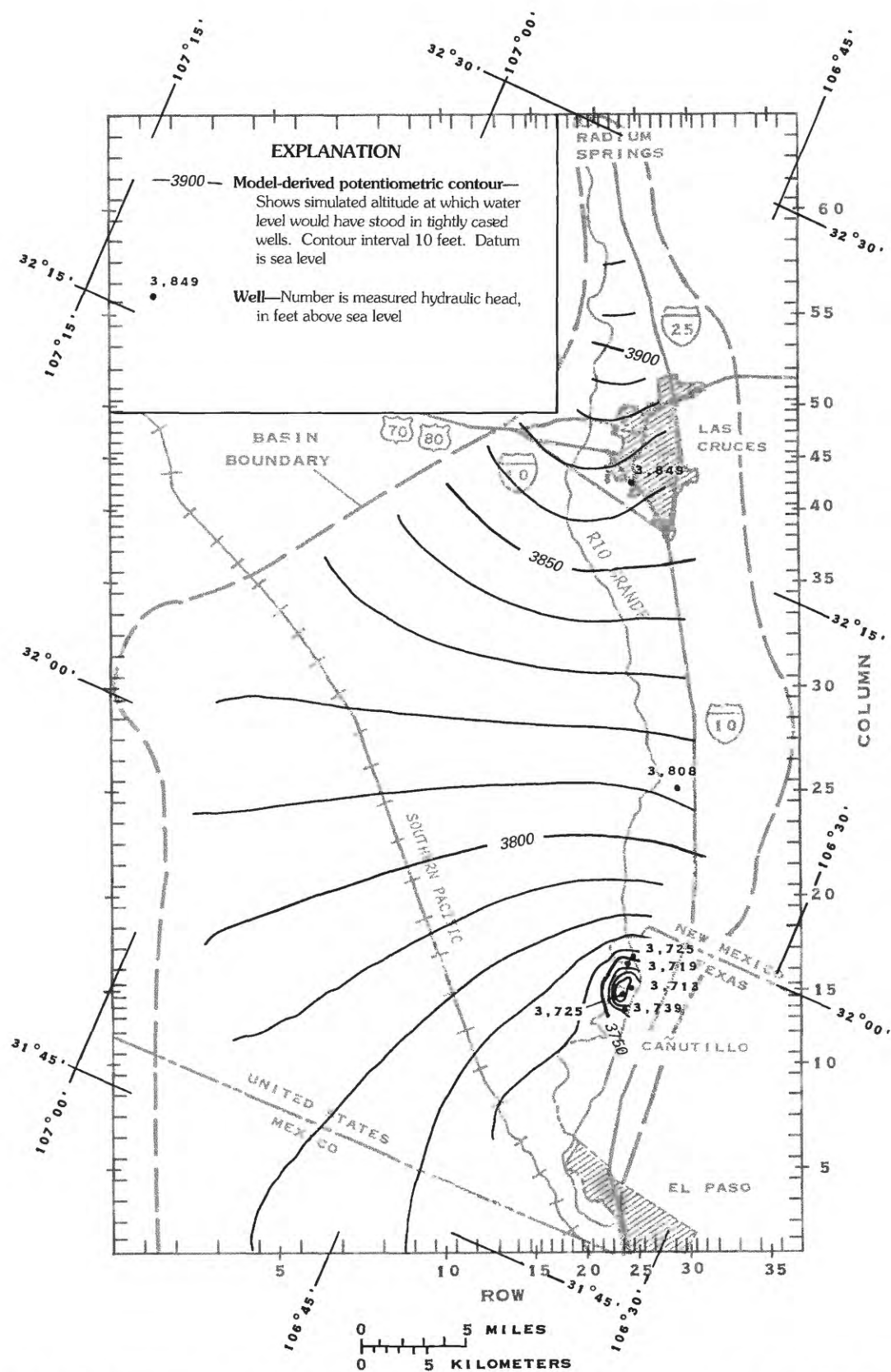
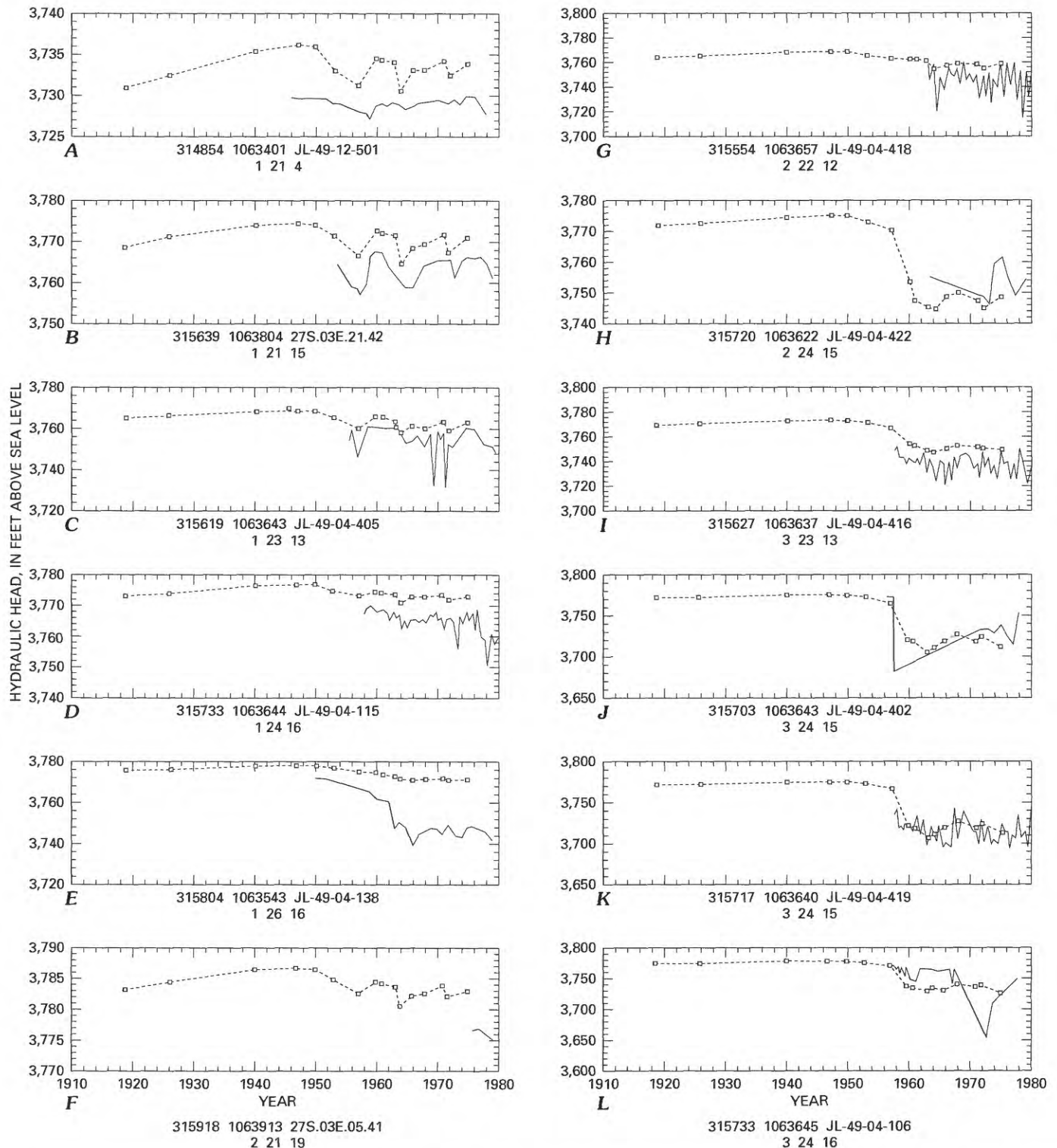


FIGURE 35.—Comparison of measured hydraulic heads and model-derived potentiometric surface for 1975-76, layer 3.



give an approximate indication of drawdowns that might be expected several miles from the well fields.

SURFACE-WATER DEPLETIONS

Annual surface-water depletions in the Rio Grande were calculated in two ways. The measured discharge

at Leasburg minus the measured discharge past the El Paso Narrows is referred to as "measured" depletion in figure 39. Depletion also was calculated from the model-derived discharges at Leasburg and El Paso Narrows (fig. 39) and is referred to as "model-derived" depletion (fig. 39). The depletion comparison provides a measure of model accuracy, but errors may tend to

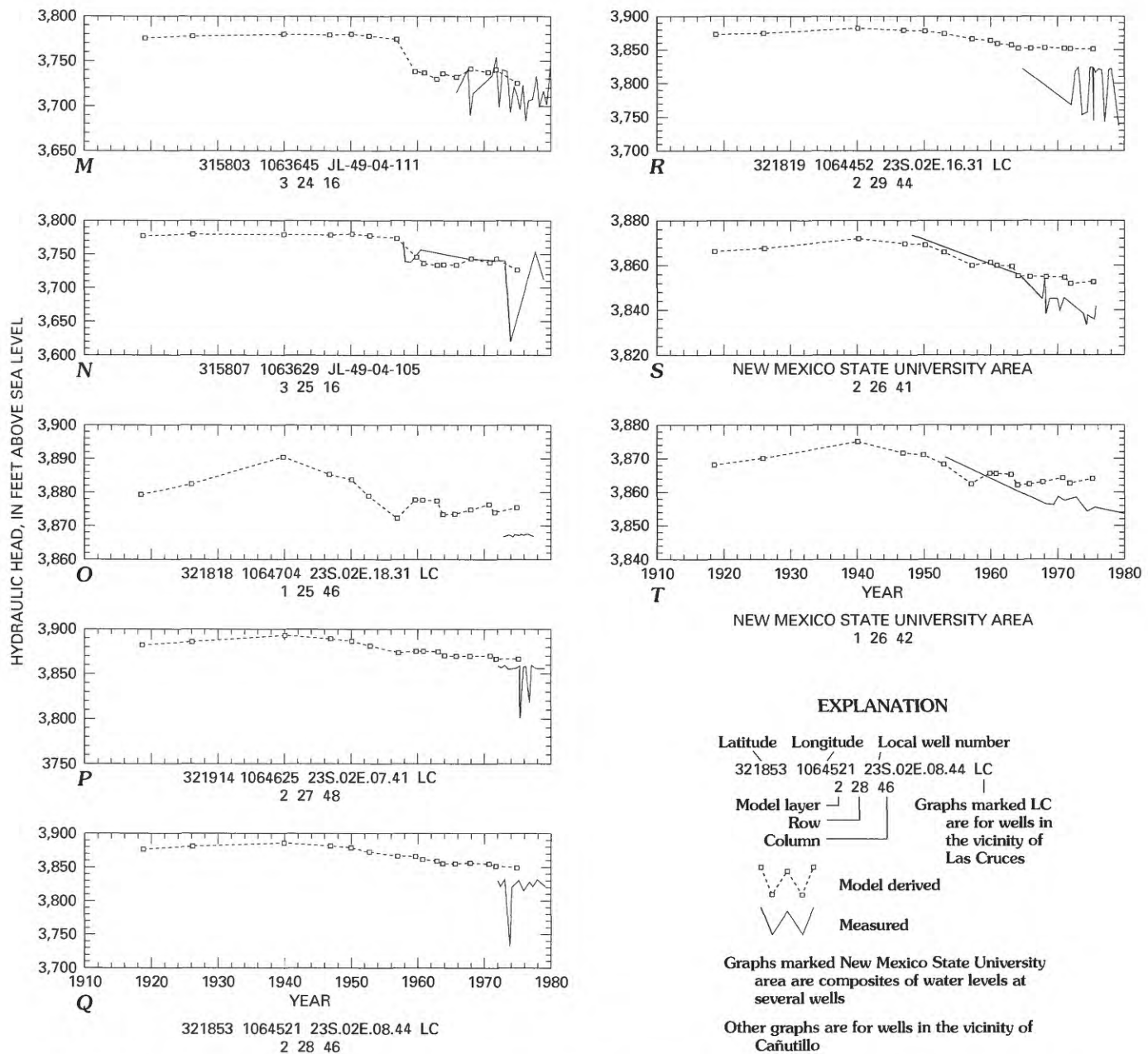


FIGURE 36 (above and facing page).—Comparison of hydrographs of measured and model-derived hydraulic heads, 1910–80.

offset each other. For example, if agricultural evapotranspiration were underestimated and other evapotranspiration properties were overestimated, or if recharge were underestimated, the model could be in error even if the depletion comparisons were close.

The measured depletions were calculated from streamflow measurements that were considered to be good. It was assumed that they might be in error by 5 percent for a given year. However, during a long period of time, if errors of measurement were assumed to be random, the accumulated error might be near zero.

The goal of model adjustment was to have model-derived depletions be within plus or minus 5 percent of measured depletions.

Model-derived depletions tend to be less than measured depletions during early years but greater during later years (table 7). No property was identified during the sensitivity analysis that affected this trend appreciably. The total measured depletion for 1941–75 was 7,701,000 acre-feet, and the model-derived depletion was 8,110,000 acre-feet, a 5-percent overestimate.

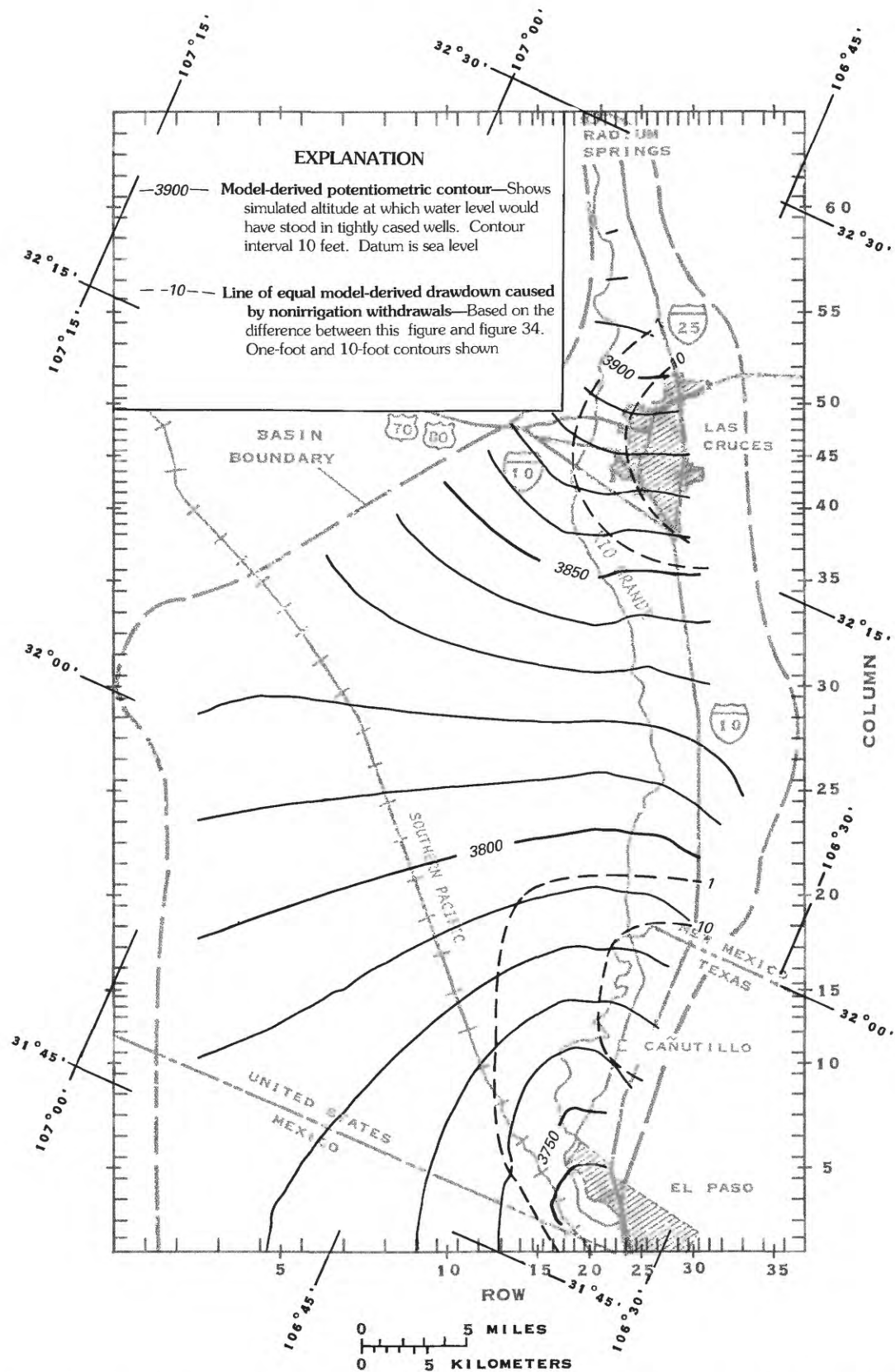


FIGURE 37.—Potentiometric surface (for 1975-76, layer 2) that might exist without nonirrigation withdrawals. Also shown are model-derived lines of equal drawdown near major well fields.

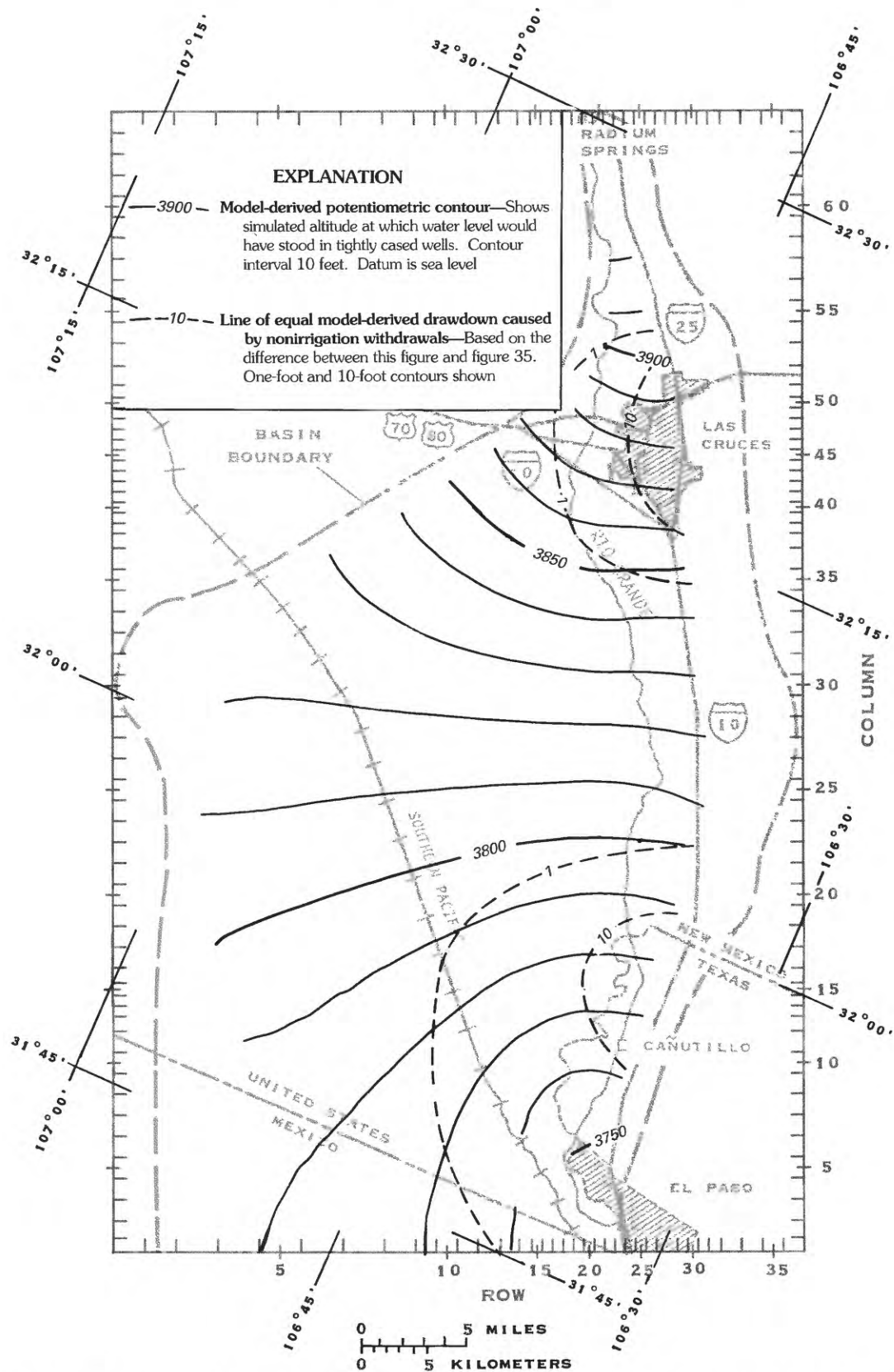


FIGURE 38.—Potentiometric surface (for 1975–76, layer 3) that might exist without nonirrigation withdrawals. Also shown are model-derived lines of equal drawdown near major well fields.

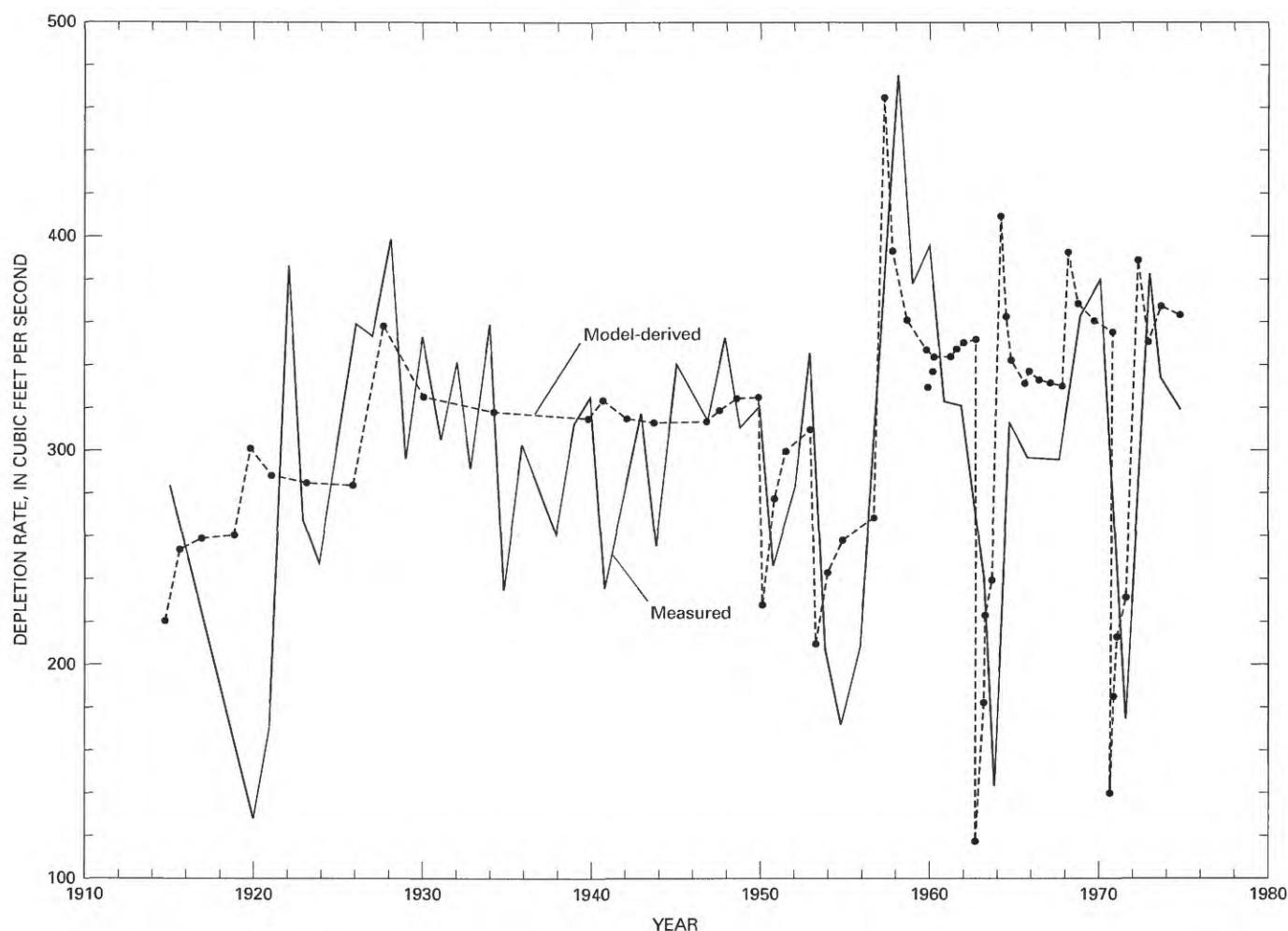


FIGURE 39.—Annual surface-water depletions calculated from measured discharges compared to depletions calculated from model-derived discharges.

DRAIN DISCHARGES

Measured and model-derived drain discharges were compared at 11 sites (fig. 40). The model-derived discharges are the flow rates for the end of each time step. The average annual measured discharges may be thought of as discharge hydrographs if it is understood that they do not indicate a continuous curve for time increments of less than a year for measured discharges. The goal of model adjustment was to simulate the shape of the measured discharge hydrographs. Precise simulation was not considered to be critical partly because the measurements were considered to be poor. It was assumed that they might be in error by 20 percent for the large discharges and by more than 20 percent for the small discharges. This assumption was based on the occurrence of slow velocities, backwater conditions, and vegetation that ordinarily affect measurement of low-gradient streams. A close match of measured and simulated discharges was expected to be somewhat less likely at small-discharge

sites than at large-discharge sites because small-discharge sites tend to represent short channels and local geologic conditions. The assumption of a uniform leakance in the calculation of specified values of *CRIV* may not have been appropriate in these particular cases. The sawtooth shape of the model-derived hydrographs mainly is due to the effect of the combination of net irrigation flux (fig. 26B), which was specified for each pumping period, with model-derived flow to and from storage and flow to head-dependent evapotranspiration, which was calculated with each time step. Because figure 26B does not represent the more jagged line E in figure 16, the curvature of the model-derived hydrographs that occurs between pumping periods is an artifact of the model. This was not considered to be a serious problem.

SYSTEM PROPERTIES ADJUSTED

Recharge rates, hydraulic conductivity, specific yield, and the Mesilla Valley boundary were adjusted.

The Mesilla Valley boundary represents a combination of streams and net irrigation flux.

RECHARGE

Recharge rates around the perimeter of the basin were at first generated by specifying the hydraulic head at each site (fig. 25) and letting the model calculate the recharge rate on the basis of values of

hydraulic conductivity under steady-state conditions. These model-derived flow rates were considered to be plausible with respect to estimates made independently. The specified-head boundary was then changed to the specified-flux boundary shown in figure 25 using the model-derived fluxes in order to allow the head to fluctuate under transient conditions. The same fluxes were used in subsequent steady-state versions of the model without further adjustment. These fluxes were

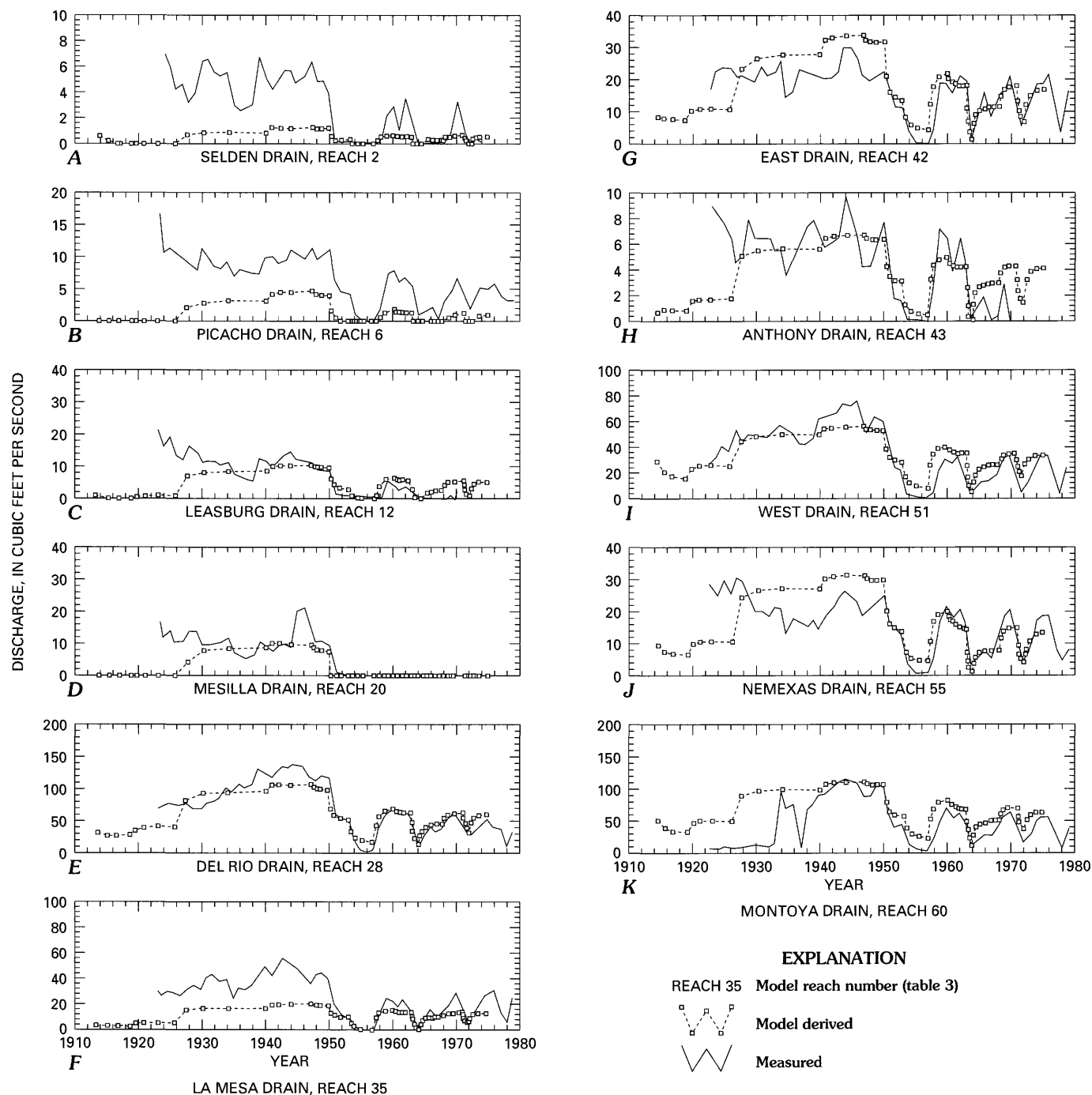


FIGURE 40.—Comparison of hydrographs of measured and model-derived drain discharges, 1910–80.

varied proportionately to precipitation for the transient version. Recharge rates estimated for the Aden Hills area were applied as specified fluxes along the East Robledo fault.

HYDRAULIC CONDUCTIVITY

Values of horizontal hydraulic conductivity were changed slightly from starting values. An exception to this was layer 3, where starting values of hydraulic conductivity were about the same as in layer 1 (about 22 feet per day for the Santa Fe Group). They were decreased to 8 feet per day after figure 13 was developed. This change generally improved the head simulation, but drawdowns were too great for layer 3 in the Cañutillo well field. The hydraulic conductivity in layer 3 in the lower Mesilla Valley area then was increased to 13 feet per day, consistent with the transmissivity reported by Leggat and others (1962, p. 32). The hydraulic conductivity for layer 2 was reduced from about 22 feet per day to 18 feet per day in order to simulate more drawdown in the Las Cruces well field.

The values of vertical hydraulic conductivity were increased during the adjustment phase. Originally, they were specified as one three-hundredth of the horizontal hydraulic conductivity at a given model block, reflecting the opinion that a layered sand and clay aquifer would be highly anisotropic. They were increased to one two-hundredth of the horizontal hydraulic conductivity in order to simulate less drawdown in the Cañutillo well field.

SPECIFIC YIELD

Specific yield was adjusted from 0.2 to 0.15 and back to 0.2. The effect of the smaller value was that model-derived drain discharges and heads for 1964 were lower—this did not improve the comparison with measured data.

MESILLA VALLEY BOUNDARY

Heads specified for the river were increased by 2 feet to simulate less flow from the aquifer to the river and, hence, more drain discharge. This change was accomplished at the expense of higher simulated heads for the valley, making head comparisons worse. An alternative would have been to decrease heads specified for the drains. A slight, 1- to 2-foot positive bias in model-derived heads as opposed to measured heads was not considered to be critical to the model.

The connection coefficient (*CRIV*) for flow to and from the river originally was set at about 10 times that of the drains, based on the assumed effective width of the river being 10 times the width of the drains. This value was reduced to about twice that of the drains to

reduce the model-derived heads in the Cañutillo area. The change was not very effective, but the lower value was retained because it was theorized that the riverbed might be more plugged than the drain bottoms. The value of *CRIV* for the drains was adjusted slightly but was eventually set back to near the original estimate.

The net irrigation flux was set to zero for the part of Las Cruces situated in the valley for 1941–75 in order to increase model-derived drawdowns for the Las Cruces well field. Drawdowns were increased slightly by 2 to 5 feet. The rationale for this adjustment was that access to ditch water may no longer exist for some small fields and gardens. In such cases, water equal to the full amount of evapotranspiration may have to be pumped from ground water, causing the net irrigation flux to be a negative value. However, the effect of streets, yards, and buildings would be to reduce the area of evapotranspiration and possibly to increase the concentration and infiltration of rainwater beyond the root zone. In addition, some ground water used for irrigation probably was already accounted for in the form of city pumpage. Thus, although the average net irrigation flux, about 1 foot per year, may be too great for Las Cruces, simulating a net withdrawal of ground water in addition to city pumpage may not be justified. A zero net irrigation flux may be as good an estimate as any.

MODEL EVALUATION

Mass balance is of rudimentary importance to the model. That is, inflow must equal outflow plus change in storage. The following table shows the mass balance, in cubic feet per second, for the initial condition (steady state) and for the end of the simulated time (1975):

	Initial condition	End of simulation (1975)
Inflow from:		
Net river seepage	320.9	76.58
Net irrigation flux00	258.83
Mountain- and slope- front recharge	14.95	15.89
Underflow in flood- plain alluvium16	.95
Outflow to:		
Net drain seepage00	-180.48
Net nonirrigation pumpage00	-56.73
Evapotranspiration from nonirrigated lands	-335.82	-112.28
Underflow in flood- plain alluvium	-.09	-.72
Net flow to storage00	-1.86
Difference12	.18
Percentage difference04	.05

The differences were judged to be acceptable. Similar differences were found for the other pumping periods. The major components of the mass balance are shown in figure 26, where the apparent differences are partly due to underflow (not shown) but are mostly due to roundoff errors of the calculations.

The model can be evaluated on the bases of what was learned about the geohydrologic system and the model's usefulness as a predictive tool. Insofar as the model yielded hydraulic heads, depletions, and flow rates that compare reasonably well with measured values, the concepts of the system seem to be consistent with each other. However, the usefulness of the model as a predictive tool may be limited by its possible nonuniqueness. Sensitivity tests and the trial-and-error adjustments indicated ways to improve the model and to improve the precision of its predictive capability.

SENSITIVITY TESTS

The sensitivity of the model was tested by setting various properties at either double or one-half the values used in the standard model. The values that were changed and results of the changes are shown in tables 6 through 9. Each test is described and given a short mnemonic name in table 6.

Tests are ranked by "score" in table 7 in order of increasing model sensitivity. The ranking is largely subjective because only a few criteria were used. The criteria were: cumulative drain discharges and cumulative surface-water depletions for 1940–75 (expressed as percent change from the standard), heads in layer 1, and heads in all layers for well fields (expressed as mean absolute change from the standard, in feet). Only the heads in layer 1 that are shown in table 5 for 1975 were used. Similarly, only heads in well fields where head hydrographs (fig. 36) existed were used because heads at most other nodes were not saved after the model program was executed. Other criteria might have resulted from grouping heads by area (such as mesa areas or valley area) or by time (such as 1947 instead of 1975). The amount of water flowing into or out of storage might have been another criterion.

The ranking in table 7 demonstrates little sensitivity to storage properties (tests SP_YIELD and STOR*.5 in tables 6–9) and greater sensitivity to values of hydraulic conductivity (T^*2 , $T^*0.5$, $VERT^*.5$, and $VERT^*2$). There is also a greater sensitivity to the extinction depth of evapotranspiration (EXT_DEPTH25, EXT_DPTH25TR, and EXT_DEPTH10) than to most other properties.

Comparison of measured values with model output for each test is shown in tables 8 and 9. This

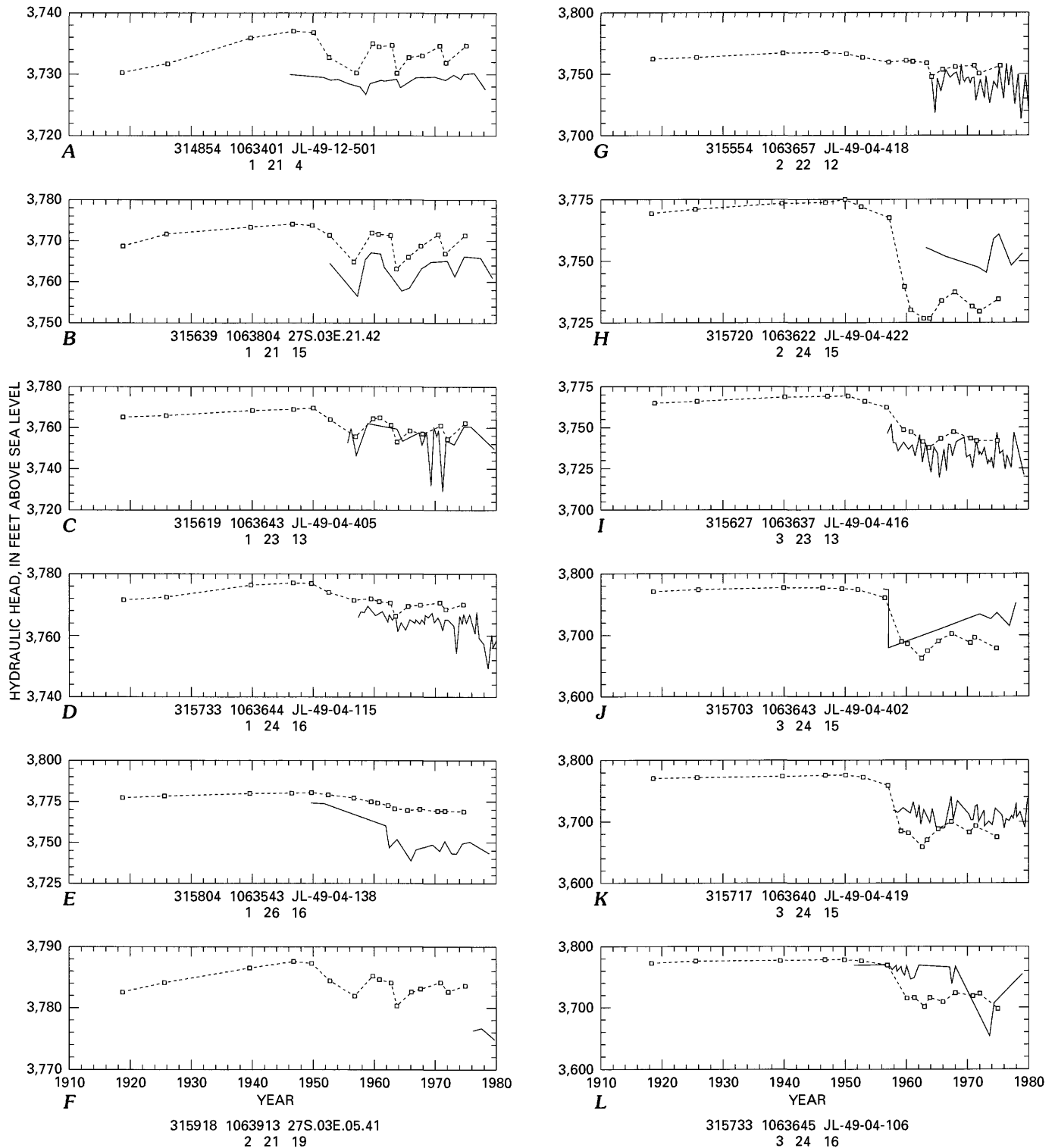
comparison may be used to evaluate the relative degree of optimization achieved by the standard simulation compared to each test.

Average differences between model-derived and measured heads (table 8) were calculated for sites listed in table 5. The sites are listed in three groups representing the mesas, the valley, and all sites. Within these spatial groups are time groups. Each time group is ranked in the order of least to greatest mean absolute difference. The test at the top of the column is the best match of measured data using mean absolute difference as the criterion. If one of the other averages had been used for the ranking, a slightly different ranking would have resulted. The standard model is not shown to have been the best match. However, the tests that showed some improvement over the standard in some groups were not generally better in all groups.

The percentage differences between model-derived and measured cumulative drain discharges, cumulative surface-water depletions, and mean absolute head differences for 1975 are shown in table 9. The cumulative drain discharges are for 1940–50, 1950–75, and 1940–75. The cumulative surface-water depletions are for 1940–75. The mean absolute head differences were taken from table 8. The "score" column indicates that nearly one-half of the tests matched the measured values as well as did the standard; one test (CRIVRIO*.5) may have matched better; and the remainder of the tests did not match the measured values as well. However, the scoring procedure is not conclusive because of its subjectivity.

The following is a description of test results in terms of changes to model-derived heads, drain discharges, and depletions. In addition to the comparisons made in tables 7–9, potentiometric maps for 1975 (not shown) were compared with figures 31–35; head hydrographs (most not shown) were compared with figure 36; and discharge hydrographs (not shown) were compared with figure 40. The term "model-derived" is implied in the remainder of this discussion where the comparison is between one model (the standard) and another (the same model with the described alteration).

Doubling transmissivity of layers 2–5 and hydraulic conductivity of layer 1 (T^*2 in tables 6–9) decreased heads by as much as 10 feet near mountain-front recharge areas and increased heads by 5–10 feet in the Cañutillo area and by 10–20 feet in the Las Cruces area. Depletion was not affected. The scoring procedure in table 7 places this test farthest from the standard. An effect only slightly less in magnitude but opposite in sign was noted when horizontal hydraulic conductivity and transmissivity were decreased by a



factor of one-half ($T*0.5$). The heads for the Las Cruces well-field area were much improved over the standard, but the heads for the Cañutillo area were unacceptably low (fig. 41). On the other hand, doubling vertical hydraulic conductivity ($VERT*2$) increased heads for the Cañutillo area by as much as 15 feet in layer 3

while increasing them by no more than 5 feet for the Las Cruces well-field area. This difference demonstrates that heads in the Cañutillo area are more sensitive to vertical and less sensitive to horizontal hydraulic conductivity than are heads in the Las Cruces well-field area.

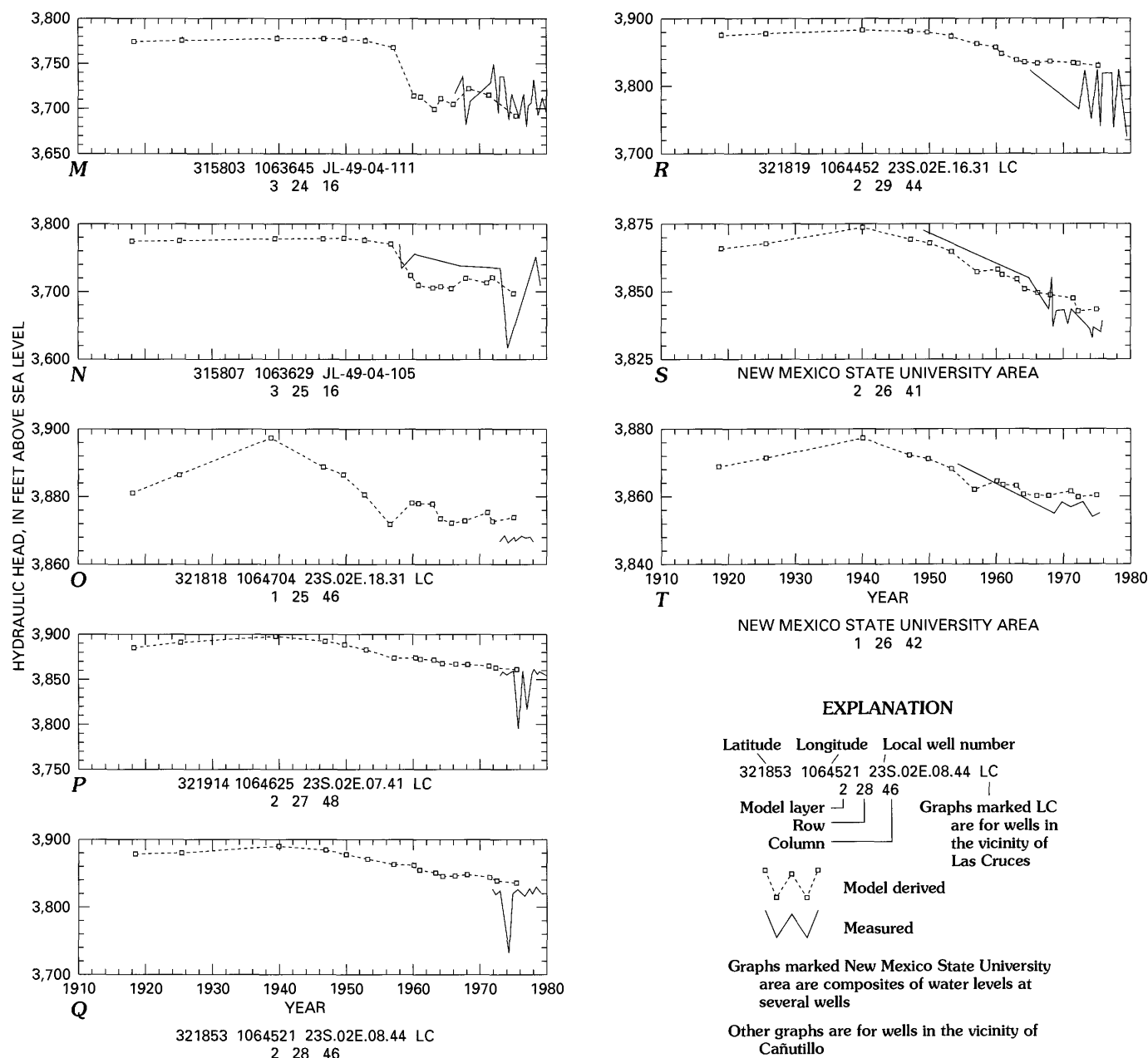


FIGURE 41 (above and facing page).—Comparison of hydrographs of measured and model-derived hydraulic heads when values of transmissivity were one-half those in the standard model.

The tests showed little sensitivity to storage. When the storage coefficient and the specific yield were reduced by one-half (STOR*.5), heads were lowered by 0.5 foot or less, and drain discharges changed little. Head hydrographs showed slightly lower heads for 1964 than those shown in figure 36 for the standard. Similarly, reducing specific yield by one-half while not changing the storage coefficient of the lower layers (SP_YIELD) had little effect. The apparent insensitivity to storage is partly because the model did

not simulate seasonal effects. The long-term insensitivity to storage was expected due to the lack of a well-defined trend in many of the hydrographs shown in figure 36 and in other hydrographs (not shown) that displayed almost no trend. The system reaches equilibrium quickly because the major stress and recharge boundaries are close together in or near the Mesilla Valley.

Changes in evapotranspiration mainly affected depletion through slight changes in drain discharges.

The changes were not evident in the drain-discharge hydrographs (not shown), but they are listed in table 7. These changes occurred both when agricultural evapotranspiration was increased from 2.2 to 2.4 acre-feet per year per acre (AGET2.4) and when evapotranspiration from nonirrigated land was increased by increasing the extinction depth to 25 feet (EXT_DEPTH25 and EXT_DPTH25TR). The effects of changes in these two kinds of evapotranspiration were so similar that an error in specification of one might easily compensate for an error in the other, yielding a model-derived depletion that might compare well with the measured value. Heads were most affected (1 to 2 feet) by changes that pertained to both the initial, steady-state condition and the transient condition (EXT_DEPTH25 and EXT_DEPTH10). These head changes persisted to 1975 in areas that were most distant from the valley. The effects on heads caused by changes that only pertained to the transient version of the model (EXT_DPTH25TR, AGET2.4, and AGET2.0) generally were less than one-half foot. In these cases, the main effect was on depletion (table 7).

Tests EXT_DEPTH25 and EXT_DPTH25TR were similar in every way except that the latter used the standard steady-state initial condition. They show the effect that the initial condition might have on the model. Head differences between the tests of about 2 feet remained in the western one-third of the model until 1975. Because there is no way to be sure that the initial condition was correct, care needs to be taken to make comparisons in such a way as to minimize these effects when studying other properties. The differences between cumulative drain discharges and cumulative depletions of these two tests were not great (tables 7 and 9).

Doubling recharge (RECH*2) had the effect of increasing heads by about 10 feet around the periphery of the basin except northeast of Las Cruces where heads increased by as much as 50 feet. Decreasing recharge by a factor of one-half (RECH*.5) had the opposite effect. Depletion was decreased by about the same flow rate as recharge was increased. Because recharge was about one-tenth of depletion, errors in recharge would be masked by slight errors in evapotranspiration.

Changing vertical hydraulic conductivity (VERT*.5 and VERT*2) had a slight effect on heads, but no effect was discernible in discharge hydrographs on drain discharges or depletion. Generally, heads were about 1 foot lower for the north end of West Mesa and about 2 feet higher for the south end when vertical hydraulic conductivity was halved (VERT*.5). The main effect was in well fields (table 7; and head maps, not shown) where heads were as much as 15 feet lower in Cañutillo and as much as 5 feet lower in Las Cruces. Doubling

vertical hydraulic conductivity (VERT*2) had effects that were similar in magnitude but opposite in sign.

Decreasing the connection coefficient (CRIV) for the drains by one-half (CRIVDRNS*.5) had the effect of increasing heads by 1 to 2 feet over most of the area. It also increased depletion by increasing evapotranspiration. Doubling CRIV (CRIVDRNS*2) decreased heads by less than a foot over most of the area and decreased depletions. The change in depletions can be ascribed to changes in head-dependent evapotranspiration. In both cases the effect on drain discharge was mixed.

Decreasing the connection coefficient (CRIV) for the river by one-half (CRIVRIO*.5) caused heads to be less than one-half foot lower over a wide area, except in the Cañutillo area where they were as much as 1 foot lower. At the same time, evapotranspiration and depletion were decreased slightly (an improvement over the standard). The overall effect was the simulated transfer of more surface water from the upper end of the valley to the lower end. Increasing CRIV for the river (CRIVRIO*2) increased heads over a wide area by less than one-half foot.

Removing the bottom two layers of the model by setting the leakance values of layers 3 and 4 to zero (BOTTOM) had little effect on discharge or head hydrographs. However, heads as expressed by contour maps were affected in some areas. Heads were about 2 feet lower in the West Mesa in layers 1–3. In layer 3, heads were about 2 feet higher in the north end of the Mesilla Valley and about 1 foot lower in the south end of the valley. A similar areal effect resulted from decreasing vertical hydraulic conductivity by one-half (VERT*.5).

When municipal and industrial withdrawals were increased by a factor of 1.2 (MUNIPMP*1.2), the main effect was in well fields (table 7), where heads were lowered by as much as 5 feet for 1975. If an error in the specification of municipal and industrial withdrawals of this magnitude were plausible, no more than about 5 feet of the mismatch between model-derived and measured heads in well fields for 1975 could be ascribed to this error.

A test of the possible effects of irrigation withdrawals from layer 2 was made where one-half the estimated irrigation withdrawals were assumed to have been from layer 2 (AGPMP-L2) for 1951–75. This test was done in order to evaluate the possible magnitude of this problem if the simulation were carried beyond 1975. After 1975, some significant part of irrigation water may have been withdrawn from more than 200 feet below the top of the aquifer. In order to do the test, some assumptions and estimates had to be made that were not made in the standard model. The effective growing-season rainfall was subtracted from the estimated evapotranspiration (2.2

feet). The difference was divided by an assumed irrigation efficiency (the part of applied water that is evapotranspired) of 0.6 to calculate the feet of water needed at land surface. From that value, the amount of water delivered to farms (Wilson and others, 1981, table 10) was subtracted; one-half of the shortfall was assumed to be withdrawn from the part of the aquifer represented by layer 1 and one-half was assumed to be withdrawn from layer 2. To keep the mass balance the same as in the standard model, the amount of withdrawal from layer 2 was added as recharge to the standard net irrigation flux applied to layer 1. The effects were minor, indicating that this problem may not be critical in simulating the time after 1975. Heads were about 2 feet lower in layer 2 in the valley area but unchanged near the edges of the model. Heads were unchanged in layer 1 in the valley area but about 1 foot lower near the edges of the valley. Drain discharges were slightly greater and surface-water depletions were slightly less (tables 7 and 9) than those simulated by the standard model.

Some aspects of the model were unaffected by the properties tested. The model-derived drain discharges generally were too small before 1950 and too large after 1950 (table 8). Similarly, model-derived heads in the valley (table 8) generally were too low for the steady-state version (pre-1915) and too high for 1975. However, heads in the mesas appeared to be too high for the steady-state version and too low for 1975. Surface-water depletions derived by the standard simulation were overestimated by a slightly greater amount for 1950–75 (6 percent) than for 1940–50 (4 percent). This trend was not changed except in the test where the connection coefficient ($CRIV$) for the drains was reduced by one-half ($CRIVDRNS*0.5$), in which case the overestimate was greater than that in the standard (8 percent for 1950–75 and 10 percent for 1940–50). These observations indicate that: (1) There was at least one important property that was not tested or was inadequately treated in the model; or (2) some data were incomplete, inappropriate, or erroneous. The second scenario probably is true in the case where certain measured heads from the 1970's were selected to approximate the steady-state condition. Also, unknown historical changes in management of the drains may be important. Some properties, such as the stream-aquifer connections or natural evapotranspiration, may have been oversimplified.

SOURCES OF WATER WITHDRAWN FOR NONIRRIGATION USES

Ground water withdrawn for nonirrigation uses (municipal, industrial, and domestic) comes from aquifer storage and boundaries. Water from storage

may be replaced ultimately by water from boundaries if storage results from elastic compression of the aquifer. However, if storage results from inelastic compression of clay lenses, water may be removed permanently and may be thought of as an ultimate, nonrenewable source. This model only treated elastic compression. Three boundaries that may be ultimate sources of water were simulated, the main one being depletion of riverflow. The model simulated river depletion in the forms of flow to and from the river and drains and as recharge of unused irrigation water that is diverted from the river. (The "diversion" was done outside the model algorithm.) Mountain- and slope-front recharge was a specified value so that the quantity was unaffected by simulated pumpage.

Another, possibly significant, ultimate source of water that is treated by the model is head-dependent evapotranspiration. As simulated heads decline, the simulated flow to head-dependent evapotranspiration declines. The difference is referred to in this discussion as "salvaged" evapotranspiration.

Another source of water is change in underflow at either end of the Mesilla Valley, which was simulated by constant-head boundaries. This source is not significant.

The ultimate sources of nearly 100 percent of withdrawals that are accounted for by this model are depletion of the river and salvaged evapotranspiration. There is an important time delay between when the water is withdrawn and when the effect is seen as salvaged evapotranspiration or depletion of river discharge. During this delay, water is removed from or added to storage in the aquifer.

Model estimates were made of the proportions of nonirrigation withdrawals that come from aquifer storage, river depletion, and salvaged evapotranspiration. These estimates were dependent on the hypotheses that: (1) The model represented the ground-water system and its boundaries reasonably well, and (2) the transmissivity of the part of the aquifer represented by layer 1 was not significantly changed by drawdowns caused by nonirrigation withdrawals. The procedure was to run a version of the model that differed from the standard in that it excluded nonirrigation withdrawals. Then, the resulting net flows to and from each possible source were compared with similar flows of the standard simulation. Specifically, the net flow to and from the river and drains derived by the altered model was subtracted from the net flow to and from the river and drains derived from the standard model. Similarly, the differences were also calculated for net flow to and from storage and flow to head-dependent evapotranspiration. These three sources accounted for about 99.8 percent of the total nonirrigation withdrawals for

1950–75. The remainder was from changes in flow at the constant-head boundaries representing underflow at either end of the Mesilla Valley. The results are shown in figure 42A.

The distance of the well fields from the valley is important for determining the lag between the time when withdrawals from the aquifer are started and the time when a similar rate of depletion shows up in the river. In order to demonstrate this principle, a hypothetical withdrawal of 50 cubic feet per second from a line of wells just west of the valley (row 14, columns 6–32, layer 2) was simulated for 1941–75. The resulting hypothetical depletion rate of the river for 1975 (fig. 42B) was not quite as great as model-derived depletion caused by historical withdrawals. This result can be contrasted with a similar hypothetical withdrawal of 50 cubic feet per second from a line of wells 8 miles southwest of the first line (row 6, columns 6–32, layer 2). The hypothetical surface-water depletion for 1975 is much less in the latter case (fig. 42C).

The hydraulic characteristics of the aquifer, especially the part of the aquifer between the well field and the boundary, govern when the effects will reach the boundary. The greater the transmissivity or the lesser the storage, the sooner the effects of withdrawals become great at the boundaries. Several tests were done to assess the effects that different values of transmissivity and storage might have on the timing of the proportion of withdrawals taken from river depletion, aquifer storage, and salvaged evapotranspiration. In order to minimize the number of tests, combinations of hydraulic conductivity and storage were used that yielded either a large or small hydraulic diffusivity. A large hydraulic diffusivity was calculated when both horizontal and vertical hydraulic conductivity were double those of the standard model and specific storage and specific yield were one-half those of the standard model. A small hydraulic diffusivity was calculated when both horizontal and vertical hydraulic conductivity were one-half those of the standard model, specific storage was double that of the standard, and specific yield was 0.3, which was 1.5 times that of the standard. These values of hydraulic diffusivity were judged to be the extremes of a plausible range.

Two tests were done for each hydraulic diffusivity, one with and one without nonirrigation withdrawals. The net flows to and from storage and the boundaries were compared for the values of hydraulic diffusivity as described above. The results are shown in figure 43.

The standard simulation generally falls between the simulations with large and small diffusivity. However, the large- and small-diffusivity versions of the model were not adjusted to match measured heads and discharges as was the standard. Nevertheless, the dashed

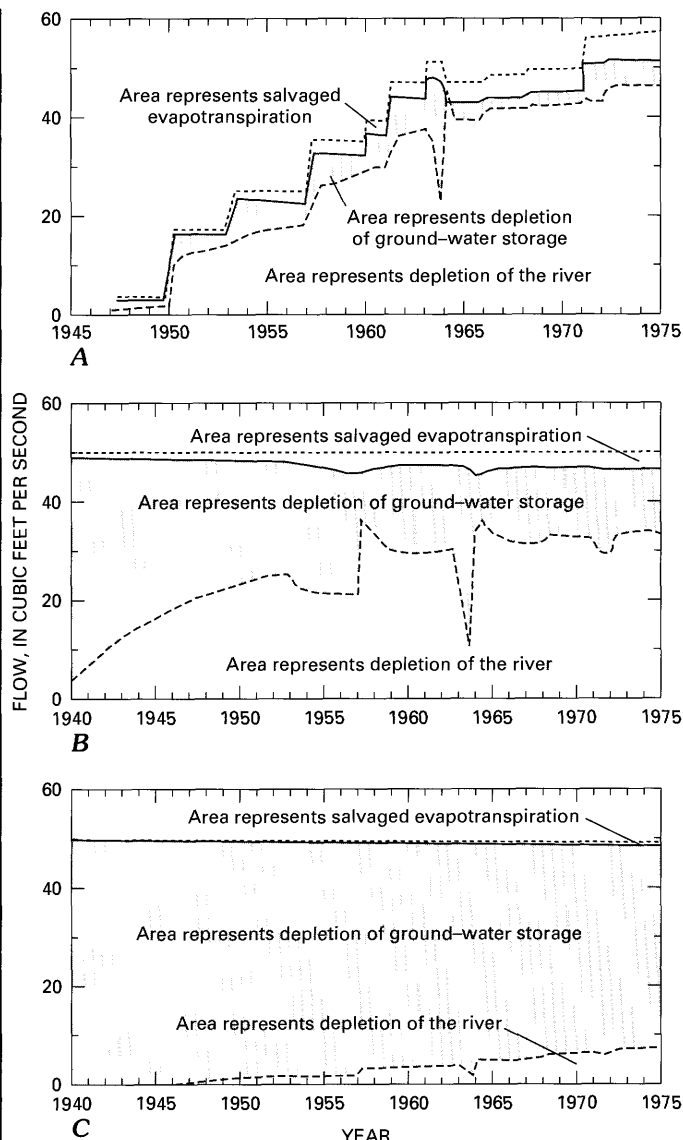


FIGURE 42.—Sources of nonirrigation withdrawals. A, Historical nonirrigation withdrawals; B, Hypothetical withdrawal of 50 cubic feet per second distributed evenly along a line in layer 2 from row 14, column 6 to row 14, column 32; C, Hypothetical withdrawal of 50 cubic feet per second distributed evenly along a line in layer 2 from row 6, column 6 to row 6, column 32.

lines in figure 43 do show the approximate magnitude of the effects of different values of diffusivity. They show, for example, that regardless of hydraulic diffusivity, the model indicates that a large part (about 80 percent) of 1975 nonirrigation withdrawals was taken from depletion of the river and that the remainder may have been about evenly divided between water taken from storage in the aquifer (fig. 43B) and from salvaged evapotranspiration (fig. 43C). (It is possible that the above proportions might be sensitive to variations in other properties.)

An effect of the drought of 1964, when a relatively large percentage of the withdrawals came from storage in the aquifer, is shown in figures 42 and 43. Later, the difference was made up from depletion of the river—the river then supplied both the withdrawals and the water returned to storage.

A greater distance between the well field and the valley would increase the effect of hydraulic diffusivity in estimates of the timing of depletion of the river caused by withdrawals. The results of a hypothetical withdrawal of 50 cubic feet per second evenly distributed along a line of wells between row 6, columns 6–32, layer 2 are shown in figure 44. This line is parallel to the first line and about 8 miles farther from the valley. The percentage of water taken from each source varied greatly with different values of hydraulic diffusivity (fig. 44). In this hypothetical case, the 1975 depletion of the river was 3 percent for small diffusivity, 15 percent for standard diffusivity, and 53 percent for large diffusivity.

PREDICTIVE CAPABILITY

The predictive capability of this model is unknown because the model was not very sensitive to what were considered to be substantial changes to input values. The simulated river depletion due to historical withdrawals near the Mesilla Valley boundary was about the same regardless of diffusivity, whereas in the hypothetical case with the withdrawals at a greater distance from the valley, the amount of river depletion varied greatly depending on the assumed diffusivity. A thorough sensitivity analysis would be necessary to assess the validity of any prediction.

SOME POSSIBLE WAYS TO IMPROVE THE MODEL

The model could be improved in several ways that became apparent during the model adjustment and sensitivity analysis. The changes probably would not be justified unless they were preceded by additional work.

ADDITIONAL MODEL ADJUSTMENT

The sensitivity tests indicate that the model could be improved by further adjustment. The tests especially indicate that the drawdowns in the Las Cruces well field could be better simulated by reducing the hydraulic conductivity of layer 2 by about one-half. At the same time, however, something would have to be done to keep the simulation of heads in the Cañutillo well field from deteriorating. Although the sensitivity tests indicate that increasing vertical hydraulic

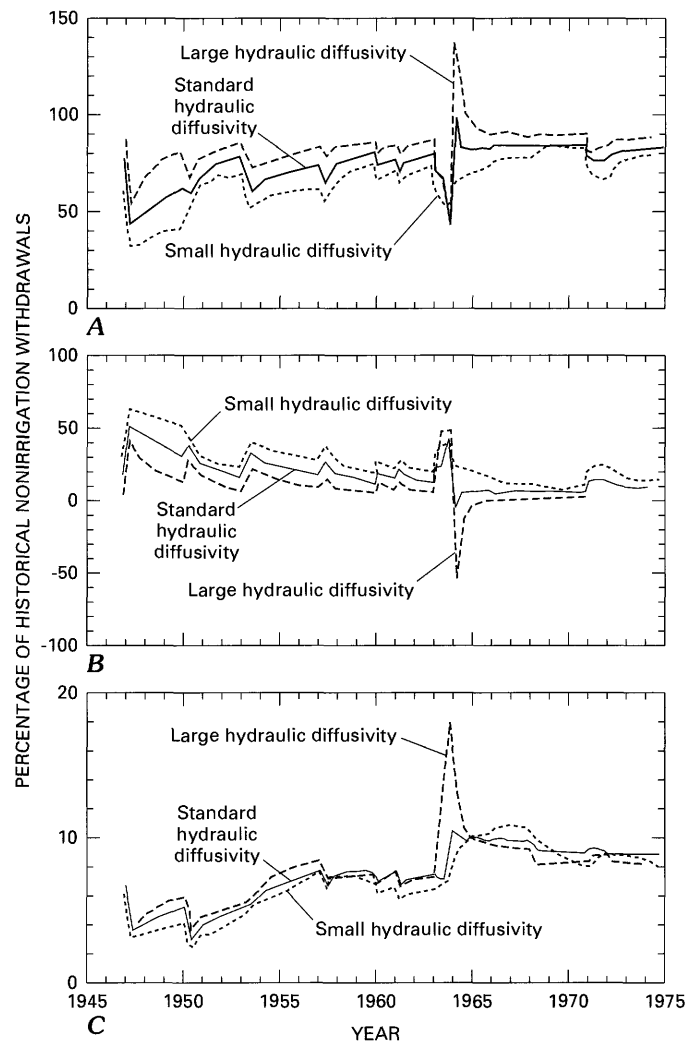


FIGURE 43.—Effect of changes in diffusivity on the sources of water for nonirrigation withdrawals. A, Percentage from river depletion; B, Percentage from ground-water storage; C, Percentage from salvaged evapotranspiration.

conductivity by a factor of two might improve the fit, these two adjustments would tend to offset each other and may not lead to a better model overall. Before further adjustments are made, an onsite evaluation of the effects of ground-water withdrawals on water levels measured in observation wells may be useful. Also, a careful examination of recent work such as that of Hawley (1984) might reveal evidence that would warrant reducing hydraulic conductivity in the part of the model that represents the Las Cruces vicinity.

The methods of estimating hydraulic conductivity (tables 1 and 2; figs. 13 and 14) were judged to be appropriate for this study. However, additional data and refinement of the analytical methods might be considered in future studies.

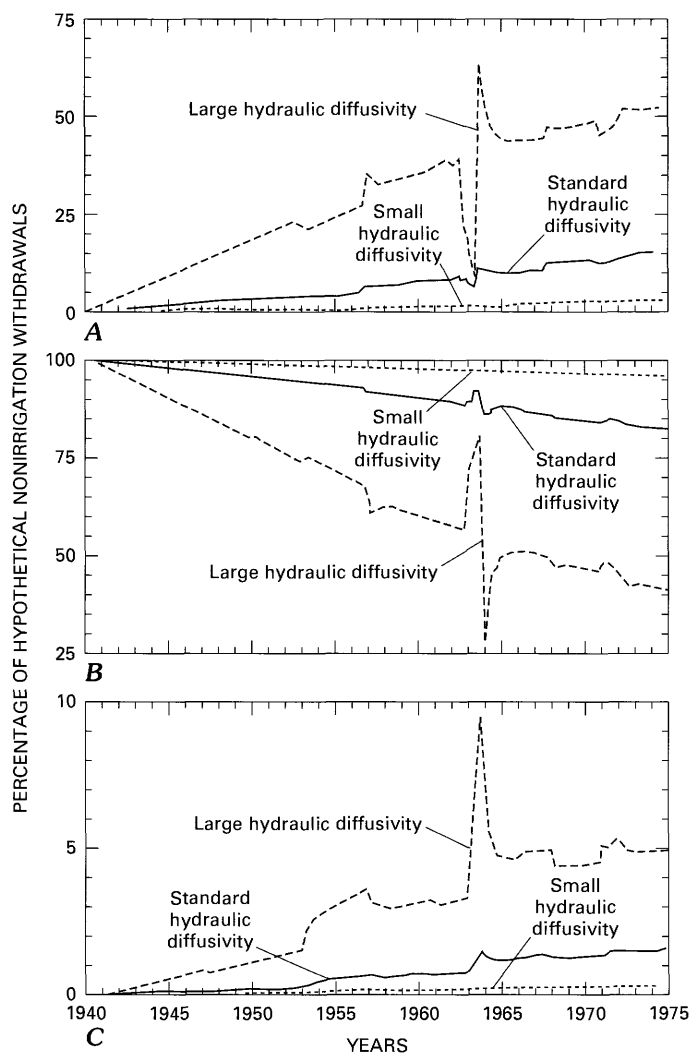


FIGURE 44.—Effect of changes in diffusivity on the sources of water for hypothetical nonirrigation withdrawals. A, Percentage from depletion of the river; B, Percentage from storage in the aquifer; C, Percentage from salvaged evapotranspiration.

Municipal ground-water withdrawals and associated drawdowns were used conceptually in this model as long-term, large-scale aquifer tests. If more measured heads in the deep pumped zones of the aquifer were available for locations several miles distant from city well fields, the model might prove to be demonstrably more sensitive to hydraulic conductivity and storage values, and it could be more closely “calibrated” with regard to these properties. However, there is a lack of information regarding boundary conditions (such as stream-aquifer connection, recharge of the aquifer by unused irrigation water, and uncontrolled withdrawals) that may prove to be critical to this concept. The results of a large-scale, well-controlled aquifer test

10 or 20 miles away from such boundaries might be easier to interpret.

During the model-adjustment phase, model-derived heads were observed to have been highly sensitive to the altitude specified for the river. The same probably is true of the drain altitudes. The overall positive bias in head differences (table 8, “all sites”) probably could be removed by lowering the heads specified for the rivers and drains by about 2 feet. This change was considered to be unnecessary because it would have had no effect on simulation of the ground-water system. Nevertheless, the absence of this bias would make the analysis of future sensitivity tests easier.

Before drain properties are adjusted, more field work needs to be done. The relative altitudes of the drains and river, such as those shown on plate 4 of Conover (1954), need to be determined in several places because the drain profiles that were used to determine the specified drain altitudes do not agree very well with altitudes shown on that plate. Also, the sites where surface discharges are measured need to be carefully evaluated as to potential problems that might cause error in the measurements. Finally, places where water is directed to the river and out of the distribution system need to be located to determine if the water flows directly into the river or if the water first flows into drains that are measured.

The connection of the river and aquifer was assumed to have been the same over the entire length of the valley. This assumption may not have been appropriate (Peterson and others, 1984, p. 27–38), especially for the area near the Cañutillo well field. The practical importance of the river-aquifer connection, with respect to prediction of river depletions that might be caused by ground-water withdrawals, may be minimized by recharge in the Mesilla Valley. The estimated recharge (net irrigation flux—fig. 16, line E) often has been in excess of 200 cubic feet per second.

The model-derived rate of evapotranspiration from nonirrigated lands tends to compensate for possible errors in other properties because it is head-dependent. This compensation could be reduced if independent estimates of evapotranspiration from nonirrigated lands were available and the model could be adjusted to match them. This change could improve the accuracy of model-derived estimates of salvaged evapotranspiration caused by withdrawals.

SHORTER TIME INCREMENTS

The model could be used to study the effects of different values of specific yield if pumping periods were shortened to 1–2 months so that seasonal changes

could be simulated. This change would require that net irrigation flux be estimated on a seasonal basis. Also, heads and drain discharges would have to be compared on a seasonal basis. However, a more practical approach might be to use a two-dimensional, cross-sectional model to refine the estimation of aquifer properties and then use the refined estimates in the regional three-dimensional model.

RESTRUCTURING OF THE GRID

The poor simulation of heads in layer 1 in the Cañutillo area indicates that vertical ground-water flow is not adequately simulated. To better simulate vertical flow, layer 1 might be divided into several layers to isolate the shallow zone of interconnection between surface-water and ground-water zones. Also, because the model appeared to be insensitive to the removal of layers 4 and 5 (which represented the deeper part of the aquifer), the computer capacity used to simulate layer 5 might be better used for an additional layer representing the shallower part of the aquifer. Transmissivity of the lowest layer in a restructured model could be increased to compensate for the additional thickness of aquifer that would be nominally below the modeled zone. In this case, the true thickness of the aquifer represented by the model layer might be used to calculate leakance. If more layers were used to represent the upper 200 feet of the aquifer, more accurate estimates of hydraulic conductivity would be appropriate, and more precise production-zone information for irrigation wells would be needed.

SIMULATION OF INELASTIC BEDS

The model did not treat the release of water from the inelastic compression of clay beds, the importance of which is not known in the Mesilla Basin. Measurements of subsidence of the land surface from year to year might show the importance of inelastic compression. Maintenance of a leveling survey for the Las Cruces and Cañutillo well fields might be useful. A careful comparison of sediments in this basin with sediments in other basins where such studies have already been conducted might help to determine if a leveling survey would be justified.

CONCLUSIONS CONCERNING THE MODEL

1. It was judged that the model successfully matched measured heads, drain discharges, and surface-water depletions reasonably well, with a few

exceptions. The two main exceptions were: (a) model-derived heads in the Las Cruces well-field area were about 20 feet too high; and (b) model-derived drain discharges generally were too small before 1950 and too large after 1950. Also, model-derived heads in layer 1 for a few sites in the Cañutillo well-field area were 10 to 20 feet too high.

2. The model indicates that the concepts ("summary of concepts" section) of the system are consistent with each other.

3. The model was insensitive to storage properties for the period simulated. Any predictions that might be made would be dependent on specification of storage properties derived from other analyses or from aquifer tests.

4. The model indicated that about 80 percent of the ground water withdrawn for nonirrigation uses during 1975 may have come from depletion of streamflow. The remainder came from storage in the aquifer and from salvaged evapotranspiration. However, the model-derived estimates of salvaged evapotranspiration may be somewhat inaccurate because head-dependent evapotranspiration tends to make up for errors in the specification of other properties.

5. The accuracy of any predicted effects of future withdrawals on depletion of streamflow would depend largely upon the accuracy of the values of hydraulic conductivity, specific yield, and specific storage simulated in the model. This is especially the case if ground-water withdrawals were to occur at great distance from the Mesilla Valley.

6. As simulated in the model, drawdowns of 1 to 10 feet in 1975 caused by historical nonirrigation withdrawals may be measurable at distances of about 5 miles west of the Las Cruces and Cañutillo well fields in or below the deep producing zones.

7. Values for several properties used in the model were not independently estimated or were based on estimates that are not considered to be very accurate. However, the model produced acceptable results with these values. They are: a ratio of horizontal to vertical hydraulic conductivity of about 200; a connection coefficient for the river channel of about twice that for the drains on a per-mile-of-length basis; a total mountain- and slope-front recharge rate of about 15 cubic feet per second for the entire basin; and an evapotranspiration rate from nonirrigated lands (head-dependent), not including large stream surfaces, of about 2.5 acre-feet per year per acre, which is more than the independently estimated rate for irrigated lands (2.2 acre-feet per acre based on Blaney and Hanson, 1965). The accuracy of these estimates was not explored.

WATER QUALITY AND GEOCHEMISTRY OF THE MESILLA BASIN

By SCOTT K. ANDERHOLM

The purpose of this part of the Mesilla Basin study was to define the areal distribution of waters of different chemical quality and to identify chemical processes that cause the differences in water quality. The area analyzed is slightly larger than the area modeled because the water quality of inflow from rocks adjacent to basin-fill deposits affects the water quality in the basin-fill deposits and because the density of water-quality data is relatively sparse within the modeled area. Although the quantity of flow into the basin from adjacent, less permeable rocks may not be significant for the flow model, the same flow may have a significant effect on the water quality of the basin.

The Mesilla Basin was divided into three areas for discussion of the chemistry of ground water: (1) west of the Mesilla Valley, (2) Mesilla Valley, and (3) east of the Mesilla Valley. This division is based on the ground-water flow system, on the differences in chemical characteristics of ground water east and west of the Mesilla Valley, and on the differences in chemical processes that occur in the Mesilla Valley compared to areas outside the Mesilla Valley.

The areas east and west of the Mesilla Valley were selected because the water-level map indicates that some ground water enters the Mesilla Basin from the east and west margins (pl. 1). The water-level map (pl. 1) does not indicate any significant flow boundaries in these areas. Ground water east of the Mesilla Valley flows westward toward the valley and ground water west of the Mesilla Valley flows southeastward, generally parallel to the valley.

Ground water along the east and west margins has different chemical characteristics that indicate differences in the chemical characteristics of recharge or inflow water. Examination of the distribution of dissolved constituents in ground water indicates that there are no large areas with significant differences or trends in the water quality within the east or west subareas.

The Mesilla Valley was selected as a separate area because the ground-water chemistry in the Mesilla Valley (river valley) is affected by infiltration of excess applied irrigation water (i.e., irrigation water applied to fields but not consumed by crops). The Mesilla Valley is the only area in the Mesilla Basin affected by this infiltration. Generally, the concentration of dissolved ions in excess applied irrigation water is much larger than the concentration of dissolved ions in ground water that is not affected by irrigation.

Examination of the water-level map of the Mesilla Basin and adjacent areas indicates regions of ground-water inflow, ground-water outflow, and the direction of ground-water movement (pl. 1). After ground water enters the Mesilla Basin (ground-water inflow), the water can mix with water already in the aquifer and chemical reactions (dissolution or precipitation of minerals, ion exchange, and chemical alteration of minerals) can occur. Mixing and chemical reactions can cause changes in the chemical characteristics of ground water as it moves through the Mesilla Basin.

It is possible that the present ground-water flow system is not an adequate representation of the past flow system because of changes in climate and resulting changes in recharge. If this is the case, the concept that ground-water chemistry at any point is the result of ground-water inflow mixing with water already in the aquifer and reacting with minerals in the aquifer as the water moves down a flow path may not be valid because the flow paths may be different and the chemistry of the ground-water inflow may be different. It has been assumed that the flow system has not changed and that the present (1985) water-quality distributions have evolved along the present flow paths.

The water-level map indicates general areas of ground-water inflow and outflow. However, inflow from adjacent bedrock units or inflow of geothermal water may not be apparent if the inflow is not large. If the chemical nature of this inflow is significantly different than other ground water in the flow system, the inflow can have a significant effect on ground-water quality in a particular area or in the entire basin. In some areas, ground-water inflow, especially geothermal water, can be recognized by large differences in ground-water quality in adjacent wells.

Geothermal anomalies have been documented in the Mesilla Basin. Ground water associated with these anomalies contains relatively large concentrations of silica, potassium, and chloride in comparison with other ground water in the Mesilla Basin (Swanberg, 1975; Icerman and Lohse, 1983). It was not possible to calculate mixing ratios of ground water containing a geothermal component because the concentration of dissolved ions was not known for an unmixed geothermal water. If the chemical nature of the inflow is not significantly different than water already in the flow system, mixing will have little effect on the water quality.

Chemical analyses used in this report generally are for water from wells completed in the Santa Fe Group; however, along the basin margins, wells may derive water from older rocks. Ground-water samples from these wells were included because data documenting

well completion generally do not exist and because ground water from older rocks along the basin margins probably is similar to ground water in the Santa Fe Group in these areas.

The density of water-quality data in the Mesilla Basin is sparse and is not evenly distributed. As a result, the description of water quality for some areas is based on chemical analyses of water from one well. It is not possible to extrapolate or predict the extent to which these chemical processes affect adjacent areas.

AREA WEST OF THE MESILLA VALLEY

The eastern boundary of this area is the approximate boundary between the entrenched Rio Grande flood plain and the adjacent upland area. The Rough and Ready Hills and the Sleeping Lady Hills were chosen as the northwestern limits of the area (pl. 5). The East Potrillo Mountains were chosen as the southwestern limits. The East Robledo fault (pl. 5) is the structural boundary along the north and west margins of the Mesilla Basin. North and west of the East Robledo fault, the Santa Fe Group is thin (265 feet in sec. 15, T. 23 S., R. 1 W.) and underlain by Tertiary volcanics, pre-Santa Fe Group rocks, and Permian rocks (Thompson and Bieberman, 1975, p. 173). South and east of the fault, the Santa Fe Group is thicker (3,790 feet in sec. 15, T. 24 S., R. 1 E.) (King and others, 1971, p. 22). Ground water to the north and west of the East Robledo fault (on the upthrown side of the fault) is considered to be inflow to the Mesilla Basin.

Water from wells 23S.1W.32.330, 23S.2W.35.411, and 23S.2W.13.314 (all of which are located north of the East Robledo fault) represents ground-water inflow along the northwest part of the area (pl. 5). The specific conductance of water ranges from 1,400 to 2,310 microsiemens (microsiemens per centimeter at 25 degrees Celsius) (table 10). The percentage of sodium plus potassium in the water is greater than 80, and the percentage of sulfate is between 40 and 60 (fig. 45).

Water from well 23S.2W.35.411 has a temperature of 36 degrees Celsius and a chloride concentration of 320 mg/L (milligrams per liter) (table 10). The temperature is high and chloride concentration is large compared to water from other wells in the area. The silica concentration in water from well 23S.1W.32.330 is 100 mg/L; this is large in comparison with water from other wells in this area. The relatively high temperature and large chloride and silica concentrations in ground water in this area may indicate a geothermal component in ground water, although ground water in this area has much larger sulfate to chloride ratios and higher percentages of sulfate than other ground water

in the Mesilla Basin that has a geothermal component. The relatively large sulfate to chloride ratio and percentage of sulfate may indicate that dissolution of gypsum is a significant process affecting this inflow water. The percentage of sulfate in ground water from the northwest part of this area generally is greater than the percentage of sulfate in other ground-water samples in the area (fig. 45). The large percentage of sodium indicates that cation exchange may also be a significant chemical process affecting this inflow water.

Water from well 25S.3W.2.213, which also is on the upthrown side of the East Robledo fault, probably represents ground-water inflow along this basin margin (pl. 1). The water has a specific conductance of 690 microsiemens and has 37 percent sulfate and 15 percent calcium (table 10 and fig. 45). The percentages of individual dissolved constituents in water from this well are similar to the percentages in water from the other three wells on the upthrown side of the East Robledo fault. However, the specific conductance of water from this well is much smaller than the specific conductance of ground water sampled in the northwest part of the area. The dissolution of gypsum and ion exchange probably are also the dominant chemical processes that affect ground-water inflow in the area of well 25S.3W.2.213.

Wells 26S.2W.15.443 and 27S.2W.25.111 are along the west margin of the basin, and water from these wells probably is representative of ground-water inflow from the west (pl. 1). The specific conductance of water from well 26S.2W.15.443 is 435 microsiemens, and the specific conductance of water from well 27S.2W.25.111 is 1,940 microsiemens (table 10). The distribution of cations and anions is similar in water from both wells. The percentage of bicarbonate is greater than 65, and the percentage of sodium is greater than 60 (fig. 45). Water from two wells in the southern Mesilla Basin (wells 27S.1E.33.130 and 27S.1W.32.000) has a distribution of anions and cations similar to the water from the two wells along the west margin (fig. 45). The larger percentage of bicarbonate in ground-water inflow in the southern basin compared with that of inflow in the northwest indicates that there may be fewer gypsum-bearing sediments in the southern basin than in the north.

Water from well 28S.1W.19.111, which is located near a large fault that separates the East Potrillo Mountains from a thick section of the Santa Fe Group (pl. 1), has a specific conductance of 7,400 microsiemens and a chloride concentration of 1,600 mg/L (table 10). Sodium is the dominant cation in water from this well. Water from this well has significantly larger concentrations of dissolved constituents than other

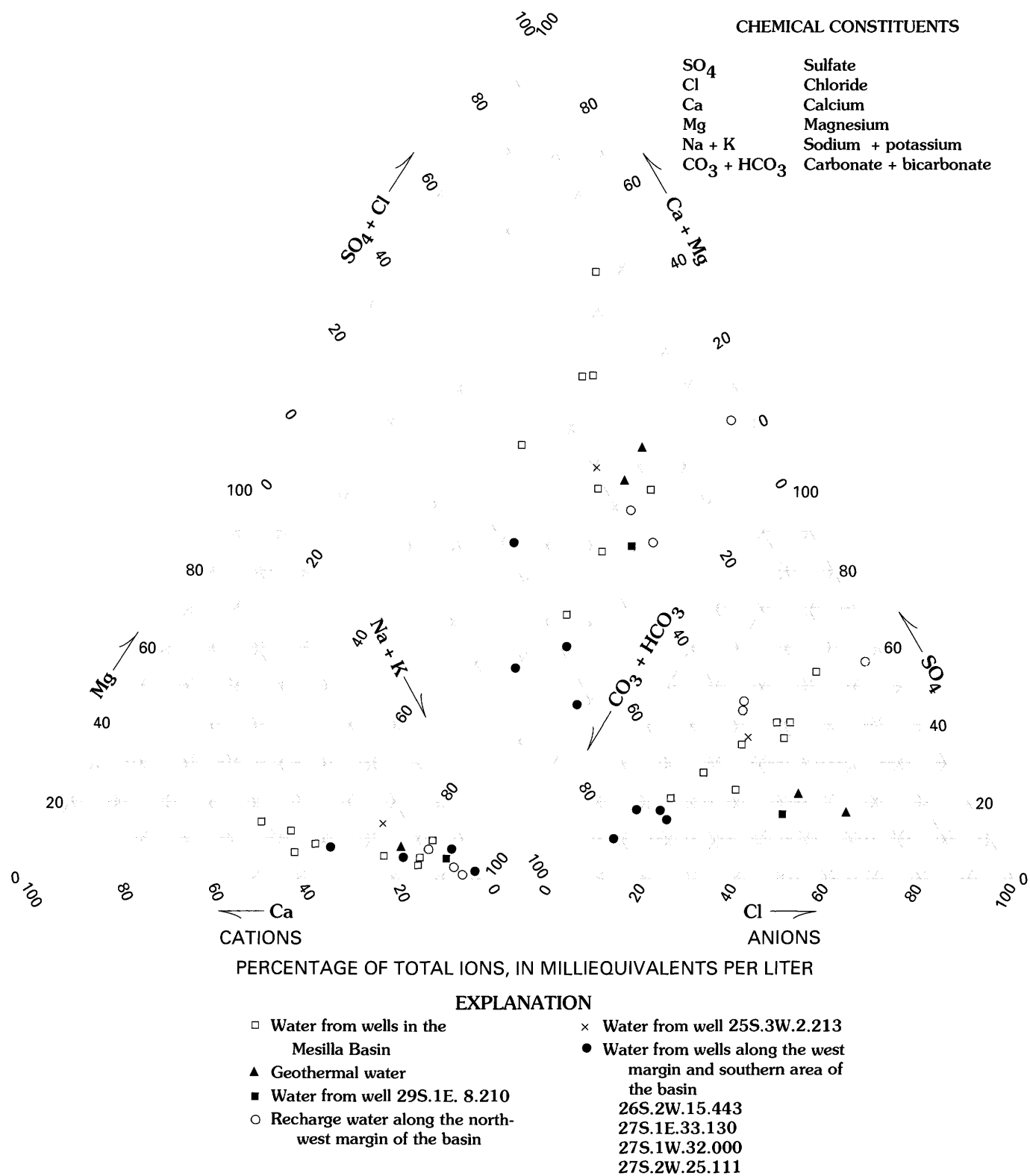


FIGURE 45.—Selected ground-water analyses from the area west of the Mesilla Valley.

ground water in the area (pl. 5). Water from this well may represent ground-water inflow from Cretaceous rocks in the East Potrillo Mountains or ground water (possibly geothermal) moving upward along the fault. The quantity of this type of ground water entering the Mesilla Basin probably is not large because water from other wells in the area does not have specific conductances and chloride concentrations as large as those in water from this well. Water from well 29S.1E.8.210 (fig. 45) has sulfate and chloride percentages similar to water from this well—this indicates that some ground water in the southernmost Mesilla Basin may be affected by this inflow.

Waters from wells 26S.1W.25.414 and 26S.1E.18.222, which are located in the central part of the area, have similar specific conductances (902 and 950 microsiemens) and a similar distribution of cations; however, the distribution of anions is different. The concentration of bicarbonate is 261 mg/L and the concentration of sulfate is 100 mg/L in water from well 26S.1W.25.414, whereas the concentration of bicarbonate is 161 mg/L and the concentration of sulfate is 150 mg/L in water from well 26S.1E.18.222. The reason for the difference in bicarbonate and sulfate concentrations is unknown.

South and east of the East Robledo fault, ground water in the Mesilla Basin west of Las Cruces (T. 23 S. and T. 24 S.) generally has a specific conductance less than 900 microsiemens (pl. 5). The percentage of sulfate generally is larger and the percentage of sodium smaller in ground water in this area compared to areas to the south (fig. 45).

Water samples were collected from several different depths in well 24S.1E.8.123 (table 10). The specific conductance and general chemical composition of ground water from the 568- to 588- and 754- to 774-foot depth intervals are similar (table 10). Ground water from the 1,380- to 1,400-foot depth interval has a smaller specific conductance, larger percentage of sodium, and larger percentage of bicarbonate than ground water from the shallower samples.

Water from well 24S.1W.22.123 has a specific conductance of 1,610 microsiemens and a chloride concentration of 230 mg/L—this value is much larger than is present in other ground water west of Las Cruces. The large chloride concentration and a potassium concentration of 35 mg/L may indicate a geothermal component in this ground water. This well is located near the East Robledo fault and may produce water that is a mixture of geothermal water that moves upward along the fault and ground-water inflow from adjacent areas.

MESILLA VALLEY

The Mesilla Valley is defined as the entrenched Rio Grande flood plain, with the exception of a small area near Radium Springs and the Leasburg Dam that is included in the area east of the Mesilla Valley (pl. 5). Most irrigated agriculture in the Mesilla Basin is in the Mesilla Valley.

The areal distribution of ground-water quality in the Mesilla Valley will not be described; instead, major factors controlling the chemistry of ground water (evapotranspiration and irrigation practices) will be described. Wilson and others (1981, pl. 4) defined water-quality zones in the Mesilla Valley on the basis of dissolved-solids concentrations and presented maps showing the areal and vertical distribution of these zones. Wilson and others (1981, p. 53) state:

The general trend of decreasing dissolved-solids concentrations with depth in shallower Mesilla Valley sediments may be attributed, in part, to the effects of surface-irrigation practices and evapotranspiration. As part of the applied water evaporates or is transpired by plants, the dissolved solids in the water are concentrated. This more saline water is recharged to the shallow ground-water system. Low vertical permeabilities resulting from interbedded clays probably retard vertical mixing, contributing to water-quality differences with depth. Local conditions such as the distribution of clay in flood-plain alluvium or the proximity to linear or point-source recharge or discharge areas (the river, canals, drains, and wells) also affect the distribution of water quality with depth.

Prior to irrigation and the damming of the Rio Grande, the concentrations of dissolved solids in water in the Rio Grande probably varied considerably during the year. In the spring, when large quantities of snowmelt runoff from the mountains in northern New Mexico and southern Colorado occurred, the dissolved-solids concentration probably was small. In the late summer, when evapotranspiration was large and flow in the river was small, the dissolved-solids concentration of water in the Rio Grande probably was quite large. Evapotranspiration along the Mesilla Valley prior to irrigation probably was immediately adjacent to the Rio Grande and was negligible a short distance away from the river. Evapotranspiration near the river concentrated salts in the soils and shallow ground water. Inflow of this shallow ground water to the Rio Grande and evaporation from the Rio Grande caused the dissolved-solids concentration of water in the Rio Grande to increase in the summer months. During

large flows in the spring, areas along the margin of the Rio Grande probably flooded; thus, salts that had concentrated in the soils were flushed out of the soils and into the river. Degradation of shallow ground-water quality probably was not extensive prior to irrigation because of this natural flushing action.

Initially, irrigation practices consisted of construction of irrigation canals that diverted water from the Rio Grande into fields that, in many cases, were a considerable distance from the Rio Grande. Part of the diverted water was evaporated, part was transpired by crops, and part infiltrated and recharged the ground-water system (excess applied irrigation water). After water became available from Elephant Butte Reservoir in 1915, clear water (water with little suspended sediment) was used for irrigation (Conover, 1954, p. 53). The clear water infiltrated faster than the sediment-laden water that was previously used, resulting in a rapid rise of ground-water levels in the irrigated part of the Mesilla Valley (Conover, 1954, p. 53). The rise in water level caused salts to build up in the soils and increased the dissolved-solids concentration in shallow ground water. This increased salinity was due to an increase in evapotranspiration that resulted from high water levels, slow rate of ground-water movement, and lack of natural flushing of this water. The rise in water levels caused waterlogging and abandonment of productive farmlands (Conover, 1954, p. 53).

The rise in water levels and abandonment of farmland resulted in the construction of open drains in the 1920's. These drains were constructed to maintain water levels at a sufficient depth below land surface so that the abandoned land could be farmed again and the deposited salts could be leached out by the application of excess irrigation water. This leaching probably resulted in a further increase in the dissolved-solids concentration in shallow ground water under irrigated parts of the river valley. Infiltration of excess applied irrigation water created downward potentiometric gradients that probably caused mixing of the local ground water in the area (i.e., ground water unaffected by irrigation) and shallow ground water that had large dissolved-solids concentrations (i.e., excess applied irrigation water).

Presently (1985), most farmers apply water to fields to meet water requirements needed for maximum growth and to flush salts that have been concentrated by evapotranspiration from the soils and shallow ground water. The ratio of the volume of water used by crops (evapotranspiration) to the volume of applied water is called irrigation efficiency. The irrigation efficiency varies from farm to farm and in each particular field because of different application rates and availability of irrigation water. In general, farmers

must apply a sufficient amount of water to keep the salts flushed from the soils because large salt concentrations in the soils or large concentrations of dissolved ions in the shallow ground water can adversely affect crop yields. The rate at which these salts are removed by the shallow ground water varies with properties of the local flow system. The flow rate of shallow ground water near a ground-water divide (generally near the midway point between two drains) may be relatively slow compared to the flow rate near a drain. The concentration of dissolved ions in shallow ground water may be large in areas where ground-water flow is relatively slow because of evapotranspiration by plants with roots at or below the water table.

In areas that are not irrigated, natural vegetation can cause salts to be concentrated in the soils and can cause large concentrations of dissolved ions to be present in the shallow ground water because there is no flushing by infiltration of excess applied irrigation water. The only flushing that occurs in these areas is natural flushing due to the shallow ground-water flow system responding to the infiltration of precipitation and fluctuating ground-water levels.

Irrigation water for the Mesilla Basin is stored in Elephant Butte and Caballo Reservoirs, upstream from the study area. Water is released from these reservoirs as it is needed in the Mesilla Valley. The concentration of dissolved ions in surface water downstream from Elephant Butte does not vary significantly during the year because of the dampening effect the large surface-water reservoir has on the changing water quality of inflow to the reservoir.

Variation in the concentration of dissolved ions in excess applied irrigation water is related to irrigation efficiency, amount of salts flushed from soils, and chemical reactions that occur. Concentrations of dissolved ions in excess applied irrigation water have been calculated assuming that salts are flushed from the soils after each irrigation. These concentrations have been calculated for several irrigation efficiencies and possible chemical reactions (table 11). The chemical reactions include precipitation of calcite and calcium for sodium ion exchange. There is no physical evidence that these reactions do occur during evapotranspiration of irrigation water, but calcite saturation is reached during evaporation of irrigation water. In the calculation, calcite precipitation was assumed to happen when the solution reached calcite saturation. Clays that have large ion-exchange capacities are found in deposits in the Mesilla Valley (Anderholm, 1985); therefore, calcium-for-sodium ion exchange is a reaction that could occur. In the calculation, it was

assumed that 0.875 mmol (millimole) of calcium is exchanged for 1.75 mmol of sodium.

In general, dissolved-solids concentrations increase with increasing irrigation efficiency. Measured irrigation efficiencies for a farm in the Rio Grande valley near San Acacia, New Mexico, were 0.62 in 1978 and 0.49 in 1979 (Gelhar and others, 1980, p. 48). The irrigation efficiencies in the Mesilla Basin probably are similar to those efficiencies, although there probably is a large range of values. Irrigation efficiencies larger than 0.5 probably are more common than those less than 0.5 because farmers may apply only as much water to the fields as is needed by the crops and because of reduced allotments available to farmers during dry years.

Since installation of the drains, many irrigation wells have been drilled in the Mesilla Valley. Initially, ground water was used to supplement surface water, but, recently, ground water is used instead of surface water in many cases. The irrigation efficiency of fields irrigated with ground water probably is greater than those irrigated with surface water because of the added cost of pumping ground water. Ground-water withdrawals have caused cones of depression near the wells, and further mixing has occurred between the shallow ground water with large concentrations of dissolved solids (due to the leaching of salts and evapotranspiration) and deep ground water that contains smaller concentrations of dissolved solids.

Wilson and others (1981, pls. 8 and 13) showed the depth to the freshwater zone (dissolved solids less than 1,000 mg/L) and water-quality zones in the Mesilla Basin. The depth to the freshwater zone and location of the different water-quality zones are transient features because increased irrigation withdrawals enhance mixing, cause the depth to the freshwater zone to increase, and cause the location of different water-quality zones to change. If withdrawals stop and upward hydraulic gradients exist, the mixed waters probably will be forced upward and the depth to the top of the freshwater zone will decrease.

AREA EAST OF THE MESILLA VALLEY

Although a small area in the Rio Grande flood plain near Radium Springs and Leasburg Dam has been included in this area, the boundary between the entrenched Rio Grande flood plain and the adjacent upland areas generally forms the western limit of the area. The San Andres, Organ, and Franklin Mountains form the eastern boundary.

Recharge to the ground-water system occurs as ground-water inflow from adjacent areas and as infiltration of runoff on alluvial fans along the

mountain fronts and in the beds of arroyos that flow out of mountainous areas along the eastern margin of the area. In general, ground-water flow is westward toward the Mesilla Valley (pl. 1).

Wells 21S.1W.14.113, 21S.1W.12.343, and 21S.1W.10.213 are near the Radium Springs Known Geothermal Resource Area. Water from each of these wells is a mixture of geothermal water and local ground water. The geothermal component is evidenced by relatively large chloride concentrations in water from these wells (table 12). Water from well 21S.1W.10.213 has a measured temperature of 53 degrees Celsius and a chloride concentration of 1,630 mg/L. This water probably contains a small component of local ground water but probably is more representative of the composition of geothermal water. Water from well 21S.1W.12.343 also has a relatively large chloride concentration (1,100 mg/L) and a potassium concentration of 79 mg/L (table 12). Large potassium concentrations are often associated with geothermal water (Fournier, 1977).

In the northeastern part of this area, Wilson and others (1981, p. 61, pl. 9) indicated a broad, poorly defined ground-water divide between the Jornada del Muerto and the Mesilla Basin. Based on the distribution of anions from chemical analyses of ground water, two types of ground water can be recognized (table 12). The percentage of sulfate plus chloride is greater than 70 for type 1 and the percentage is between 40 and 50 for type 2 (fig. 46). Type 1 generally has a larger specific conductance than type 2 (table 12).

Type 1 water is found north of type 2 water (pl. 5). Type 1 water probably is derived from the San Andres Mountains, which are composed of Paleozoic sedimentary rocks that contain gypsum (Kottlowski, 1975). Type 2 water probably is derived from the Organ Mountains, which are composed mainly of igneous rocks. The ground water derived from the San Andres Mountains (type 1) probably comes in contact with more soluble materials than type 2 ground water—this may explain the difference in specific conductance between the two water types.

Water from deep wells along the western edge of water types 1 and 2 has a different distribution of anions and cations than either water type. Water from well 22S.2E.13.441, which is 430 feet deep, is type 2 and contains an amount of calcium plus magnesium equal to approximately 63 percent (table 13). Water from well 22S.2E.24.422 (sample interval 1,120 to 1,140 feet) and well 22S.2E.23.111 (well depth 662 feet) contains amounts of calcium plus magnesium equal to 3 and 23 percent, respectively. The well depth, water level, and approximate amounts of calcium plus

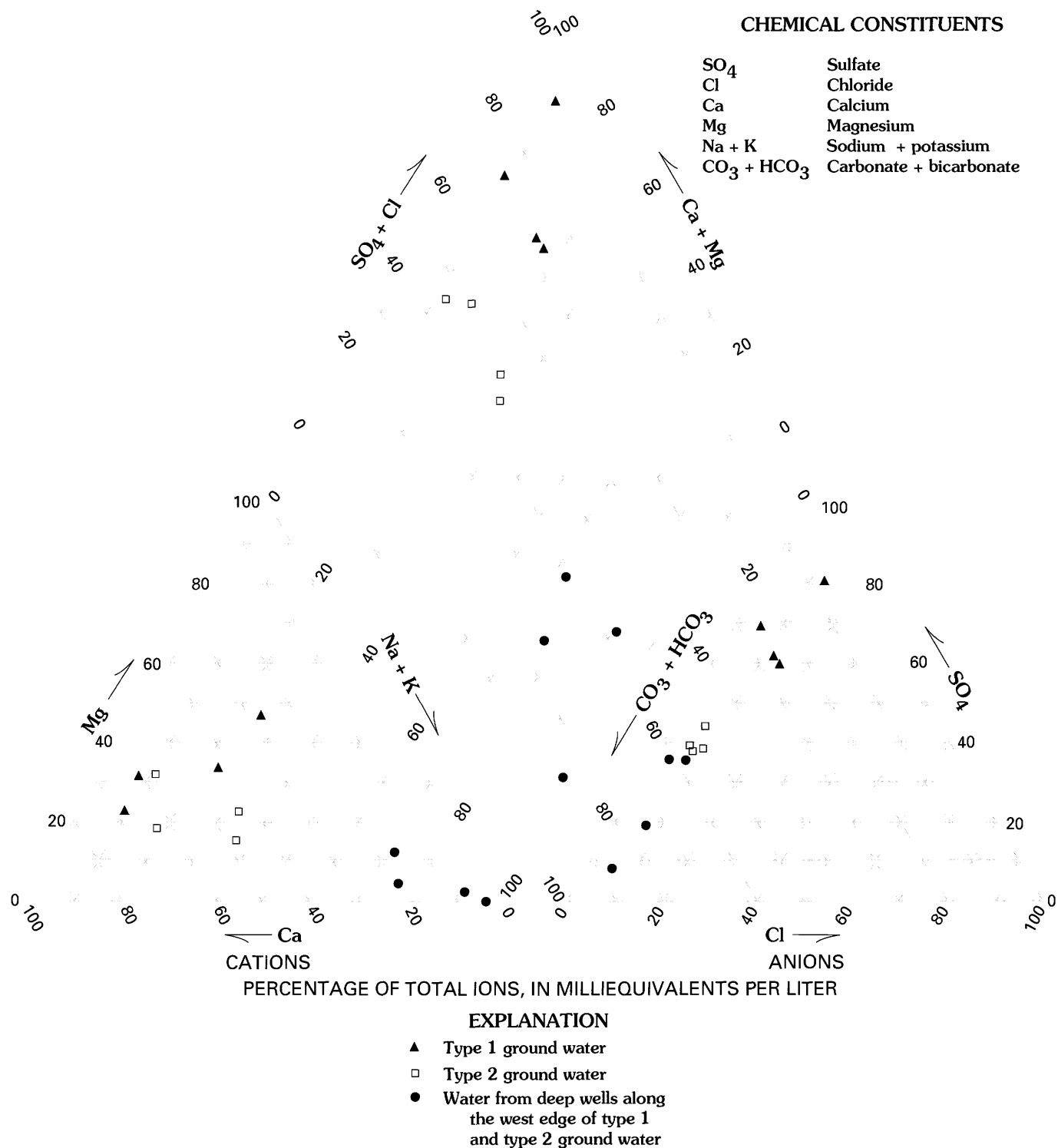


FIGURE 46.—Selected ground-water analyses from the area east of the Mesilla Valley.

magnesium and sulfate plus chloride for sampling sites in this area are shown in table 13. The amounts of calcium plus magnesium and sulfate plus chloride shown in this table are smaller in the deep samples

than in the shallow samples (water types 1 and 2). The small amount of calcium plus magnesium in the deep ground water may indicate that calcium-for-sodium ion exchange occurs in deep ground water.

Ground water west of the poorly defined ground-water divide between the Jornada del Muerto and the Mesilla Basin has smaller sulfate concentrations than ground water east of the divide. Ground-water-quality data used in this study are not sufficient to prove or disprove the presence and location of the ground-water divide. The fact that the smallest specific conductances are near the location of the ground-water divide of Wilson and others (1981) may suggest that recharge occurs in this area.

In the Fillmore Pass area, the distribution of anions and the range of specific conductance are quite variable (pl. 5). Water from well 25S.4E.17.442 has a specific conductance of 818 microsiemens and a sulfate concentration that is three times greater than the chloride concentration (pl. 5). Water from well 25S.4E.8.000 has a specific conductance of 743 microsiemens and a chloride concentration that is greater than the sulfate concentration. Water from wells 25S.4E.18.242 and 25S.3E.12.413 has a specific conductance of approximately 2,000 microsiemens and a chloride concentration that is greater than the sulfate concentration. The wide range of concentrations in a small area may indicate that there are several ground-water inflow sources with different chemical compositions. One inflow water probably contains large chloride concentrations. Another type probably is similar to the composition of water derived from well 25S.4E.17.442.

Water from many wells along the eastern side of the basin has relatively large chloride concentrations in comparison with other ground water in the basin. Conover (1954, p. 87) reported that the east drain that runs along the eastern side of the valley from Anthony to Mesquite had the poorest quality water of any drains in the Mesilla Basin. The large chloride concentrations and poor-quality ground water along the east side of the Mesilla Basin are probably due to the inflow of geothermal water.

Swanberg (1975) characterized the thermal waters in the Mesilla Basin. He used chemical geothermometers (silica and sodium potassium calcium) to calculate maximum reservoir temperatures of as much as 230 degrees Celsius. Swanberg found that the highest geochemical temperatures occurred along the valley fault and decreased rapidly and systematically away from the fault. This valley fault runs along the eastern side of the Mesilla Valley. Swanberg (1975) postulated that the valley fault acts as a conduit for ascending geothermal water.

Icerman and Lohse (1983) used shallow-temperature-gradient holes to delineate the magnitude and extent of the geothermal resources of the area. They found a thermal anomaly that they suggested

may result from a fault-controlled hydrothermal system 28 miles long and ranging in width from 2.5 to 5 miles (fig. 47). Icerman and Lohse (1983, p. 75) also suggested that geothermal waters may ascend along basement faults and then flow laterally to the west and mix with the cooler, less mineralized ground water of the Mesilla Basin. This mixing causes wide ranges in chemical composition of ground water in the area east of the Mesilla Valley because of the wide range in mixing ratios and the difference in chemical composition of the cooler, less mineralized water (inflow water from adjacent areas).

The geothermal water contains large concentrations of chloride, silica, and potassium. A plot of chloride versus potassium concentrations shows that there are two linear trends in the data (fig. 48). The difference in the two trends does not seem to be related to geographical areas. If the trends represent dilution trends (geothermal water diluted or mixed with recharge water), the divergence of the trends with increasing concentration suggests that there may be two end members of geothermal water.

Inflow of geothermal water does not seem to be restricted to a small area but instead seems to be distributed along the entire eastern side of the Mesilla Basin, as indicated by the large potassium, chloride, and silica concentrations in ground water along the east side of the basin (table 12 and pl. 5). The largest potassium concentrations occur in water from wells 25S.3E.6.212 and 23S.2E.25.321 (table 12). The sample from well 23S.2E.25.321 was collected from Paleozoic limestone, and the temperature of the sample was approximately 68 degrees Celsius (Icerman and Lohse, 1983, p. 137-140). Fournier (1977) presented a method to calculate geothermal reservoir temperatures using silica (Si), sodium (Na), potassium (K), and calcium (Ca) concentrations in ground-water samples. Silica geothermometer temperatures calculated for selected water analyses ranged from 90 to 112 degrees Celsius (table 14). Na/K geothermometer-calculated temperatures ranged from 168 to 248 degrees Celsius and Na/K/Ca geothermometer-calculated temperatures ranged from 175 to 219 degrees Celsius. These calculations indicate that the reservoir temperatures are much hotter than the temperature of water from well 23S.2E.25.321. This temperature difference also seems to indicate that the water from well 23S.2E.25.321 and from other wells in the area has already mixed with cooler and probably less mineralized ground water.

The large differences between the calculated silica geothermometer temperatures and the Na/K and Na/K/Ca geothermometer temperatures also may indicate mixing. The mixing of geothermal water and

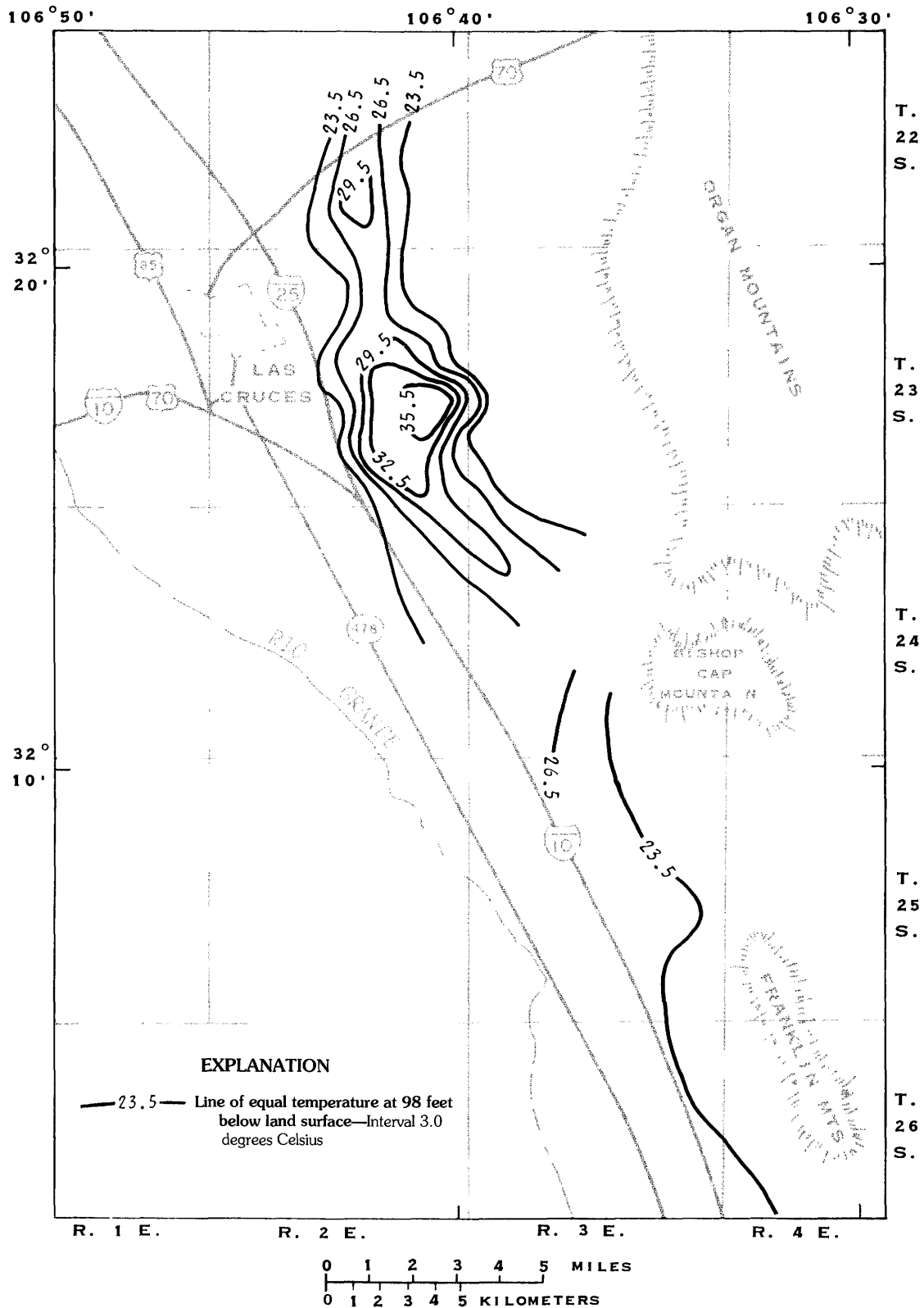


FIGURE 47.—Location of the thermal anomaly along the east side of the Mesilla Basin. Modified from Icerman and Lohse (1983).

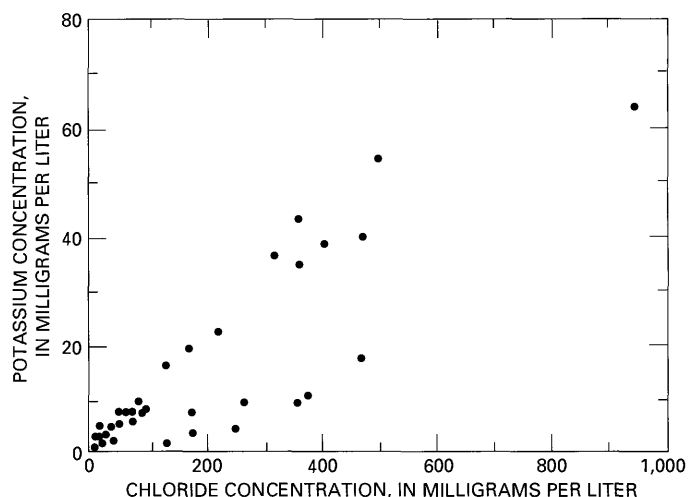


FIGURE 48.—Chloride versus potassium concentrations for selected ground-water analyses in the area east of the Mesilla Valley.

shallow ground water containing relatively small dissolved-solids concentrations would probably have a greater effect on the calculated silica geothermometer temperatures than on the Na/K and Na/K/Ca geothermometer temperatures.

In the southern part of the area east of the Mesilla Valley, large chloride concentrations are present in analyses of water from wells 29S.4E.6.243 and JL-49-12-106. These analyses do not have large silica concentrations, and the sulfate to chloride ratio is greater than the ratio in geothermal water. These differences may indicate that the water is not of geothermal origin or, if the water is of geothermal origin, that the composition is different from other geothermal water in the basin. Leggat and others (1962, p. 36) indicated that, at the south and east ends of the Mesilla Basin, large dissolved-solids concentrations occur, and the base of the freshwater zone becomes shallower to the south and east. Wilson and others (1981, pls. 8 and 15) also showed that, in the southeast area of the basin, the freshwater zone is shallow and thin, and the dissolved-solids concentration is greater than 3,000 mg/L close to the land surface. Upward vertical gradients in this area indicate upward movement of deep basin water. Upward-moving deep basin water would be expected to contain large concentrations of dissolved ions. The wide range in chemical composition of ground water in the southern Mesilla Basin may be due to differences in mixing ratios of shallow ground water, recharge water from the Franklin Mountains, and upward-moving deep basin ground water.

CONCLUSIONS CONCERNING BASIN GEOCHEMISTRY

The chemistry of ground water in the area west of the Mesilla Valley is controlled by the chemical nature of inflow water. Along the northwest margin of the basin, inflow water has a specific conductance between 1,400 and 2,310 microsiemens. Sulfate is the dominant anion and sodium is the dominant cation in this inflow water. Two types of ground-water inflow occur along the southwestern margin of the basin. Bicarbonate and sodium are the dominant ions in type 1, which has a specific conductance of less than 1,940 microsiemens. Chloride and sodium are the dominant ions in type 2. The specific conductance of water from the one well that receives this type of inflow is 7,400 microsiemens. This water probably represents geothermal water or water that moves upward along a major fault that separates the East Potrillo Mountains from the Mesilla Basin.

Ground water in the Mesilla Basin west of Las Cruces generally has a specific conductance less than 900 microsiemens. Sulfate is the dominant anion in this ground water. Water samples from a well completed at several different depths in this area indicate that the specific conductance decreases and the percentage of bicarbonate increases with depth.

The chemical composition of ground water in the Mesilla Valley varies areally and vertically. The large variation in the chemical composition is due to mixing of excess applied irrigation water and water in the aquifer. The excess applied irrigation water generally has larger dissolved-solids concentrations than water deep in the aquifer; thus, the shallow mixed water generally has larger dissolved-solids concentrations than water deep in the aquifer. The location of the transition zone between these two water types is probably a transient feature that moves in response to ground-water withdrawals.

Two types of ground water occur in the northeastern part of the area east of the Mesilla Valley. The differences in ground-water types may be due to the different rock types in their recharge areas. The percentage of sulfate plus chloride and specific conductance are greater in recharge from the San Andres Mountains than in recharge from the Organ Mountains. In the area near Radium Springs, inflow of geothermal water with large chloride concentrations controls the chemical nature of ground water.

Inflow of geothermal water with large chloride, silica, and potassium concentrations mixes with cool, less mineralized water along the eastern side of the

Mesilla Basin. Calculated chemical-geothermometer temperatures indicate that the geothermal reservoir temperatures may be as high as 230 degrees Celsius.

In the southeast corner of the basin, the freshwater zone (less than 1,000 mg/L dissolved solids) is thin. Ground water having large concentrations of chloride and dissolved solids in the southeastern corner of the basin probably is caused by upward flow of deep basin water.

SUMMARY

The basin-fill deposits, composed of the Santa Fe Group and flood-plain alluvium, form a three-dimensional ground-water flow system in the Mesilla Basin. The lateral extent and depth of the system are defined by bedrock consisting of igneous-intrusive and metamorphic rocks, Paleozoic and Mesozoic sedimentary rocks, and lower Tertiary sedimentary and volcanic rocks. The estimated values of hydraulic conductivity of the Santa Fe Group ranged from 1 to 100 feet per day. The estimated values of hydraulic conductivity of the shallow part of the aquifer (flood-plain alluvium and upper part of the Santa Fe Group) ranged from 10 to 437 feet per day. Values of hydraulic conductivity of the bedrock are much smaller than those of the basin-fill deposits. Mountain- and slope-front recharge may be about 15 cubic feet per second; however, most flow into and out of the ground-water flow system occurs at or near the land surface in the Mesilla Valley and is the result of complex interactions among the Rio Grande, drains, canals, evapotranspiration, and ground-water withdrawals. Generally, ground-water recharge occurs beneath the Rio Grande, the canals, and the irrigated lands; discharge occurs at drains and wells. These flows fluctuate seasonally, and in the intermediate term (1–5 years), they fluctuate with the availability of surface water. In the long term, they do not fluctuate much. Ground-water flow generally is away from the Mesilla Valley near Las Cruces and back toward the valley in the southern part of the basin.

A finite-difference ground-water flow model consisting of 36 rows, 64 columns, and 5 layers was used to simulate the flow system from 1915 to 1975. The model simulated ground-water flow to and from the Rio Grande and the system of drains that empties into the Rio Grande. The model also simulated evapotranspiration from irrigated and nonirrigated lands in the Mesilla Valley and ground-water withdrawals for irrigation. Mountain- and slope-front recharge (about 15 cubic feet per second) was estimated by an empirical formula and modeled as specified fluxes. Pumpage of

ground water for municipal, industrial, and domestic uses (about 58 cubic feet per second in 1975) was either reported or estimated from population data and was simulated as specified fluxes.

Values of hydraulic conductivity of the uppermost layer generally were about 22 feet per day if the layer represented the Santa Fe Group and about 70 feet per day if the layer represented the flood-plain alluvium and the upper part of the underlying Santa Fe Group. Values of hydraulic conductivity of other layers representing the Santa Fe Group ranged from 3 to 22 feet per day. The ratio of horizontal to vertical hydraulic conductivity was estimated to be 200:1.

The model matched measured hydraulic heads, drain discharges, and river depletions reasonably well, with a few exceptions. Model-derived hydraulic heads in the Las Cruces well-field area were about 20 feet too high, and model-derived drain discharges generally were too small before 1950 and too large after 1950. Also, model-derived hydraulic heads in the top layer for a few sites in the Cañutillo well-field area were 10 to 20 feet too high.

According to sensitivity analyses, the model was insensitive to storage properties for the period simulated. Any predictions that might be made would be dependent on specification of storage properties derived from other analyses or from aquifer tests.

The model indicated that about 80 percent of the ground water withdrawn for nonirrigation uses during 1975 may have come from depletion of streamflow. The remainder came from storage in the aquifer and from salvaged evapotranspiration. The accuracy of any predicted effects of future withdrawals on depletion of streamflow would depend largely upon the accuracy of the values of hydraulic conductivity, specific yield, and specific storage simulated in the model. This is especially the case if ground-water withdrawals were to occur at great distance from the Mesilla Valley.

West of the Mesilla Valley, the chemical nature of inflow water from areas adjacent to the Mesilla Basin determines ground-water chemistry. Along the north-west margin of the basin, inflow has a specific conductance between 1,400 and 2,310 microsiemens; sulfate is the dominant anion, and sodium is the dominant cation. Along the southwestern margin, two types of inflow occur. Bicarbonate and sodium are the dominant ions in type 1, which has a specific conductance of less than 1,940 microsiemens. Chloride and sodium are the dominant ions in type 2. The specific conductance from the one well that derives this type of inflow is 7,400 microsiemens. This water probably represents geothermal water or water that moves upward along a major fault that separates the East Potrillo Mountains from the Mesilla Basin.

West of Las Cruces, ground water generally has a specific conductance less than 900 microsiemens; specific conductance decreases and the percentage of bicarbonate increases with depth. Sulfate is the dominant anion in this ground water.

The chemical composition of ground water in the Mesilla Valley varies areally and vertically due to mixing of excess applied irrigation water and water in the aquifer. Shallow water generally has larger dissolved-solids concentrations than water deep in the aquifer. The location of the transition zone between these two water types is probably a transient feature that moves in response to ground-water withdrawals.

In the northeastern part of the basin, the differences in ground-water types may be due to the different rock types in recharge areas. The percentage of sulfate plus chloride and the specific conductance are greater in recharge from the San Andres Mountains than in recharge from the Organ Mountains. Near Radium Springs, inflow of geothermal water causes large chloride concentrations.

Inflow of geothermal water with large chloride, silica, and potassium concentrations mixes with cool, less mineralized water along the eastern side of the Mesilla Basin. Calculated chemical-geothermometer temperatures indicate that the geothermal reservoir temperatures may be as high as 230 degrees Celsius.

In the southeast corner of the basin, the freshwater zone (containing less than 1,000 mg/L dissolved solids) is thin. Ground water having large concentrations of chloride and dissolved solids in this area probably is caused by upward flow of water from great depth in the basin.

SELECTED REFERENCES

- Anderholm, S.K., 1985, Clay-sized fraction and powdered whole-rock X-ray analysis from alluvial-basin deposits in central and southern New Mexico: U.S. Geological Survey Open-File Report 85-173, 18 p.
- Bachman, G.O., and Mehnert, H.H., 1978, New K-Ar dates the late Pliocene to Holocene geomorphic history of the central Rio Grande region, New Mexico: Geological Society of America Bulletin, v. 89, no. 2, p. 283-292.
- Ball, D.M., 1974, Ground-water model for the Mesilla Valley for 1960 through 1973: Las Cruces, New Mexico State University, unpub. M.S. thesis, 120 p.
- Barker, F.C., 1898, Irrigation in Mesilla Valley, New Mexico: U.S. Geological Survey Water-Supply Paper 10, 50 p.
- Belcher, R.C., 1975, The geomorphic evolution of the Rio Grande: Waco, Tex., Baylor University, Baylor Geological Studies Bulletin 29, 64 p.
- Berggren, W.A., and Van Couvering, J.A., 1974, The late Neogene, *reprinted from Palaeogeography, Palaeoclimatology, Palaeoecology*: Amsterdam, Elsevier Scientific Publishing Co., v. 16, no. 1-2, 228 p.
- Bieberman, R.A., compiler, 1957, Petroleum exploration map of Doña Ana County, New Mexico: New Mexico Bureau of Mines and Mineral Resources Exploration Map 17, periodically revised.
- Birch, F.S., 1980, Three-dimensional gravity model of the basin hydrologic parameters in New Mexico: Unpublished report prepared for the U.S. Geological Survey by the University of New Mexico under contract 14-08-0001-17899, 27 p.
- Blaney, H.F., and Hanson, E.G., 1965, Consumptive use and water requirements in New Mexico: New Mexico State Engineer Technical Report 32, 82 p.
- Bryan, Kirk, 1938, Geology and ground-water conditions of the Rio Grande depression in Colorado and New Mexico, in [U.S.] National Resources Planning Board, Regional Planning Part 6, The Rio Grande joint investigation in the upper Rio Grande basin in Colorado, New Mexico, and Texas, 1936-1937: Washington, U.S. Government Printing Office, v. 1, pt. 2, sec. 1, p. 197-225.
- Bryan, Kirk, and McCann, F.T., 1937, The Ceja del Rio Puerco—A border feature of the Basin and Range Province in New Mexico: Journal of Geology, v. 45, p. 801-828.
- Chapin, C.E., Chamberlin, R.M., Osburn, G.R., White, C.W., and Sanford, A.R., 1978, Exploration framework of the Socorro geothermal area, New Mexico: New Mexico Geological Society Special Publication 7, p. 115-129.
- Chapin, C.E., and Seager, W.R., 1975, Evolution of the Rio Grande Rift in the Socorro and Las Cruces areas: New Mexico Geological Society Guidebook, 26th Field Conference, p. 297-321.
- Classen and Rowland, Consulting Engineers, 1948, Report on survey and study of municipal water works system, and future requirements of supply and facilities for the City of Las Cruces, New Mexico: El Paso, Tex., Classen and Rowland, 23 p.
- Clemons, R.E., 1976, Sierra de las Uvas ash-flow field, south-central New Mexico: New Mexico Geological Society Special Publication 6, p. 115-121.
- Conover, C.S., 1954, Ground-water conditions in the Rincon and Mesilla Valleys and adjacent areas in New Mexico: U.S. Geological Survey Water-Supply Paper 1230, 200 p.
- Dane, C.H., and Bachman, G.O., 1965, Geologic map of New Mexico: U.S. Geological Survey, scale 1:500,000, 2 sheets.
- Davis, S.N., and DeWiest, R.J.M., 1966, Hydrology: New York, John Wiley and Sons, 463 p.
- Debler, E.B., 1932, Final report on Middle Rio Grande investigations: U.S. Department of Interior, Bureau of Reclamation, 145 p.
- Dinwiddie, G.A., 1967, Rio Grande basin—Geography, geology, and hydrology, in Water Resources of New Mexico: New Mexico State Planning Office, p. 129-142.
- Dinwiddie, G.A., Mourant, W.A., and Basler, J.A., 1966, Municipal water supplies and uses, southwestern New Mexico: New Mexico State Engineer Technical Report 29D, 98 p.
- Dunham, K.C., 1935, The geology of the Organ Mountains, with an account of Doña Ana County, New Mexico: New Mexico Bureau of Mines and Mineral Resources Bulletin 11, 272 p.
- Field, J.W., no date, New Mexico State University 1966-67 annual domestic water survey: Las Cruces, New Mexico State University, 21 p.
- no date, Static water table, New Mexico State University campus annual report no. 1, 1 July 1968-1 July 1969: Las Cruces, New Mexico State University, 9 p.
- no date, Static water table, New Mexico State University campus tri-annual report no. 2, 1 July 1968-1 July 1971: Las Cruces, New Mexico State University, 11 p.

- _____, no date, New Mexico State University campus annual water report, 1 July 1972–1 July 1973: Las Cruces, New Mexico State University, 9 p.
- _____, no date, New Mexico State University campus annual water report, 1 July 1973–1 July 1974: Las Cruces, New Mexico State University, 10 p.
- _____, no date, New Mexico State University campus annual water report, 1 July 1974–1 July 1975: Las Cruces, New Mexico State University, 10 p.
- Fournier, R.O., 1977, Chemical geothermometers and mixing models for geothermal systems: *Geothermics*, v. 5, p. 41–50.
- Freeze, R.A., and Cherry, J.A., 1979, *Groundwater*: Englewood Cliffs, N.J., Prentice-Hall, 604 p.
- Gabin, V.L., and Lesperance, L.E., 1975, New Mexico climatological data, precipitation, temperature, evaporation, and wind, monthly and annual means, 1850–1975: Socorro, N. Mex., W.K. Summers and Associates, 436 p.
- Galusha, Ted, 1966, The Zia Sand Formation, new early to medial Miocene beds in New Mexico: *American Museum Novitates*, no. 2271, p. 1–12.
- _____, 1974, Dating rocks of the Santa Fe Group—Programs and problems: New Mexico Geological Society Guidebook, 25th Field Conference, p. 283–286.
- Galusha, Ted, and Blick, J.C., 1971, Stratigraphy of the Santa Fe Group, New Mexico: *American Museum of Natural History Bulletin*, v. 144, article 1, 125 p.
- Gates, J.S., White, D.E., Stanley, W.D., and Ackerman, H.D., 1978, Availability of fresh and slightly saline ground water in the basins of westernmost Texas: U.S. Geological Survey Open-File Report 78–663, 115 p.
- Gelhar, L.W., and McLin, S.G., 1979, Evaluation of a hydrosalinity model of irrigation return-flow water quality in the Mesilla Valley, New Mexico: U.S. Environmental Protection Agency 600/2–79–173, Robert S. Kerr Environmental Research Laboratory, 192 p.
- Gelhar, L.W., Wierenga, P.J., Duffy, C.J., Rehfeldt, K.R., Senn, R.B., Simonett, M., Yeh, T.C., Gutjahr, A.L., Strong, W.R., and Bustamante, A., 1980, Irrigation return-flow studies at San Acacia, New Mexico—Monitoring, modeling, and variability: Socorro, New Mexico Institute of Mining and Technology Hydrology Research Program Report H-3, 195 p.
- Harbeck, G.E., Jr., Kohler, M.A., Koberg, G.E., and others, 1958, Water-loss investigations—Lake Mead studies: U.S. Geological Survey Professional Paper 298, 100 p.
- Hawley, J.W., 1975, Quaternary history of Doña Ana County region, south-central New Mexico, in *Guidebook of the Las Cruces Country*: New Mexico Geological Society, 26th Field Conference, p. 139–150.
- _____, 1978, Correlation chart 2—Middle to upper Cenozoic stratigraphic units in selected areas of the Rio Grande Rift in New Mexico, in Hawley, J.W., ed., *Guidebook to Rio Grande Rift in New Mexico and Colorado*: New Mexico Bureau of Mines and Mineral Resources Circular 163, p. 239–241.
- _____, 1984, Hydrogeologic cross sections of the Mesilla Bolson area, Doña Ana County, New Mexico, and El Paso County, Texas: New Mexico Bureau of Mines and Mineral Resources Open-File Report 190, 10 p.
- Hawley, J.W., and Kottowski, F.E., 1969, Quaternary geology of the south-central New Mexico border region, in *Border Stratigraphy Symposium*: New Mexico Bureau of Mines and Mineral Resources Circular 104, p. 89–115.
- Hawley, J.W., Kottowski, F.E., Strain, W.S., Seager, W.R., King, W.E., and LeMone, D.V., 1969, The Santa Fe Group in the south-central New Mexico border region, in *Border Stratigraphy Symposium*: New Mexico Bureau of Mines and Mineral Resources Circular 104, p. 52–76.
- Hearne, G.A., 1982, Supplement to the New Mexico three-dimensional model (Supplement to Open-File Report 80–421): U.S. Geological Survey Open-File Report 82–857, 89 p.
- Hearne, G.A., and Dewey, J.D., 1988, Hydrologic analysis of the Rio Grande basin above Embudo, New Mexico, Colorado and New Mexico: U.S. Geological Survey Water-Resources Investigations Report 86–4113, 244 p.
- Hoffer, J.M., 1971, Mineralogy and petrology of the Santo Tomas–Black Mountains basalt field, Potrillo volcanics, south-central New Mexico: *Geological Society of America Bulletin*, v. 82, no. 3, p. 603–612.
- _____, 1976, Geology of Potrillo basalt field, south-central New Mexico: New Mexico Bureau of Mines and Mineral Resources Circular 149, 30 p.
- Icerman, Larry, and Lohse, R.L., 1983, Geothermal low-temperature reservoir assessment in Doña Ana County, New Mexico: New Mexico Energy Research and Development Institute Report 2–69–2202, 188 p.
- Izett, G.A., 1977, Volcanic ash beds in continental deposits of the southern high plains—Their bearing on the time of the Blencoe–Irvingtonian faunal transition [abs.]: *Geological Society of America, Abstracts with Programs*, v. 9, no. 7, p. 1,034.
- Johnson, A.I., 1967, Specific yield—Compilation of specific yields for various materials: U.S. Geological Survey Water-Supply Paper 1662–D, 74 p.
- Kelley, V.C., 1977, Geology of Albuquerque Basin, New Mexico: New Mexico Bureau of Mines and Mineral Resources Memoir 33, 59 p.
- Kelley, V.C., and Silver, Caswell, 1952, Geology of the Caballo Mountains: Albuquerque, University of New Mexico Publications in Geology, no. 4, 286 p.
- King, W.E., and Hawley, J.W., 1975, Geology and ground-water resources of the Las Cruces area, New Mexico, in *Guidebook of the Las Cruces Country*: New Mexico Geological Society, 26th Field Conference, p. 195–204.
- King, W.E., Hawley, J.W., Taylor, A.M., and Wilson, R.P., 1971, Geology and ground-water resources of central and western Doña Ana County, New Mexico: New Mexico Bureau of Mines and Mineral Resources Hydrologic Report 1, 64 p.
- Kottowski, F.E., 1953, Tertiary-Quaternary sediments of the Rio Grande valley in southern New Mexico—Road log, Las Cruces to Caballo, in *Guidebook of southwestern New Mexico*: New Mexico Geological Society, Fourth Field Conference, p. 144–148.
- _____, 1975, Stratigraphy of the San Andres Mountains in south-central New Mexico, in *Guidebook of the Las Cruces Country*: New Mexico Geological Society, 26th Field Conference, p. 95–104.
- Kottowski, F.E., Flower, R.H., Thompson, M.L., and Foster, R.W., 1956, Stratigraphic studies of the San Andres Mountains, New Mexico: New Mexico Bureau of Mines and Mineral Resources Memoir 1, 132 p.
- Kudo, A.M., Kelley, B.C., Damon, P.E., and Shafiqullah, M., 1977, K-Ar ages of basalt flows at Canjilon Hill, Isleta volcano, and the Cat Hills volcanic field, Albuquerque-Belen Basin, central New Mexico: *Isochron/West*, no. 18, p. 15–16.
- Lambert, P.W., 1968, Quaternary stratigraphy of the Albuquerque area, New Mexico: Albuquerque, University of New Mexico, Ph.D. dissertation, 257 p.
- Lansford, R.R., Sorensen, E.F., Creel, B.J., Latham, R.D., and Wile, W.W., 1976, Sources of irrigation water and irrigated and dry cropland acreages in New Mexico, by county: Las Cruces, New Mexico State University Agricultural Experiment Station Research Report 324, 39 p.

- Lansford, R.R., Sorensen, E.F., Gollehon, N.R., Fisburn, M., Loslebon, L., Creel, B.J., and West, F.G., 1980, Sources of irrigation water and irrigated and dry cropland acreages in New Mexico, by county, 1974–1979: Las Cruces, New Mexico State University Agricultural Experiment Station Research Report 422, 39 p.
- Lee, W.T., 1907, Water resources of the Rio Grande valley in New Mexico and their development: U.S. Geological Survey Water-Supply Paper 188, 59 p.
- Leggat, E.R., Lowry, M.E., and Hood, J.W., 1962, Ground-water resources of the lower Mesilla Valley, Texas and New Mexico: Texas Water Commission Bulletin 6203, 191 p.
- Lizarraga, S.P., 1978, A non-linear lumped-parameter model for the Mesilla Valley, New Mexico: Socorro, New Mexico Institute of Mining and Technology, unpub. M.S. thesis, 43 p.
- Lohman, S.W., 1972, Ground-water hydraulics: U.S. Geological Survey Professional Paper 708, 80 p.
- Lovejoy, E.M.P., and Hawley, J.W., 1978, Road log, El Paso to New Mexico-Texas State line, in Hawley, J.W., ed., Guidebook to the Rio Grande Rift: New Mexico Bureau of Mines and Mineral Resources Circular 163, p. 57–68.
- Machette, M.N., 1978, Geologic map of the San Acacia quadrangle, Socorro County, New Mexico: U.S. Geological Survey Geologic Quadrangle Map GQ-1415, scale 1:24,000.
- Malm, N.R., and Houghton, F.E., 1977, Climatic guide, Las Cruces, 1851–1976: Las Cruces, New Mexico State University Agricultural Experiment Station Research Report 350, 20 p.
- Manley, Kim, 1978, Geologic map of Bernalillo northwest quadrangle, Sandoval County, New Mexico: U.S. Geological Survey Geologic Quadrangle Map GQ-1446, scale 1:24,000.
- McDonald, M.G., and Harbaugh, A.W., 1984, A modular three-dimensional finite-difference ground-water flow model: U.S. Geological Survey Open-File Report 83–875, 528 p.
- Meinzer, O.E., 1923, The occurrence of ground water in the United States, with a discussion of principles: U.S. Geological Survey Water-Supply Paper 489, 321 p.
- Miller, R.S., 1988, User's guide for RIV2—A package for routing and accounting of river discharge for a modular, three-dimensional, finite-difference, ground-water flow model: U.S. Geological Survey Open-File Report 88–345, 33 p.
- Peterson, D.M., Khaleel, Raz, and Hawley, J.W., 1984, Quasi three-dimensional modeling of groundwater flow in the Mesilla Bolson, New Mexico and Texas: New Mexico Water Resources Research Institute Technical Completion Report, Project No. 1–3–45645, October 1984, 185 p.
- Poland, J.F., Lofgren, B.E., Ireland, R.L., and Pugh, R.G., 1975, Land subsidence in the San Joaquin Valley, California, as of 1972: U.S. Geological Survey Professional Paper 437–H, 78 p.
- Posson, D.R., Hearne, G.A., Tracy, J.V., and Frenzel, P.F., 1980, A computer program for simulating geohydrologic systems in three dimensions: U.S. Geological Survey Open-File Report 80–421, 795 p.
- Randall, Alan, and Dewbre, Joe, 1972, Inventory of water diversions and rate structures for cities, towns, and villages in New Mexico: Las Cruces, New Mexico State University Agricultural Experiment Station Technical Report 241, 50 p.
- Richardson, G.L., Gebhard, T.G., Jr., and Brutsaert, W.F., 1972, Water-table investigation in the Mesilla Valley: Las Cruces, New Mexico State University Engineering Experiment Station Technical Report 76, 206 p.
- Ruhe, R.V., 1967, Geomorphic surfaces and surficial deposits in southern New Mexico: New Mexico Bureau of Mines and Mineral Resources Memoir 18, 66 p.
- Seager, W.R., 1973, Resurgent volcano-tectonic depression of Oligocene age, south-central New Mexico: Geological Society of America Bulletin, v. 84, no. 11, p. 3,611–3,626.
- , 1975, Cenozoic tectonic evolution of the Las Cruces area, New Mexico, in Guidebook of the Las Cruces Country: New Mexico Geological Society, 26th Field Conference, p. 241–250.
- Seager, W.R., Hawley, J.W., and Clemons, R.E., 1971, Geology of San Diego Mountain area, Doña Ana County, New Mexico: New Mexico Bureau of Mines and Mineral Resources Bulletin 97, 38 p.
- Seager, W.R., Shafiqullah, M., Hawley, J.W., and Marvin, R.F., 1984, New K-Ar dates from basalts and the evolution of the southern Rio Grande Rift: Geological Society of America Bulletin 95, p. 87–99.
- Slichter, C.S., 1905, Observations on the ground waters of the Rio Grande valley: U.S. Geological Survey Water-Supply Paper 141, 83 p.
- Sorensen, E.F., 1977, Water use by categories in New Mexico counties and river basins, and irrigated and dry cropland acreage in 1975: New Mexico State Engineer Technical Report 41, 34 p.
- , 1982, Water use by categories in New Mexico counties and river basins, and irrigated acreage in 1980: New Mexico State Engineer Technical Report 44, 51 p.
- Spiegel, Zane, 1958, Ground-water trends in New Mexico: New Mexico Professional Engineer, March, pt. 1, p. 8–12, and April, pt. 2, p. 8–11.
- Stone, H.L., 1968, Iterative solution of implicit approximations of multidimensional partial differential equations: Society for Industrial and Applied Mathematics Journal on Numerical Analysis, v. 5, no. 3, p. 530–558.
- Strain, W.S., 1966, Blancan mammalian fauna and Pleistocene formations, Hudspeth County, Texas: Texas Memorial Museum Bulletin 10, 55 p.
- , 1969, Late Cenozoic strata of the El Paso area, in Border Stratigraphy Symposium: New Mexico Bureau of Mines and Mineral Resources Circular 104, p. 122–123.
- Swanberg, C.A., 1975, Detection of geothermal components in ground waters of Doña Ana County, southern Rio Grande Rift, New Mexico, in Guidebook of the Las Cruces Country: New Mexico Geological Society, 26th Field Conference, p. 175–180.
- Taylor, A.M., 1967, Geohydrologic investigations in the Mesilla Valley, New Mexico: Las Cruces, New Mexico State University, unpub. M.S. thesis, 130 p.
- Theis, C.V., 1936, Ground-water supplies near Las Cruces, New Mexico: U.S. Geological Survey unpub. report, 9 p.
- Thompson, Sam, III, and Bieberman, R.A., 1975, Oil and gas exploration wells in Doña Ana County, New Mexico, in Guidebook of the Las Cruces Country: New Mexico Geological Society, 26th Field Conference, p. 171–174.
- Titus, F.B., Jr., 1967, Central closed basins—Geography, geology, and hydrology, in Water Resources of New Mexico: New Mexico State Planning Office, p. 99–111.
- Trescott, P.C., 1975, Documentation of finite-difference model for simulation of three-dimensional ground-water flow: U.S. Geological Survey Open-File Report 75–438, 32 p.
- Trescott, P.C., and Larson, S.P., 1976, Documentation of finite-difference model for simulation of three-dimensional ground-water flow (Supplement to Open-File Report 75–438): U.S. Geological Survey Open-File Report 76–591, 21 p.
- Trescott, P.C., Pinder, G.F., and Larson, S.P., 1976, Finite-difference model for aquifer simulation in two dimensions with results of numerical experiments: Techniques of Water-Resources Investigations of the U.S. Geological Survey, book 7, chap. C1, 116 p.
- U.S. Bureau of Reclamation, 1973, New Mexico water resources assessment for planning purposes: v. II, supporting data, 440 p.

- U.S. Department of Agriculture, Weather Bureau, 1931-40, Climatological data, New Mexico section, annual reports 1930-39: v. 34-43, no. 13.
- U.S. Department of Commerce, Bureau of the Census, 1952a, Census of population, 1950, v. II, Characteristics of the population: pt. 31, New Mexico, 138 p.
- _____. 1952b, Census of population, 1950, v. II, Characteristics of the population: pt. 43, Texas, 607 p.
- _____. 1982a, Census of population, 1980, v. 1, Characteristics of the population, Chapter A, Number of inhabitants: pt. 33, New Mexico, 37 p.
- _____. 1982b, Census of population, 1980, v. 1, Characteristics of the population, Chapter A, Number of inhabitants: pt. 45, Texas, sec. 4.
- U.S. Department of Commerce, Environmental Science Services Administration, 1966-70, Climatological data, New Mexico annual summaries 1965-69: v. 69-73, no. 13.
- _____. 1966-70, Climatological data, Texas annual summaries 1965-69: v. 70-74, no. 13.
- U.S. Department of Commerce, National Oceanic and Atmospheric Administration, 1971-81, Climatological data, New Mexico annual summaries 1970-80: v. 74-84, no. 13.
- _____. 1971-81, Climatological data, Texas annual summaries 1970-80: v. 75-85, no. 13.
- U.S. Department of Commerce, Weather Bureau, 1941-65, Climatological data, New Mexico annual summaries 1940-64: v. 44-68, no. 13.
- _____. 1958, Climatology of the United States no. 11-36, Climatic summary of the United States—Supplement for 1931 through 1952, Texas: 147 p.
- _____. 1962-65, Climatological data, Texas annual summaries 1961-64: v. 66-69, no. 13.
- _____. 1965, Climatology of the United States no. 86-36, Decennial census of United States climate—Climatic summary of the United States—Supplement for 1951 through 1960, Texas: 197 p.
- U.S. Department of State, International Boundary and Water Commission, United States and Mexico, no date, Flow in the Rio Grande and related data from San Marcial, New Mexico, to the Gulf of Mexico: Summary of Water Bulletin no. 1, 1889-1955, 89 p.
- U.S. Geological Survey, 1981, Water resources data—New Mexico, Water year 1980: U.S. Geological Survey Water-Data Report NM-80-1, 679 p.
- Updegraph, D.C., and Gelhar, L.W., 1978, Parameter estimation for a lumped-parameter ground-water model of the Mesilla Valley, New Mexico: New Mexico Water Resources Research Institute Report 097, 69 p.
- Walton, W.C., 1962, Selected analytical methods for well and aquifer evaluation: Illinois State Water Survey Bulletin 49, 81 p.
- Weir, J.E., 1965, Geology and availability of ground water in the northern part of White Sands Missile Range and vicinity, New Mexico: U.S. Geological Survey Water-Supply Paper 1802, 78 p.
- Wen, Cheng-Lee, 1983, A study of bolson-fill thickness in the southern Rio Grande Rift, southern New Mexico, west Texas, and northern Chihuahua: University of Texas at El Paso, unpub. M.S. thesis, 74 p.
- Wilkins, D.W., Scott, W.B., and Kaehler, C.A., 1980, Planning report for the Southwest Alluvial Basins (east) Regional Aquifer-System Analysis, parts of Colorado, New Mexico, and Texas: U.S. Geological Survey Open-File Report 80-564, 39 p.
- Wilson, C.A., and White, R.R., 1984, Geohydrology of the central Mesilla Valley, Doña Ana County, New Mexico: U.S. Geological Survey Water-Resources Investigations 82-555, 144 p.
- Wilson, C.A., White, R.R., Orr, B.R., and Roybal, R.G., 1981, Water resources of the Rincon and Mesilla Valleys and adjacent areas, New Mexico: New Mexico State Engineer Technical Report 43, 514 p.
- Woodward, L.A., Callender, J.F., Seager, W.R., Chapin, C.E., Gries, J.C., Shaffer, W.L., and Zilinski, R.E., 1978, Tectonic map of Rio Grande Rift region in New Mexico, Chihuahua, and Texas, in Hawley, J.W., ed., Guidebook to Rio Grande Rift in New Mexico and Colorado: New Mexico Bureau of Mines and Mineral Resources Circular 163, sheet 2.
- Yeo, H.W., 1928, Report on irrigation in the Rio Grande basin in Texas above Fort Quitman and in New Mexico during 1907, 1920, and 1928, v. 1: New Mexico State Engineer report, 283 p.
- Zohdy, A.A.R., Jackson, D.B., Mattick, R.E., and Peterson, D.L., 1969, Geophysical surveys for ground water at White Sands Missile Range, New Mexico: U.S. Geological Survey Open-File Report 69-326, 31 p. [plus supplemental information].

TABLES 1–14

SOUTHWEST ALLUVIAL BASINS RASA PROJECT

TABLE 1.—*Estimated values of hydraulic conductivity of the Santa Fe Group*

[Open interval is the depth below land surface of the interval of hydraulic connection to the aquifer. No inference as to the type of opening is made. K is the estimated hydraulic conductivity. Adjusted interval is the open interval below the water table. No adjustment was made for wells in the valley where the water table was relatively shallow (about 15 feet)]

Latitude	Longitude	Well number	Open interval (feet)	K (feet per day)	Adjusted interval (feet)
32°22'23"	106°49'16"	22S.1E.22.444	252-273	2	
			504-525	18	
			672-693	4	
32°19'46"	106°50'28"	23S.1E.4.434	335-355	25	
32°19'17"	106°48'20"	23S.1E.11.214	384-404	7	
			510-530	7	
			640-660	9	
32°19'17"	106°48'20"	23S.1E.11.214a	465-485	55	
32°18'30"	106°47'30"	23S.1E.13.411	600-620	19	
			961-981	19	
			1,260-1,280	3	
			1,448-1,468	1	
32°18'30"	106°47'30"	23S.1E.13.411b	429-629	19	
32°20'09"	106°45'23"	23S.2E.5.321	392-620	20	212-440
32°19'14"	106°46'33"	23S.2E.7.122	213-360	26	153-300
32°19'14"	106°46'25"	23S.2E.7.411	281-381	44	221-321
32°18'56"	106°45'28"	23S.2E.8.433	430-716	12	280-566
32°18'19"	106°44'52"	23S.2E.16.314	381-591	13	231-441
32°18'32"	106°45'13"	23S.2E.17.243	410-700	10	280-570
32°16'28"	106°45'58"	23S.2E.29.331	243-458	50	
32°16'42"	106°46'04"	23S.2E.30.243a	205-225	26	
			310-330	47	
			430-450	48	
			650-670	5	
32°13'35"	106°47'21"	24S.1E.13.221a	140-370	60	
32°14'10"	106°46'27"	24S.2E.7.231	170-460	47	
32°13'24"	106°43'26"	24S.2E.15.231a	463-484	36	
32°13'08"	106°45'38"	24S.2E.17.322	180-464	38	
32°13'14"	106°45'10"	24S.2E.17.423a	310-680	41	
32°12'36"	106°44'45"	24S.2E.21.123	170-480	68	
32°10'47"	106°43'06"	24S.2E.36.131	392-412	8	
			507-527	12	
32°08'26"	106°51'12"	25S.1E.16.114	600-1,650	12	250-1,300
32°09'42"	106°44'17"	25S.2E.4.141	242-262	5	
			505-525	5	
			660-680	2	
32°06'29"	106°42'51"	25S.2E.26.114	251-272	7	
			503-524	16	
			651-672	8	
32°07'37"	106°39'57"	25S.3E.17.111a	437-457	2	
			675-685	2	
32°05'40"	106°36'40"	25S.3E.28.434	225-245	45	
			730-750	14	
			1,200-1,220	6	
32°00'54"	106°53'39"	26S.1W.25.414	443-563	24	53-173
32°04'14"	106°39'58"	26S.3E.6.442	307-597	35	

TABLE 1.—*Estimated values of hydraulic conductivity of the Santa Fe Group—Continued*

Latitude	Longitude	Well number	Open interval (feet)	K (feet per day)	Adjusted interval (feet)
32°03'37"	106°39'13"	26S.3E.8.143	400–420	3	
			945–965	1	
			1,410–1,430	34	
			1,660–1,680	2	
32°02'45"	106°37'47"	26S.3E.15.322	310–330	10	
			565–585	100	
			670–690	29	
			820–840	3	
			1,050–1,070	13	
31°56'25"	106°39'17"	27S.3E.20.432	195–215	12	
			450–470	18	
			640–660	14	
31°51'11"	106°39'18"	28S.3E.20.432	163–320	24	53–210
31°50'50"	106°38'49"	28S.3E.28.114	240–350	25	110–220
31°50'44"	106°38'08"	28S.3E.28.241	135–285	51	75–225
31°50'46"	106°39'29"	28S.3E.29.231	201–350	26	71–220
31°47'24"	106°35'07"	29S.3E.13.223	300–320	1	120–140
			390–410	8	210–230

TABLE 2.—*Estimated values of hydraulic conductivity of the shallow part of the aquifer in the Mesilla Valley (flood-plain alluvium and upper part of the Santa Fe Group)*

[The hydraulic conductivity was estimated to be the specific capacity multiplied by 170 and divided by the difference between the well depth and the water level]

Latitude	Longitude	Well number	Well depth (feet)	Water level (feet)	Specific capacity (gallons per minute per foot)	Estimated hydraulic conductivity (feet per day)
32°28'05"	106°54'06"	21S.1W.24.133	100	7	39	71
32°25'52"	106°51'50"	21S.1E.32.344	185	11	64	63
32°24'35"	106°51'25"	22S.1E.8.234	178	8	83	83
32°24'06"	106°50'05"	22S.1E.16.122	140	8	64	82
32°22'50"	106°51'20"	22S.1E.20.244	142	10	80	103
32°23'00"	106°51'00"	22S.1E.21.113	180	10	68	68
32°22'20"	106°42'10"	22S.2E.26.214	100	14	102	202
32°20'27"	106°49'39"	23S.1E.3.213	145	15	49	64
32°20'30"	106°49'20"	23S.1E.3.221	145	14	82	106
32°20'30"	106°51'02"	23S.1E.4.114	138	38	43	73
32°18'30"	106°50'40"	23S.1E.16.142	111	16	71	127
32°17'35"	106°50'00"	23S.1E.22.133	133	10	72	100
32°17'13"	106°48'32"	23S.1E.23.433	120	23	120	210
32°16'07"	106°50'26"	23S.1E.33.214	130	18	20	30
32°16'05"	106°49'50"	23S.1E.34.141	120	8	46	70
32°16'00"	106°49'50"	23S.1E.34.143	109	7	86	143
32°15'44"	106°48'08"	23S.1E.35.424	80	21	151	435
32°15'40"	106°48'15"	23S.1E.35.442	80	19	60	167
32°15'45"	106°47'40"	23S.1E.36.324	225	21	44	37
32°16'45"	106°45'20"	23S.2E.29.234	230	95	28	35

SOUTHWEST ALLUVIAL BASINS RASA PROJECT

TABLE 2.—*Estimated values of hydraulic conductivity of the shallow part of the aquifer in the Mesilla Valley (flood-plain alluvium and upper part of the Santa Fe Group)—Continued*

Latitude	Longitude	Well number	Well depth (feet)	Water level (feet)	Specific capacity (gallons per minute per foot)	Estimated hydraulic conductivity (feet per day)
32°14'55"	106°44'55"	24S.2E.4.313	160	19	49	59
32°14'18"	106°45'47"	24S.2E.8.114	214	18	49	43
32°13'55"	106°44'05"	24S.2E.9.442	140	15	51	69
32°14'30"	106°43'35"	24S.2E.10.122	240	81	33	35
32°14'20"	106°43'20"	24S.2E.10.213	240	79	31	33
32°13'25"	106°43'50"	24S.2E.15.132	114	14	61	104
32°13'10"	106°43'30"	24S.2E.15.324	150	16	43	55
32°13'05"	106°44'25"	24S.2E.16.431	150	14	50	63
32°13'00"	106°45'35"	24S.2E.17.413	90	11	50	108
32°13'05"	106°45'15"	24S.2E.18.244	199	13	66	60
32°12'20"	106°43'47"	24S.2E.22.311	191	15	45	43
32°12'40"	106°42'50"	24S.2E.23.112	90	13	198	437
32°11'20"	106°43'20"	24S.2E.27.432	85	13	63	149
32°09'50"	106°41'20"	25S.2E.1.233	186	10	14	14
32°09'55"	106°41'05"	25S.2E.1.242	350	13	24	12
32°09'40"	106°41'55"	25S.2E.1.313	131	12	62	89
32°09'30"	106°41'10"	25S.2E.1.441	120	10	55	85
32°09'44"	106°44'07"	25S.2E.4.422	95	15	48	102
32°09'06"	106°42'36"	25S.2E.11.142	130	9	62	87
32°09'05"	106°41'20"	25S.2E.12.213	65	14	68	227
32°06'58"	106°43'49"	25S.2E.22.314	200	19	47	44
32°06'50"	106°41'05"	25S.2E.24.444	120	10	88	136
32°05'20"	106°42'10"	25S.2E.35.424	116	11	21	34
32°08'14"	106°40'01"	25S.3E.18.224	250	8	14	10
32°07'50"	106°40'15"	25S.3E.18.423	156	9	95	110
32°07'30"	106°39'50"	25S.3E.20.112	120	9	18	28
32°07'00"	106°39'20"	25S.3E.20.411	125	8	34	49
32°05'30"	106°40'55"	25S.3E.31.131	125	9	154	226
32°05'48"	106°38'37"	25S.3E.33.112	100	11	10	19
32°03'30"	106°41'05"	26S.2E.12.422	100	10	135	255
32°04'05"	106°38'26"	26S.3E.4.433	130	9	36	51
32°04'55"	106°39'20"	26S.3E.5.212	80	12	51	128
32°04'35"	106°40'25"	26S.3E.6.233	110	12	66	114
32°04'30"	106°40'55"	26S.3E.6.311	120	10	44	68
32°04'15"	106°40'15"	26S.3E.6.441	203	12	20	18
32°02'40"	106°39'55"	26S.3E.17.313	116	11	163	264
32°02'35"	106°39'55"	26S.3E.17.331	120	8	46	70
31°59'44"	106°39'14"	27S.3E.5.212	139	9	84	110
31°59'30"	106°39'00"	27S.3E.5.242	143	12	93	121
31°59'25"	106°39'00"	27S.3E.5.244	148	12	110	138
31°58'30"	106°38'08"	27S.3E.9.243	136	9	44	59
31°57'32"	106°39'24"	27S.3E.17.411	120	14	59	95
31°55'30"	106°39'06"	27S.3E.29.441	216	11	58	48

TABLE 2.—*Estimated values of hydraulic conductivity of the shallow part of the aquifer in the Mesilla Valley (flood-plain alluvium and upper part of the Santa Fe Group)—Continued*

Latitude	Longitude	Well number	Well depth (feet)	Water level (feet)	Specific capacity (gallons per minute per foot)	Estimated hydraulic conductivity (feet per day)
31°54'51"	106°38'35"	27S.3E.33.324	130	12	58	84
31°54'02"	106°39'00"	28S.3E.5.422	122	9	33	50
31°58'47"	106°38'09"	JL-49-03-303	80	11	46	113
31°57'34"	106°36'27"	JL-49-04-142	150	7	39	46
31°56'17"	106°36'56"	JL-49-04-403	155	8	17	20
31°56'19"	106°36'21"	JL-49-04-406	152	8	23	27
31°55'57"	106°36'18"	JL-49-04-412	160	8	23	26
31°55'37"	106°36'15"	JL-49-04-415	122	7	28	41
31°55'57"	106°36'58"	JL-49-04-420	155	7	13	15

TABLE 3.—*River and drain specifications*

Row	Column	Specified head in stream (feet)	Connection coefficient, CRIV (feet squared per second)
Initial condition (steady state)			
River reach 1 (discharges to reach 2)			
20	63	3,964	13.93
19	63	3,963	6.96
20	62	3,958	6.96
21	62	3,955	13.93
21	61	3,952	13.93
20	60	3,950	13.93
21	59	3,944	13.93
22	58	3,936	13.93
23	58	3,934	13.93
22	57	3,927	13.93
23	56	3,923	13.93
22	56	3,918	6.96
21	56	3,917	6.96
21	55	3,911	13.93
22	55	3,909	6.96
23	54	3,908	13.93
22	54	3,907	6.96
21	53	3,902	15.33
21	52	3,898	12.54
21	51	3,893	4.18
20	51	3,891	4.18
20	50	3,889	3.48
20	49	3,886	3.48
20	48	3,883	3.48
20	47	3,881	3.48
19	47	3,879	3.48
19	46	3,878	3.48
19	45	3,877	3.48
19	44	3,876	3.48
19	43	3,875	3.48
19	42	3,874	3.48

TABLE 3.—*River and drain specifications—Continued*

Row	Column	Specified head in stream (feet)	Connection coefficient, CRIV (feet squared per second)
Initial condition (steady state)—Continued			
River reach 1 (discharges to reach 2)—Continued			
18	42	3,873	3.48
18	41	3,871	3.48
18	40	3,870	3.48
18	39	3,868	3.48
18	38	3,866	3.48
19	38	3,866	3.48
19	37	3,865	9.75
20	36	3,859	13.93
21	36	3,857	6.96
22	35	3,854	13.93
23	34	3,850	13.93
24	33	3,845	13.93
24	32	3,841	13.93
24	31	3,838	13.93
25	30	3,834	13.93
26	30	3,834	6.96
25	29	3,829	13.93
25	28	3,826	13.93
26	27	3,820	13.93
26	26	3,817	13.93
26	25	3,814	1.39
25	25	3,813	2.78
25	24	3,809	2.78
24	24	3,806	2.78
23	24	3,805	2.78
23	23	3,804	2.78
24	23	3,801	2.78
23	22	3,797	2.78
23	21	3,792	2.78
23	20	3,791	2.78
22	20	3,788	2.78

TABLE 3.—River and drain specifications—Continued

Row	Column	Specified head in stream (feet)	Connection coefficient, CRIV (feet squared per second)
Initial condition (steady state)—Continued			
River reach 1 (discharges to reach 2)—Continued			
21	19	3,786	2.78
21	18	3,783	2.78
20	18	3,782	2.78
19	18	3,781	2.78
19	17	3,779	2.78
19	16	3,777	1.95
20	16	3,776	1.95
18	15	3,776	1.67
20	15	3,773	1.67
19	14	3,769	.69
17	14	3,775	.69
17	13	3,774	0.69
19	13	3,768	.69
18	12	3,770	1.95
17	12	3,771	1.95
16	11	3,768	2.78
18	11	3,768	2.78
16	10	3,764	2.78
18	10	3,761	2.78
River reach 2 (discharges to reach 3)			
23	15	3,776	0.83
22	15	3,771	.83
21	15	3,770	.83
21	14	3,769	.69
21	13	3,768	.69
21	12	3,766	1.95
20	11	3,762	2.78
River reach 3 (discharges to reach 4)			
19	10	3,758	2.78
16	9	3,758	2.78
17	9	3,758	2.78
19	9	3,756	2.78
River reach 4 (discharges to reach 5)			
26	19	3,787	2.78
25	18	3,779	2.78
25	17	3,777	2.78
25	16	3,775	1.95
24	15	3,773	1.67
24	14	3,771	.69
23	13	3,769	.69
22	12	3,767	1.95
22	11	3,764	2.78
21	10	3,759	2.78
21	9	3,755	2.78
20	8	3,750	2.78
River reach 5 (last reach)			
19	8	3,750	2.78

TABLE 3.—River and drain specifications—Continued

Row	Column	Specified head in stream (feet)	Connection coefficient, CRIV (feet squared per second)
Initial condition (steady state)—Continued			
River reach 5 (last reach)—Continued			
17	8	3,748	2.78
19	7	3,746	2.78
20	7	3,745	2.78
18	7	3,745	2.78
17	7	3,745	2.78
18	6	3,740	2.78
19	6	3,740	2.78
20	6	3,740	2.78
18	5	3,735	2.78
19	5	3,734	2.78
20	5	3,734	2.78
21	4	3,731	2.78
20	4	3,733	2.78
19	4	3,731	2.78
20	3	3,729	2.78
21	3	3,729	2.78
22	3	3,727	2.78
22	2	3,725	2.23
Simulation for 1915 to 1975			
River reach 1 (discharges to reach 4)			
20	64	3,956	0.00
20	63	3,950	1.40
20	62	3,946	.69
21	62	3,943	.69
21	61	3,941	1.40
20	60	3,938	1.40
21	59	3,933	1.40
Drain reach 2 (discharges to reach 3)			
22	62	3,948	0.33
22	61	3,942	.55
Drain reach 3 (discharges to reach 4)			
22	60	3,940	0.55
22	59	3,934	.55
River reach 4 (discharges to reach 5)			
22	58	3,927	1.40
22	57	3,924	1.40
21	56	3,920	1.40
21	55	3,915	1.40
22	55	3,912	.55
22	54	3,907	1.40
22	53	3,903	.76
21	53	3,901	.76
21	52	3,896	1.26
21	51	3,893	.84
20	50	3,891	.70
20	49	3,888	.70
20	48	3,885	.70
20	47	3,883	.70

TABLE 3.—River and drain specifications—Continued

Row	Column	Specified head in stream (feet)	Connection coefficient, CRIV (feet squared per second)
Simulation for 1915 to 1975—Continued			
River reach 4 (discharges to reach 5—Continued)			
20	46	3,882	.34
19	46	3,881	.34
River reach 5 (discharges to reach 7)			
19	45	3,880	0.70
18	44	3,877	.70
18	43	3,874	.70
18	42	3,872	.70
18	41	3,871	.70
18	40	3,869	.70
Drain reach 6 (discharges to reach 7)			
20	51	3,888	0.33
19	50	3,884	.28
19	49	3,883	.28
19	48	3,881	.28
19	47	3,880	.28
18	46	3,879	.28
17	45	3,877	.28
17	44	3,875	.28
17	43	3,873	.28
17	42	3,873	.28
17	41	3,873	.28
18	40	3,873	.28
River reach 7 (discharges to reach 9)			
18	39	3,867	0.70
18	38	3,866	.70
19	37	3,862	.98
20	36	3,859	1.40
21	35	3,855	1.40
22	34	3,848	1.40
23	33	3,841	1.40
24	32	3,838	1.40
Drain reach 8 (discharges to reach 9)			
20	36	3,852	0.33
21	35	3,848	.55
22	34	3,844	.55
23	33	3,840	.55
24	32	3,836	.55
River reach 9 (discharges to reach 30)			
24	31	3,833	1.40
25	30	3,830	1.40
25	29	3,825	1.40
26	28	3,820	1.40
26	27	3,816	1.40
27	26	3,812	1.40
Drain reach 10 (discharges to reach 12)			
23	59	3,932	0.28
23	58	3,927	.55

TABLE 3.—River and drain specifications—Continued

Row	Column	Specified head in stream (feet)	Connection coefficient, CRIV (feet squared per second)
Simulation for 1915 to 1975—Continued			
Drain reach 10 (discharges to reach 12)			
23	57	3,924	.55
23	56	3,919	.55
23	55	3,914	.55
Drain reach 11 (discharges to reach 12)			
22	56	3,917	0.55
22	55	3,914	.28
Drain reach 12 (discharges to reach 13)			
24	54	3,910	0.55
Drain reach 13 (discharges to reach 15)			
24	53	3,906	0.61
23	52	3,902	.25
22	52	3,893	.50
Drain reach 14 (discharges to reach 15)			
23	54	3,905	0.22
22	53	3,900	.36
21	53	3,897	.24
21	52	3,895	.25
21	50	3,886	.28
21	49	3,885	.28
21	48	3,883	.28
21	47	3,881	.28
20	46	3,877	.28
20	45	3,875	.28
19	44	3,872	.28
19	43	3,870	.28
19	42	3,868	.28
19	41	3,866	.28
19	40	3,864	.28
Drain reach 16 (discharges to reach 17)			
19	44	3,872	0.28
18	43	3,870	.28
18	42	3,868	.28
18	41	3,866	.28
18	40	3,864	.28
Drain reach 17 (discharges to reach 21)			
19	39	3,860	0.28
19	38	3,857	.28
20	37	3,855	.39
20	36	3,852	.28
21	36	3,850	.28
22	35	3,846	.28
Drain reach 18 (discharges to reach 20)			
25	55	3,919	0.55
25	54	3,914	.55
25	53	3,908	.61
26	52	3,902	.50

TABLE 3.—River and drain specifications—Continued

Row	Column	Specified head in stream (feet)	Connection coefficient, CRIV (feet squared per second)
Simulation for 1915 to 1975—Continued			
Drainreach 18 (discharges to reach 20)—Continued			
25	51	3,898	0.33
25	50	3,895	.28
24	50	3,893	.28
23	50	3,892	.28
Drain reach 19 (discharges to reach 20)			
23	51	3,895	0.33
Drain reach 20 (discharges to reach 21)			
23	49	3,890	0.28
23	48	3,887	.28
23	47	3,885	.28
23	46	3,884	.28
22	45	3,881	.28
21	44	3,878	.28
21	43	3,875	.28
21	42	3,873	.28
21	41	3,871	.28
21	40	3,868	.28
22	39	3,865	.28
22	38	3,863	.28
22	37	3,860	.39
22	36	3,855	.55
Drain reach 21 (discharges to reach 25)			
23	35	3,843	0.55
23	34	3,840	.55
24	33	3,833	.55
Drain reach 22 (discharges to reach 24)			
23	43	3,873	0.28
24	43	3,871	.28
25	43	3,868	.28
25	42	3,866	.28
25	41	3,863	.28
24	41	3,861	.28
23	40	3,858	.28
23	39	3,856	.28
24	38	3,853	.28
Drain reach 23 (discharges to reach 24)			
25	39	3,858	0.28
25	38	3,856	.28
Drain reach 24 (discharges to reach 25)			
24	37	3,850	0.39
24	36	3,845	.55
25	35	3,840	.55
25	34	3,836	.55
25	33	3,833	.28
Drain reach 25 (discharges to reach 28)			
24	32	3,831	0.55
25	31	3,826	.55

TABLE 3.—River and drain specifications—Continued

Row	Column	Specified head in stream (feet)	Connection coefficient, CRIV (feet squared per second)
Simulation for 1915 to 1975—Continued			
Drain reach 26 (discharges to reach 28)			
24	31	3,827	0.28
Drain reach 27 (discharges to reach 28)			
26	32	3,830	0.55
26	31	3,824	.55
Drain reach 28 (discharges to reach 29)			
26	30	3,822	0.55
26	29	3,818	.55
26	28	3,816	.55
Drain reach 29 (discharges to reach 30)			
27	27	3,813	0.55
27	26	3,811	.39
River reach 30 (discharges to reach 39)			
26	25	3,810	0.97
25	25	3,808	.41
25	24	3,805	1.40
24	23	3,801	1.40
24	22	3,797	1.40
Drain reach 31 (discharges to reach 33)			
19	36	3,850	0.55
20	35	3,846	.55
20	34	3,843	.55
21	33	3,841	.55
21	32	3,838	.44
22	32	3,836	.28
23	32	3,833	.55
Drain reach 32 (discharges to reach 33)			
22	34	3,843	0.22
22	33	3,840	.28
23	33	3,837	.28
Drain reach 33 (discharges to reach 35)			
23	31	3,828	0.55
Drain reach 34 (discharges to reach 35)			
22	31	3,829	0.22
Drain reach 35 (discharges to reach 36)			
23	30	3,825	0.22
24	30	3,824	.33
24	29	3,822	.55
23	28	3,817	.55
23	27	3,811	.55
22	26	3,808	.55
Drain reach 36 (discharges to reach 38)			
22	25	3,806	0.55

TABLE 3.—River and drain specifications—Continued

Row	Column	Specified head in stream (feet)	Connection coefficient, CRIV (feet squared per second)
Simulation for 1915 to 1975—Continued			
Drain reach 36 (discharges to reach 38)—Continued			
22	24	3,804	1.12
23	24	3,802	.55
Drain reach 37 (discharges to reach 38)			
25	28	3,819	0.39
25	27	3,814	.55
24	26	3,809	.55
24	25	3,805	.55
Drain reach 38 (discharges to reach 39)			
23	23	3,797	0.55
23	22	3,794	.44
River reach 39 (discharges to reach 46)			
23	21	3,795	1.40
23	20	3,791	1.40
23	19	3,786	1.40
24	18	3,781	1.40
24	17	3,780	1.40
25	16	3,777	.98
Drain reach 40 (discharges to reach 42)			
27	35	3,847	0.22
27	34	3,843	.55
27	33	3,839	.55
27	32	3,835	.55
27	31	3,831	.55
27	30	3,827	.55
28	29	3,823	.55
28	28	3,819	.55
28	27	3,815	.55
28	26	3,811	.55
28	25	3,806	.55
27	25	3,806	.55
Drain reach 41 (discharges to reach 42)			
27	27	3,814	0.39
27	26	3,810	.55
Drain reach 42 (discharges to reach 45)			
27	24	3,800	0.55
28	23	3,796	.55
28	22	3,794	.16
27	22	3,792	.39
27	21	3,790	.55
27	20	3,786	.55
27	19	3,783	.55
26	18	3,777	.55
25	17	3,774	.55
Drain reach 43 (discharges to reach 44)			
26	24	3,800	0.44
26	23	3,798	.55
25	22	3,794	.55

TABLE 3.—River and drain specifications—Continued

Row	Column	Specified head in stream (feet)	Connection coefficient, CRIV (feet squared per second)
Simulation for 1915 to 1975—Continued			
Drain reach 43 (discharges to reach 44)—Continued			
25	21	3,790	.55
Drain reach 44 (discharges to reach 45)			
25	20	3,786	0.55
25	19	3,782	.55
25	18	3,778	.55
Drain reach 45 (discharges to reach 46)			
25	16	3,771	0.19
River reach 46 (discharges to reach 57)			
25	15	3,776	0.84
24	14	3,773	.70
24	13	3,771	.70
23	12	3,769	.98
23	11	3,766	1.40
22	10	3,763	1.40
21	9	3,756	1.40
20	8	3,753	1.40
19	7	3,749	1.40
Drain reach 47 (discharges to reach 49)			
21	31	3,831	0.33
20	31	3,830	.55
20	30	3,825	.22
21	30	3,825	.33
21	29	3,819	.55
21	28	3,816	.55
21	27	3,813	.55
21	26	3,805	.55
21	25	3,802	.55
21	24	3,800	.55
21	23	3,796	.55
21	22	3,792	.55
20	21	3,788	.55
20	20	3,784	.55
20	19	3,779	.55
19	18	3,777	0.55
19	17	3,771	.55
18	16	3,768	.39
18	15	3,765	.33
18	14	3,763	.28
18	13	3,761	.28
18	12	3,759	.39
18	11	3,755	.55
Drain reach 48 (discharges to reach 49)			
20	14	3,770	0.28
20	13	3,765	.28
19	12	3,760	.39
19	11	3,755	.16
Drain reach 49 (discharges to reach 51)			
18	10	3,750	0.22
17	10	3,748	.33

TABLE 3.—River and drain specifications—Continued

Row	Column	Specified head in stream (feet)	Connection coefficient, CRIV (feet squared per second)
Simulation for 1915 to 1975—Continued			
Drain reach 49 (discharges to reach 51)—Continued			
17	9	3,746	.55
Drain reach 50 (discharges to reach 51)			
16	9	3,746	0.22
Drain reach 51 (discharges to reach 56)			
17	8	3,743	0.55
Drain reach 52 (discharges to reach 56)			
19	10	3,755	0.33
19	9	3,746	.28
18	9	3,746	.28
18	8	3,743	.55
Drain reach 53 (discharges to reach 55)			
23	23	3,798	0.50
22	22	3,792	.55
22	21	3,790	.55
22	20	3,785	.55
22	19	3,785	.55
22	18	3,785	.55
21	17	3,780	.55
21	16	3,774	.39
21	15	3,771	.23
22	15	3,768	.10
22	14	3,765	.28
Drain reach 54 (discharges to reach 55)			
23	18	3,774	0.28
23	17	3,773	.55
23	16	3,773	.39
23	15	3,765	.33
Drain reach 55 (discharges to reach 56)			
22	13	3,762	0.28
22	12	3,758	.39
21	11	3,755	.55
21	10	3,752	.55
20	9	3,748	.55
19	8	3,744	.55
Drain reach 56 (discharges to reach 59)			
18	7	3,739	0.55
River reach 57 (discharges to reach 63)			
18	6	3,745	1.40
18	5	3,741	1.40
19	4	3,738	1.40
19	3	3,734	.69
20	3	3,731	0.69
21	3	3,730	.69
22	3	3,728	.69

TABLE 3.—River and drain specifications—Continued

Row	Column	Specified head in stream (feet)	Connection coefficient, CRIV (feet squared per second)
Simulation for 1915 to 1975—Continued			
Drain reach 58 (discharges to reach 60)			
21	8	3,745	0.44
20	7	3,740	.55
20	6	3,735	.55
20	5	3,730	.55
Drain reach 59 (discharges to reach 60)			
19	5	3,734	0.28
Drain reach 60 (discharges to reach 61)			
20	4	3,729	0.55
Drain reach 61 (discharges to reach 63)			
21	3	3,728	0.22
22	3	3,728	.39
Drain reach 62 (discharges to reach 63)			
18	5	3,734	0.28
19	4	3,732	.55
19	3	3,731	.22
20	3	3,729	.28
21	3	3,728	.28
22	3	3,728	.28
Reach 63 (last reach)¹			
23	2	3,726	0.00

¹Reach 63 was an artifice. It was used as an accumulator for reaches 57, 61, and 62.

[In cubic feet per second]

Location within model (block)		Pumping period																													
		1915		1920		1927		1941		1948		1951		1954		1958		1961		1962		1964		1965		1967		1969		1972	
		1915	1919	1920	1926	1940	1947	1950	1954	1957	1960	1961	1963	1964	1966	1968	1971	1972	1975												
1	18	4	0.000	0.000	0.000	0.000	0.000	0.000	-1.117	-2.360	-2.820	-2.650	-2.627	-2.407	-2.236	-2.307	-2.357	-3.238	-3.336												
1	19	4	0.000	0.000	0.000	0.000	0.000	0.000	-6.104	-2.102	-1.161	-1.081	-1.071	-0.981	-0.911	-0.940	-0.961	-1.321	-1.361												
1	20	2	0.000	0.000	0.000	0.000	0.000	-0.007	-0.021	-0.021	-0.021	-0.021	-0.021	-0.021	-0.021	-0.021	-0.021	-0.021	-0.021												
1	22	11	0.000	0.000	0.000	0.000	0.000	0.000	-0.633	-1.077	-0.080	-0.970	-0.913	-0.914	-0.422	-0.694	-0.650	-0.662	-0.493												
1	22	13	0.000	0.000	0.000	0.000	0.000	0.000	-0.633	2.497	0.791	0.952	2.085	-3.767	-2.204	-2.881	-2.071	-3.171	-2.000												
1	23	11	0.000	0.000	0.000	0.000	0.000	0.000	-0.703	-0.605	-0.605	-0.974	-0.958	-0.945	-0.443	-1.485	-1.446	-1.946	-1.247												
1	23	12	0.000	0.000	0.000	0.000	0.000	0.000	-1.267	-2.550	-1.782	-1.316	-2.944	-2.651	-1.597	-2.149	-1.715	-2.170	-1.569												
1	23	13	0.000	0.000	0.000	0.000	0.000	0.000	-0.633	-1.613	-0.504	-0.202	-1.058	-1.062	-1.040	-1.646	-1.085	-1.372	-0.844												
1	23	42	0.000	0.000	0.000	0.000	0.000	0.000	0.000	0.000	0.000	0.006	0.014	0.019	0.033	0.039	0.037	.041	.060												
1	23	51	0.000	0.000	0.000	0.000	0.000	0.000	0.000	0.000	0.000	0.000	0.000	0.009	0.015	0.018	0.017	0.020	0.032												
1	24	11	0.000	0.000	0.000	0.000	0.000	0.000	0.000	0.000	0.000	0.000	0.000	0.000	0.000	0.000	-0.001	-0.063	-0.023												
1	24	13	0.000	0.000	0.000	0.000	0.000	0.000	-0.633	-0.860	-0.638	-0.312	-0.441	-0.271	-0.379	-0.959	-0.643	-0.608	-0.520												
1	24	14	0.000	0.000	0.000	0.000	0.000	0.000	0.000	0.000	0.000	0.000	0.000	0.000	-0.341	-0.964	-1.234	1.684	-1.085												
1	24	47	0.000	-0.046	-0.043	0.302	0.302	0.302	0.302	0.302	0.302	0.302	0.302	0.302	0.302	0.302	0.302	0.302	0.302												
1	25	39	0.000	0.000	0.000	0.000	0.000	0.000	0.000	0.000	0.000	0.000	0.000	0.000	0.004	0.007	0.007	0.008	0.012												
1	27	39	0.000	0.000	0.000	0.000	0.000	0.000	0.000	0.000	0.000	0.000	0.000	0.000	0.009	0.018	0.023	0.031	0.046												
1	28	43	0.000	0.000	0.000	0.000	0.000	0.000	-0.372	-1.137	-1.053	-0.935	-0.824	-0.820	-0.802	-0.714	-0.216	0.001	0.001												
1	28	46	-0.302	-0.302	-0.479	-1.285	-2.968	-0.000	-3.041	-2.578	-2.411	-2.175	-1.953	-1.944	-0.302	-0.302	-0.302	-0.302	-0.302												
1	29	43	0.000	0.000	0.000	0.000	0.000	0.000	-0.372	-1.137	-1.053	-0.935	-0.824	-0.820	-0.802	-0.714	-0.701	-0.658	-0.710												
2	13	8	0.000	0.000	0.000	0.000	0.000	0.000	0.000	0.000	0.000	0.000	0.000	0.000	0.000	0.000	0.000	0.000	-0.787												
2	13	9	0.000	0.000	0.000	0.000	0.000	0.000	0.000	0.000	0.000	0.000	0.000	0.000	0.000	0.000	0.000	0.000	-0.380												
2	14	7	0.000	0.000	0.000	0.000	0.000	0.000	0.000	0.000	0.000	0.000	0.000	0.000	0.000	0.000	0.000	0.000	-0.787												
2	15	7	0.000	0.000	0.000	0.000	0.000	0.000	0.000	0.000	0.000	0.000	0.000	0.000	0.000	0.000	0.000	0.000	-0.787												
2	19	16	-0.047	-0.066	-0.051	-0.062	-0.053	-0.053	-0.052	-0.052	-0.052	-0.052	-0.052	-0.052	-0.052	-0.052	-0.052	-0.052	-0.052												
2	19	49	0.000	0.000	0.000	-0.002	-0.027	-0.029	-0.029	-0.029	-0.029	-0.029	-0.029	-0.029	-0.029	-0.029	-0.029	-0.029	-0.029												
2	21	13	0.000	0.000	0.000	0.000	0.000	0.000	0.000	0.000	0.000	0.000	0.000	-0.554	-1.847	-0.559	-0.126	-0.133	-0.066												
2	21	23	0.000	-0.038	-0.053	-0.033	-0.030	-0.030	-0.030	-0.030	-0.030	-0.030	-0.030	-0.030	-0.030	0.000	-0.030	-0.030	-0.030												
2	22	13	0.000	0.000	0.000	0.000	0.000	0.000	0.000	0.000	0.000	0.000	0.000	0.000	0.000	0.000	0.000	0.000	-0.210												
2	22	31	0.000	0.000	0.000	0.000	0.000	-0.058	-0.059	-0.059	-0.059	-0.059	-0.059	-0.059	-0.059	-0.059	-0.059	-0.059	-0.059												
2	22	43	-0.072	-0.094	-0.129	-0.107	-0.119	-0.119	-0.122	-0.122	-0.122	-0.122	-0.122	-0.122	-0.122	-0.122	-0.122	-0.122	-0.122												

TABLE 4.—Schedule of nonagricultural withdrawals specified in the model—Continued

Location within model (block)	Pumping period															
	1915 1919	1920 1926	1927 1940	1941 1947	1948 1950	1951 1953	1954 1957	1958 1960	1961 1963	1962 1963	1964 1966	1965 1966	1967 1968	1969 1971	1972	1973 1975
2 23 12	0.000	0.000	0.000	0.000	0.000	0.000	0.000	0.000	0.000	0.000	-2.025	-0.865	-0.790	-1.738	-1.968	-0.768
2 23 28	-0.039	-0.054	-0.061	-0.054	-0.059	-0.059	-0.059	-0.059	-0.059	-0.059	-0.059	-0.059	-0.059	-0.059	-0.059	-0.059
2 23 42	0.000	0.000	0.000	0.000	0.000	0.000	0.000	0.000	0.013	-0.030	-0.039	-0.068	-0.081	-0.078	-0.087	-0.126
2 23 51	0.000	0.000	0.000	0.000	0.000	0.000	0.000	0.000	0.000	0.000	-0.018	-0.029	-0.034	-0.033	-0.039	-0.064
2 23 52	0.000	0.000	-0.023	-0.029	-0.029	-0.029	-0.029	-0.029	-0.029	-0.029	-0.029	-0.029	-0.029	-0.029	-0.029	-0.029
2 23 58	0.000	0.000	-0.002	-0.022	-0.022	-0.022	-0.022	-0.022	-0.022	-0.022	-0.022	-0.022	-0.022	-0.022	-0.022	-0.022
2 24 14	0.000	0.000	0.000	0.000	0.000	0.000	0.000	0.000	0.000	0.000	0.000	-0.248	-0.711	-0.745	-2.187	-1.234
2 24 15	0.000	0.000	0.000	0.000	0.000	0.000	0.000	-3.072	-4.288	-4.190	-3.894	-3.164	-3.023	-3.610	-3.511	-2.507
2 24 16	0.000	0.000	0.000	0.000	0.000	0.000	0.000	0.000	0.000	0.000	0.000	0.000	0.000	-0.014	-0.096	-0.376
2 24 17	0.000	0.000	0.000	0.000	0.000	0.000	0.000	0.000	0.000	0.000	0.000	-0.386	-0.799	-0.384	-2.156	-1.288
2 24 41	0.000	-0.050	-0.080	-0.116	-0.168	-0.178	-0.178	-0.178	-0.178	-0.178	-0.178	-0.178	-0.178	-0.137	-0.116	-0.116
2 25 39	0.000	0.000	0.000	0.000	0.000	0.000	0.000	0.000	0.000	0.000	-0.001	-0.008	-0.014	-0.013	-0.016	-0.025
2 25 42	0.000	0.000	0.000	0.000	0.000	0.000	0.000	-0.670	-0.937	-0.826	-0.822	-0.804	-0.716	-0.703	-0.660	-0.712
2 26 10	0.000	0.000	0.000	0.000	0.000	0.000	0.000	0.000	0.000	0.000	0.000	0.000	0.000	-0.009	-0.028	-0.028
2 26 16	0.000	0.000	0.000	0.000	0.000	0.000	0.000	0.000	0.000	0.000	0.000	0.000	0.000	0.000	0.000	-0.003
2 26 17	0.000	0.000	0.000	0.000	0.000	0.000	0.000	-0.200	-0.240	-0.202	-0.116	-0.378	-0.296	-0.370	-0.243	-0.240
2 26 31	0.000	0.000	-0.002	-0.022	-0.022	-0.022	-0.022	-0.022	-0.022	-0.022	-0.022	-0.022	-0.022	-0.015	-0.001	-0.001
2 26 41	0.000	0.000	-0.016	-0.174	-0.239	-0.299	-0.421	-0.575	-0.723	-0.806	-0.949	-1.162	-1.256	-1.639	-1.969	-2.020
2 26 47	0.000	0.000	0.000	0.000	0.000	-1.369	-1.138	-1.054	-0.936	-0.825	-0.821	-0.803	-0.715	-0.702	-0.659	-0.711
2 26 49	0.000	0.000	0.000	0.000	0.000	0.000	-1.138	-1.054	-0.936	-0.825	-0.821	-0.803	-0.715	-0.702	-0.659	-0.711
2 26 55	-0.038	-0.037	-0.033	-0.033	-0.033	-0.033	-0.033	-0.033	-0.033	-0.033	-0.033	-0.033	-0.033	-0.036	-0.054	-0.074
2 27 15	0.000	0.000	0.000	0.000	0.000	0.000	0.000	0.000	-0.381	-0.403	-0.475	-0.125	-0.153	-0.309	-0.580	-0.598
2 27 17	0.000	0.000	0.000	0.000	0.000	-0.135	-0.919	-0.514	-1.283	-1.732	-2.470	-2.202	-3.101	-2.466	-2.181	-1.837
2 27 18	0.000	0.000	0.000	0.000	0.000	0.000	-0.169	-0.198	-0.207	-0.232	-0.222	-0.237	-0.290	-0.356	-0.291	-0.128
2 27 19	-0.038	-0.042	-0.053	-0.059	-0.059	-0.059	-0.059	-0.059	-0.059	-0.059	-0.059	-0.067	-0.097	-0.129	-0.139	-0.142
2 27 36	0.000	0.000	-0.002	-0.023	-0.025	-0.025	-0.025	-0.025	-0.025	-0.025	-0.025	-0.025	-0.025	-0.025	-0.025	-0.025
2 27 39	0.000	0.000	0.000	0.000	0.000	0.000	0.000	0.000	0.000	0.000	-0.001	-0.018	-0.035	-0.046	-0.061	-0.092
2 27 50	0.000	0.000	0.000	0.000	0.000	0.000	0.000	-1.054	-0.936	-0.825	-0.821	-0.803	-0.715	-0.702	-0.659	-0.711
2 28 14	0.000	0.000	0.000	0.000	0.000	0.000	0.000	0.000	0.000	-0.049	-0.076	-0.074	-0.087	-0.098	-0.102	-0.144
2 28 17	0.000	0.000	-0.034	-0.283	-0.290	-0.496	-0.530	-0.530	-0.530	-0.551	-0.481	-0.501	-0.457	-0.523	-0.597	-0.501
2 28 44	0.000	0.000	0.000	0.000	0.000	0.000	0.000	0.000	0.000	0.000	0.000	-0.395	-0.716	-0.703	-0.660	-0.712
2 28 45	0.000	0.000	0.000	0.000	0.000	0.000	0.000	0.000	0.000	0.000	0.000	0.000	-0.715	-0.703	-0.660	-0.712
2 28 46	0.000	0.000	0.000	0.000	0.000	0.000	0.000	-0.300	-0.936	-0.825	-0.821	-0.803	-0.715	-0.932	-1.318	-1.421
2 28 48	0.000	0.000	0.000	0.000	0.000	0.000	0.000	0.000	0.000	0.000	0.000	0.000	0.000	-0.230	-0.659	-0.711
2 28 49	0.000	0.000	0.000	0.000	0.000	0.000	0.000	0.000	0.000	0.000	0.000	0.000	0.000	-0.703	-0.660	-0.712

TABLE 4.—Schedule of nonagricultural withdrawals specified in the model—Continued

Location within model (block)	Pumping period															
	1915	1920	1926	1940	1941	1948	1951	1954	1958	1961	1962	1964	1966	1967	1969	1973
	1919	1926	1940	1947	1950	1953	1957	1960	1963	1968	1971	1975				
2 28 50	0.000	0.000	0.000	0.000	0.000	0.000	0.000	0.000	0.000	0.000	0.000	-0.821	-1.198	-1.431	-1.405	-1.318
2 29 23	0.000	-0.033	-0.042	-0.021	-0.021	-0.021	-0.021	-0.021	-0.021	-0.021	-0.021	-0.021	-0.021	-0.021	-0.021	-0.021
2 29 43	0.000	0.000	0.000	0.000	0.000	0.000	-0.581	-1.054	-0.936	-0.936	-0.825	-0.821	-0.803	-0.715	-0.702	-0.659
2 29 44	0.000	0.000	0.000	0.000	0.000	0.000	0.000	-0.300	-0.936	-0.936	-0.825	-0.821	-0.803	-0.715	-0.702	-0.659
2 29 45	0.000	0.000	0.000	0.000	0.000	0.000	0.000	0.000	0.000	0.000	-0.826	-0.822	-0.804	-0.716	-0.703	-0.660
2 29 46	0.000	0.000	0.000	0.000	0.000	0.000	0.000	0.000	0.000	0.000	-0.826	-1.643	-1.607	-1.432	-1.406	-1.319
3 24 15	0.000	0.000	0.000	0.000	0.000	0.000	-0.940	-6.794	-6.693	-6.693	-9.118	-7.805	-5.566	-4.974	-6.494	-6.429
3 24 16	0.000	0.000	0.000	0.000	0.000	0.000	-0.147	-3.149	-2.184	-2.184	-2.321	-0.597	-2.174	-1.343	-1.610	-1.888
3 24 17	0.000	0.000	0.000	0.000	0.000	0.000	0.000	0.000	-0.334	-0.334	-2.040	-3.746	-4.480	-3.657	-1.626	-1.367
3 25 16	0.000	0.000	0.000	0.000	0.000	0.000	0.000	-1.455	-3.175	-3.175	-2.249	-2.396	-2.588	-1.858	-2.595	-1.654
3 26 16	0.000	0.000	0.000	0.000	0.000	0.000	0.000	0.000	0.000	0.000	0.000	0.000	0.000	0.000	0.000	0.015
3 27 18	0.000	0.000	0.000	0.000	0.000	0.000	0.000	0.000	0.000	0.000	0.000	0.000	0.000	0.000	0.000	-0.252
Totals	-0.54	-0.76	-1.14	-2.10	-3.93	-17.56	-25.06	-35.33	-39.56	-47.49	-51.91	-48.99	-47.63	-49.74	-55.99	-56.73

SOUTHWEST ALLUVIAL BASINS RASA PROJECT

TABLE 5.—Differences between measured and model-derived hydraulic heads

[NA, well number not available. Hydraulic-head data from Lee, 1907, pl. X]

Latitude	Longitude	Well number	Mode		Measured hydraulic head (feet)	Model- derived hydraulic head (feet)	Difference (feet)
			Col- umn	Row			
					Initial condition (steady-state version)		
Layer 1							
31°53'55"	106°59'06"	28S.1W.6.323	3	21	3,813.00	3,805.70	-7.30
31°48'12"	106°51'28"	29S.1E.8.210	5	10	3,801.00	3,787.00	-14.00
32°03'09"	106°52'16"	26S.1E.18.222	8	28	3,815.00	3,817.30	2.30
31°59'55"	106°49'03"	26S.1E.35.333	9	23	3,796.00	3,804.00	8.00
31°49'52"	106°41'35"	28S.2E.36.142	11	8	3,776.00	3,769.30	-6.70
31°51'18"	106°42'26"	28S.2E.23.324	11	10	3,783.00	3,773.40	-9.60
32°05'28"	106°47'02"	25S.2E.31.133	13	28	3,814.00	3,817.80	3.80
31°50'50"	106°38'49"	28S.3E.28.114	14	8	3,756.00	3,759.20	3.20
32°02'50"	106°45'02"	26S.2E.17.244	14	25	3,803.00	3,807.70	4.70
31°47'30"	106°33'55"	29S.4E.18.222	20	2	3,730.00	3,728.70	-1.30
--	--	NA	20	20	3,787.00	3,787.10	.10
--	--	NA	21	22	3,792.00	3,792.80	.80
--	--	NA	21	32	3,837.00	3,834.30	-2.70
--	--	NA	22	26	3,813.00	3,808.50	-4.50
--	--	NA	22	28	3,827.00	3,814.20	-12.80
--	--	NA	23	11	3,762.00	3,763.20	1.20
--	--	NA	24	50	3,882.00	3,884.30	2.30
--	--	NA	24	55	3,907.00	3,909.50	2.50
--	--	NA	25	35	3,847.00	3,842.60	-4.40
--	--	NA	26	39	3,862.00	3,859.00	-3.00
--	--	NA	27	23	3,797.00	3,795.70	-1.30
31°57'41"	106°34'29"	JL-49-04-202	28	14	3,771.00	3,777.50	6.50
--	--	NA	28	25	3,807.00	3,807.80	.80
32°17'57"	106°44'17"	23S.2E.21.221	29	43	3,849.00	3,871.90	22.90
32°08'24"	106°35'50"	25S.3E.13.111	33	28	3,812.00	3,824.10	12.10
Initial condition (steady-state version)							
Layer 2							
31°49'26"	106°37'55"	28S.3E.34.331	14	6	3,749.00	3,756.30	7.30
31°59'18"	106°39'13"	27S.3E.5.412	21	19	3,777.00	3,784.30	7.30
31°55'54"	106°36'57"	JL-49-04-418	22	13	3,760.00	3,768.60	8.60
32°14'10"	106°46'27"	24S.2E.7.231	22	37	3,854.00	3,855.30	1.30
31°57'03"	106°36'43"	JL-49-04-427	24	15	3,760.00	3,772.60	12.60
31°58'19	106°37'07"	JL-49-04-110	24	17	3,768.00	3,776.10	8.10
32°13'04"	106°45'14"	24S.2E.17.423	24	35	3,845.00	3,845.60	.60
32°09'46"	106°41'51"	25S.2E.1.312	26	31	3,824.00	3,830.80	6.80
32°23'24"	106°48'52"	22S.1E.14.341	26	55	3,911.00	3,906.90	-4.10
32°22'20"	106°47'10"	22S.1E.25.222	28	53	3,898.00	3,895.30	-2.70
32°00'59"	106°35'24"	26S.3E.25.411	30	19	3,784.00	3,789.90	5.90
32°08'11"	106°33'58"	25S.4E.18.242	35	26	3,815.00	3,825.40	10.40

TABLE 5.—Differences between measured and model-derived hydraulic heads—Continued

Latitude	Longitude	Well number	Mode		Measured	Model-	Difference (feet)
			Row	Col- umn	hydraulic	derived	
					head (feet)	head (feet)	
Initial condition (steady-state version)							
Layer 3							
32°08'26"	106°51'12"	25S.4E.16.114	11	33	3,837.00	3,832.90	-4.10
31°57'17"	106°36'40"	JL-49-04-419	24	15	3,774.00	3,773.90	-.10
31°57'33"	106°36'45"	JL-49-04-106	24	16	3,771.00	3,775.90	4.90
32°04'02"	106°38'55"	26S.3E.9.111	26	23	3,802.00	3,800.20	-1.80
32°00'17"	106°36'35"	26S.3E.35.141	27	19	3,766.00	3,785.70	19.70
Comparison for end of 1947							
Layer 1							
31°49'15"	106°53'13"	29S.1E.6.110	4	12	3,865.00	3,791.40	-73.60
31°55'21"	106°54'27"	27S.1W.26.430	5	21	3,803.60	3,803.30	-.30
32°02'19"	106°57'04"	26S.1W.16.330	5	29	3,804.00	3,819.00	15.00
31°49'15"	106°46'34"	28S.2E.31.340	7	9	3,811.50	3,780.50	-31.00
31°57'45"	106°51'27"	27S.1E.17.210	7	22	3,780.00	3,803.20	23.20
32°00'47"	106°53'26"	26S.1W.25.410	7	26	3,760.00	3,812.60	52.60
32°02'58"	106°52'12"	26S.1E.18.220	8	28	3,820.00	3,817.70	-2.30
32°07'09"	106°52'16"	25S.1E.19.240	9	32	3,785.00	3,828.60	43.60
32°09'23"	106°53'03"	25S.1E.6.330	10	35	3,910.00	3,837.80	-72.20
31°59'57"	106°46'18"	26S.2E.31.410	11	22	3,808.00	3,800.20	-7.80
31°51'38"	106°41'43"	28S.2E.24.110	12	10	3,782.00	3,769.70	-12.30
32°05'25"	106°46'52"	25S.2E.31.130	13	28	3,820.00	3,818.90	-1.10
32°02'47"	106°45'02"	26S.2E.17.240	14	25	3,804.00	3,808.70	4.70
32°17'02"	106°52'36"	23S.1E.30.210	14	48	3,882.30	3,874.80	-7.50
31°54'10"	106°39'05"	28S.3E.5.140	16	11	3,767.60	3,765.00	-2.60
31°47'47"	106°35'40"	29S.3E.12.300	17	3	3,747.20	3,745.30	-1.90
32°17'25"	106°51'01"	23S.1E.21.314	17	48	3,887.10	3,883.10	-4.00
31°47'10"	106°34'22"	29S.4E.18.233	18	2	3,750.00	3,742.10	-7.90
31°47'39"	106°34'02"	29S.4E.7.440	19	2	3,745.70	3,737.90	-7.80
31°59'35"	106°40'26"	27S.3E.6.213	19	20	3,768.00	3,791.20	23.20
32°00'28"	106°40'40"	26S.3E.31.123	19	21	3,790.00	3,792.50	2.50
32°06'30"	106°44'03"	25S.2E.28.220	19	28	3,815.30	3,819.70	4.40
32°01'20"	106°40'48"	26S.3E.30.114	20	22	3,791.70	3,795.40	3.70
32°15'25"	106°48'07"	23S.1E.36.333	20	41	3,863.70	3,871.50	7.80
32°15'59"	106°48'35"	23S.1E.35.231	20	43	3,866.50	3,875.50	9.00
32°16'39"	106°48'45"	23S.1E.26.311	20	45	3,870.00	3,879.00	9.00
31°48'54"	106°34'01"	JL-49-12-501	21	4	3,729.50	3,736.10	6.60
32°01'40"	106°40'19"	26S.3E.19.432	21	22	3,789.80	3,794.70	4.90
32°15'03"	106°47'37"	24S.1E.1.144	21	40	3,862.50	3,869.40	6.90
32°19'02"	106°49'13"	23S.1E.10.442	21	50	3,885.10	3,889.50	4.40
32°22'04"	106°50'45"	22S.1E.28.142	21	54	3,907.60	3,909.50	1.90
31°57'37"	106°37'36"	27S.3E.15.143	22	16	3,771.60	3,777.00	5.40
32°09'44"	106°44'03"	25S.2E.4.422	22	32	3,824.40	3,837.80	13.40
32°24'29"	106°51'44"	22S.1E.8.421	22	57	3,916.50	3,924.10	7.60

TABLE 5.—Differences between measured and model-derived hydraulic heads—Continued

Latitude	Longitude	Well number	Mode		Measured	Model-	Difference (feet)
			Row	Col- umn	hydraulic	hydraulic	
					head (feet)	head (feet)	
Comparison for end of 1947—Continued							
Layer 1—Continued							
32°26'18"	106°52'27"	21S.1E.31.412	22	60	3,935.40	3,939.10	3.70
32°28'42"	106°53'54"	21S.1W.13.323	22	62	3,947.60	3,946.70	−.90
32°29'34"	106°54'40"	21S.1W.11.431	22	63	3,956.00	3,951.90	−4.10
32°16'06"	106°46'35"	23S.2E.31.213	23	42	3,865.90	3,874.30	8.40
32°23'10"	106°50'37"	22S.1E.21.211	23	56	3,909.60	3,919.10	9.50
32°06'56"	106°41'28"	25S.2E.24.413	24	28	3,813.80	3,820.10	6.30
32°16'45"	106°46'20"	23S.2E.30.412	24	43	3,867.40	3,874.90	7.50
32°06'52"	106°40'58"	25S.3E.19.331	25	27	3,814.10	3,815.80	1.70
32°14'43"	106°45'06"	24S.2E.5.422	25	38	3,858.40	3,860.40	2.00
32°19'48"	106°47'19"	23S.1E.1.443	25	50	3,887.50	3,896.10	8.60
32°23'23"	106°49'37"	22S.1E.15.431	25	55	3,908.40	3,918.90	10.50
32°10'11"	106°42'14"	25S.2E.2.221	26	31	3,829.00	3,828.80	−.20
32°12'00"	106°43'05"	24S.2E.22.444	26	34	3,839.00	3,843.80	4.80
32°16'46"	106°45'18"	23S.2E.29.243	26	42	3,867.60	3,871.30	3.70
32°18'46"	106°45'19"	23S.2E.17.210	28	46	3,863.10	3,875.70	12.60
32°18'59"	106°45'19"	23S.2E.8.434	28	47	3,870.30	3,883.90	13.60
32°20'45"	106°46'37"	22S.2E.31.340	28	51	3,896.00	3,899.40	3.40
32°10'10"	106°40'16"	24S.3E.31.430	29	31	3,817.00	3,833.80	16.80
32°07'19"	106°37'25"	25S.3E.22.120	32	26	3,825.00	3,819.50	−5.50
32°08'53"	106°59'18"	25S.2W.12.240	6	36	3,842.00	3,829.10	−12.90
Comparison for end of 1975							
Layer 1							
31°53'55"	106°59'06"	28S.1W.6.323	3	21	3,813.37	3,805.60	−7.77
31°59'08"	107°00'50"	27S.2W.2.411	3	27	3,823.60	3,817.10	−6.50
32°03'06"	107°03'36"	26S.2W.17.214	3	32	3,828.80	3,824.50	−4.30
32°02'30"	107°01'31"	26S.2W.15.443	4	31	3,833.70	3,822.20	−11.50
31°55'36"	106°54'46"	27S.1W.26.413	5	21	3,810.69	3,803.20	−7.49
32°00'54"	106°53'39"	26S.1W.25.414	7	26	3,822.00	3,812.60	−9.40
32°07'46"	106°57'20"	25S.1W.16.331	7	35	3,835.00	3,831.10	−3.90
32°03'09"	106°52'16"	26S.1E.18.222	8	28	3,814.47	3,817.60	3.13
31°59'55"	106°49'03"	26S.1E.35.333	9	23	3,795.50	3,803.70	8.20
32°12'39"	106°56'01"	24S.1W.22.123	9	41	3,872.53	3,844.80	−27.73
32°06'51"	106°51'11"	25S.1E.21.331	10	31	3,836.17	3,826.50	−9.67
32°11'23"	106°53'23"	24S.1W.25.422	10	37	3,848.00	3,842.50	−5.50
31°49'52"	106°41'35"	28S.2E.36.142	11	8	3,776.35	3,767.10	−9.25
31°51'18"	106°42'26"	28S.2E.23.324	11	10	3,782.47	3,770.80	−11.67
32°08'26"	106°51'12"	25S.1E.16.114	11	33	3,836.69	3,833.30	−3.39
32°05'28"	106°47'02"	25S.2E.31.133	13	28	3,814.30	3,818.30	4.00
31°50'50"	106°38'49"	28S.3E.28.114	14	8	3,754.95	3,755.00	.05
31°52'12"	106°38'19"	28S.3E.16.414	16	9	3,749.45	3,750.50	1.05
32°16'07"	106°50'26"	23S.1E.33.214	16	45	3,876.70	3,873.90	−2.80
31°54'27"	106°38'57"	28S.3E.4.111	17	11	3,759.36	3,759.90	.54

TABLE 5.—Differences between measured and model-derived hydraulic heads—Continued

Latitude	Longitude	Well number	Mode		Measured	Model-	Difference (feet)
			Row	Col- umn	hydraulic	derived	
					head (feet)	head (feet)	
Comparison for end of 1975—Continued							
Layer 1—Continued							
31°54'57"	106°39'05"	27S.3E.32.244	17	12	3,762.65	3,763.90	1.25
32°17'36"	106°50'59"	23S.1E.20.134	17	48	3,877.15	3,880.50	3.35
31°51'52"	106°37'19"	JL-49-12-108	18	8	3,746.61	3,745.50	-1.11
31°58'37"	106°40'25"	27S.3E.7.231	18	18	3,779.71	3,779.60	-.11
32°15'39"	106°49'22"	23S.1E.34.423	18	43	3,874.85	3,872.80	-2.05
31°48'25"	106°34'50"	29S.4E.7.111	19	4	3,731.53	3,734.60	3.07
31°55'30"	106°38'33"	27S.3E.28.341	19	13	3,765.59	3,765.70	.11
31°59'28"	106°40'23"	27S.3E.6.231	19	19	3,782.88	3,784.60	1.72
31°59'53"	106°40'39"	26S.3E.31.341	19	20	3,784.04	3,788.40	4.36
32°18'53"	106°50'40"	23S.1E.9.433	19	51	3,890.87	3,890.60	-.27
31°49'20"	106°34'38"	JL-49-12-502	20	4	3,752.15	3,732.30	-19.85
31°51'52"	106°35'39"	JL-49-12-103	20	7	3,747.55	3,744.20	-3.35
32°00'44"	106°40'41"	26S.3E.30.343	20	21	3,789.23	3,789.80	.57
32°15'44"	106°48'08"	23S.1E.35.424	20	42	3,861.49	3,870.80	9.31
32°19'21"	106°50'01"	23S.1E.10.134	20	51	3,893.93	3,890.50	-3.43
31°48'54"	106°34'01"	JL-49-12-501	21	4	3,729.80	3,733.90	4.10
31°56'39"	106°38'04"	27S.3E.21.421	21	15	3,765.74	3,770.80	5.06
31°59'10"	106°39'13"	27S.3E.5.414	21	19	3,776.12	3,785.10	8.98
32°00'41"	106°39'45"	26S.3E.29.334	21	20	3,786.85	3,788.10	1.25
32°03'36"	106°41'11"	26S.2E.12.421	21	24	3,805.12	3,802.10	-3.02
32°26'11"	106°53'09"	21S.1W.36.221	21	60	3,932.88	3,938.10	5.22
32°27'17"	106°53'31"	21S.1W.25.232	21	61	3,942.00	3,941.20	-.80
31°55'51"	106°37'22"	JL-49-04-407	22	13	3,763.27	3,761.10	-2.17
31°55'52"	106°37'11"	JL-49-04-408	22	13	3,762.56	3,761.10	-1.46
31°57'48"	106°37'58"	27S.3E.16.224	22	17	3,771.76	3,777.00	5.24
31°58'31"	106°38'10"	27S.3E.9.243	22	17	3,775.61	3,777.00	1.39
32°03'41"	106°40'34"	26S.3E.7.144	22	24	3,800.59	3,803.40	2.81
32°20'10"	106°49'14"	23S.1E.3.422	22	52	3,890.22	3,896.10	5.88
31°55'56"	106°36'31"	JL-49-04-417	23	12	3,758.51	3,762.70	4.19
31°56'19"	106°36'43"	JL-49-04-405	23	13	3,758.88	3,762.80	3.92
31°59'28"	106°38'10"	27S.3E.4.241	23	18	3,780.18	3,779.50	-.68
31°57'33"	106°36'44"	JL-49-04-115	24	16	3,767.24	3,772.90	5.66
32°09'06"	106°42'36"	25S.2E.11.142	24	30	3,824.37	3,826.60	2.23
32°18'18"	106°47'04"	23S.2E.18.313	24	47	3,867.40	3,880.80	13.40
32°18'27"	106°47'35"	23S.1E.13.411	24	47	3,868.35	3,880.80	12.45
31°56'37"	106°35'43"	JL-49-04-436	25	13	3,751.45	3,764.90	13.45
31°57'11"	106°35'42"	JL-49-04-439	25	14	3,747.97	3,767.70	19.73
31°59'06"	106°36'51"	JL-49-04-122	25	18	3,778.33	3,779.00	.67
31°58'04"	106°35'43"	JL-49-04-138	26	16	3,748.42	3,771.70	23.28
32°16'53"	106°45'18"	23S.2E.29.234	26	42	3,858.00	3,863.90	5.90
32°08'46"	106°40'48"	25S.3E.7.312	27	29	3,818.09	3,823.20	5.11

SOUTHWEST ALLUVIAL BASINS RASA PROJECT

TABLE 5.—Differences between measured and model-derived hydraulic heads—Continued

Latitude	Longitude	Well number	Mode		Measured	Model-	Difference (feet)
			Row	Col- umn	hydraulic	derived	
					head (feet)	head (feet)	
Comparison for end of 1975—Continued							
Layer 1—Continued							
32°12'05"	106°42'43"	24S.2E.23.341	27	33	3,836.87	3,838.60	1.73
31°59'53"	106°35'40"	JL-49-04-102	28	18	3,767.45	3,780.20	12.75
31°59'56"	106°35'31"	JL-49-04-101	28	18	3,790.50	3,780.20	-10.30
32°04'56"	106°37'31"	26S.3E.3.344	28	23	3,801.54	3,798.70	-2.84
32°05'48"	106°38'37"	25S.3E.33.112	28	25	3,803.11	3,808.60	5.49
32°22'10"	106°46'40"	22S.2E.30.123	29	53	3,890.98	3,909.80	18.82
32°08'24"	106°35'50"	25S.3E.13.111	34	27	3,812.00	3,827.00	15.00
Comparison for end of 1975							
Layer 2							
31°59'18"	106°39'13"	27S.3E.5.412	21	19	3,776.76	3,783.10	6.34
31°55'54"	106°36'57"	JL-49-04-418	22	12	3,758.84	3,758.10	-.74
31°56'19"	106°37'05"	JL-49-04-404	22	13	3,758.23	3,758.40	.17
32°14'10"	106°46'27"	24S.2E.7.231	22	37	3,854.20	3,856.40	2.20
31°55'56"	106°36'45"	JL-49-04-410	23	12	3,760.62	3,756.10	-4.52
31°56'52"	106°36'23"	JL-49-04-425	24	14	3,746.07	3,751.40	5.33
31°57'03"	106°36'43"	JL-49-04-427	24	15	3,752.63	3,748.60	-4.03
31°57'20"	106°36'22"	JL-49-04-422	24	15	3,754.35	3,748.60	-5.75
31°58'19"	106°37'07"	JL-49-04-110	24	17	3,762.88	3,763.80	.92
32°04'14"	106°39'58"	26S.3E.6.42	24	24	3,799.09	3,803.70	4.61
31°58'03"	106°35'43"	JL-49-04-165	26	16	3,737.46	3,759.60	22.14
32°16'23"	106°44'56"	23S.2E.28.333	26	41	3,838.00	3,851.90	13.90
32°19'14"	106°46'25"	23S.2E.7.411	27	48	3,856.72	3,866.80	10.08
32°18'32"	106°45'13"	23S.2E.17.243	28	46	3,834.68	3,850.50	15.82
32°18'53"	106°45'21"	23S.2E.8.443	28	47	3,815.91	3,858.20	42.29
32°22'20"	106°47'10"	22S.1E.25.222	28	53	3,897.70	3,898.80	1.10
32°18'19"	106°44'52"	23S.2E.16.314	29	45	3,819.71	3,845.80	26.09
32°19'56"	106°45'31"	23S.2E.5.342	29	49	3,836.79	3,863.40	26.61
Comparison for end of 1975							
Layer 3							
31°56'27"	106°36'37"	JL-49-04-416	23	13	3,738.59	3,747.80	9.21
31°57'03"	106°36'43"	JL-49-04-402	24	15	3,724.90	3,712.80	-12.10
31°57'17"	106°36'40"	JL-49-04-419	24	15	3,712.70	3,712.80	.10
31°58'03"	106°36'45"	JL-49-04-111	24	16	3,719.34	3,722.30	2.96
31°58'17"	106°37'06"	JL-49-04-113	24	17	3,724.64	3,744.00	19.36
32°16'40"	106°46'12"	23S.2E.30.243	25	42	3,849.00	3,861.70	12.70
32°05'50"	106°38'15"	25S.3E.28.434	29	25	3,808.00	3,811.10	3.10

TABLE 6.—Description of sensitivity tests

Test name	Test description
QAL	Values of hydraulic conductivity in layer 1, representing the upper 200 feet of sediments, flood-plain alluvium, and Santa Fe Group, were set equal to twice those in the standard.
SP_YIELD	Specific yield for layer 1 was set equal to 0.1.
EXT_DEPTH25	Extinction depth for head-dependent evapotranspiration was set equal to 25 feet below land surface for both the steady-state and transient versions.
EXT_DEPTH10	Extinction depth for head-dependent evapotranspiration was set equal to 10 feet below land surface for both the steady-state and transient versions.
T*2	Values of transmissivity of layers 1–5 were set equal to double those in the standard.
T*0.5	Values of transmissivity of layers 1–5 were set equal to one-half those in the standard.
BOTTOM	The leakance values of layers 3 and 4 were set equal to 0, effectively removing the lower two layers from the model.
CRIVRIO*2	The connection coefficients for the river were set equal to twice those in the standard.
CRIVRIO*.5	The connection coefficients for the river were set equal to one-half those in the standard.
CRIVDRNS*2	The connection coefficients for the drains were set equal to twice those in the standard.
CRIVDRNS*.5	The connection coefficients for the drains were set equal to one-half those in the standard.
EXT_DPTH25TR	The extinction depth for head-dependent evapotranspiration was set equal to 25 feet for the transient version only.
AGET2.4	The net irrigation–return flow was changed to simulate 0.2 acre–foot/acre more evapotranspiration from irrigated lands than was simulated in the standard.
AGET2.0	The net irrigation–return flow was changed to simulate 0.2 acre–foot/acre less evapotranspiration from irrigated lands than was simulated in the standard.
MUNIPMP*1.2	Municipal and industrial pumpages were set equal to 1.2 times those in the standard.
MUNIPMP*0.0	Municipal and industrial pumpages were set equal to zero.
RECH*2	Mountain-front and slope-front recharges were set equal to twice those in the standard.
RECH*.5	Mountain-front and slope-front recharges were set equal to one-half those in the standard.
STOR*.5	Storage and specific yield were set equal to one-half those in the standard.
VERT*2	Values of vertical hydraulic conductivity of all layers were set equal to twice those in the standard.
VERT*.5	Values of vertical hydraulic conductivity of all layers were set equal to one-half those in the standard.
AGPMP–L2	One-half of the estimated irrigation pumpage was taken from layer 2 for 1951–75.

TABLE 7.—*Comparison of flows and heads of sensitivity tests with those of the standard*

[See table 6 for description of tests. Drain-flow volumes were totaled for 1941–75. The differences are shown as percentages of the volumes derived by the standard simulation. Percentage change in depletion volumes was calculated in the same way. The mean absolute change in layer 1 heads is the mean of the absolute value of the difference between the head calculated by each test and the head calculated by the standard at the nodes shown in the part of table 5 labeled "Comparison for end of 1975," "Layer 1." These nodes were selected because heads calculated at other nodes in layer 1 generally were not saved after execution of the test. The mean absolute change in well-field heads was calculated in the same way, and the nodes selected were those for which hydrographs had been saved (fig. 41). These nodes were in or near the parts of the model representing the Las Cruces and Cañutillo well fields. The score was calculated on the basis of all four columns. For a given entry in each column, a partial score was calculated as the absolute value of the entry divided by the mean absolute value of all entries in the column. The total of the partial scores for a given line is shown as the score. The greater the score, the greater was the effect of the given test. These scores were used only to rank the tests in this table.]

Test name	Change in cumulative drain flow, 1941–75 (percent)	Change in cumulative surface-water depletion, 1941–75 (percent)	Mean absolute change in layer 1 heads, 1975 (feet)	Mean absolute change in well-field heads, 1975 (feet)	Score
STANDARD	0.0	0.0	0.0	0.0	0.0
SP_YIELD	–1.0	0.0	0.1	0.1	0.4
STOR*.5	–1.0	0.0	0.1	0.1	0.4
BOTTOM	–1.0	0.0	0.4	0.8	1.5
CRIVRIO*2	5.0	1.0	0.2	0.3	1.7
AGPMP–L2	1.0	–2.0	0.3	1.1	2.1
CRIVRIO*.5	–6.0	–1.0	0.3	0.4	2.2
RECH*.5	–2.0	2.0	0.9	0.5	3.0
VERT*2	1.0	0.0	0.2	4.7	3.7
AGET2.4	–7.0	6.0	0.2	0.3	3.8
AGET2.0	7.0	–6.0	0.2	0.3	3.8
MUNIPMP*1.2	–1.0	1.0	0.3	4.7	4.1
VERT*.5	0.0	0.0	0.3	5.8	4.4
CRIVDRNS*2	16.0	–2.0	0.6	0.6	4.8
EXT_DEPTH10	10.0	–8.0	0.4	0.3	5.5
T*0.5	–8.0	0.0	1.8	1.1	5.5
RECH*2	5.0	–4.0	1.6	0.9	6.0
CRIVDRNS*.5	–19.0	3.0	0.8	0.8	6.2
EXT_DPTH25TR	–14.0	11.0	0.4	0.6	7.4
EXT_DEPTH25	–15.0	11.0	0.7	0.6	8.2
T*2	10.0	0.0	1.2	8.0	9.2

TABLE 8.—Average differences, in feet, between model-derived and measured heads for the standard and each sensitivity test

[See table 6 for description of tests. SS, steady-state initial condition]

Test name	Time	Arithmetic mean	Mean absolute	Median	Root mean square
Sites on the mesas only					
EXT_DEPTH25	SS	-0.99	7.01	0.55	8.88
RECH*.5	SS	-.67	7.18	1.40	9.32
T*2	SS	.52	7.25	2.20	9.28
CRIVRIO*.5	SS	.67	7.42	2.40	9.43
VERT*.5	SS	1.55	7.42	2.85	9.43
STANDARD	SS	1.04	7.52	2.75	9.45
VERT*2	SS	.72	7.57	2.70	9.46
BOTTOM	SS	.01	7.58	1.55	9.92
CRIVRIO*2	SS	1.27	7.60	3.00	9.48
T*0.5	SS	2.90	7.77	3.80	9.97
EXT_DEPTH10	SS	2.17	7.97	3.55	9.93
RECH*2	SS	4.25	8.15	4.85	10.81
T*0.5	1975	.90	7.80	-.82	11.27
RECH*2	1975	1.53	7.88	.01	11.62
EXT_DEPTH10	1975	-2.62	8.27	-4.20	10.32
VERT*2	1975	-3.26	8.42	-4.55	10.34
CRIVRIO*2	1975	-3.08	8.45	-4.70	10.47
CRIVDRNS*.5	1975	-2.68	8.46	-4.55	10.42
AGET2.4	1975	-3.41	8.52	-5.00	10.52
STANDARD	1975	-3.28	8.53	-4.90	10.54
EXT_DPTH25TR	1975	-3.60	8.55	-5.15	10.54
AGET2.0	1975	-3.15	8.55	-4.85	10.55
MUNIPMP*1.2	1975	-3.36	8.55	-4.95	10.53
MUNIPMP*0.0	1975	-2.84	8.64	-4.80	10.62
SP_YIELD	1975	-3.43	8.66	-4.90	10.65
STOR*.5	1975	-3.43	8.66	-4.90	10.65
CRIVDRNS*2	1975	-3.68	8.67	-5.15	10.65
AGPMP-L2	1975	-3.89	8.68	-5.45	10.69
CRIVRIO*.5	1975	-3.58	8.70	-5.30	10.69
VERT*.5	1975	-3.28	8.70	-5.40	10.81
EXT_DEPTH25	1925	-4.50	9.09	-6.30	11.02
BOTTOM	1975	-4.40	9.30	-6.00	11.21
T*2	1975	-5.64	9.37	-8.23	11.23
RECH*.5	1975	-5.83	9.47	-8.50	11.30
Sites in the valley only					
EXT_DEPTH10	SS	0.01	2.66	1.05	3.65
T*2	SS	-.68	2.67	.50	3.69
CRIVRIO*.5	SS	-2.14	2.98	-1.05	4.52
VERT*2	SS	-1.58	2.98	-.45	4.34
RECH*2	SS	-1.26	3.01	-.20	4.33
STANDARD	SS	-1.75	3.03	-.60	4.43
RECH*.5	SS	-1.98	3.03	-1.50	4.50
BOTTOM	SS	-1.73	3.06	-.75	4.48
VERT*.5	SS	-1.88	3.10	-.70	4.53
CRIVRIO*2	SS	-1.53	3.11	-.30	4.41

TABLE 8.—Average differences, in feet, between model-derived and measured heads for the standard and each sensitivity test—Continued

Test name	Time	Arithmetic mean	Mean absolute	Median	Root mean square
Sites in the valley only—Continued					
T*0.5	SS	-2.68	3.48	-1.55	5.25
EXT_DEPTH25	SS	-5.28	5.28	-3.75	7.05
EXT_DEPTH25	1975	1.32	3.66	.75	5.23
MUNIPMP*1.2	1947	1.92	11.39	4.05	19.22
SP_YIELD	1947	2.08	11.41	4.10	19.24
STOR*.5	1947	2.08	11.41	4.10	19.24
VERT*.5	1947	2.03	11.42	4.10	19.19
EXT_DEPTH25	1947	1.29	11.43	3.55	19.27
CRIVRIO*2	1947	2.04	11.45	4.10	19.24
STANDARD	1947	1.98	11.46	4.05	19.26
AGPMP-L2	1947	1.98	11.46	4.05	19.26
CRIVRIO*.5	1947	1.91	11.48	4.05	19.27
EXT_DEPTH10	1947	2.39	11.49	4.25	19.26
VERT*2	1947	1.97	11.50	4.10	19.30
RECH*.5	1947	1.19	11.51	3.75	19.36
AGET2.0	1947	2.14	11.53	4.25	19.29
BOTTOM	1947	1.60	11.58	3.90	19.32
RECH*2	1947	3.46	11.67	5.05	19.28
T*0.5	1947	3.29	11.71	4.65	19.35
MUNIPMP*0.0	1947	2.29	11.76	4.30	19.51
CRIVDRNS*.5	1947	3.26	12.28	5.80	19.62
EXT_DPTH25TR	1975	2.43	6.99	.79	10.15
MUNIPMP*1.2	1975	1.55	7.01	1.25	9.77
AGPMP-L2	1975	2.29	7.06	1.26	10.17
CRIVDRNS*2	1975	2.30	7.07	.80	10.28
AGET2.4	1975	2.69	7.08	1.33	10.27
EXT_DEPTH25	1975	2.21	7.09	.79	10.24
CRIVRIO*.5	1975	2.58	7.12	1.62	10.31
VERT*.5	1975	1.42	7.14	.80	10.00
STANDARD	1975	2.90	7.19	1.72	10.40
SP_YIELD	1975	2.84	7.19	1.72	10.36
STOR*.5	1975	2.84	7.19	1.72	10.36
RECH*.5	1975	2.09	7.23	1.33	10.30
CRIVRIO*2	1975	3.13	7.26	1.82	10.48
EXT_DEPTH10	1975	3.28	7.27	1.92	10.49
AGET2.0	1975	3.11	7.31	2.02	10.53
BOTTOM	1975	2.57	7.37	1.33	10.62
RECH*2	1975	4.44	7.38	2.60	11.21
T*0.5	1975	1.19	7.42	1.75	11.11
CRIVDRNS*.5	1975	3.72	7.54	3.11	10.64
VERT*2	1975	4.03	7.79	2.81	11.42
T*2	1975	4.34	8.66	2.45	12.64
MUNIPMP*0.0	1975	9.57	12.96	4.40	20.43

TABLE 9.—*Differences between model-derived and measured drain discharges, surface-water depletions, and 1975 heads*

[See table 6 for description of tests. Measured drain discharges were totaled for the time periods shown, as were the model-derived drain discharges. The differences are shown as percentages of the measured totals. Percentage differences in depletions were calculated in the same way. The mean absolute head difference is the same as in table 8 for 1975, at all sites. The score was calculated on the basis of the last three columns (difference in cumulative drain discharges for 1940–75, difference in cumulative depletion, and mean absolute head difference). For a given entry in each of these columns, a partial score was calculated as the absolute value of the entry divided by the mean absolute value of all entries in the column. The total of the partial scores for a given line is shown as the score. The lower the score, the better the comparison of model-derived and measured values with respect to the three columns that were scored. These scores were used only to rank the tests in this table]

Test name	Difference in cumulative drain discharges			Difference in cumulative surface-water depletion	Mean absolute head difference	Score
	1940–50 (percent)	1950–75 (percent)	1940–75 (percent)	1940–75 (percent)	1975 (feet)	
CRIVRIO*.5	–12.0	11.0	–2.0	4.0	7.1	1.9
BOTTOM	–11.0	21.0	3.0	5.0	7.3	2.2
RECH*.5	–13.0	19.0	1.0	7.0	7.2	2.2
VERT*.5	–11.0	21.0	3.0	5.0	7.1	2.2
STANDARD	–11.0	22.0	4.0	5.0	7.1	2.3
SP_YIELD	–11.0	21.0	3.0	6.0	7.1	2.3
MUNIPMP*1.2	–11.0	19.0	2.0	7.0	7.0	2.3
STOR*.5	–11.0	21.0	3.0	6.0	7.1	2.3
AGPMP–L2	–11.0	25.0	5.0	4.0	7.0	2.3
RECH*2	–8.0	30.0	9.0	1.0	7.3	2.4
VERT*2	–11.0	24.0	5.0	5.0	7.7	2.5
T*0.5	–14.0	7.0	–5.0	6.0	7.4	2.6
AGET2.0	–7.0	33.0	11.0	–1.0	7.3	2.7
CRIVRIO*2	–10.0	32.0	9.0	6.0	7.2	3.2
AGET2.4	–16.0	12.0	–3.0	12.0	7.0	3.2
EXT_DEPTH10	–6.0	39.0	14.0	–3.0	7.2	3.4
T*2	–9.0	42.0	14.0	5.0	8.6	3.9
CRIVDRNS*2	1.0	44.0	20.0	3.0	7.0	4.2
CRIVDRNS*.5	–28.0	–2.0	–16.0	9.0	7.5	4.6
EXT_DEPTH25	–19.0	–2.0	–11.0	17.0	7.0	5.1
EXT_DPTH25TR	–19.0	–1.0	–11.0	17.0	6.9	5.1

TABLE 10.—Selected ground-water analyses from the area west of the Mesilla Valley

[Well depth, asterisk (*) indicates water level (in feet below land surface), °C, degrees Celsius; mg/L, milligrams per liter; dashes indicate no data]

Well number	Date sampled	Well depth or sample interval (feet below land surface)	Specific conductance (microsiemens per centimeter at 25 °C)	pH (units)	Temperature (°C)	Dissolved solids (mg/L)	Calcium (mg/L)	Magnesium (mg/L)	Sodium (mg/L)	Sodium plus potassium (mg/L as sodium)	Potassium (mg/L)	Bicarbonate (mg/L)	Carbonate (mg/L)	Sulfate (mg/L)	Chloride (mg/L)	Fluoride (mg/L)	Silica (SiO ₂) (mg/L)
Recharge water along the northwest margin of the basin																	
25S.3W.2.213	80-08-20	527	690	7.8	26.0	--	23	12.0	120	--	1.6	170	--	130	59	1.2	31
23S.1W.32.330	55-03-16	501	1,510	7.7	21.5	1,040	16	2.4	--	320.0	--	320	--	320	100	2.8	100
23S.2W.35.411	73-01-11	1,050	2,310	8.6	36.0	--	23	.3	460	--	3.2	47	1	610	320	6.0	24
23S.2W.13.314	72-11-14	300	1,400	8.0	21.0	--	29	10.0	260	--	15.0	304	--	280	97	2.7	51
Ground water from wells along the southwest margin of the basin																	
28S.1W.19.111	62-05-04	400	7,400	7.3	--	4,770	240	53.0	--	1,400.0	--	1,200	--	770	1,600	2.7	60
27S.2W.25.111	73-03-21	600	1,940	6.8	27.0	--	130	22.0	290	--	42.0	903	--	170	130	1.5	81
26S.2W.15.443	74-06-25	437	435	8.1	26.0	--	13	2.6	73	--	11.0	205	--	21	11	1.6	71
Ground water in the Mesilla Basin																	
29S.1E.8.210	81-04-11	565	1,120	8.5	--	1,040	18	8.7	--	310.0	--	360	--	120	220	1.6	44
28S.2E.24.100	47-05-01	550	1,180	--	--	--	24	10.0	240	--	--	360	11	200	69	1.5	--
27S.1E.23.130	72-05-26	--	871	8.2	27.0	--	7	7.7	170	--	14.0	357	--	73	45	2.6	57
27S.1W.32.000	75-03-03	280	1,210	--	--	--	2	1.2	300	--	5.4	525	--	100	42	7.5	48
26S.1W.25.414	73-03-31	--	902	--	--	--	13	10.0	170	--	11.0	261	--	100	90	1.5	40
26S.1E.18.222	76-05-06	430	950	8.1	33.5	554	20	4.8	170	--	4.1	161	--	150	98	1.4	34
24S.1W.25.422	75-02-03	370	688	8.0	--	431	26	4.4	110	--	6.1	167	--	110	57	.9	26
24S.1W.22.123	75-03-06	--	1,610	--	23.0	--	50	10.0	270	--	35.0	316	--	160	230	2.4	30
24S.1E.8.123	75-01-30	568-588	884	8.1	19.0	548	56	8.9	110	--	4.1	150	--	160	94	.6	18
		754-774	909	8.0	19.0	577	66	7.6	110	--	4.3	172	--	170	91	.5	21
		1,380-1,400	736	8.3	21.0	462	20	2.8	140	--	13.0	288	--	73	40	2.3	27
23S.1E.33.422	72-10-30	209	742	8.0	18.0	--	84	11.0	--	--	--	182	--	120	76	--	--
23S.1E.30.422	82-08-11	--	657	7.8	23.5	348	52	5.8	63	--	8.9	--	--	51	96	.4	26
23S.1E.20.114	72-11-01	565	599	7.9	16.0	--	44	8.6	68	--	3.4	205	--	83	42	.9	27
23S.1E.17.423	72-11-01	26 *	1,940	8.0	18.0	--	190	40.0	230	--	7.6	212	--	580	250	.7	35

TABLE 11.—Concentrations of dissolved ions in excess applied irrigation water for different irrigation efficiencies and chemical reactions

[All concentrations in milligrams per liter]

	Dissolved solids	Calcium	Magnesium	Sodium	Potassium	Bicarbonate	Sulfate	Chloride
Initial surface water, Rio Grande below Elephant Butte, May 14, 1980	274	46	7.7	38	4.2	146	86	19
Excess applied irrigation water, irrigation efficiency of 0.4	457	77	12.8	63	7.0	243	143	32
Excess applied irrigation water, irrigation efficiency of 0.5	548	92	15.4	76	8.4	292	172	38
Excess applied irrigation water, irrigation efficiency of 0.6	685	115	19.3	95	10.5	365	215	48
Excess applied irrigation water, irrigation efficiency of 0.7	913	153	25.7	127	14.0	487	287	63
Excess applied irrigation water, irrigation efficiency of 0.8	1,361	230	38.5	190	21.0	730	430	86
Excess applied irrigation water, irrigation efficiency of 0.6, precipitation of cal- cite after saturation of calcite is reached	646	92	19.3	95	10.5	332	215	48
Excess applied irrigation water, irrigation efficiency of 0.6, calcium-for-sodium ion exchange	690	80	19.3	135	10.5	365	215	48

TABLE 12.—Selected ground-water analyses from the area east of the Mesilla Valley

[Well depth, asterisk (*) indicates water level (in feet below land surface); °C, degrees Celsius; mg/L, milligrams per liter; dashes indicate no data]

Well number	Date sampled	Well depth or sample interval (feet below land surface)	Specific conductance (microsiemens per centimeter at 25 °C)	pH (units)	Temperature (°C)	Dissolved solids (mg/L)	Calcium (mg/L)	Magnesium (mg/L)	Sodium (mg/L)	Sodium plus potassium (mg/L as sodium)	Potassium (mg/L)	Bicarbonate (mg/L)	Carbonate (mg/L)	Sulfate (mg/L)	Chloride (mg/L)	Fluoride (mg/L)	Silica (SiO ₂) (mg/L)
29S.4E.18.233	74-12-03	200	1,840	8.0	25.5	1,220	130	24.0	220	--	23.0	103	--	460	220	0.9	26
29S.3E.12.422	74-12-04	--	3,630	8.0	13.5	--	250	11.0	--	--	--	37	--	990	520	--	--
29S.4E.6.243	76-03-12	40	--	7.7	16.5	--	520	150.0	3,600	--	38.0	443	--	3,600	4,000	1.1	9
JL-49-12-204	52-01-10	382	1,340	6.6	--	782	69	57.0	108	--	--	246	--	166	187	1.1	18
JL-49-12-106	53-11-05	194-238	6,200	7.9	--	4,010	69	48.0	1,310	--	--	182	--	1,150	1,320	1.8	24
JL-49-04-724	51-03-30	124	2,630	8.0	--	1,740	93	45.0	455	--	--	487	--	499	358	--	46
JL-49-03-908	52-03-26	125	1,760	8.0	--	1,110	24	29.0	337	--	--	466	--	240	192	--	57
JL-49-04-501	53-08-31	218-279	1,590	7.8	--	983	60	30.0	236	--	12.0	216	--	269	232	2.6	11
JL-49-04-205	52-11-12	517	1,810	8.0	--	1,100	101	64.0	202	--	--	251	--	271	318	--	19
JL-49-03-322	53-11-12	195-238	650	7.8	--	400	21	3.8	110	--	2.3	120	--	112	69	.3	22
28S.3E.2.122	75-06-19	--	1,800	--	20.0	--	120	10.0	230	--	4.3	231	--	420	180	.8	41
			2,470	8.0	23.5	--	84	56.0	--	--	--	192	--	410	420	--	--
			759	8.5	27.0	--	16	.1	140	--	2.3	56	4	99	130	.5	22
26S.3E.36.143	72-05-17	--	1,870	8.4	24.5	--	64	25.0	260	--	11.0	194	1	180	380	.9	37
26S.3E.26.224	75-06-12	42-62	2,110	7.1	20.5	--	84	27.0	310	--	35.0	359	--	220	360	1.0	39
26S.3E.14.434	74-05-09	268	2,180	7.6	23.5	--	140	45.0	230	--	44.0	408	--	200	360	.3	52
26S.3E.11.111	73-03-28	478-501	1,120	7.7	31.0	--	25	3.6	220	--	8.1	359	--	170	73	1.1	36
26S.3E.2.342	73-03-27	718	2,330	8.0	27.0	--	39	14.0	450	--	18.0	257	--	240	470	2.4	21
25S.4E.17.442	54-01-03	647-690	818	8.0	--	--	22	6.4	150	--	6.2	180	--	180	49	.5	14
25S.4E.18.242	53-12-06	987	1,920	7.5	--	--	140	29.0	220	--	9.8	230	--	230	360	--	38
25S.3E.8.421	73-03-02	372	2,480	7.3	--	--	160	27.0	350	--	39.0	655	--	210	400	1.2	46
25S.3E.12.413	72-09-12	360-560	2,090	7.6	--	--	130	24.0	290	--	37.0	514	--	210	320	.7	40
25S.4E.8.000	53-05-23	--	743	7.9	--	429	37	8.8	93	--	8.0	180	--	66	91	.3	30
25S.3E.8.214	72-11-01	250	2,870	7.7	31.5	--	170	30.0	420	--	40.0	612	--	270	470	1.4	53
25S.3E.6.212	72-09-12	400	4,590	7.7	25.0	--	230	58.0	710	--	64.0	582	--	510	940	1.7	62
24S.4E.35.000	53-05-04	580	657	7.9	--	--	33	8.1	89	--	8.1	180	--	70	68	.3	28
24S.2E.14.122	72-09-18	160-512	1,420	7.8	24.0	--	87	16.0	210	--	20.0	390	--	180	170	1.9	47

TABLE 12.—Selected ground-water analyses from the area east of the Mesilla Valley—Continued

[Well depth, asterisk (*) indicates water level (in feet below land surface); °C, degrees Celsius; mg/L, milligrams per liter; dashes indicate no data]

Well number	Date sampled	Well depth or sample interval (feet below land surface)	Specific conductance (microsiemens per centimeter at 25 °C)	pH (units)	Temperature (°C)	Dissolved solids (mg/L)	Calcium (mg/L)	Magnesium (mg/L)	Sodium (mg/L)	Sodium plus potassium (mg/L as sodium)	Potassium (mg/L)	Bicarbonate (mg/L)	Carbonate (mg/L)	Sulfate (mg/L)	Chloride (mg/L)	Fluoride (mg/L)	Silica (SiO ₂) (mg/L)
24S.3E.5.330	48-03-25	--	--	--	20.5	--	15	9.4	--	140.0	--	350	7	41	20	--	--
23S.2E.5.321	75-06-27	392-438	740	--	26.5	500	47	17.0	99	--	10.0	213	--	110	82	0.7	27
23S.2E.9.332	74-06-28	612	860	7.8	--	528	70	19.0	73	--	8.3	182	--	140	93	.6	31
23S.2E.16.314	75-06-30	381-591	600	--	--	404	58	12.0	59	--	6.8	159	--	88	73	.7	28
23S.2E.21.223	72-05-24	420-526	1,430	7.7	--	961	130	30.0	160	--	10.0	304	--	170	270	.5	40
23S.2E.34.412	72-12-01	486	1,100	8.2	--	691	55	9.9	160	--	17.0	283	--	140	130	1.6	38
23S.2E.25.321	81-11-	645	2,580	8.5	--	1,626	129	31.0	398	--	54.7	394	--	300	496	2.2	56
22S.2E.32.222	72-05-26	450	1,270	8.1	25.5	--	76	26.0	150	--	5.2	124	--	140	250	.7	31
Ground water from the Radium Springs area																	
21S.1W.14.113	73-12-14	105	1,470	7.9	21.0	--	100	14.0	190	--	15.0	237	--	210	220	0.4	33
21S.1W.12.343	73-12-11	67 *	3,840	8.0	23.5	--	34	29.0	710	--	79.0	180	--	110	1,100	1.1	4
21S.1W.10.213	57-04-29	--	6,210	8.2	53.0	--	--	--	--	--	--	420	--	263	1,630	--	--
Type 1 ground water																	
22S.3E.11.441	57-04-17	460	801	8.2	--	--	110	34.0	--	18.0	--	140	--	290	14	1.2	29
22S.3E.2.214	65-05-26	--	1,960	7.4	--	--	320	66.0	--	54.0	--	100	--	900	110	1.0	38
21S.3E.33.142	73-04-10	700	850	7.7	--	--	76	36.0	46	--	3.4	150	--	270	36	.9	47
21S.3E.19.444	73-03-21	529	742	7.7	25.0	--	42	43.0	44	--	3.0	126	--	220	38	.8	25
Type 2 ground water																	
22S.3E.23.143	73-03-28	225	647	7.7	--	--	82	27.0	14	--	5.7	231	--	130	16	1.1	23
22S.3E.17.134	73-03-29	490-540	513	7.6	--	--	46	15.0	38	--	3.2	168	--	100	18	.8	32
22S.2E.13.441	48-03-26	430	349	--	--	--	34	7.0	--	30.0	--	120	--	65	9	--	--
22S.3E.8.144	73-08-02	500-590	533	7.8	25.5	--	69	13.0	21	--	2.2	171	--	120	13	.2	33
Ground water along the western margin of types 1 and 2 ground water																	
22S.2E.24.422	73-08-30	1,120-1,140	564	8.8	28.0	402	3	0.2	130	--	0.9	313	8	28	8	3.5	15
22S.2E.21.131	73-03-21	1,000	537	8.0	26.0	--	7	1.6	110	--	2.3	191	--	94	13	1.1	25
22S.2E.23.111	73-03-29	662	286	8.2	--	--	11	2.1	52	--	1.7	132	--	28	6	.7	27
22S.3E.6.111	76-09-02	1,150-1,170	520	8.1	29.0	340	18	8.2	94	--	3.4	216	--	99	5	.9	30

TABLE 13.—Well depth, water level, and percentages of calcium plus magnesium and sulfate plus chloride for selected sites in the northeastern part of the Mesilla Basin

[* indicates well depth]

Well number	Sample interval (feet below land surface)	Water level (feet below land surface)	Calcium plus magnesium (percent)	Sulfate plus chloride (percent)
Type 1 ground water				
22S.3E.11.441	460*	--	92	74
22S.3E.2.214	253*	56	91	92
21S.3E.33.142	700*	594	77	73
21S.3E.19.444	529*	393	74	74
Type 2 ground water				
22S.3E.23.143	225*	108	90	45
22S.3E.17.134	490–540	--	67	48
22S.2E.13.441	430*	--	63	45
22S.3E.8.144	500–590	480	83	50
Ground water along the western margin of types 1 and 2 water				
22S.2E.24.222	1,120–1,140	397	3	12
22S.2E.23.111	662*	--	23	27
22S.2E.21.131	1,000*	470	9	42
22S.3E.6.111	1,150–1,170	350	28	38

TABLE 14.—Calculated chemical-geothermometer temperatures for selected ground-water analyses in the Mesilla Basin

[All temperatures are in degrees Celsius; Si, silica; Na, sodium; K, potassium; Ca, calcium]

Well number	Geothermometer temperatures		
	Si	Na/K	Na/K/Ca
26S.3E.26.224	90	184	185
26S.3E.14.434	104	227	204
25S.3E.8.421	98	183	179
25S.3E.12.413	92	194	185
25S.3E.8.214	105	172	175
25S.3E.6.212	112	168	179
23S.2E.25.321	107	248	219